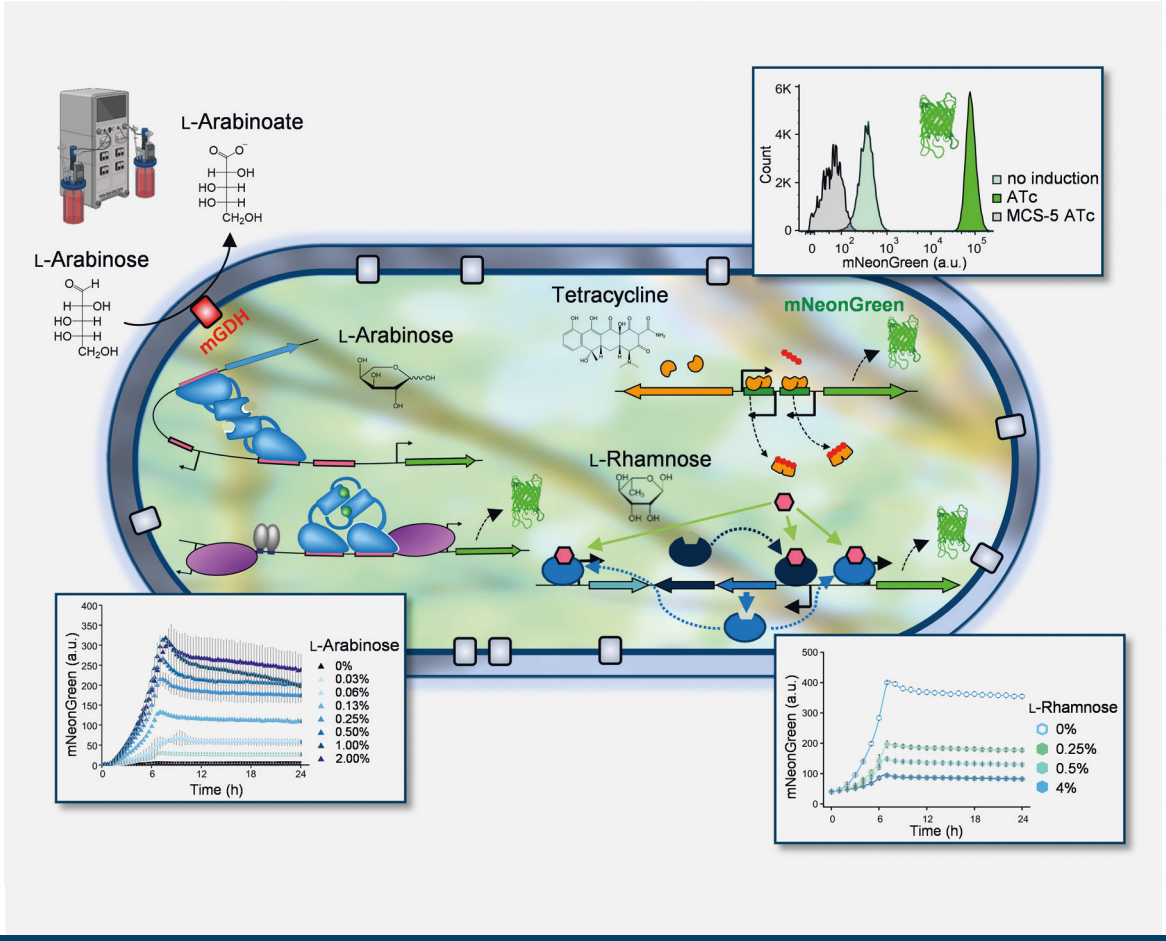

Establishing regulatable expression systems in the acetic acid bacterium *Gluconobacter oxydans* 621H

Philipp Moritz Fricke

Schlüsseltechnologien / Key Technologies
Band / Volume 258
ISBN 978-3-95806-642-7

Mitglied der Helmholtz-Gemeinschaft

JÜLICH
Forschungszentrum

Schriften des Forschungszentrums Jülich
Reihe Schlüsseltechnologien / Key Technologies Band / Volume 258

Forschungszentrum Jülich GmbH
Institut für Bio-und Geowissenschaften
Biotechnologie (IBG-1)

Establishing regulatable expression systems in the acetic acid bacterium *Gluconobacter oxydans* 621H

Philipp Moritz Fricke

Schriften des Forschungszentrums Jülich
Reihe Schlüsseltechnologien / Key Technologies Band / Volume 258

ISSN 1866-1807 ISBN 978-3-95806-642-7

Bibliografische Information der Deutschen Nationalbibliothek.
Die Deutsche Nationalbibliothek verzeichnet diese Publikation in der
Deutschen Nationalbibliografie; detaillierte Bibliografische Daten
sind im Internet über http://dnb.d-nb.de abrufbar.

Herausgeber und Vertrieb:	Forschungszentrum Jülich GmbH Zentralbibliothek, Verlag 52425 Jülich Tel.: +49 2461 61-5368 Fax: +49 2461 61-6103 zb-publikation@fz-juelich.de www.fz-juelich.de/zb
Umschlaggestaltung:	Grafische Medien, Forschungszentrum Jülich GmbH
Druck:	Grafische Medien, Forschungszentrum Jülich GmbH
Copyright:	Forschungszentrum Jülich 2022

Schriften des Forschungszentrums Jülich
Reihe Schlüsseltechnologien / Key Technologies, Band / Volume 258

D 61 (Diss. Düsseldorf, Univ., 2022)

ISSN 1866-1807
ISBN 978-3-95806-642-7

Vollständig frei verfügbar über das Publikationsportal des Forschungszentrums Jülich (JuSER)
unter www.fz-juelich.de/zb/openaccess.

Results described in this dissertation are part of the following publications and manuscripts in preparation:

Publications:

Fricke, P. M., Link, T., Gätgens, J., Sonntag, C., Otto, M., Bott, M., & Polen, T. (2020). A tunable L-arabinose-inducible expression plasmid for the acetic acid bacterium *Gluconobacter oxydans*. **Applied Microbiology and Biotechnology 104: 9267–9282.**
doi:10.1007/s00253-020–10905-4

Fricke, P. M., Klemm, A., Bott, M., & Polen, T. (2021a)**.** On the way toward regulatable expression systems in acetic acid bacteria: target gene expression and use cases. **Applied Microbiology and Biotechnology 105: 3423–3456.**
doi:10.1007/s00253-021-11269-z

Fricke, P. M., Lürkens, M., Hünnefeld, M., J., Sonntag, C., Bott, M., Davari, M. D. & Polen, T. (2021b). Highly tunable TetR-dependent target gene expression in the acetic acid bacterium *Gluconobacter oxydans*. **Applied Microbiology and Biotechnology 105: 6835–6852.**
doi:10.1007/s00253-021-11473-x

Submitted manuscript:

Fricke, P. M., Hartmann, R., Wirtz, A., Bott, M., & Polen, T. Production of L-arabinonic acid from renewable L-arabinose by the acetic acid bacterium *Gluconobacter oxydans*. **Submitted to Bioresource Technology.**

Manuscripts in preparation:

Fricke P.M., Gries M., Mürköster M., Sonntag C., Gätgens J., Bott M., Polen T. The L-rhamnose-dependent regulator RhaS and its target promoters expand the toolkit for regulatable gene expression in the acetic acid bacterium *Gluconobacter oxydans*.

Fricke P.M., Klemm A., Derksen S., Degner U., Sonntag C., Bott M., Polen T. Endogenous promoters enabling tunable citrate-dependent target gene expression in the acetic acid bacterium *Gluconobacter oxydans*.

Table of content

Abbreviations:

ATc	Anhydrotetracycline
bp	Base pair
cAMP	Cyclic adenosine monophosphate
ChAP-Seq	Chromatin affinity purification DNA sequencing
CO_2	Carbon dioxide
DNA	Deoxyribonucleic acid
EDP	Entner-Doudoroff Pathway
EMP	Embden–Meyerhof–Parnas
et al.	*et alii*
$FAD/FADH_2$	Flavin adenine dinucleotide
$FeSO_4$	Iron(II) sulfate
IPTG	Isopropyl-β-D-1-thiogalactopyranoside
mNG	mNeonGreen
mRNA	Messenger ribonucleic acid
$NAD^+/NADH$	Nicotinamide adenine dinucleotide
$NADP^+/NADPH$	Nicotinamide adenine dinucleotide phosphate
OD_{600}	Optical density (600 nm)
PPP	Pentose phosphate pathway
PQQ	Pyrroloquinoline quinone
Q10	Ubiquinone–10
RBS	Ribosome binding site
RNAP	RNA polymerase
TCA	Tricarboxylic acid cycle
TSS	Transcription start site

Further abbreviations not included in this section are according to international standards, for example listed in the author guidelines of the FEBS Journal.

Abstract

Among industrially relevant microorganisms, the acetic acid bacterium *Gluconobacter oxydans* is valued for its ability to incompletely oxidize a vast number of carbohydrates stereo- and regio-specifically. Biotechnological production processes involving *G. oxydans* strains so far utilized exclusively constitutive target gene expression. Regulatable promoters used in *G. oxydans* suffered from low induction fold-changes and relatively high basal promoter activity already when not induced. This study aimed to establish regulatable promoter systems in *G. oxydans* that allow tuned target gene expression in an effector-dependent manner. For this purpose, expression plasmids were constructed to test four well-characterized heterologous regulator-promoter pairs in *G. oxydans.* Additionally, screenings were performed to identify regulatable endogenous *G. oxydans* promoters responding to a metabolite given as an external stimulus and suitable for controlled gene expression.

When transferred into *G. oxydans*, the AraC-P_{araBAD} system from *Escherichia coli* MC4100 permitted tight repression of target gene expression in the absence of L-arabinose and up to 480-fold induction when maximally induced with L-arabinose. At inducer concentrations from 0.1 to 1% (w/v) L-arabinose, reporter gene expression from P_{araBAD} was highly tunable. Furthermore, L-arabinose was found to be oxidized to L-arabinonic acid by the membrane-bound glucose dehydrogenase GdhM, resulting in an acidification of the medium and pH-dependent loss of intracellular reporter protein activity. This loss could be circumvented by pH-controlled cultivation or use of the *gdhM* deletion strain BP.6.

The oxidation product L-arabinonic acid is a valuable compound with potential use in various applications ranging from the production of pharmaceuticals to semi-conductor materials and composite cements. By using *G. oxydans* 621H, more than 120 g/L L-arabinonic acid could be produced from 160 g/L L-arabinose within 144 h in pH-controlled fed-batch cultivations. This high titer exceeded the ones previously reported for engineered *E. coli* or *Saccharomyces cerevisiae* strains more than threefold. Plasmid-based overexpression of *gdhM* to increase the enzyme activity did not improve the productivity possibly due to detrimental effects on the membrane integrity.

Besides the AraC-P_{araBAD} system, the suitability of the transposon Tn*10*-based TetR-P_{tet} system and of the LacI-P_{lacUV5} system, both originating from *E. coli*, was tested in *G. oxydans*. In contrast to AraC-P_{araBAD}, these inducible expression systems rely on target gene repression. The TetR-P_{tet} system outperformed the AraC-P_{araBAD} system, since in *G. oxydans* it showed extremely low basal expression and a concentration-dependent gradual increase of target gene expression upon induction with anhydrotetracycline. A maximal induction of up to 3,500-fold was obtained with 200 ng/mL anhydrotetracycline. Terminator sequences, plasmid backbone, antibiotic resistance gene, and the insertion of an additional known ribosome-binding site affected the performance of this system. In *G. oxydans*, only moderate inducible gene expression from P_{lacUV5} made this system the weakest of the regulator-promoter pairs tested in this work. Due to relatively high leakiness of non-induced P_{lacUV5}, induction with 1 mM IPTG was only 40-fold.

With the RhaSR-P_{rhaBAD} system from *E. coli*, a regulator-promoter pair was found that – contrary to *E. coli* – allows L-rhamnose-dependent knockdown of gene expression in *G. oxydans* instead of induction. P_{rhaBAD} was very strong in *G. oxydans* and activated by the presence of RhaS in the absence of L-rhamnose, while with increasing L-rhamnose concentrations the P_{rhaBAD} activity was reduced by 92% in a RhaS-dependent manner. In contrast, expression from the RhaS-dependent promoter P_{rhaT} was L-rhamnose-inducible in

G. oxydans as in *E. coli*. Since P_{rhaT} was rather weak in *G. oxydans*, the induction was tunable up to 10-fold. This could be of advantage for expression of 'difficult' enzymes.

In the DNA microarray-based genome-wide stimulon screenings for regulated endogenous promotors, transcription of GOX0532 and GOX0536 encoding ExbB and a ferrisiderophore receptor both likely involved in iron uptake were found to be increased 45-fold when exposed to 1% (w/v) citrate as stimulus. Supplementation of the growth medium with 8 µM $FeSO_4$ reduced the basal expression from both promoters und thereby increased induction ratios. Probably induced by iron-limitation through Fe^{3+}-citrate chelation, expression from $P_{GOX0532}$ and $P_{GOX0536}$ could be upregulated >270-fold when 5 x 50 mM citrate was added to the medium in intervals of 1.5 h. ChAP-Seq experiments confirmed that the ferric uptake regulator Fur (GOX0771) binds to the promoter region $P_{GOX0536}$.

Beside these original studies, a review on expression systems and their applications in acetic acid bacteria (AAB) was published covering the years from 1985, when the first plasmids were used in AAB, up to the end of 2020. Screening of 6097 AAB-related publications revealed that expression plasmids have been reported for merely nine out of 49 AAB genera currently described, and six major expression plasmid lineages were identified. According to this AAB-related literature search, the AraC-P_{araBAD} and TetR-P_{tet} systems developed by us for *G. oxydans* are the first regulatable expression system with induction ratios >40-fold in this group of bacteria. They provide new options in future strain development and may be transferable to other AAB species.

Zusammenfassung

Das Essigsäurebakterium *Gluconobacter oxydans* wird unter den industriell relevanten Mikroorganismen für seine Fähigkeit geschätzt, eine Vielzahl von Kohlenhydraten stereo- und regiospezifisch unvollständig zu oxidieren. Bisherige biotechnologische Verfahren mit *G. oxydans* verwendeten für die zielgerichtete Genexpression ausschließlich konstitutive Promotoren. Die regulierbaren Promotoren, die in *G. oxydans* oder anderen Essigsäurebakterien untersucht wurden, zeigten eine sehr hohe Basalaktivität unter nicht induzierten Bedingungen, was zu einem geringen Induktionsverhältnis führte. Das Ziel dieser Doktorarbeit war es, ein regulierbares Promotorsystem in *G. oxydans* zu etablieren, dass die Expression ausgewählter Gene durch die Konzentration eines Induktors steuern kann. Zu diesem Zweck wurden vier bekannte und gut charakterisierte Regulator-Promotor-Paare in *G. oxydans* mit Hilfe von Expressionsplasmiden getestet. Außerdem wurde versucht, regulierbare endogene *G. oxydans*-Promotoren zu identifizieren, die auf die Zugabe eines Metaboliten als externen Stimulus reagieren und so für eine kontrollierte Genexpression geeignet sind.

In *G. oxydans* getestet, ermöglichte das AraC-P_{araBAD}-System aus *Escherichia coli* MC4100 eine starke Repression der Transkription in Abwesenheit von L-Arabinose sowie eine bis zu 480-fach erhöhte Genexpression bei vollständiger Induktion mit L-Arabinose. Die Genexpression von P_{araBAD} war durch den Einsatz von Induktorkonzentrationen von 0,1-1% (w/v) L-Arabinose gut modulierbar. Außerdem wurde gezeigt, dass die Oxidation von L-Arabinose zu L-Arabinsäure durch die membrangebundene Glucose-Dehydrogenase GdhM zu einer Ansäuerung des Mediums und damit zu einem pH-abhängigen Verlust der Reporterproteinaktivität führte. In pH-kontrollierten Fermentationen oder durch die Verwendung des GdhM-Deletionsstamms BP.6 konnte dieser Verlust umgangen werden.

Das Oxidationsprodukt L-Arabinsäure ist ein wertvoller Rohstoff, der in vielen Prozessen unter anderem bei der Herstellung bestimmter Pharmazeutika, Halbleitermaterialien und Verbundzementen Anwendung findet. Durch die Verwendung von *G. oxydans* 621H wurde in pH-kontrollierten Fed-Batch-Kultivierungen innerhalb von 144 Stunden mehr als 120 g/L L-Arabinsäure aus 160 g/L L-Arabinose hergestellt. Dieser hohe Titer übertraf die Titer, die zuvor für gentechnisch veränderte *E. coli* oder *Saccharomyces cerevisiae* berichtet wurden, um mehr als das Dreifache. Die Plasmid-basierte Überexpression von *gdhM* zur Erhöhung der Enzymaktivität führte, möglicherweise aufgrund nachteiliger Auswirkungen auf die Membranintegrität, zu keiner Verbesserung der Produktivität.

Neben dem AraC-P_{araBAD}-System wurden mit dem Transposon Tn*10*-basiertem TetR-P_{tet}-System und dem LacI-P_{lacUV5}-System zwei weitere induzierbare Expressionssysteme aus *E. coli* in *G. oxydans* getestet. Im Gegensatz zu AraC-P_{araBAD} beruhen diese induzierbaren Expressionssysteme auf der Transkriptionsrepression von Zielgenen. Die Leistung des TetR-P_{tet}-Systems übertraf die des AraC-P_{araBAD}-Systems. Unter nicht induzierten Bedingungen zeigte das TetR-P_{tet}-System eine sehr geringe basale Expression, die durch die Konzentration des Induktors graduell gesteigert werden konnte. Unter Verwendung von 200 ng/ml Anhydrotetracyclin wurde ein maximales Induktionsverhältnis von 3.500 ermittelt. Terminatorsequenzen, Wahl des Expressionsplasmids, Antibiotikaresistenzgen und die Insertion einer zusätzlichen, bekannten Ribosomenbindestelle beeinflussten die Leistungsfähigkeit dieses Systems. Die deutlich geringere Induzierbarkeit von P_{lacUV5} in *G. oxydans* hingegen machte dieses System zum schwächsten der hier getesteten Regulator-Promotor-Paare. Aufgrund der hohen Basalaktivität wurde mit P_{lacUV5} nur eine 40-fache Induktion mit 1 mM IPTG erzielt.

Mit dem RhaSR-P_{rhaBAD}-System von *E. coli* wurde ein Regulator-Promotor-Paar gefunden, das – im Gegensatz zu *E. coli* – einen L-Rhamnose-abhängigen Knockdown anstelle einer Induktion der Genexpression in *G. oxydans* ermöglichte. P_{rhaBAD} führte in *G. oxydans* zu einer sehr starken Expression und wurde durch die Anwesenheit von RhaS in Abwesenheit von L-Rhamnose aktiviert. Mit steigender L-Rhamnose-Konzentration wurde die P_{rhaBAD}-Aktivität RhaS-abhängig um bis zu 92% reduziert. Im Gegensatz dazu war die Expression des RhaS-abhängigen Permease-Promotors P_{rhaT} in *G. oxydans* genauso wie in *E. coli* induzierbar. P_{rhaT} zeigte in *G. oxydans* eine schwache Expressionsstärke, welche durch die L-Rhamnosekonzentration maximal 10-fach induziert werden konnte. Ein derartiger Promotor wäre möglicherweise für die Expression von „schwierigen" Enzymen von Vorteil.

In DNA-Microarray-basierten genomweiten Stimulon-Screenings auf regulierte endogene Promotoren wurde gezeigt, dass sich die Transkription der *G. oxydans*-Gene GOX0532 und GOX0536 um das 45-fache erhöhte, wenn dem Medium 1% (w/v) Citrat zugesetzt wurde. Die Gene GOX0532 und GOX0536 kodieren für ExbB und einen Eisen-Siderophore Rezeptor, die beide wahrscheinlich an der Eisenaufnahme beteiligt sind. Die Supplementierung des Mediums mit 8 µM $FeSO_4$ reduzierte die basale Expression beider Promotoren und erhöhte dadurch die Induktionsraten. Wahrscheinlich induziert durch Eisenlimitierung verursacht durch Citrate-Fe^{3+}-Chelatierung, konnte die Expression von $P_{GOX0532}$ und $P_{GOX0536}$ >270-fach hochreguliert werden, wenn das Medium mit 5 x 50 mM Citrat in Intervallen von 1,5 Stunden versetzt wurden. ChAP-Seq Analysen bestätigten, dass der Transkriptionsfaktor Fur (*ferric uptake regulator*) (GOX0771) Promotorbereiche von $P_{GOX0536}$ bindet.

Neben diesen Originalstudien wurde in einem Minireview ein Überblick über Expressionssysteme und ihre Anwendungen in Essigsäurebakterien veröffentlicht, der die Jahre von 1985, als die ersten Plasmide in Essigsäurebakterien verwendet wurden, bis Ende 2020 umfasste. In 6.097 Veröffentlichungen zu Essigsäurebakterien wurde lediglich für neun von 49 beschriebenen Gattungen über die Verwendung von Expressionsplasmiden berichtet. Innerhalb der beschriebenen Expressionsplasmide wurden sechs Hauptplasmidlinien identifiziert. Gemäß der Literaturrecherche sind die für *G. oxydans* entwickelten Systeme AraC-P_{araBAD} und TetR-P_{tet} die ersten regulierbaren Expressionssystem in dieser Bakteriengruppe, die eine >40-fach Induktion erlauben. Sie bieten neue Optionen für die zukünftige Stammentwicklung von *G. oxydans* und können möglicherweise auf andere Essigsäurebakterien-Arten übertragen werden.

1 Introduction

1.1 *Gluconobacter oxydans*

The family of acetic acid bacteria (AAB) belongs to the α-subclass of *Proteobacteria* and currently comprises 50 genera, including the well-known and extensively studied genera *Acetobacter*, *Gluconobacter*, *Gluconacetobacter*, *Acidiphilium*, *Komagataeibacter*, *Roseomonas*, *Asaia*, *Acidocella* and *Acidomonas* (Yamada & Yukphan, 2008, NCBI Taxonomy Browser, November 2021). The Gram-negative *Gluconobacter oxydans* is a prominent member of the *Acetobacteraceae* family and used in industrial biotechnology. *G. oxydans* is strictly aerobic, rod-shaped and strives in environments that are rich in carbohydrates, such as rotten fruits, flowers and alcoholic beverages (Kersters et al. 2006). The bacterium is acidophilic with a pH optimum of 5-6 and its preferred growth temperature is 25-30 °C. Cells are ellipsoidal to rod-shaped with a size of 0.5-0.8 x 0.9-4.2 µm but can develop enlarged irregular and filamentous cell forms, *e.g.* when exposed to osmotic stress (Ley et al. 1984, De Muynck et al. 2007, Zahid et al. 2015). *G. oxydans* was the first AAB to be fully sequenced (Prust et al. 2005). The genome of *G. oxydans* with a G+C content is 60.8 % comprises a circular chromosome of 2.7 Mb and five plasmids ranging from 2.7 to 163 kb. From the 2,664 predicted protein-coding open reading frames (ORFs), 1,877 ORFs were assigned to a specific function. Moreover, genome sequencing identified 103 transposase genes and 82 insertion sequences (IS), which might cause a genetic instability of *G. oxydans* (Kondo & Horinouchi, 1997, Prust et al. 2005). Additionally and most striking, 75 ORFs were annotated to encode putative oxidoreductases with unknown functions. 32 membrane-bound dehydrogenases (DHs) were predicted and substrate specificity of some of them has been elucidated, underlining the industrial potential of the bacterium (Deppenmeier et al. 2002, Prust et al. 2005, Mientus et al. 2017). Recently, the genome sequence of *G. oxydans* 621H was improved by combining Nanopore and Illumina sequencing (Kranz et al. 2017).

1.1.1 Biotechnological relevance of *G. oxydans*

G. oxydans has been used in biotechnological applications for more than 90 years, primarily because of its ability to rapidly and incompletely oxidize sugars, sugar alcohols and polyols stereo- and regiospecifically with its many membrane-bound DHs active in the periplasm (Gupta et al. 2001, Deppenmeier et al. 2002, Merfort et al. 2006). The location of these periplasmic enzymes pose the advantage that no uptake of substrates into the cytoplasm is required and that desired products often diffuse via porins in the outer membrane back into the medium where they accumulate in large quantities (Matsushita et al. 1994, Kulhánek, 1989, Chen, 2007). The most prominent process involving *G. oxydans* is the Reichstein-Grüssner

synthesis of vitamin C, where the chemically difficult conversion of D-sorbitol to L-sorbose is catalyzed by membrane-bound DHs of the bacterium (Pappenberger & Hohmann, 2014). Furthermore, *G. oxydans* is used for the synthesis of the pharmaceutical compound and skin tanning agent dihydroxyacetone through oxidation of glycerol as well as for the synthesis of 6-amino-L-sorbose from 1-amino-D-sorbitol, which is a precursor of the anti-diabetic drug miglitol (Schedel, 2001, Deppenmeier et al. 2002, Gätgens et al. 2007, Mamlouk & Gullo, 2013). Moreover, *G. oxydans* and enzymes isolated from the bacterium are utilized as biosensors for sugars, alcohols and biological oxygen demand (Švitel et al. 2006, Kitova et al. 2021). All in all, the functions of some oxidoreductases still remain to be elucidated, signifying that *G. oxydans*' potential for biotechnological application has not been fully exploited yet.

1.1.2 Carbon metabolism of *G. oxydans*

Like all AAB, *G. oxydans* is known for its incomplete oxidation of carbohydrates. The preferred carbon- and energy sources of the chemoorganotrophic bacterium are in descending order D-mannitol, D-sorbitol, glycerol, D-fructose, and D-glucose (De Ley et al. 1984, Gupta *et al.* 2001, Kersters et al. 2006). In defined mineral salts medium *G. oxydans* grows poorly and reaches only very low biomass yields (Olijve & Kok, 1979, Raspor & Goranovič, 2008). The above mentioned substrates are primarily oxidized by one or more of the many DHs active in the periplasm that use pyrroloquinoline quinone (PQQ), PQQ plus cytochrome *c*, or flavin adenine dinucleotide (FAD) as prosthetic groups (Ameyama et al. 1987, Peters et al. 2013). The oxidation products such as aldehydes, ketones or organic acids are released into the environment where they accumulate near-quantitatively, often acidifying the habitat and making it more hostile for competing organisms (Olijve & Kok, 1979, Deppenmeier et al. 2002). Periplasmic oxidation is linked to the respiratory chain by ubiquinone (Q_{10}), enabling transfer of electrons via terminal oxidases of the proton-pumping cytochrome bo_3- and the non-proton pumping cytochrome *bd*-type from ubiquinol to oxygen (Richhardt et al. 2013). Interestingly, while the genes encoding a cytochrome bc_1 complex and soluble cytochrome *c* were identified in the genome of *G. oxydans*, no gene encoding a cytochrome *c* oxidase was found. The electrochemical proton gradient across the cytoplasmic membrane drives ATP synthesis by two F_1F_O-type ATP synthases (Prust et al. 2005, Hanke et al. 2012). A metabolic flux analysis using ^{13}C-labeled glucose showed that from the initially provided substrate only a small percentage enters the cell and is either completely oxidized to CO_2 or utilized for anabolic reactions. For example 90% of the provided glucose is oxidized to gluconate and partially further to 2-ketogluconate in the periplasm and only 10% enters the cytoplasm. From these 10%, cytoplasmic enzymes oxidize 91% again to gluconate and merely 9% is phosphorylated to glucose-6-phosphate. A part of the gluconate is phosphorylated to 6-phosphogluconate which enters, like the glucose-6-phosphate, the central carbon metabolism (Hanke et al. 2013).

This inefficient use of substrate explains the low biomass yield of 0.09 $g_{cdw}/g_{glucose}$ for *G. oxydans* strain IFO3293 in comparison to *e.g. Escherichia coli* (0.49 $g_{cdw}/g_{glucose}$) and *Bacillus subtilis* (0.32 $g_{cdw}/g_{glucose}$) (Dauner et al. 2002, Soini et al. 2008, Krajewski et al. 2010, Richhardt et al. 2012).

Central carbon metabolism of *G. oxydans* is characterized by the absence of a complete Embden-Meyerhof-Parnas pathway and tricarboxylic acid cycle (TCA). A key enzyme of glycolysis, phosphofructokinase, as well as succinyl-CoA-synthetase and succinate DH of the TCA are missing, forcing *G. oxydans* to oxidize sugars intracellularly primarily via the pentose-phosphate pathway (PPP) and the Entner-Doudoroff-pathway (EDP) (Fig. 1). Furthermore, *G. oxydans* unlike other members of the *Acetobacteraceae* family is not capable to utilize acetate as a carbon source because the genes encoding the isocitrate lyase and malate synthase of the glyoxylate shunt and the acetate kinase as well as the phosphotransacetylase are missing (Prust et al. 2005, Bringer & Bott, 2016). Comparison of deletion mutants lacking key enzymes of the EDP or PPP revealed that the main route for sugars entering the cytoplasmic catabolism is the PPP while the EDP appeared to be dispensable (Richhardt et al. 2012). Furthermore, due to the lack of the phosphofructokinase, fructose-6-phosphate derived from the PPP is isomerized again to glucose-6-phosphate, which reenters the oxidative PPP leading to a cyclic carbon flux (Hanke et al. 2013). A non-proton-pumping NADH DH transfers electrons from EDP-derived NADH to the ubiquinone pool (Kersters & De Ley, 1968, Prust et al. 2005). Additionally, when required, a membrane-bound transhydrogenase transfer electrons from NADPH to NAD^+ or NADH to $NADP^+$. Oxidation of ubiquinol and transfer of respective electrons to oxygen is catalyzed by the above mentioned cytochrome bo_3- and cytochrome *bd*-type terminal oxidases. Experiments to complete the TCA cycle by replacing the genes encoding cytoplasmic and membrane-bound glucose DH as well as pyruvate decarboxylase with heterologous genes encoding succinate DH, succinyl synthetase and a second type II NADH DH, all taken from other *Acetobacteraceae*, increased the biomass yield by 60% (Kiefler et al. 2017). Furthermore, recent studies suggest that excessive periplasmic substrate oxidation causes intracellular insufficient oxidation of reducing equivalents due to oxygen limitation leading to increased expression of the transhydrogenase and an alcohol DH. These enzymes enable the regeneration of $NAD(P)^+$ by transferring electrons from NADPH to NAD^+ and further to acetaldehyde derived from pyruvate decarboxylation to form ethanol. GoxR, the only representative of the fumarate-nitrate reduction regulator (FNR) family in *G. oxydans*, regulates this adaptation (Schweikert et al. 2021).

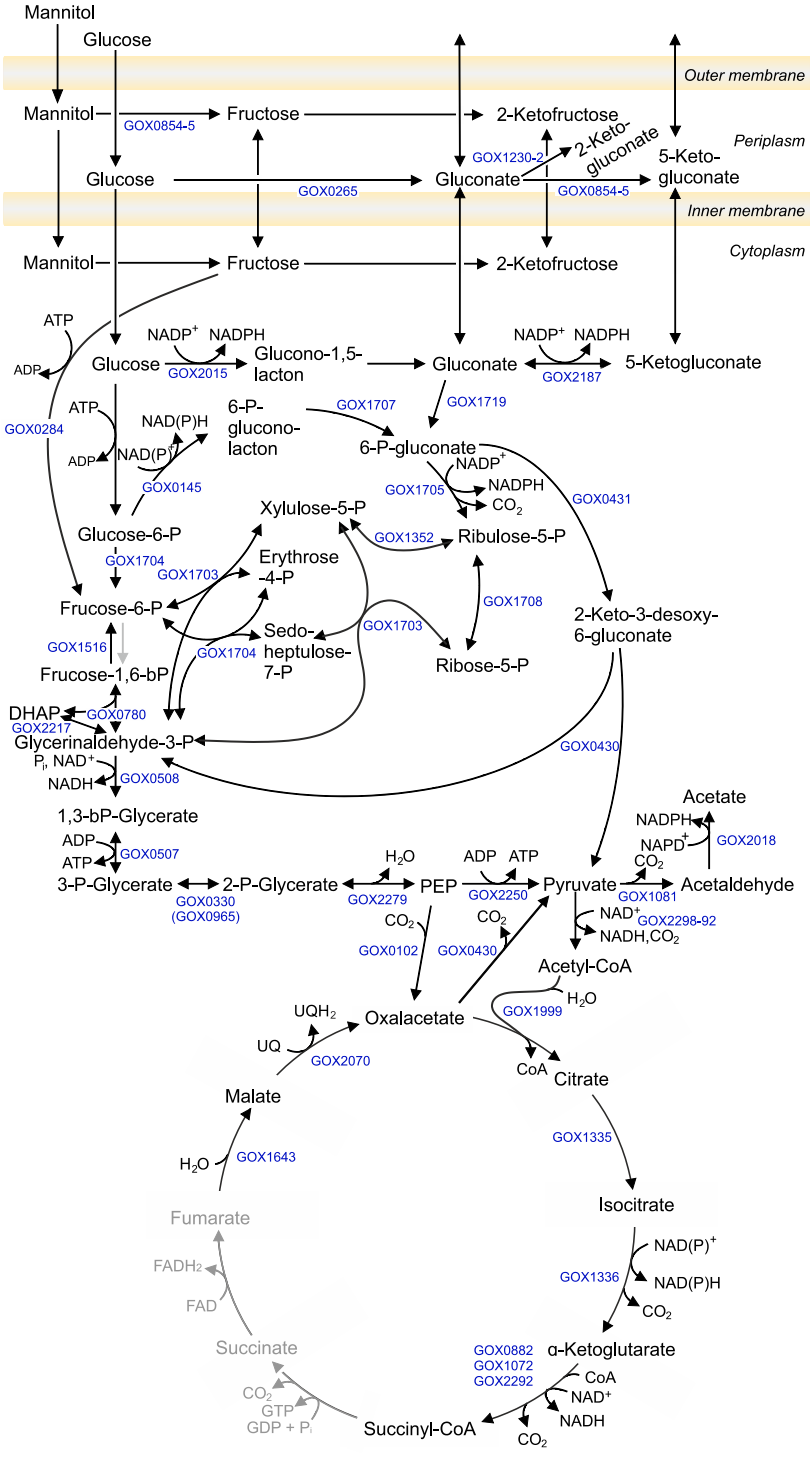

Fig. 1 Scheme of central carbon metabolism of *G. oxydans* with the substrates glucose and mannitol. Grey marked reactions are missing in *G. oxydans* 621H. Modified from Richhardt et al. (2013) and Kiefler (2016).

1.2 Expression and promoter systems

For basic research as well as biotechnological applications, it is often beneficial to fine-tune the expression of target genes for controlled protein production. Using tools that permit a regulation of gene expression supports objectives that range from low levels of expression for the adjustment of metabolic pathways to high-level protein synthesis at industrial scales (Brautaset et al. 2009). Furthermore, characterization of enzymes in regard to their substrates, products and mode of action benefits from overexpression of the corresponding genes to obtain large quantities of the proteins. While maximal protein synthesis is desired, overexpression may cause insoluble inclusion bodies containing aberrantly folded, inactive proteins. Therefore, protein overproduction often benefits from regulatable systems that enable controlled expression of target genes to achieve maximal target protein titers and avoid loss of protein due to inclusion bodies. Also transmembrane, periplasmic or secreted proteins may require gene expression to be carefully tuned to adjust it to the capacity of the translocation apparatus (Rosenberg, 1998, Mergulhão & Monteiro, 2004). Similarly, for the expression of genes whose products are toxic for the host, it is advisable to apply an expression system that allows tight control and fine-tuning of transcription. Moreover, metabolic burden caused by the synthesis of proteins that are not constantly needed can be circumvented when gene expression only starts at a desired time point, *e.g.* it can be beneficial to first acquire high cell titers in a fermentation process before the production phase is initiated (Saïda et al. 2006, Terpe, 2006).

Expression of a gene or operon is initiated from a DNA sequence called promoter that is located upstream from the corresponding gene/operon. Promoter recognition by the RNA polymerase (RNAP) holoenzyme (RNAP + σ factor) and the initiation of transcription is the most frequently regulated step that modulates gene expression (Browning & Busby, 2004, Haugen et al. 2008). A promoter is characterized by a number of core elements that are recognized by the RNAP holoenzyme including:

I) upstream (UP) element (–37 to –58), recognized by a C-terminal domain of the α-subunits of the RNAP holoenzyme ($\alpha_2\beta\beta'\omega\sigma$)
II) –35 element (–35 to –30), recognized by domain 4 of the σ factor
III) extended –10 element (–17 to –14), recognized by domain 3 of the σ factor
IV) –10 element (–12 to –7), recognized by domain 2 of the σ factor
V) discrimination region (–6 to –4), recognized by domain 1 of the σ factor
VI) transcription start site (TSS, designated as +1), first nucleotide of the transcript

Additionally, on the promoter or in close proximity of it there can be specific operator sequence motifs that are recognized and bound by transcription factors (TFs). Depending on the presence or absence of these operator sites and TFs, the respective gene downstream of the promoter is either constantly (constitutively) transcribed or transcription initiation requires a

change in TF-DNA binding caused by a conformational change of the TF due to a specific stimulus. The DNA-binding domain of bacterial TFs, often consisting of a helix-turn-helix motif, recognizes a specific 4-5 base pair (bp) DNA motif on the operator site. Given that such a motif occurs statistically every 4^5 bp, homodimerization or homooligomerization of TF proteins in combination with direct or inverted repeats within the operator is required to achieve regulatory specificity (Browning & Busby, 2016). TFs can be distinguished by their mode of regulation in repressors and activators. Repressors bind operator sites that often overlap with core promoter elements, thereby sterically hindering RNAP holoenzyme to interact with the promoter and initiate transcription. Alternatively, when a repressor multimer simultaneously binds sites located up- and downstream from the promotor, transcription may be repressed by DNA looping, which makes the core elements inaccessible for RNAP (Browning & Busby, 2004, Semsey et al. 2004, Swint-Kruse & Matthews, 2009). Activators usually assist RNAP holoenzyme in promoter binding through protein-protein interaction, thereby increasing transcription activity from the respective promoter. Activator binding sites are often located upstream from core elements, allowing activator interaction with the C-terminal domain of the α-subunits of the RNAP. Other activators bind sites slightly overlap with the –35 element and thereby assist the recruitment of the σ factor (Lee et al. 2012). Thirdly, activators may bind sites located in between the –10 and –35 elements. In these cases, the activated activator alters the non-optimal spacing between –10 and –35 regions to a spacing that enables binding of the RNA polymerase (Brown et al. 2003, Philips et al. 2015).

1.2.1 Constitutive expression systems in *G. oxydans*

The first expression plasmids for *Gluconobacter* were reported in 1985 (Fukaya et al. 1985). Since then until the start of this thesis, 64 publications reported the construction of expression plasmids with the goal to express a specific gene (reviewed by Fricke et al. 2021a). From these expression plasmids, the pBBR1MCS derivatives based on the very small plasmid from *Bordetella bronchiseptica* were used most often and are considered as the major expression plasmid lineage in *Gluconobacter* (Fig. 2) (Antoine & Locht, 1992, Fricke et al. 2021a).

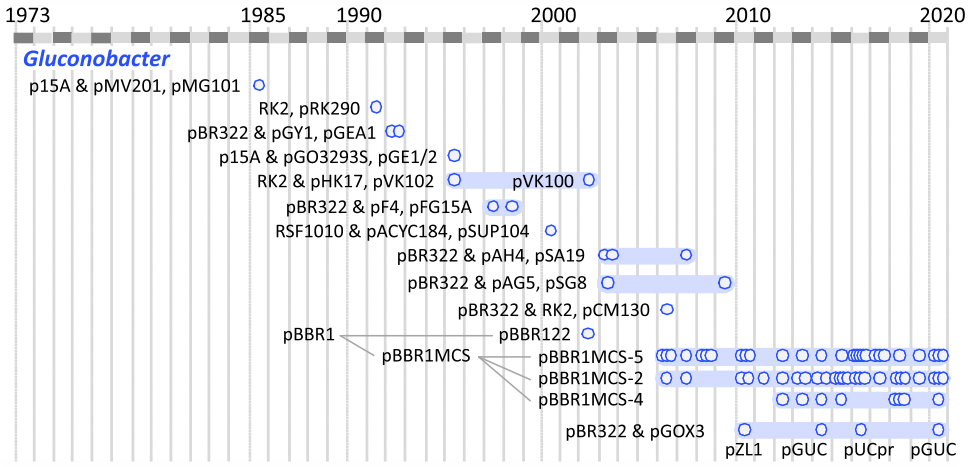

Fig. 2 Time plot illustrating major lineages and diversity of expression plasmids and their origins of replication hitherto used in the AAB genus *Gluconobacter* according to the publications (o) in the WoSCC database. Modified from Fricke et al. (2021a).

In earlier works strong promoters from *E. coli* and phage λ, such as P_{tufB}, P_L, P_{tac} and P_{lac}, were applied for various purposes in *G. oxydans*. All these heterologous promoters were used for constitutive gene expression with *E. coli* P_{tufB}, exhibiting the strongest expression in *G. oxydans* (Saito et al. 1997, Tonouchi et al. 2003). Later works focused on native *G. oxydans* promoters enabling stronger expression than previously obtained with heterologous pomoters. For example, promoter P_{tufB} derived from the elongation factor TU gene from the *G. oxydans* strains 621H and H24 and P_{gdh} from the glucose DH gene led to higher target gene expression than *E. coli* P_{tufB} (Merfort et al. 2006, Zhang et al. 2010, Hu et al. 2015). The variety of expression with different strength was increased when the promoters $P_{GOX0384}$, $P_{GOX0452}$ and $P_{GOX0264}$ of the ribosomal protein S12, L13 and L35 genes were classified as weak, moderate and strong (Kallnik et al. 2010, Kallnik, 2012). Since then these promoters have been frequently used in multiple applications (Meyer et al. 2013, Kosciow et al. 2014, Kiefler et al. 2015, Kosciow et al. 2016, Kiefler et al. 2017, Herweg et al. 2018, Siemen et al. 2018, Blank & Schweiger, 2018, Hoffmann et al. 2020, Battling et al. 2020). In search of strong promoters, $P_{GOX0169}$ controlling expression of GOX0169 encoding a hypothetical transmembrane protein was identified and compared to $P_{GOX0264}$, $P_{GOX0452}$ and P_{tufB} (*G. oxydans* 621H) by means of expressing a gene for a fluorescent reporter protein. According to biomass-specific fluorescence, the strength of these promoters decreased in the order $P_{GOX0169}$, $P_{GOX0264}$, P_{tufB} (*G. oxydans* 621H), and P_{0452} (Shi et al. 2014, Yuan et al. 2016).

1.2.2 Regulatable expression in *G. oxydans* and other acetic acid bacteria

When this thesis started, only very few studies reported attempts to implement a regulatable expression system in *G. oxydans* or other AAB. To establish a functional

heterologous inducible expression system, besides the inducible promoter, the gene encoding the respective regulator needs to be expressed from the expression plasmid or the genome of the host. First experiments trying to control gene expression using *E. coli* P_{lac} in *G. oxydans* showed very low gene (*lacZ*) expression when induced with IPTG in comparison to *E. coli*. Additonally, repression of P_{lac} by LacI seemed to be impaired, leading to high leakiness in the absence of an inducer (Condon et al.1991, Kallnik et al. 2010). Similar results were obtained for the AAB *Komagataeibacter xylinus* using the fluorescent protein mRFP as reporter. Also in this case high basal expression levels under non-induced conditions and low induction fold changes were reported (Liu et al. 2020). In *Komagataeibacter rhaeticus* iGEM, induction of gene expression was tested with the TetR-P_{tet} and LuxR-P_{lux} systems using the same reporter as for *K. xylinus*. Due to the high leakiness of non-induced P_{tet}, very low (~1.5-fold) induction ratios were reported. Furthermore, *N*-acyl homoserine-lactone (AHL)-induced expression from P_{lux} was very strong, but due to high basal expression also exhibited low induction ratios (3−5-fold). *K. rhaeticus* iGEM naturally produces and secretes cellulose, which forms interconnected pellicles around the cell. Interestingly, higher induced *mRFP* expression and lower leakiness was observed when inducibility of the LuxR-P_{lux} system was tested with cells encased in cellulose pellicles (Florea et al. 2016). Furthermore, controlled gene expression with the LuxR-P_{lux} and AraC-P_{araBAD} system was investigated in the AAB *K. xylinus*, *K. rhaeticus* iGEM, and *Gluconacetobacter hansenii*. For all three strains, with the LuxR-P_{lux} regulator-promoter pair fluorescence intensities increased 26−36-fold upon AHL-supplementation. Similar to the TetR-P_{tet} and LacI-P_{lac} systems, P_{araBAD} suffered from leaky expression in the absence of inducer, resulting in low induction ratios (5−11-fold) (Teh et al. 2019). In summary, only few regulatable expression systems with low to moderate induction ratios were successfully established for AAB when this PhD thesis was started.

1.2.3 The LacI-P_{lac} system from *Escherichia coli*

The *lac* operon from *E. coli* and the inducibility of its transcription from P_{lac} has been studied intensively for more than 60 years (Jacob & Monod, 1961). It enables the bacterium to sense lactose and rapidly adapt its metabolism towards the utilization of the disaccharide. The LacI-P_{lacI} system is schematically illustrated in Figure 3a. The *lac* operon consists of three structural genes, *lacZ*, *lacY* and *lacA* encoding a β-galactosidase, a lactose permease and transacetylase, respectively. LacZ cleaves lactose, consisting of galactose and glucose linked by a β-1,4 O-glycosidic bond, into the monosaccharides for further metabolization; LacY is a secondary transporter for the uptake of lactose using the proton gradient across the cytoplasmic membrane as driving force; LacA catalyzes the transfers of an acetyl group from acetyl coenzyme A to the 6-hydroxyl group of the galactosides. Upstream of P_{lac} and in the same orientation as the operon, *lacI* encoding the repressor LacI is expressed constitutively

from P_{lacI}. Repression of the operon is mediated by LacI that binds three different operator sites within the promoter region (*O1*, *O2*, *O3*). *O1* is centered around +11, partially overlapping with the TSS, while *O2* and *O3* are located 401 bp downstream and 92 bp upstream from *O1* overlapping with the *lacZ* and *lacI* coding regions, respectively (Reznikoff, 1992, Müller-Hill, 1998). Besides the cleavage of the disaccharide, LacZ isomerizes lactose to allolactose (β-1,6 linkage), which is bound by LacI and initiates a conformational change of the repressor that causes its release from the DNA and allows initiation of transcription. As an analogon of allolactose, isopropyl β-D-1-thiogalactopyranoside (IPTG) can also induce P_{lac}-derived gene expression. Furthermore, because in contrast to allolactose IPTG is not metabolized by the cells, inducer concentrations do not decrease during cultivations (Jacob & Monod, 1961, Hansen et al. 1998, reviewed by Santillán & Mackey, 2008). The LacI tetramer is composed of two functional homodimers that can each bind one operator site. Thus, one tetramer can bind two operator sites simultaneously (Kania & Brown, 1976). For repression, binding to the *O1* site is required as binding of *O2* or *O3* alone has close to no effect on expression of the *lac* operon in *E. coli*. LacI bound only to *O1* reduces expression 18-fold, while *O1* and *O2* or *O1* and *O3* bound cooperatively decreases expression 700- and 440-fold, respectively, and overall increases stability of DNA binding by LacI. With all three operator sites bound by LacI, a repression level of 1300-fold can be reached. This strong cooperative effect in repression is partly caused by DNA looping mediated by the LacI tetramer (Oehler et al. 1990). Besides LacI repression, the *lac* operon is regulated by catabolite repression. Controlled by the glucose-specific phosphoenolpyruvate:carbohydrate phosphotransferase system (PTS), the intracellular cyclic adenosine monophosphate (cAMP) concentration increases when extracellular glucose becomes scarce. cAMP binding by the cAMP receptor protein (CRP), also known as CAP (catabolite activator protein), initiates a conformational change that enables the protein to bind a CRP-binding motif located upstream from P_{lac}. By doing so, CRP-cAMP interacts with the α-subunit of the RNAP, thereby assisting transcription initiation from the promoter (Reznikoff, 1992). In *G. oxydans*, EII^B and EII^C of the PTS are missing and the function of EI, HPr, EII^A, and HPr kinase is unclear (Prust et al. 2005).

The promoter P_{lacUV5} used in this work differs from wild-type P_{lac} by two point mutation in the –10 element, making the promoter independent of activator proteins and increasing its efficiency of RNAP recruitment (Silverstone et al. 1970, Studier & Moffatt, 1986, Noel & Reznikoff, 2000). In *G. oxydans,* it is not very likely that other catabolites interfere with gene regulation from P_{lac} through CRP, as the only member the CRP/FNR superfamily of transcriptional regulators, GoxR, belongs to the FNR and not the CRP protein family (Prust et al. 2005, Schweikert et al. 2021).

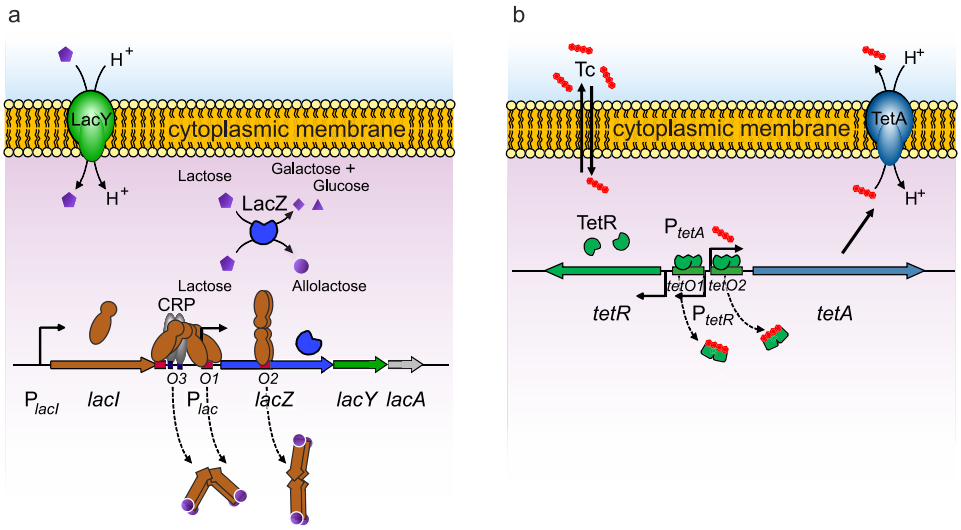

Fig. 3 Schematic illustration of the regulatory mechanisms of the regulator-promoter pairs LacI-P_{lac} (**a**) from *E. coli* and TetR-P_{tet} from transposon Tn*10* (**b**). Repression of P_{lac} is abolished when allolactose derived from isomerization of lactose by LacZ interacts with the repressor LacI. For de-repression of P_{tet} by TetR, tetracycline (Tc) (or its less toxic analogon anhydrotetracycline) needs to interact with TetR, thereby enabling *tetA* expression and efflux of Tc. TetR-P_{tet} mechanism modified from Grkovic et al. (2002).

1.2.4 The TetR-P_{tet} system from *Escherichia coli* transposon Tn*10*

The TetR-P_{tet} system conveys the resistance towards the antibiotic tetracycline. Although known from many different bacteria, TetR-P_{tet} from transposon Tn*10* has been best characterized (Grkovic et al. 2002). Since even low expression of *tetA* encoding a proton-dependent antiporter for the antibiotic is disadvantageous for bacteria in the absence of tetracycline, a highly sensitive inducible expression system evolved for *tetA* (McMurry et al. 1980, Nguyen et al. 1989). Tetracycline diffuses across the membrane and binds as a complex with Mg^{2+} the repressor TetR, causing the protein to release its operator sites within the *tetA* promoter P_{tet}, thereby rapidly inducing *tetA* expression (Fig. 3b). Two operator sites ($tetO_1$ and $tetO_2$) are located 11 bp apart from one another with $tetO_1$ covering 19 bp between the –10 and –35 regions and $tetO_2$ overlapping with the TSS of *tetA*. Facing the opposite direction, two promoters that overlap with P_{tet} negatively autoregulate expression of *tetR* (reviewed by Bertram & Hillen, 2008). TetR dimers bind both operators noncooperatively leading in case of $tetO_1$ to the inhibition of both, *tetA* and *tetR* expression. TetR occupying $tetO_2$ primarily downregulates expression of *tetA* for the reason that one of the two *tetR* promoters remains almost completely active (Meier et al.1988). Both operator sites vary in their sequence resulting in a higher affinity of TetR for $tetO_2$ ensuring that no excessive amount of TetA is synthesized (Kleinschmidt et al. 1991). The often-used analogon of tetracycline, anhydrotetracycline, binds

TetR approximately 35-fold stronger while exhibiting a reduced antibiotic activity (Fig. 3b) (Degenkolb et al. 1991, Oliva et al. 1992, Terpe, 2006).

1.2.5 The AraC-P_{araBAD} system from *Escherichia coli*

Different from P_{lac} and P_{tet}, transcription of the *araBAD* operon from the promoter P_{araBAD} is regulated by a TF (AraC) that is involved in both repression and activation of gene expression (Dunn & Schleif, 1984, Hahn et al. 1984, Guzman et al. 1995). The *E. coli* operon *araBAD* encodes enzymes necessary for the conversion of the five-carbon sugar L-arabinose that can be found as a constituent of some plant cell walls to D-xylulose-5-phosphate, which enters the PPP (Gross & Englesberg, 1959). In *E. coli* efficient transcription of *araBAD* only takes place when L-arabinose is present and the concentration of the preferred carbon source glucose is low, as expression from the promoter is also activated by CRP-cAMP the same way as previously described for P_{lac}. In the absence of the P_{araBAD}-inducer L-arabinose, a dimer of AraC binds two promoter sites called I_1 and O_2, thereby looping the intervening 194 bp of DNA and repressing transcription from P_{araBAD}. Binding of L-arabinose to AraC causes a conformational change with the consequence that one subunit releases the distal O_2 site and instead binds the I_2 site that is located in close proximity of I_1. By doing so, AraC assists RNAP in promoter binding and stimulates the transition from the closed to the open RNAP-DNA complex necessary for transcription (Fig. 4a) (reviewed by Schleif, 2010). Besides controlling P_{araBAD}-derived expression, AraC also negatively autoregulates its own expression from the divergently orientated promoter P_C through binding of the O_1 site that is overlapping with core elements of P_C (Hahn & Schleif, 1983, Harmer et al. 2001). In *E. coli* L-arabinose enters the cell via two transport systems, the low-affinity, high capacity proton-symporter AraE and the high-affinity, low capacity ABC transporter AraFGH. Expression of both transport systems is also controlled by the AraC-L-arabinose complex (Kolodrubetz & Schleif, 1981, Horazdovsky & Hogg, 1989). AraC-P_{araBAD} is frequently applied for heterologous inducible expression as it combines high level of target gene expression with tight regulation of protein synthesis using the inexpensive inducer L-arabinose (Terpe, 2006).

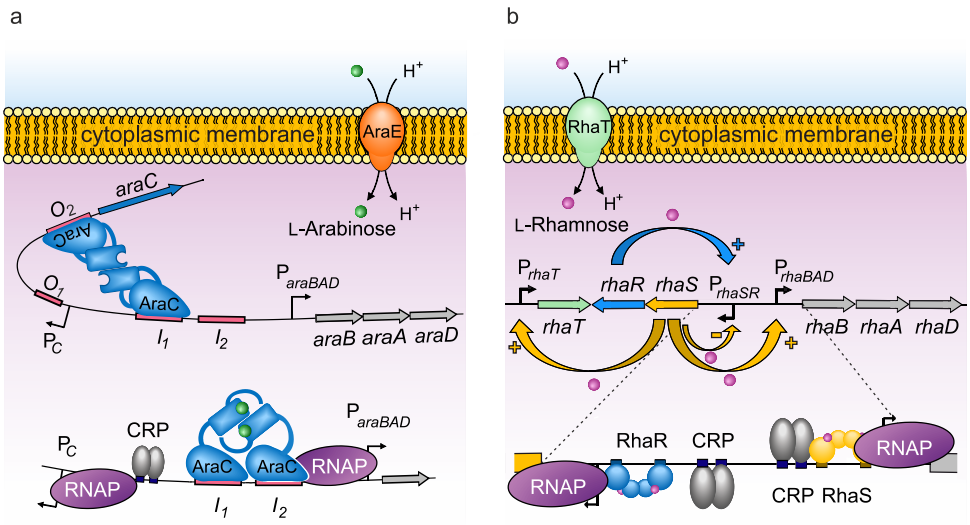

Fig. 4 Schematic illustration of the regulatory mechanisms of the *E. coli* regulator-promoter pairs AraC-P_{araBAD} (**a**) and RhaSR-P_{rhaBAD} (**b**). The regulator AraC represses transcription from P_{araBAD} in the absence of L-arabinose through DNA looping and activates transcription when bound to L-arabinose. From the two regulators RhaS and RhaR, only RhaS activates transcription from P_{rhaBAD} and P_{rhaT} in the presence of L-rhamnose. Bound to L-rhamnose, RhaR increases expression of the *rhaSR* operon. Modified from Schleif (2010) and Egan & Schleif (1993).

1.2.6 The RhaSR-P_{rhaBAD} system from *Escherichia coli*

The regulator-promoter system RhaSR-P_{rhaBAD} exhibits many similarities to AraC-P_{araBAD}. Based on the utilization of L-rhamnose, the *E. coli rhaBAD* operon encoding enzymes required for the degradation of the sugar in the rather uncommon L-conformation is induced when L-rhamnose is present und glucose concentrations are low. Unlike all other expression systems discussed before, P_{rhaBAD} involves two regulators, RhaR and RhaS, both belonging to the AraC/XylS family of regulators. The genes *rhaR* and *rhaS* are transcribed as polycistronic mRNA from the promoter P_{rhaSR} and are located adjacent to P_{rhaBAD} in divergent orientation (Fig. 4b). In the presence of L-rhamnose, a homodimer of RhaR activates transcription from P_{rhaSR}, increasing its own and *rhaS* expression. Dimeric RhaS in turn induces transcription from P_{rhaBAD} once L-rhamnose is bound (Power, 1967, Tobin & Schleif, 1987, Egan & Schleif, 1993). Interestingly, binding of L-rhamnose effects RhaR and RhaS differently. While RhaR cannot effectively recruit RNAP for transcription without L-rhamnose, DNA binding of RhaS is hampered in the absence of the inducer (Kolin et al. 2008). Besides P_{rhaBAD}, expression from the promoter P_{rhaT} with *rhaT* encoding a L-rhamnose-proton symporter in the cytoplasmic membrane is activated by RhaS (Vía et al. 1996). All RhaS and RhaR binding sites consist of two half-sites of 17 bp. For RhaS, two half-sites are located within P_{rhaBAD} (*rhaI1* and *rhaI2*) and

two within P_{rhaT} (*rhaI5* and *rhaI6*). The two RhaR half-sites within P_{rhaSR} are termed *rhaI3* and *rhaI4*. In *E. coli* expression from P_{rhaBAD}, P_{rhaT} and P_{rhaSR} is also activated by CRP-cAMP when glucose concentrations are low (Egan & Schleif, 1993, Vía et al. 1996, Holcroft & Egan, 2000).

1.3 Aims of this thesis

G. oxydans has been used since the 1930s for various industrial applications due to its exceptional ability to incompletely oxidize carbohydrates in the periplasm. In spite of this long-standing experience, applications requiring target gene expression made only use of promoters conveying constitutive gene expression. All attempts in *G. oxydans* or other AAB to control gene expression in an inducer-dependent manner suffered from high basal expression under non-induced conditions and thus relative low fold-changes upon induction. Synthesis of desired enzymes for industrial applications at a defined time point as well as for basic research and metabolic engineering approaches including tight control of metabolic pathways could benefit from regulatable expression systems. This work aimed to establish regulatable expression systems for *G. oxydans* 621H. For that purpose, well-known regulatable expression systems from *E. coli* such as the AraC-P_{araBAD}, TetR-P_{tet}, LacI-P_{lac} and RhaSR-P_{rhaBAD} systems should be tested in *G. oxydans.* By means of expressing different reporter genes, the performance of these heterologous regulator-promoter pairs should be studied using pBBR1MCS-based plasmids and in selected cases also with genomically integrated expression systems. Another aim was the identification of endogenous *G. oxydans* promoters that respond to stimulating effector molecules by altering the expression of the corresponding target gene upon supplementation. Once such promoters and their respective regulators have been identified, they would not only expand the scarce knowledge of regulatory networks in *G. oxydans*, but could also allow regulation of target gene expression in a *G. oxydans* strain that is not classified as a genetically modified organism (GMO).

2 Results:

2.1 A tunable L-arabinose-inducible expression plasmid for the acetic acid bacterium *Gluconobacter oxydans*

Fricke, P. M., Link, T., Gätgens, J., Sonntag, C., Otto, M., Bott, M., & Polen, T. (2020). A tunable L-arabinose-inducible expression plasmid for the acetic acid bacterium *Gluconobacter oxydans*. **Applied Microbiology and Biotechnology 104:9267–9282.**

doi:10.1007/s00253-020–10905-4

Author's contributions:
PMF and TL selected the reporters and constructed the plasmids. PMF carried out all growth experiments to test strains with and without plasmids and performed the data analysis. JG performed the GC-TOF-MS experiments and analyzed the data. PMF and CS performed the FACS analysis and analyzed the data. PMF and MO performed the DASbox cultivations. TP designed and supervised the study. PMF, MB, and TP wrote the manuscript. All authors read and approved the final manuscript.

Overall contribution PF: 75%

Applied Microbiology and Biotechnology
https://doi.org/10.1007/s00253-020-10905-4

APPLIED GENETICS AND MOLECULAR BIOTECHNOLOGY

A tunable L-arabinose-inducible expression plasmid for the acetic acid bacterium *Gluconobacter oxydans*

Philipp Moritz Fricke[1] · Tobias Link[1] · Jochem Gätgens[1] · Christiane Sonntag[1] · Maike Otto[1] · Michael Bott[1] · Tino Polen[1]

Received: 1 August 2020 / Revised: 4 September 2020 / Accepted: 10 September 2020

Abstract

The acetic acid bacterium (AAB) *Gluconobacter oxydans* incompletely oxidizes a wide variety of carbohydrates and is therefore used industrially for oxidative biotransformations. For *G. oxydans*, no system was available that allows regulatable plasmid-based expression. We found that the L-arabinose-inducible P_{BAD} promoter and the transcriptional regulator AraC from *Escherichia coli* MC4100 performed very well in *G. oxydans*. The respective pBBR1-based plasmids showed very low basal expression of the reporters β-glucuronidase and mNeonGreen, up to 480-fold induction with 1% L-arabinose, and tunability from 0.1 to 1% L-arabinose. In *G. oxydans* 621H, L-arabinose was oxidized by the membrane-bound glucose dehydrogenase, which is absent in the multi-deletion strain BP.6. Nevertheless, AraC-P_{BAD} performed similar in both strains in the exponential phase, indicating that a gene knockout is not required for application of AraC-P_{BAD} in wild-type *G. oxydans* strains. However, the oxidation product arabinonic acid strongly contributed to the acidification of the growth medium in 621H cultures during the stationary phase, which resulted in drastically decreased reporter activities in 621H (pH 3.3) but not in BP.6 cultures (pH 4.4). These activities could be strongly increased quickly solely by incubating stationary cells in D-mannitol-free medium adjusted to pH 6, indicating that the reporters were hardly degraded yet rather became inactive. In a pH-controlled bioreactor, these reporter activities remained high in the stationary phase (pH 6). Finally, we created a multiple cloning vector with *araC*-P_{BAD} based on pBBR1MCS-5. Together, we demonstrated superior functionality and good tunability of an AraC-P_{BAD} system in *G. oxydans* that could possibly also be used in other AAB.

Key points

- *We found the AraC-P_{BAD} system from E. coli MC4100 was well tunable in G. oxydans.*
- *In the absence of AraC or L-arabinose, expression from P_{BAD} was extremely low.*
- *This araC-P_{BAD} system could also be fully functional in other acetic acid bacteria.*

Keywords AraC · P_{BAD} promoter · Induction · mNeonGreen · β-D-Glucuronidase UidA · Membrane-bound dehydrogenase

Electronic supplementary material The online version of this article (https://doi.org/10.1007/s00253-020-10905-4) contains supplementary material, which is available to authorized users.

✉ Tino Polen
t.polen@fz-juelich.de

Philipp Moritz Fricke
p.fricke@fz-juelich.de

Tobias Link
tobias.link@tum.de

Jochem Gätgens
j.gaetgens@fz-juelich.de

Christiane Sonntag
c.sonntag@fz-juelich.de

Maike Otto
maike.otto@bsse.ethz.ch

Michael Bott
m.bott@fz-juelich.de

[1] IBG-1: Biotechnology, Institute of Bio- and Geosciences, Forschungszentrum Jülich GmbH, 52425 Jülich, Germany

Published online: 25 September 2020

Introduction

Controlled expression of target genes to produce proteins for various purposes in a bacterial cell culture at a defined time point is often beneficial or even required in basic research and in biotechnological applications. For inducible expression, various plasmids have been developed and established in many bacteria including *Escherichia coli*, *Pseudomonas* sp., *Ralstonia* sp., *Bacillus* sp., *Lactoccocus* sp., *Streptomyces* sp., mycobacteria, corynebacteria, halophilic bacteria, and others (reviewed in, for example, Chen 2012; Connell 2001; Dilworth et al. 2018; Evans and Mizrahi 2015; Forstner et al. 2007; Gruber et al. 2015; Parachin et al. 2012; Schnappinger and Ehrt 2014; Terpe 2006; Valero 2012). Prominent classical examples are the well-known LacI-, TetR-, and AraC-dependent systems (as well as optimized or modified versions thereof) for inducible expression by addition of the respective inducer. For acetic acid bacteria (AAB), including the most frequently used and studied genera *Acetobacter*, *Gluconobacter*, *Gluconacetobacter*, *Komagataeibacter*, and *Acidiphilium*, a low-cost, tight, and strongly inducible expression system has not been reported yet in the literature to the best of our knowledge. Apparently, for the heterologous systems, leakiness is a major issue responsible for the relatively low induction ratios (induced/non-induced) in AAB. In *Komagataeibacter rhaeticus* iGEM, the TetR-dependent system from transposon Tn*10* with the inducible promoter P_{tet} exhibited approximately only 1.5-fold induction due to high leakiness in the absence of the inducer anhydrotetracycline (Florea et al. 2016). The native L-arabinose-inducible AraC-dependent P_{BAD} system from *E. coli* exhibited approximately only 5- to 12-fold induction in *Gluconacetobacter xylinus* ATCC 700178, *Gluconacetobacter hansenii* ATCC 53582, and *Komagataeibacter rhaeticus* iGEM due to high basal expression and required a high concentration (4%, *w*/*v*) of the inducer L-arabinose (Teh et al. 2019). The performance of IPTG-inducible *Lac*I-dependent expression has not been reported yet for AAB according to the literature.

The AAB *G. oxydans* is industrially used for oxidative biotransformations of carbohydrates to produce, e.g., L-sorbose, a precursor in vitamin C production, dihydroxyacetone, a substance used for tanning lotions, or 6-amino-L-sorbose, a precursor of the antidiabetic drug miglitol (Ameyama et al. 1981; Gupta et al. 2001; Hekmat et al. 2003; Saito et al. 1997; Tkac et al. 2001; Wang et al. 2016). The beneficial ability of *G. oxydans* is the regio- and stereoselective incomplete oxidation of a variety of substrates (e.g., sugars and sugar alcohols) in the periplasm by membrane-bound dehydrogenases (mDHs) and release of resulting products into the cultivation medium (Mamlouk and Gullo 2013; Mientus et al. 2017; Pappenberger and Hohmann 2014). For the fully functional expression of mDHs in *G. oxydans*, the promoters of the alcohol dehydrogenase ($P_{GOX1067\text{-}68}$) and the inositol dehydrogenase ($P_{GOX1857}$) have been used in shuttle vectors (Mientus et al. 2017). While $P_{GOX1857}$ is repressed in the presence of glucose (Hölscher et al. 2007), $P_{GOX1067\text{-}68}$ showed constitutive activity with good expression (Mientus et al. 2017). Other *G. oxydans* promoters classified as strong, moderate, and weak are the constitutive promoters $P_{GOX0264}$, $P_{GOX0452}$, and $P_{GOX0384}$ from genes encoding ribosomal proteins (Kallnik et al. 2010). Expression from moderate $P_{GOX0452}$ has been used to successfully produce membrane-bound PQQ-dependent glucose dehydrogenase (GOX0265) for purification and characterization (Meyer et al. 2013). Expression from weak $P_{GOX0384}$ has been used to successfully produce the succinate dehydrogenase from *Acetobacter pasteurianus* in *G. oxydans* as a first step toward a complete tricarboxylic acid cycle (Kiefler et al. 2015). In earlier work with *G. oxydans*, constitutive P_{tufB} from *G. oxydans* and from *E. coli* as well as P_{lac} from *E. coli* have been used (Merfort et al. 2006a, b; Schleyer et al. 2008; Tonouchi et al. 2003; Zhang et al. 2010). Since there is no Lac repressor homolog in *G. oxydans*, also P_{lac} is constitutive in *G. oxydans*. Together, the resulting expression plasmids with all these promoters do not allow for gradually induced expression of target genes at a desired time.

Therefore, to provide for *G. oxydans* a tight and strongly inducible plasmid, we tested AraC-P_{BAD} from the *E. coli* K12 derivative MC4100 in a pBBR1-based vector. The plasmids constructed in this study exhibited very low basal reporter gene expression and L-arabinose-dependent induction ratios up to 480-fold. GC-TOF-MS analysis confirmed oxidation of the inducer L-arabinose to L-arabinonic acid contributing to the acidification of the growth medium in shake flasks. This additional acidification turned out to be critical for the activity of intracellular reporter proteins in the stationary phase and could be eliminated by mDH deletion or pH-controlled conditions.

Materials and methods

Bacterial strains, plasmids, and culture conditions

Strains and plasmids used or created in this study are listed in Table 1. *G. oxydans* strains were routinely cultivated at 30 °C and 180 rpm in D-mannitol medium containing 4% (*w*/*v*) D-mannitol, 5 g L^{-1} yeast extract, 1 g L^{-1} KH_2PO_4, 1 g L^{-1} $(NH_4)_2SO_4$, and 2.5 g L^{-1} $MgSO_4 \times 7H_2O$ and supplemented with 50 μg mL^{-1} cefoxitin. Unless stated otherwise, for shake flask cultivations, 50 mL of D-mannitol medium in 500 mL shaking flasks with three baffles was inoculated from overnight starter cultures to an initial optical density at 600 nm (OD_{600}) of 0.3 (UV-1800, Shimadzu). If required for induction tests, L-arabinonic acid was supplemented as Li^+ salt

Table 1 Strains and plasmids used or constructed in this study

	Relevant characteristics	Reference/source
Strain		
E. coli DH5α	*supE*44, Δ*lacU*169 (Φ80*lacZ*ΔM15), *hsdR*17 (r_K^- m_K^+), *recA1*, *endA1*, *gyrA96*, *thi-1*, *relA1*	Hanahan (1983)
E. coli S17-1	Δ*recA*, *endA1*, *hsdR17*, *supE44*, *thi*-1, *tra*$^+$	Simon et al. (1983)
G. oxydans 621H	DSM 2343	DSMZ
G. oxydans BP.6	621H derivative carrying Δ*upp* and gene deletions for six mDHs	Peters et al. (2013)
Plasmid		
pBAD/Myc-His A	Vector for dose-dependent expression of recombinant proteins containing a 6×His tag in *E. coli*	Invitrogen
pBBR1MCS-2	Derivative of pBBR1MCS; Km^R	Kovach et al. (1995)
pBBR1MCS-2-*araC*-P_{BAD}-*uidA*	Derivative of pBBR1MCS-2 carrying reporter gene *uidA* controlled by L-arabinose-induced promoter P_{BAD} and *araC* encoding P_{BAD} regulator AraC	This work
pBBR1MCS-2-*araC*-P_{BAD}-*mNG*	Derivative of pBBR1MCS-2-*araC*-P_{BAD}-*uidA* using reporter gene *mNG* instead of *uidA*	This work
pBBR1MCS-2-$P_{GOX0264}$-*mNG*	Derivative of pBBR1MCS-2 carrying reporter gene *mNG* controlled by the strong constitutive promoter of GOX0264	This work
pBBR1MCS-5	Derivative of pBBR1MCS; Gm^R	Kovach et al. (1995)
pBBR1MCS-5-*araC*-P_{BAD}-*uidA*	Derivative of pBBR1MCS-5 carrying reporter gene *uidA* controlled by L-arabinose-induced promoter P_{BAD} and *araC* encoding P_{BAD} regulator AraC	This work
pBBR1MCS-5-*araC*-P_{BAD}-*mNG*	Derivative of pBBR1MCS-5-*araC*-P_{BAD}-*uidA* using reporter gene *mNG* instead of *uidA*	This work
pBBR1MCS-5-P_{BAD}-*mNG*	Derivative of pBBR1MCS-5-*araC*-P_{BAD}-*mNG*, lacking the regulator gene *araC* and carrying the terminator of *gdhM* (GOX0265) upstream of P_{BAD}	This work
pBBR1MCS-5-*araE-araC*-P_{BAD}-*mNG*	Derivative of pBBR1MCS-5-*araC*-P_{BAD}-*mNG* carrying gene *araE* encoding L-arabinose transporter AraE	This work
pBBR1MCS-5-*araC*-P_{BAD}-MCS	pBBR1MCS-5-based empty vector for AraC-P_{BAD}-dependent expression of target genes cloned into the MCS provided	This work
pBBR1MCS-5-*araC*-P_{BAD}-MCS-*mNG*	Derivative of pBBR1MCS-5-*araC*-P_{BAD}-MCS with *mNG* as reporter gene inserted into the MCS when using the restriction enzymes *Nde*I and *Xho*I	This work

directly to the medium. The pH of the supplemented medium was adjusted to pH 6, cold sterile filtered and directly used for cultivation. Cultivations of *G. oxydans* harboring pBBR1MCS-2- or pBBR1MCS-5-based plasmids were supplemented with 50 μg mL^{-1} kanamycin or 10 μg mL^{-1} gentamicin, respectively (Kovach et al. 1995). *Escherichia coli* strains were routinely cultivated in lysogeny broth (LB) medium at 37 °C and 160 rpm. If appropriate, 50 μg mL^{-1} kanamycin or 10 μg mL^{-1} gentamicin was added to the medium. *G. oxydans* was transformed by conjugation using *E. coli* S17-1 as a donor (Kiefler et al. 2017). All *E. coli* strains were made competent and transformed by $CaCl_2$ procedure (Hanahan 1983).

Enzymatic determination of L-arabinose concentrations

L-Arabinose concentrations in the medium of the *G. oxydans* strains 621H and BP.6 were determined using the enzymatic L-arabinose and D-galactose rapid assay kit (Megazyme). All samples were measured in microplates according to the manufacturer's instructions by monitoring NADH formation as increase in absorption at 340 nm in a multi-well reader (infinite M1000 PRO, Tecan).

DNA microarray analysis

To analyze short-term gene expression changes in response to a pulse of 1% (*w*/*v*) L-arabinose, the transcriptomes of *G. oxydans* 621H cultivated in complex medium with 4% (*w*/*v*) D-mannitol were compared with the control. In the mid-exponential growth phase, 1% (*w*/*v*) L-arabinose was supplemented and the same volume of water in another 621H culture as a control. After 30 min of cultivation, each cell suspension was harvested by centrifugation (4500×*g*, 5 min, 4 °C). The resulting cell pellets were directly frozen in liquid nitrogen and stored at − 80 °C until RNA preparation. The preparation of RNA, cDNA synthesis, hybridization using Agilent's 4-plex DNA microarray platform, and data analysis were carried out as described (Kranz et al. 2018).

Recombinant DNA work

All DNA oligonucleotides used in this study were synthesized by Eurofins MWG and are listed in Table S1. All enzymes for recombinant DNA work were purchased from Thermo Scientific. DNA manipulations by polymerase chain reaction (PCR), restriction, and ligation reactions followed standard protocols (Sambrook et al. 1989). Reporter plasmids were constructed from amplified DNA fragments and the restricted broad-host vectors pBBR1MCS-2 or pBBR1MCS-5 in a one-step isothermal Gibson assembly (Gibson et al. 2009). The terminator sequence BBa_B1002 from the iGEM parts library was placed downstream of the reporter genes. For DNA amplification by PCR, Q5 polymerase was used according to the conditions recommended by the manufacturer (New England Biolabs). All DNA modifications used to obtain designed plasmids were performed with *E. coli* DH5α. Plasmids were isolated from *E. coli* using a QIAprep spin miniprep kit (Qiagen). The plasmid inserts constructed in this work were checked by DNA sequencing (Eurofins MWG).

Construction of plasmids

Plasmid pBBR1MCS-2-*araC*-P_{BAD}-*uidA* was constructed using the primer pairs PF1/PF2 and PF3/PF4 to generate a 1253-bp DNA fragment with *araC*-P_{BAD} from the commercially available plasmid pBAD/*Myc*-His A (Invitrogen/Thermo Fischer) and a 1886-bp DNA fragment with *uidA* from *E. coli* K12 genomic DNA and the terminator BBa_B1002 inserted by elongating the 5′-end of PF4. Plasmid pBBR1MCS-2-*araC*-P_{BAD}-*mNG* was constructed using the primer pairs PF1/PF5 and PF6/PF7 to generate a 1,238 bp DNA fragment with *araC*-P_{BAD} and a 790 bp DNA fragment with *mNG* and terminator BBa_B1002, respectively. For insertion of the two overlapping DNA fragments into pBBR1MCS-2 by Gibson assembly (50 °C; 1 h), pBBR1MCS-2 was restricted by the endonucleases *Sac*I and *Kpn*I. Elongated 5′-ends in primers PF2/PF3 and PF5/PF6 were used to introduce downstream of P_{BAD} and 6 bp upstream of the start codon of *mNG* or *uidA*, the artificial Shine-Dalgarno sequence AGGAGA (Hentschel et al. 2013). To change the plasmid backbone from pBBR1MCS-2 to pBBR1MCS-5, *araC*-P_{BAD}-*uidA* and *araC*-P_{BAD}-*mNG* were excised and ligated into pBBR1MCS-5 using *Sac*I and *Eco*81I.

The plasmid pBBR1MCS-5-P_{BAD}-*mNG* was constructed using the primer pair PF8/PF9 to obtain a 1164-bp DNA fragment P_{BAD}-*mNG* from pBBR1MCS-5-*araC*-P_{BAD}-*mNG*. The resulting fragment was cloned into pBBR1MCS-5 using *Bam*HI and *Xho*I. To prevent undesired transcripts initiating from P_{BAD}, the *G. oxydans* terminator of *gdhM* (GOX0265) was inserted upstream of P_{BAD}.

Plasmid pBBR1MCS-5-*araE-araC*-P_{BAD}-*mNG* was constructed by insertion of *araE* into pBBR1MCS-5-*araC*-P_{BAD}-*mNG*. For that, pBBR1MCS-5-*araC*-P_{BAD}-*mNG* was restricted by the enzymes *Asc*I and *Eco*81I and a 1576-bp DNA fragment comprising *araE* without own promoter, amplified with the primer pair PF10/PF11 from *E. coli* K12 genomic DNA, was integrated downstream of *araC* by Gibson assembly. PF10 and PF11 contained elongated 5′-ends to insert the T7 terminator sequence downstream of *araE* and a Shine-Dalgarno sequence upstream of *araE* between *araE* and *araC*. Thus, *araE* and *araC* are expected to be expressed as a polycistronic transcript from the *araC* promoter.

Plasmid pBBR1MCS-5-*araC*-P_{BAD}-MCS as an empty vector with a ribosome-binding site, a new *Nde*I site upstream of the multiple cloning site (MCS) and the iGEM terminator sequence BBa_B1002 was constructed in two steps. In the first step, the DNA fragment *araC*-P_{BAD} generated with the primer pair PF12/PF13 was inserted into *Bsh*TI/*Sac*I-restricted pBBR1MCS-5 by Gibson assembly keeping the original MCS from pBBR1MCS-5. In the second step, the terminator sequence BBa_B1002 was integrated downstream of the MCS by integration of a DNA fragment amplified with the primer pair PF14/PF15. For the integration of the terminator sequence, the plasmid obtained in step one was restricted with *Xho*I and *Sph*I.

Plasmid pBBR1MCS-5-*araC*-P_{BAD}-MCS-*mNG* was constructed from pBBR1MCS-5 by integration of the DNA fragments *araC*-P_{BAD} and *mNG*-BBa_B1002 in a Gibson assembly. In the amplification of the DNA fragments, the restriction sites *Nde*I and *Xho*I were integrated resulting in the same sequence as it would have been obtained *via* classical restriction cloning of *mNG* into pBBR1MCS-5-*araC*-P_{BAD}-MCS using the restriction enzymes *Nde*I and *Xho*I. The DNA fragments *araC*-P_{BAD} and *mNG*-BBa_B1002 were amplified with the primer pairs PF1/PF16 and PF17/PF18, respectively. For integration, pBBR1MCS-5 was restricted using the restriction enzymes *Bsh*TI and *Kpn*I.

Measurements of fluorescence protein and enzyme activity

For online monitoring of expression induction and relative promoter strengths of promoter–reporter constructs in *G. oxydans*, the fluorescence protein mNeonGreen (mNG) was used (Shaner et al. 2013). In shake flask experiments, *mNG* expression in *G. oxydans* was induced by addition of 1% (*w*/*v*) L-arabinose from a 50% (*w*/*v*) stock solution. Reference cultures were supplemented with an equal volume of water. In intervals, growth (OD_{600}) and fluorescence emission was monitored by a spectrophotometer (UV-1800, Shimadzu) and a Tecan Reader (λ_{ex} 504 nm/λ_{em} 517 nm; gain 60; ex/em bandwidth 5 nm; infinite M1000 PRO, Tecan), respectively. In BioLector cultivations using 48-well

Flowerplates® (m2p-labs), batches of 800 µL of D-mannitol medium were inoculated from overnight precultures and incubated (1200 rpm; 85% humidity, 30 °C). Over a period of up to 30 h, cell growth and fluorescence was monitored in each well simultaneously by measuring the backscatter ($A_{620\ nm}$; gain 20) and fluorescence emission (λ_{ex} 510 nm/λ_{em} 532 nm; gain 60). Typically, mean values and standard deviations of all experiments were derived from at least three biological replicates.

For enzymatic reporter assays, β-D-glucuronidase (UidA) was used (Kallnik et al. 2010). UidA activity was determined in a Miller assay essentially as described (Miller 1992). Immediately after inoculation of *G. oxydans* shake flask cultures, *uidA* expression was induced by the addition of 1% (*w*/*v*) L-arabinose. Non-induced cultures supplemented with an equal volume of water were used as controls. In intervals, 500 µL samples were taken to determine OD_{600} and UidA activity. For permeabilization of the cells, 30 µL of the culture broth in appropriate dilutions in assay buffer was incubated in a 96-well plate (20 min; 30 °C) with 100 µL of prewarmed Z-mix (54.6 mM $Na_2HPO_4 \times 7H_2O$, 36.4 mM $NaH_2PO_4 \times H_2O$, 9.1 mM KCl, 0.9 mM $MgSO_4$, 45.5 mM DTT, 4.5% (*v*/*v*) chloroform, 0.5% (*w*/*v*) SDS, pH 7). After the addition of 100 µL of prewarmed 4-nitrophenyl-β-D-glucopyranoside (4 g L^{-1}) using a multichannel pipette, β-D-glucuronidase activity was monitored measuring the absorption of *p*-nitrophenol in intervals of 1 min at 420 nm (infinite M1000 PRO, Tecan). From all constructs, at least three biological replicates were measured in triplicates to determine mean values and standard deviations.

Cell flow cytometer analysis

For single cell analysis of reporter gene expression, the *G. oxydans* strains 621H and BP.6 carrying the plasmid pBBR1MCS-5-*araC*-P_{BAD}-*mNG* were analyzed using a BD FACSAria II cell sorter (BD Biosciences) equipped with a 70-µm nozzle run with a sheath pressure of 70 psi. Using the 488 nm laser beam, the front scatter (FSC) and side scatter (SSC) were recorded as small-angle (axial) and perpendicular scatter, respectively. Combining a 502-nm-long-pass and 530/30 nm band-pass filter, the emitted mNG fluorescence from the SSC signal was detected. Fluorescence data were acquired using a two-step gating strategy: at first, signals from cell debris and electronic noise were excluded by gating a population in a FSC-H vs. an SSC-H plot. Secondly, to perform singlet discrimination, from the resulting population the FSC-H signal was plotted against FSC-W. The gated singlet population was used for fluorescence acquisition in all experiments. While the total event rate during measurements never exceeded 15,000 events/s, for each sample, the signals of 100,000 events were recorded. For FACS device control and data analysis, FACSDiva 7.0.1 software (BD Biosciences) was used. Gated events (n = 100,000) were used for data analysis in FlowJo for Windows 10.4.2 (FlowJo, LLC) and Prism 7.04 (GraphPad Software) to visualize FACS data.

Bioreactor cultivation of *G. oxydans*

Bioreactor cultivations were conducted in DASbox® mini-bioreactors controlled by DASware software (Eppendorf). In 385-mL glass vessels equipped with two 6-bladed Rushton-type impellers, O_2 (InPro® 6800 series, Mettler-Toledo), pH (EasyFerm Plus K8 120, Hamilton), and temperature sensors, 150-mL 4% (*w*/*v*) D-mannitol medium was inoculated to an initial OD_{600} of 0.3 (30 °C). The initial gas flow rate was set to 6 sL h^{-1}. Starting agitation frequency was 500 rpm. The pH was maintained at 6 by automatic titration using H_2SO_4 or KOH stocks (1.5 M). Dissolved oxygen tension in the medium was maintained ≥ 30% by a cascade of first adjusting the agitation speed to a maximum of 1200 rpm, then by rising the O_2 concentration in the supplied gas up to 80% (*v*/*v*) and eventually by increasing the gas flow rate. In intervals, samples were taken from the culture broth and OD_{600} as well as fluorescence were determined as described above.

L-Arabinose biotransformation for the analysis of oxidation products

To identify the reaction products of L-arabinose oxidation by *G. oxydans* strains, cells were grown in 25 mL of D-mannitol medium in 500 mL shake flasks to an OD_{600} of 1.6, centrifuged (4000×*g*, 5 min) and washed twice with 1 mM HEPES (pH 7). The pellet was resuspended in 25 mL biotransformation buffer (33.9 g L^{-1} Na_2HPO_4, 15 g L^{-1} KH_2PO_4, 5 g L^{-1} NH_4Cl, 2.5 g L^{-1} NaCl, 0.49 g L^{-1} $MgSO_4$, 0.02 g L^{-1} $CaCl_2$) supplemented with 1% (*w*/*v*) L-arabinose. The cell suspensions were incubated for 24 h at 30 °C on a shaker (180 rpm). Afterwards, cells were centrifuged (4000×*g*, 5 min) and the cell-free supernatant was analyzed using a gas chromatograph (Agilent 6890N, Agilent Technologies) coupled to a Waters Micromass GCT Premier high-resolution time-of-flight mass spectrometer (Waters). Sample derivatization, GC-TOF-MS operation, and peak identification were essentially conducted as described (Paczia et al. 2012). Biotransformation medium without cells was used as reference.

Results

Growth of *G. oxydans* 621H in the presence of L-arabinose

In the present study, we wanted to test L-arabinose-dependent gene expression in *G. oxydans* 621H to provide a regulatable

expression plasmid for this AAB, similar to AraC-dependent vectors constructed for *E. coli* (Guzman et al. 1995). In such a system, the inducer L-arabinose needs to enter the cell where it binds to the transcriptional regulator AraC (Schleif 2010). In the case of *G. oxydans* 621H, L-arabinose was reported to be oxidized already in the periplasm by the membrane-bound glucose DH GdhM (GOX0265) (Mientus et al. 2017; Peters et al. 2013). Thus, the presence of L-arabinose could affect the growth of *G. oxydans* 621H by using it as an energy source through oxidation, thereby inactivating the inducer. The *G. oxydans* multi-deletion strain BP.6 lacks GdhM and exhibited no L-arabinose-oxidizing activity anymore (Peters et al. 2013). Therefore, we first tested the impact of L-arabinose on growth of the *G. oxydans* strains 621H and BP.6 in shake flasks. In complex medium supplemented with 1% (*w*/*v*) L-arabinose instead of D-mannitol, growth of *G. oxydans* 621H was very poor and OD_{600} merely doubled within 8 h, while strain BP.6 did not grow at all (Fig. 1a). In medium supplemented with 4% (*w*/*v*) D-mannitol plus 1% (*w*/*v*) L-arabinose, both strains grew very similar ($\mu = 0.18 \pm 0.01\ h^{-1}$ for 621H and $0.17 \pm 0.01\ h^{-1}$ for BP.6) compared with the control condition with 4% (*w*/*v*) D-mannitol, yet without arabinose ($\mu = 0.18 \pm 0.01\ h^{-1}$ for 621H and $0.17 \pm 0.01\ h^{-1}$ for BP.6). In the stationary phase, both strains reached similar final OD_{600} values independent of the L-arabinose supplementation (621H OD_{600} with D-mannitol 3.84 ± 0.18 and with D-mannitol + L-arabinose 3.65 ± 0.28; BP.6 OD_{600} with D-mannitol 3.48 ± 0.26 and with D-mannitol + L-arabinose 3.66 ± 0.08). The concentration of L-arabinose supplemented to the medium did not decrease without cells or with BP.6 cells, while in the 621H cultures L-arabinose was decreased by approximately 80% within 24 h (Fig. 1b). This suggested that L-arabinose or its oxidation product did not impair growth of *G. oxydans*.

L-Arabinose is oxidized to L-arabinonic acid and hardly affected global gene expression

Based on the measurement of whole cell L-arabinose-oxidation activities of *G. oxydans* mDH deletion strains and of specifically complemented strains using DCPIP as electron acceptor, the membrane-bound glucose DH is expected to be responsible for L-arabinose oxidation (Mientus et al. 2017; Peters et al. 2013). Therefore, we tested the *G. oxydans* strains 621H and BP.6 for L-arabinose oxidation and analyzed the product(s) by GC-TOF-MS analysis. The multi-deletion strain BP.6 lacks six mDHs including the membrane-bound glucose DH GdhM (GOX0265) and still possesses the cytosolic glucose DH (GOX2015) GdhS (Peters et al. 2013). Cell suspensions of each strain with an OD_{600} of 1.6 were incubated for 24 h at 30 °C and 180 rpm in biotransformation buffer supplemented with 1% (*w*/*v*) L-arabinose. Afterwards, cell-free supernatants were obtained for GC-TOF-MS measurements. Strain 621H clearly oxidized L-arabinose, and L-arabinonic acid was identified as the product, while strain BP.6 consumed only minor amounts of L-arabinose and formed minor amounts of L-arabinonic acid (Fig. S1). The 621H sample showed two new peaks at retention times (R_t) 13.49 and 14.74 min. The peak at R_t 13.49 min had an *m*/*z* value of 364, corresponding to arabinonic acid γ-1,4-lactone with 3 TMS groups. The peak at R_t 14.74 min had an *m*/*z* value of 511, corresponding to arabinonic acid with 5 TMS groups and a methyl group split off. According to the comparable arbitrary peak areas, data indicated that GdhM did significantly contribute to L-arabinose oxidation. For strain BP.6, only a very low amount of L-arabinonic acid was found (~ 3%) compared with 621H. Together, this indicated that L-arabinose was indeed mainly oxidized by the membrane-bound glucose DH, while the contribution of the cytosolic glucose DH GdhS or another enzyme remaining in strain BP.6 was negligible.

To check whether the addition of L-arabinose as an inducer possibly affects short-term global gene expression in *G. oxydans* 621H, transcriptomes were compared using DNA microarrays. Addition of 1% (*w*/*v*) L-arabinose in the mid-exponential growth phase to 621H cells cultured in complex medium with D-mannitol had only very little effects on the relative mRNA levels within 30 min (Table S2). The highest mRNA level increase (2-fold) was found for GOX0707 encoding the DNA protection during starvation protein Dps followed by six hypothetical proteins (1.6- to 1.9-fold). The strongest mRNA level decrease (0.46-fold) was observed for GOX0536 encoding a hydroxamate-type ferrisiderophore receptor followed by its neighboring genes GOX0532 (0.57-fold) and GOX0531 (0.59-fold) encoding the ExbB and ExbD proteins of the TonB-ExbB-ExbD system as well as GOX0758 (0.56-fold) encoding a porin protein. There is no obvious functional link between these genes and L-arabinose metabolism.

Construction of AraC-dependent L-arabinose-inducible expression plasmids

Based on the tight high-level expression vectors containing the P_{BAD} promoter developed for *E. coli* (Guzman et al. 1995), Invitrogen commercialized the AraC-P_{BAD} system for dose-dependent expression of genes with plasmid pBAD/Myc-His A useful for expression of potentially toxic or essential genes in *E. coli*. The *araC* sequence used in pBAD/Myc-His A corresponds to the *araC* sequence of the widely used MC4100 lineage of *E. coli* K12 (Casadaban 1976). It differs in nine codons from *araC* of the *E. coli* K12 reference strain MG1655, which could be of advantage for expression in *G. oxydans*. Six of the nine different codons cluster in the region of the helix-turn-helix motif responsible for DNA binding at the C terminus of AraC (Brunelle and Schleif 1989). Five of these six codons exhibit much higher usage frequency in *G. oxydans* when using *araC* from MC4100 instead of

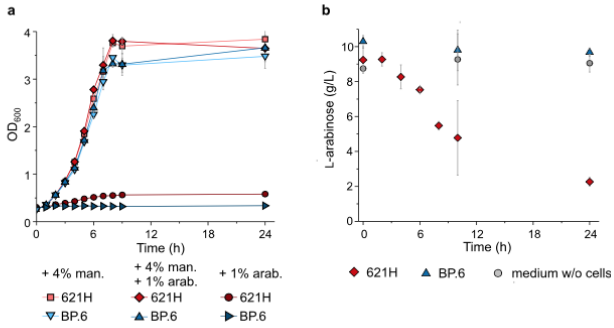

Fig. 1 Comparisons of the *G. oxydans* strains 621H and BP.6. **a** Growth (OD_{600}) in shake flasks in complex medium with 4% (*w/v*) D-mannitol or 1% (*w/v*) L-arabinose as well as both 4% (*w/v*) D-mannitol plus 1% (*w/v*) L-arabinose. **b** Arabinose concentrations in complex medium with 4% (*w/v*) D-mannitol plus 1% (*w/v*) L-arabinose in shake flasks. Data represent mean ± SD from three biological replicates

MG1655 (Table S3). Consequently, the AraC-dependent promoter P_{BAD} flanked by *araC* from MC4100 and the reporter gene *uidA* or *mNeonGreen* was integrated into the multiple cloning site (MCS) as described in "Materials and methods." To enable efficient translation of the reporter, 16 nt containing a proven Shine-Dalgarno sequence functional in *G. oxydans* was placed between P_{BAD} and the reporter gene. Furthermore, as a terminator sequence, BBa_B1002 was inserted downstream of the reporter genes. We also constructed a reporter plasmid without *araC* to test the AraC dependence of P_{BAD} in *G. oxydans*. Another reporter plasmid additionally carried the L-arabinose transporter gene *araE* to test the sensitivity of induction towards L-arabinose (Fig. S2).

Performance of the AraC-P_{BAD} system with enzyme reporter UidA in shake flasks

With the pBBR1MCS-5-*araC*-P_{BAD}-*uidA* plasmid, we tested the basal expression and the induction by L-arabinose using the reporter enzyme β-D-glucuronidase. Besides *G. oxydans* 621H, which oxidizes L-arabinose by mDHs, we also used the multi-deletion strain BP.6 that is almost unable to oxidize L-arabinose to check whether AraC-P_{BAD} performs better in BP.6 than in 621H. Both strains were grown in shake flasks using D-mannitol medium with and without 1% (*w/v*) L-arabinose. For strain 621H, the highest UidA activity was observed at the end of the exponential phase after approximately 9 h with 12,772 ± 1604 MU compared with 146 ± 47 MU in the control cultures without L-arabinose, the latter indicating very low basal expression (Fig. 2a). Strain BP.6 exhibited 11,780 ± 813 MU after 9 h in induced cultures compared with 225 ± 29 MU in the non-induced controls. Surprisingly, UidA activity in L-arabinose-supplemented *G. oxydans* 621H was highly reduced after 24 h (2,007 ± 583 MU), while UidA activity in BP.6 remained high after 24 h (13,209 ± 715 MU). When compared with the non-induced cultures, maximal UidA induction ratios of 87 and 59 were calculated for 621H and BP.6, respectively (Table 2). The lower ratio calculated for BP.6 was primarily due to the somewhat higher basal expression under non-induced condition, while the absolute UidA activity in BP.6 under induced conditions was similar as that in 621H. Generally, the UidA activities in the non-induced cultures did barely surpass the background activity values determined in cell-free control samples. This indicated that the expression plasmid pBBR1MCS-5-*araC*-P_{BAD}-*uidA* showed very low basal expression of P_{BAD} in the absence of L-arabinose.

Performance of the AraC-P_{BAD} system with the fluorescence reporter protein mNeonGreen

For continuous determination of reporter gene expression and its dynamics as well as to verify the strong induction of P_{BAD} and AraC dependence in *G. oxydans*, we also tested the fluorescence reporter protein mNeonGreen (mNG). In all tests with plasmid pBBR1MCS-5-*araC*-P_{BAD}-*mNG*, the mNG fluorescence signals in non-induced cultures did barely surpass the background signals of cell-free control samples, suggesting also a very low basal expression of *mNG*. In shake flask cultivations with 1% (*w/v*) L-arabinose, the mNG fluorescence in *G. oxydans* 621H peaked approximately after 8 h (Fig. 2b). At the end of the cultivation (24 h), the mNG fluorescence was much lower in strain 621H, while in strain BP.6, the mNG fluorescence was further increased. The maximal induction ratios based on the absolute or the biomass-specific mNG fluorescence were calculated to be 289 ± 75 or 327 ± 71 for strain 621H and 431 ± 14 or 481 ± 38 for BP.6, respectively (Table 3). In microscale BioLector cultivations, a similar induction profile was observed (Fig. 2c). The maximal induction ratios based on specific fluorescence were calculated to be 222 ± 8 for 621H and 192 ± 8 for BP.6. Again, after entering the stationary phase, the specific mNG fluorescence steadily decreased and reached zero after about 16 h in strain 621H, while for strain BP.6, the decrease was much weaker reduced over time and remained high. This was in contrast with the shake flask cultivations, where mNG

Table 2 L-Arabinose-dependent induction fold changes calculated from UidA activities in *G oxydans* strains 621H and BP.6 carrying plasmid pBBR1MCS-5-*araC*-P_{BAD}-*uidA*

Time (h)	621H	BP.6
2	62 ± 30	16 ± 5
4	93 ± 67	35 ± 7
7	50 ± 7	34 ± 12
9	98 ± 46	53 ± 3
24	7 ± 4	52 ± 3

Cells were cultivated in shake flasks in D-mannitol medium without and with 1% (*w*/*v*) L-arabinose for induction (Fig. 2a). Data represent mean ± SD from three biological replicates

fluorescence increased in the stationary phase in strain BP.6 (Fig. 2b). In the late stationary phase (16–24 h), the backscatter values of the 621H cultures supplemented with 1% (*w*/*v*) L-arabinose steadily increased further. Measurements of the OD_{600} in a photometer showed no differences between L-arabinose-supplemented strain 621H and the non-supplemented 621H cultures. Additional control measurements with cell-free complex medium adjusted to different pH values (pH 6, 4.5, 4, and 3.3) revealed differences in backscatters already in cell-free medium due to the differences in pH that could not be observed in OD_{600} measurements in a photometer. This suggested that the steady increase of backscatter values in L-arabinose-induced 621H cultures in the stationary phase resulted from a stronger acidification of the growth medium that cannot be detected by OD_{600} measurements in a photometer. Taken together, the newly constructed expression plasmids for *G. oxydans* based on the AraC-P_{BAD} system exhibited very low basal expression of the reporter proteins UidA and mNG and very strong induction by 1% (*w*/*v*) L-arabinose both in shake flask and in microscale BioLector cultivations (up to 480-fold).

The P_{BAD} promoter is AraC-dependent in *G. oxydans* and tunable by varying the L-arabinose concentrations

In *E. coli*, the regulator AraC acts as a repressor of P_{BAD} in the absence of L-arabinose by bending the promoter DNA and stimulates transcription from P_{BAD} when L-arabinose is present (Schleif 2010; Soisson et al. 1997). To rule out the possibility that in *G. oxydans* P_{BAD} is either repressed or activated by a *G. oxydans* protein, the plasmid pBBR1MCS-5-P_{BAD}-*mNG* missing the *araC* gene was constructed and tested in *G. oxydans* 621H. In this experiment, no differences in fluorescence were observed between induced and non-induced cells, thus no induction was observed with 1% (*w*/*v*) L-arabinose when AraC was absent (Fig. S3). This result showed that the inducibility of P_{BAD} in *G. oxydans* is independent of endogenous proteins and indeed specifically dependent on

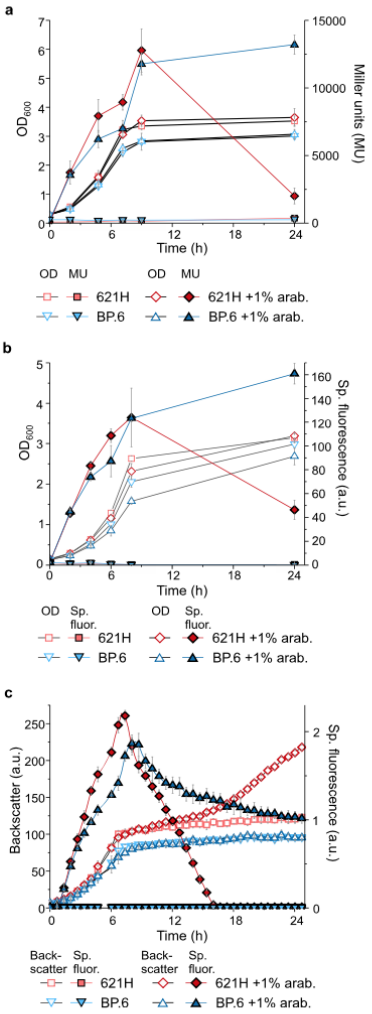

Fig. 2 Comparisons of the *G. oxydans* strains 621H and BP.6. **a** Growth and UidA activity in Miller units (MU) in strains 621H and BP.6 carrying plasmid pBBR1MCS-5-*araC*-P_{BAD}-*uidA* in L-arabinose-induced and non-induced condition in shake flasks. **b** Growth and specific mNeonGreen (mNG) fluorescence in strains 621H and BP.6 carrying plasmid pBBR1MCS-5-*araC*-P_{BAD}-*mNG* in L-arabinose-induced and non-induced condition in shake flasks. The mNG fluorescence was measured in a Tecan reader. The specific fluorescence was calculated from absolute fluorescence per OD_{600}. **c** Growth according to backscatter and specific mNG fluorescence in strains 621H and BP.6 carrying plasmid pBBR1MCS-5-*araC*-P_{BAD}-*mNG* in L-arabinose-induced and non-induced condition in microscale BioLector cultivations. The specific fluorescence was calculated from absolute fluorescence per backscatter. For induction, always 1% (*w*/*v*) L-arabinose was added to the D-mannitol medium. For all experiments, data represent mean ± SD from three biological replicates

heterologous AraC. Furthermore, in the absence of AraC the reporter is almost not expressed from P_{BAD}, thus repression of P_{BAD} by AraC seemed not to be required in *G. oxydans*.

The tunability of the AraC-P_{BAD} system in *G. oxydans* was tested with a range of L-arabinose concentrations. The mNG fluorescence gradually increased similarly in strains 621H and BP.6 with increasing concentrations of L-arabinose (Fig. 3). Compared with 1% (*w*/*v*) L-arabinose, supplementation with 2% (*w*/*v*) L-arabinose did not lead to a significant increase in mNG fluorescence, indicating saturation of induction at close to 1% (*w*/*v*) inducer. Whereas only a small decrease of the mNG fluorescence was observed in the stationary phase for the BP.6 cultures induced with the highest L-arabinose concentrations, mNG fluorescence for strain 621H decreased to zero in the stationary phase for the cultures induced with more than 0.5% (*w*/*v*) L-arabinose. In contrast, no decrease was observed for the 621H cultures with up to 0.25% L-arabinose, clearly suggesting a correlation between L-arabinonic acid formation and loss in mNG fluorescence signals.

Overall, in the exponential growth phase, the performance of the AraC-P_{BAD} system was very similar in the L-arabinose-oxidizing strain 621H compared with the multi-deletion strain BP.6. Therefore, we asked whether the oxidation product L-arabinonic acid could possibly also act as an inducer on AraC, thereby compensating for the decrease in L-arabinose by its oxidation in 621H cultures. To test this, we added 1% (*w*/*v*) of L-arabinonic acid to mannitol medium and monitored the mNG fluorescence of strain 621H with pBBR1MCS-5-*araC*-P_{BAD}-*mNG* in BioLector cultivations. L-Arabinonic acid did not induce the AraC-P_{BAD} system, since the cultures exhibited a similar background fluorescence as non-induced 621H cultures without L-arabinose or L-arabinonic acid (Fig. S4).

Table 3 L-Arabinose-dependent induction fold changes calculated from mNG signals in *G. oxydans* strains 621H and BP.6 carrying plasmid pBBR1MCS-5-*araC*-P_{BAD}-*mNG*

Time (h)	abs. fluorescence-fold		sp. fluorescence-fold	
	621H	BP.6	621H	BP.6
2	38 ± 4	31 ± 4	39 ± 2	32 ± 3
4	51 ± 4	35 ± 2	53 ± 3	38 ± 2
6	126 ± 12	73 ± 9	140 ± 13	88 ± 14
8	289 ± 75	194 ± 8	327 ± 71	254 ± 16
24	128 ± 61	431 ± 14	125 ± 58	481 ± 38
30	45 ± 15	327 ± 20	48 ± 16	392 ± 28

Cells were cultivated in shake flasks in D-mannitol medium with and without 1% (*w*/*v*) L-arabinose for induction (Fig. 2b). Fold changes (1% L-arabinose vs. no inducer) were calculated from absolute mNG fluorescence signals (abs.) and from backscatter-related biomass-specific mNG fluorescence signals (sp.). Data represent mean ± SD from three biological replicates

The experiments described above showed that L-arabinose is able to activate AraC in *G. oxydans*, yet it is unknown how L-arabinose enters the *G. oxydans* cytoplasm. Knowledge on sugar transport systems in *G. oxydans* is scarce in general and no data are available for L-arabinose to our knowledge. The *E. coli* protein AraE is a low-affinity high-capacity L-arabinose transporter (Khlebnikov et al. 2001). To facilitate L-arabinose uptake by *G. oxydans* and thereby possibly improving the sensitivity of the L-arabinose-inducible system, plasmid pBBR1MCS-5-*araE-araC*-P_{BAD}-*mNG* was constructed containing *araE* including a Shine-Dalgarno sequence directly downstream of *araC*. This should enable co-transcription of *araC* and *araE* from P_{araC}. When analyzing strain 621H carrying plasmid pBBR1MCS-5-*araE-araC*-P_{BAD}-*mNG* with 0.1 and 0.5% (*w*/*v*) L-arabinose, however, the specific fluorescence was 40 to 60% lower compared with strain 621H carrying the plasmid without *araE* (Fig. S5). Thus, no increase in sensitivity towards the inducer was observed with pBBR1MCS-5-*araE-araC*-P_{BAD}-*mNG* under the conditions tested.

Acidification of the growth medium is responsible for the decrease in reporter activities

In the experiments described above, both UidA activity and mNG fluorescence strongly decreased in the stationary phase of the 621H cultures induced with 1% (*w*/*v*) L-arabinose but not in the BP.6 cultures. The decrease correlated with the L-arabinose concentration and was absent at concentrations up to 0.25% (*w*/*v*). This clearly indicated that oxidation of L-arabinose affected the dynamics of the reporter activities. According to previous data and our GC-TOF-MS results, strain 621H oxidizes L-arabinose to L-arabinonic acid by the membrane-bound glucose DH, which is absent in strain BP.6 (Mientus et al. 2017). With a pK_a of 3.39 (https://hmdb.ca/metabolites/HMDB0000539), formation of L-arabinonic acid caused an additional acidification of the growth medium. The pH values of the D-mannitol media of strains 621H and BP.6 supplemented with 1% (*w*/*v*) L-arabinose decreased from initially pH 6.0 to 3.3 ± 0.1 and 4.4 ± 0.1, respectively, after 24 h. In contrast, the pH values of the non-induced cultures were 4.7 ± 0.1 and 4.6 ± 0.1 for 621H and BP.6, respectively, after 24 h. These data confirm that L-arabinose oxidation to L-arabinonic acid by strain 621H leads to a stronger acidification of the medium.

Bacteria typically exhibit energy-dependent mechanisms for cytoplasmic pH homeostasis in order to survive during exposure to acidic or alkaline conditions. The observed decreases in mNG fluorescence suggested that due to the formation of L-arabinonic acid, the cytoplasmic pH in strain 621H increasingly acidified in the stationary phase when cells starved for energy. Recently, it was shown for the mNG protein that a shift from pH 6 to 4 is sufficient to reduce the mNG

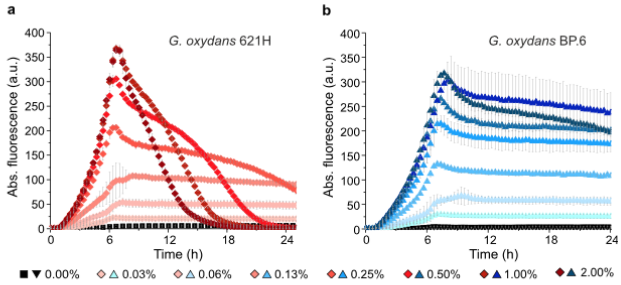

Fig. 3 L-Arabinose-dependent modulation of expression in the *G. oxydans* strains 621H (**a**) and BP.6 (**b**) carrying plasmid pBBR1MCS-5-*araC*-P_{BAD}-*mNG* in microscale BioLector cultivations. Reporter gene mNG expression was induced with increasing concentrations of L-arabinose from 0.03 to 2% (*w*/*v*) as indicated. Data represent mean ± SD from three biological replicates

fluorescence by approximately 75% (Steiert et al. 2018). As described above, the pH values of induced 621H cultures after 24 h were even lower than pH 4. Consequently, we tested whether fresh D-mannitol-free and L-arabinose-free medium adjusted to different pH values could restore the mNG fluorescence of stationary phase 621H cells cultivated with 1% (*w*/*v*) L-arabinose. For this test, we used plasmid pBBR1MCS-2-$P_{GOX0264}$-*mNG* in order to constitutively express *mNG* from the strong promoter of GOX0264. As expected, when cultivated with L-arabinose the mNG fluorescence was clearly decreased in the stationary phase, while without L-arabinose the mNG fluorescence remained high (Fig. S6a). Incubation of the cells grown with L-arabinose for 1 h in fresh medium adjusted to pH 3.5, 4.9, and 6.2 gradually recovered the mNG fluorescence (Fig. S6b). This result indicated that the decrease in mNG fluorescence in 621H cells was hardly due to degradation of the mNG protein in the stationary phase. Rather, the strong acidification of the growth medium by L-arabinonic acid formation in 621H cultures affected the cytoplasmic pH during the stationary phase which in turn was responsible for the decrease in mNG fluorescence. Furthermore, for *G. oxydans* 621H carrying pBBR1MCS-5-*araC*-P_{BAD}-*uidA* grown with 1% (*w*/*v*) L-arabinose, the loss of UidA activity in the stationary phase (24 h) was also restored partly when cells were transferred for 1 h into fresh medium adjusted to pH 6 (Fig. S6c, d).

To analyze the induction of the Ara*C*-P_{BAD} system in *G. oxydans* and the pH-dependent decrease and recovery in mNG fluorescence on the single cell level, flow cytometer analysis was applied. For strain 621H, 8 h after induction, 91% of all cells exhibited high fluorescence signals (approximately 40,000 a.u.) within the chosen gate, indicating a high population homogeneity close to the end of the exponential growth phase (Fig. 4a). 26 h after induction, when the pH of the medium was 3.3 ± 0.1, the overall fluorescence was diminished and two distinct populations at approximately 10,000 a.u. and approximately 600 a.u. emerged. Transferring the 621H cells into D-mannitol-free and L-arabinose-free medium adjusted to pH 6 resulted in a recovery of the mNG fluorescence in a single population with 83% exhibiting a fluorescence signal of approximately 30,000 a.u.. For *G. oxydans* BP.6, also a strong induction with a high

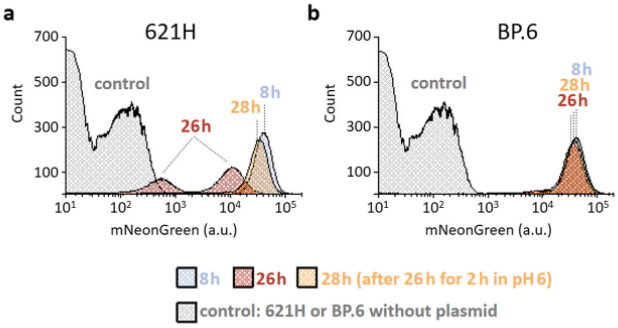

Fig. 4 FACS analysis of the *G. oxydans* strains 621H (**a**) and BP.6 (**b**) carrying plasmid pBBR1MCS-5-*araC*-P_{BAD}-*mNG*. Cells were grown in shake flasks with D-mannitol medium and induced with 1% (*w*/*v*) L-arabinose. FACS analysis was performed 8 and 26 h after induction. After 26 h, cells were transferred into fresh L-arabinose- and D-mannitol-free medium adjusted to pH 6 followed by incubation on a rotary shaker for 2 h. As a control, 621H or BP.6 cells without plasmids also grown in D-mannitol medium with 1% (*w*/*v*) L-arabinose were used. Total counts per sample represent 100,000 events and only appears to be different due to the logarithmic scale on the *x*-axis

homogeneity and a fluorescence of about 40,000 a.u. was observed after 8 h. These signals were hardly decreased in the stationary phase after 26 h (pH 4.4 ± 0.1) and were not affected by the transfer into fresh medium adjusted to pH 6 (Fig. 4b). These single cell results are in line with the assumption that additional acidification of the growth medium causes a stronger intracellular acidification in the stationary phase. Furthermore, the single cell data showed that the AraC-P_{BAD} system enabled a highly uniform induction response in the cells.

UidA activity and mNG fluorescence are stable in pH-controlled bioreactor cultivations

In the following, pH-controlled bioreactor cultivations were carried out to circumvent effects due to acidification of the medium when assaying the performance of the L-arabinose-inducible AraC-P_{BAD}-system in *G. oxydans*. Therefore, *G. oxydans* strains 621H and BP.6 carrying pBBR1MCS-5-*araC*-P_{BAD}-*uidA* and pBBR1MCS-5-*araC*-P_{BAD}-*mNG* were grown in DASbox® mini bioreactors under controlled conditions at pH 6 and dissolved oxygen concentrations above 30%. Sufficient oxygen levels are crucial for maturation of the chromophore (Shaner et al. 2013). After the 24-h fermentation in D-mannitol medium with 1% (*w*/*v*) L-arabinose, the total volume of potassium hydroxide solution consumed to maintain pH 6 in the 621H cultures (11.2 ± 0.7 mL) was much higher compared with the BP.6 cultures (6.0 ± 1.0 mL), which is in line with the L-arabinose oxidation by strain 621H yielding L-arabinonic acid. As expected, when maintaining a constant pH of 6 throughout the cultivation, neither the mNG fluorescence nor the UidA activity decreased in the stationary phase in 621H cells oxidizing L-arabinose (Fig. 5).

Providing an AraC-P_{BAD}-dependent plasmid with a multiple cloning site as empty vector

Albeit an AraC-P_{BAD}-dependent expression plasmid with genes of interest could be easily obtained by Gibson assembly in an all-in-one fragment mixture cloning, we wanted to provide an AraC-P_{BAD}-dependent plasmid for *G. oxydans* with a multiple cloning site as an empty vector for classical restriction enzyme-based cloning attempts to insert genes of interest. Therefore, we assembled *araC*-P_{BAD} with the multiple cloning site from pBBR1MCS-5 and the terminator sequence BBa_B1002 from the iGEM parts library in plasmid pBBR1MCS-5 to obtain plasmid pBBR1MCS-5-*araC*-P_{BAD}-MCS as an empty vector (Fig. 6). In this plasmid, the ribosome binding site AGGAGA was included upstream of the *Nde*I site newly created upstream of the original MCS by exchanging a single G to a C. To check the functionality and inducibility of AraC-P_{BAD} in this empty vector as a multiple cloning reference plasmid, we created the reporter plasmid pBBR1MCS-5-*araC*-P_{BAD}-MCS-*mNG* by Gibson assembly resulting in the same sequence as it would have been obtained *via* classical restriction cloning of *mNG* using the restriction enzymes *Nde*I and *Xho*I. When the resulting plasmid pBBR1MCS-5-*araC*-P_{BAD}-MCS-*mNG* was tested in strain 621H, again strong induction in the presence of L-arabinose was observed and the basal expression in the absence of L-arabinose was again very low (Fig. S7). However, for unknown reasons the specific mNG fluorescence reached only approximately 40% of the maximum observed with the test plasmid always used before and not having the multiple cloning site or remaining parts thereof. Nevertheless, this demonstrated that plasmid pBBR1MCS-5-*araC*-P_{BAD}-MCS was also functional and could serve as a multiple cloning vector to insert fragments containing genes of interest and if required own ribosome binding sites.

Discussion

For the AAB *G. oxydans*, no expression plasmid was available that shows very low background expression and allows strong and tunable target gene expression. In this study, we found that the AraC-P_{BAD} system derived from *E. coli* K12 MC4100 performed very well in *G. oxydans* with the pBBR1 plasmid backbone. It exhibited very low basal reporter gene expression, induction ratios up to 480-fold, and gradually increased expression in an L-arabinose concentration-dependent manner. Typically, the regulatable expression plasmids tested in AAB species and reported so far suffered from very leaky expression in the absence of the respective inducer, resulting in very low induction ratios for the promoters P_{BAD}, P_{Tet} or P_{Lux}, while the overall expression was strong according to the reporter activities (Florea et al. 2016; Teh et al. 2019). Among these three promoters, the best induction ratios were only 5- to 12-fold for the L-arabinose-inducible AraC-P_{BAD} system from *E. coli* when used in *G. xylinus* 700178, *G. hansenii* 53582, or *K. rhaeticus* iGEM (Teh et al. 2019). The reason for the leakiness in AAB reported for the repressor-regulated promoters is not clear. It seems the binding of the repressors to their target DNA sequences is not strong enough in the cytoplasm of AAB or there is not enough repressor protein. However, in the case of AraC the mechanism of transcriptional gene regulation is different compared with those of the pure repressor proteins TetR, LuxR, and LacI, which just dissociate from their operators when their respective inducer is bound to the protein. In *E. coli*, AraC does not only repress P_{BAD} by looping the DNA when bound to specific target sequences in the absence of L-arabinose but also is essential for activation of P_{BAD} in the presence of L-arabinose *via* a modified binding to target sequences, causing unlooping of the promoter DNA and stimulation of both the binding of RNA polymerase and the transition from the closed to the open promoter complex

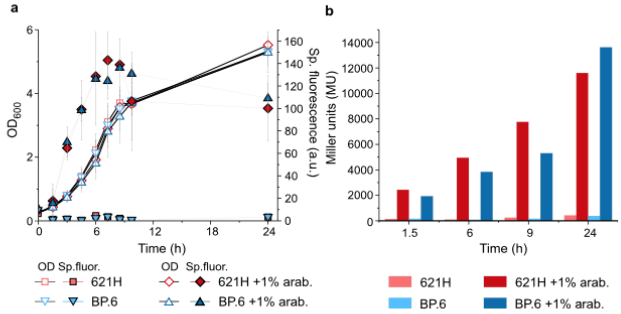

Fig. 5 L-Arabinose-inducible reporter gene expression in DASbox fermentations in pH-controlled conditions (pH 6). Both, mNG and UidA activity remained high in *G. oxydans* 621H carrying plasmid pBBR1MCS-5-*araC*-P_{BAD}-*mNG* (**a**) or pBBR1MCS-5-*araC*-P_{BAD}-*uidA* (**b**) 24 h after induction with 1% (*w*/*v*) L-arabinose when pH 6 was maintained

(Schleif 2010; Soisson et al. 1997). Additionally, in *E. coli*, the cAMP receptor protein (CRP) also plays an important role in the induction of P_{BAD} by stimulating the opening of the DNA loop and either the binding of the RNA polymerase or the transition to the open complex (Schleif 2010). In the genome of *G. oxydans*, there is only a single protein (GOX0974/GOX_RS06010) predicted to belong to the CRP/FNR superfamily of transcriptional regulators (Korner et al. 2003; Kranz et al. 2017; Prust et al. 2005). According to our data, this protein is a member of the FNR family and not a cAMP-binding protein of the CRP family (unpublished). Therefore, CRP appears to be absent in *G. oxydans*. Furthermore, with plasmid pBBR1MCS-5-P_{BAD}-*mNG* missing the *araC* gene, we confirmed that the induction by L-arabinose specifically depended on AraC and not on an endogenous *G. oxydans* protein. The absence of AraC and therefore the missing repression of P_{BAD} was not sufficient to allow transcription from P_{BAD} in *G. oxydans*. A CRP likely absent in *G. oxydans* could be the reason. This is important in view of leakiness, yet we cannot rule out that in the absence of AraC P_{BAD} is somehow repressed by a *G. oxydans* protein that is displaced from P_{BAD} when AraC is present. Nevertheless, the activation indicated that in *G. oxydans*, AraC was functional and required as a transcriptional activator of P_{BAD}, thus heterologous AraC bound to the respective promoter DNA in the cytoplasm and interacted with the RNA polymerase of *G. oxydans*, yet AraC was not required to repress P_{BAD}. Therefore, using transcriptional activation instead of derepression and considering CRP may circumvent the high leakiness of the classical repressor-based expression plasmids in AAB. However, the reason why AraC-P_{BAD} from *E. coli* did not perform well in *G. xylinus* 700178, *G. hansenii* 53582, or *K. rhaeticus* iGEM remains unclear (Teh et al. 2019). We used the *araC*-P_{BAD} sequence from *E. coli* K12 MC4100 that exhibits much better codon usage frequencies in *G. oxydans* for five rare *E. coli* K12 MG1655 codons located in the C-terminal helix-turn-helix region of AraC responsible for DNA binding. The effects of the different *araC* codon usage frequencies from MC4100 vs.

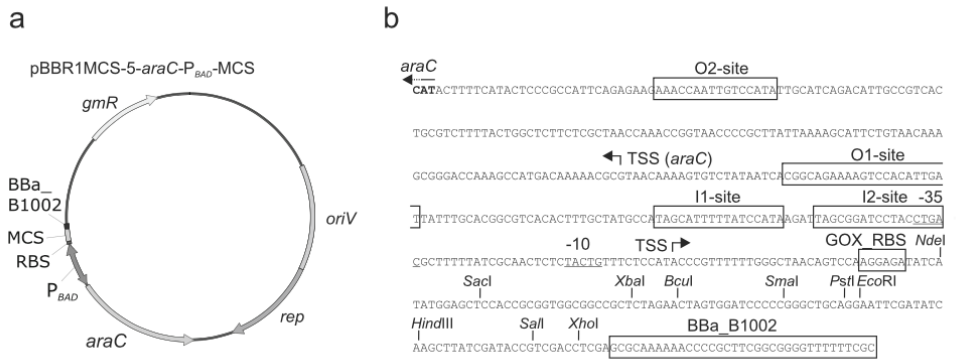

Fig. 6 Scheme of the pBBR1MCS-5-based *araC*-P_{BAD} plasmid with a multiple cloning site (**a**) and sequence information details (**b**). The ribosome-binding site AGGAGA (GOX_RBS) is included and usable when the insert cloning is carried out on the 5′-end by *Nde*I; otherwise, another RBS needs to be included in the insert upstream of the gene of interest. The iGEM terminator sequence of BBa_B1002 is located downstream of the multiple cloning site (MCS)

MG1655 in AAB are unknown. Furthermore, differences in the constructed plasmids such as terminators used and the orientations of plasmid-based reporter and resistance genes to each other, as well as further little sequence-specific differences may affect the formation or stability of their transcripts and the resulting translation, thereby affecting the overall performance of the AraC-P_{BAD} systems in AAB. This can already be seen in the result that even in *G. oxydans* with plasmid pBBR1MCS-5-*araC*-P_{BAD}-MCS-*mNG*, which was very similar to the extremely well-performing plasmid pBBR1MCS-5-*araC*-P_{BAD}-*mNG*, only approximately 40% of the maximal specific mNG fluorescence was found. This indicated that already the single G to C exchange between the RBS and the ATG start codon to create an *Nde*I site or the short remaining MCS sequence from the *Xho*I site (CTCGAG) after the stop codon directly upstream of the terminator sequence and overlapping with it by the last G, or even both, somehow negatively affected the resulting *mNG* transcript or its translation more drastically than one would expect. Further studies are required to analyze these sequence effects in AAB in more detail.

For induction of the AraC-P_{BAD} system in *E. coli*, typically a concentration in the range from 0.001 to 0.2% of L-arabinose is sufficient (Guzman et al. 1995; Narayanan et al. 2006). In this study with *G. oxydans* and plasmid pBBR1MCS-5-*araC*-P_{BAD}-*mNG*, a range of approximately 0.1 to 1% of L-arabinose was required for minimal and maximal induction. This range is much higher compared with *E. coli* and reflects an altered inducer responsiveness of the AraC-P_{BAD} system in *G. oxydans*. The GC-TOF-MS analysis demonstrated that L-arabinose was oxidized by the membrane-bound glucose DH in strain 621H. Nevertheless, in the multi-deletion strain BP.6 almost completely unable to oxidize L-arabinose, the L-arabinose responsiveness of the AraC-P_{BAD} system was similar as that of strain 621H. Thus, oxidation and the resulting decrease of L-arabinose did not reduce the responsiveness of the AraC-P_{BAD} system, although the oxidation product L-arabinonic acid did not act as an inducer on AraC. Therefore, usage of the AraC-P_{BAD} system in *G. oxydans* is not limited to strains that are unable to oxidize L-arabinose.

The lowered responsiveness of the AraC-P_{BAD} system in *G. oxydans* to L-arabinose might be caused by a very low uptake of the sugar into the cell. Attempts to improve uptake by expression of the *E. coli araE* gene encoding a secondary transporter for L-arabinose did not increase the responsiveness and even had a negative effect on the expression of the reporter gene *mNG* in our case. The reason for this result is unclear. It might be related to the co-expression of *araE* with *araC* resulting in a longer transcript than *araE* or *araC* mRNA alone. The longer transcript could be less stable or could form secondary structures that negatively affect the translation process, both yielding less AraC activator protein. Additional experiments with separate expression of *araE* from a constitutive promotor independent of *araC*-P_{BAD} or alternative arabinose transporter genes are necessary to elucidate the potential to improve the responsiveness of the *araC*-P_{BAD} system in *G. oxydans* (Khlebnikov et al. 2001). An endogenous L-arabinose transporter is not known in *G. oxydans* (Prust et al. 2005). A BLAST search with the *E. coli* AraE protein sequence in the *G. oxydans* proteome revealed three proteins with 46 to 56% sequence identity. GOX0808 (56% identity) is annotated as a galactose-proton symporter, GOX0649 (51% identity) as a sugar-proton symporter, and GOX1971 (46% identity) also as a galactose-proton symporter. One or several of these transporters might be promiscuous and poorly take up L-arabinose as a side reaction. No data are available on the substrates, properties, and physiological functions of these transporters.

With respect to the question if L-arabinose can be degraded within *G. oxydans* cells, our results in which this sugar was used in complex medium as sole supplement and as co-substrate with D-mannitol argue against this possibility. With L-arabinose alone strain 621H showed maximally one doubling while strain BP.6 showed no growth at all. This suggested that oxidation of L-arabinose somewhat contributed to generate energy in 621H for growth, yet not in BP.6 unable to oxidize L-arabinose. In *E. coli* and other bacteria, L-arabinose is catabolized *via* an initial isomerization to L-ribulose catalyzed by AraA, followed by phosphorylation to L-ribulose 5-phosphate catalyzed by AraB, and epimerization to D-xylulose 5-phosphate catalyzed by AraD (Englesberg 1961; Englesberg et al. 1962). In *G. oxydans*, homologs of AraA and AraD are absent and only a protein annotated as ribulokinase (GOX2186) showing 26% sequence identity to *E. coli* AraB was found. Therefore, L-arabinose taken up by *G. oxydans* is probably not converted to an intermediate like D-xylulose 5-phosphate that could be catabolized in the pentose phosphate pathway.

The oxidation of L-arabinose by *G. oxydans* 621H did not affect the inducibility of P_{BAD}, yet as a side effect the growth medium was much more acidified due to the formation of L-arabinonic acid. Therefore, when expressing target genes encoding pH-sensitive proteins in batch cultures without pH control, the use of a *G. oxydans* strain like BP.6 that lacks the ability to oxidize L-arabinose is beneficial to preserve the activity of the target protein in the stationary phase. In the case of strain 621H, additional acidification of the medium due to L-arabinonic acid formation resulted in a severe loss of UidA activity and mNG fluorescence in the stationary phase. Both, UidA activity and mNG fluorescence could be partly or almost fully recovered by solely transferring the cells into fresh medium adjusted to pH 6, indicating that at least the mNG protein was hardly degraded. The activity of the β-D-glucuronidase UidA is reduced by half when the pH is lowered to 4.3 compared with the activity in the optimal range of pH 5.0 to 7.5 (Jefferson et al. 1986). For mNG, it was shown that

between pH 5 and 6, three different protonated forms of the chromophore are present. When lowering the pH from 6 to 4, the acidic form becomes predominant, which decreases the fluorescence intensity by half and at pH 3 the mNG fluorescence is completely lost (Steiert et al. 2018). Our flow cytometry analysis revealed the occurrence of two subpopulations of 621H cells with reduced mNG fluorescence 26 h after induction in medium with a pH of 3.3. These two subpopulations might reflect a different progress in cytoplasmic acidification of 621H cells coping with pH 3.3 in the stationary phase. After resuspension in fresh medium with pH 6, mNG fluorescence was recovered and the two subpopulations merged into a single population. In strain BP.6, which is unable to oxidize L-arabinose, flow cytometry revealed that the acidification of the medium from pH 6 to 4.4 had only a marginal effect on mNG fluorescence. As the studies with isolated mNG demonstrated a strong decrease in fluorescence at pH 4.4 (Steiert et al. 2018), this result indicates that the intracellular pH in BP.6 cells must be higher than that in 621H cells. Bacteria have evolved various mechanisms for pH homeostasis in order to maintain the cytoplasmic pH in a range that enables survival and growth (reviewed in, for example, Baker-Austin and Dopson 2007; Follmann et al. 2009; Krulwich et al. 2011). For *G. oxydans*, the mechanisms of pH homeostasis have not yet been studied. We previously compared global gene expression of *G. oxydans* 621H cells grown at pH 4 and at pH 6 and observed 35 genes which were upregulated at pH 4 more than twofold and 37 genes that were downregulated more than twofold (Hanke et al. 2012). Obvious mechanisms for pH homeostasis could not be deduced from these data. In summary, the comparison of mNG fluorescence in strains 621H and BP.6 suggested that *G. oxydans* is well able to perform reasonable pH homeostasis at pH 4.4 and less able at pH 3.3. However, when maintaining the medium at pH 6, *e.g.*, by cultivation of the cells with pH control, the acidification due to L-arabinose oxidation can be avoided also in *G. oxydans* 621H, preserving the activity of proteins synthesized under the control of P_{BAD}. Together, our results demonstrate the functionality and potential of L-arabinose-inducible gene expression as a tool for *G. oxydans* and possibly also for other AAB.

Acknowledgments We are grateful to Lion Flachbart for providing the reporter mNeonGreen and for helpful discussions. We also thank Nick Wierckx or helpful discussion and Armin Ehrenreich for kindly providing *G. oxydans* strain BP.6 carrying multiple deletions of mDHs. For technical support, we thank Sabrina Derksen.

Availability of data and material The microarray data are accessible in NCBI's Gene Expression Omnibus through accession number GSE151596.

Authors' contributions PMF and TL selected the reporters and constructed the plasmids. PMF carried out all growth experiments to test strains with and without constructs and performed the data analysis. JG performed the GC-TOF-MS and data analysis. PMF and CS performed the FACS analysis and analyzed the data. PMF and MO performed the DASbox cultivations. TP designed and supervised the study. PMF, MB, and TP wrote the manuscript. All authors read and approved the final manuscript.

Funding Open Access funding enabled and organized by Projekt DEAL. We are grateful to the Federal Ministry of Education and Research (BMBF) for generous financial support of the project IMPRES (031B0370B). The funding organization did not influence the design of the study or collection, analysis, and interpretation of data, or writing the manuscript.

Compliance with ethical standards

Conflicts of interest The authors declare that they have no conflict of interest.

Ethical statement This article does not contain any studies with human participants or animals performed by any of the authors.

References

Ameyama M, Shinagawa E, Matsushita K, Adachi O (1981) D-fructose dehydrogenase of *Gluconobacter industrius*: purification, characterization, and application to enzymatic microdetermination of D-fructose. J Bacteriol 145(2):814–823

Baker-Austin C, Dopson M (2007) Life in acid: pH homeostasis in acidophiles. Trends Microbiol 15(4):165–171. https://doi.org/10.1016/j.tim.2007.02.005

Brunelle A, Schleif R (1989) Determining residue-base interactions between AraC-protein and *araI* DNA. J Mol Biol 209(4):607–622. https://doi.org/10.1016/0022-2836(89)90598-6

Casadaban MJ (1976) Transposition and fusion of the *lac* genes to selected promoters in *Escherichia coli* using bacteriophage lambda and Mu. J Mol Biol 104(3):541–555. https://doi.org/10.1016/0022-2836(76)90119-4

Chen R (2012) Bacterial expression systems for recombinant protein production: *E. coli* and beyond. Biotechnol Adv 30(5):1102–1107. https://doi.org/10.1016/j.biotechadv.2011.09.013

Connell ND (2001) Expression systems for use in actinomycetes and related organisms. Curr Opin Biotechnol 12(5):446–449. https://doi.org/10.1016/S0958-1669(00)00243-3

Dilworth MV, Piel MS, Bettaney KE, Ma P, Luo J, Sharples D, Poyner DR, Gross SR, Moncoq K, Henderson PJF, Miroux B, Bill RM (2018) Microbial expression systems for membrane proteins. Methods 147:3–39. https://doi.org/10.1016/j.ymeth.2018.04.009

Englesberg E (1961) Enzymatic characterization of 17 L-arabinose negative mutants of *Escherichia coli*. J Bacteriol 81:996–1006

Englesberg E, Anderson RL, Weinberg R, Lee N, Hoffee P, Huttenhauer G, Boyer H (1962) L-Arabinose-sensitive, L-ribulose 5-phosphate 4-epimerase-deficient mutants of *Escherichia coli*. J Bacteriol 84:137–146

Evans JC, Mizrahi V (2015) The application of tetracycline regulated gene expression systems in the validation of novel drug targets in *Mycobacterium tuberculosis*. Front Microbiol 6:812. https://doi.org/10.3389/fmicb.2015.00812

Florea M, Hagemann H, Santosa G, Abbott J, Micklem CN, Spencer-Milnes X, Garcia LD, Paschou D, Lazenbatt C, Kong DZ, Chughtai H, Jensen K, Freemont PS, Kitney R, Reeve B, Ellis T (2016) Engineering control of bacterial cellulose production using a genetic toolkit and a new cellulose-producing strain. Proc Natl Acad Sci 113(24):E3431–E3440. https://doi.org/10.1073/pnas.1522985113

Follmann M, Ochrombel I, Kramer R, Trotschel C, Poetsch A, Ruckert C, Huser A, Persicke M, Seiferling D, Kalinowski J, Marin K (2009) Functional genomics of pH homeostasis in *Corynebacterium glutamicum* revealed novel links between pH response, oxidative stress, iron homeostasis and methionine synthesis. BMC Genomics 10. https://doi.org/10.1186/1471-2164-10-621

Forstner M, Leder L, Mayr LM (2007) Optimization of protein expression systems for modern drug discovery. Expert Rev Proteomics 4(1):67–78. https://doi.org/10.1586/14789450.4.1.67

Gibson DG, Young L, Chuang RY, Venter JC, Hutchison CA, Smith HO (2009) Enzymatic assembly of DNA molecules up to several hundred kilobases. Nat Methods 6(5):343–U41. https://doi.org/10.1038/Nmeth.1318

Gruber S, Schwab H, Koefinger P (2015) Versatile plasmid-based expression systems for Gram-negative bacteria-General essentials exemplified with the bacterium *Ralstonia eutropha* H16. New Biotechnol 32(6):552–558. https://doi.org/10.1016/j.nbt.2015.03.015

Gupta A, Singh VK, Qazi GN, Kumar A (2001) *Gluconobacter oxydans*: its biotechnological applications. J Mol Microbiol Biotechnol 3(3):445–456

Guzman LM, Belin D, Carson MJ, Beckwith J (1995) Tight regulation, modulation, and high-level expression by vectors containing the arabinose P_{BAD} promoter. J Bacteriol 177(14):4121–4130. https://doi.org/10.1128/jb.177.14.4121-4130.1995

Hanahan D (1983) Studies on transformation of *Escherichia coli* with plasmids. J Mol Biol 166(4):557–580

Hanke T, Richhardt J, Polen T, Sahm H, Bringer S, Bott M (2012) Influence of oxygen limitation, absence of the cytochrome bc(1) complex and low pH on global gene expression in *Gluconobacter oxydans* 621H using DNA microarray technology. J Biotechnol 157(3):359–372. https://doi.org/10.1016/j.jbiotec.2011.12.020

Hekmat D, Bauer R, Fricke J (2003) Optimization of the microbial synthesis of dihydroxyacetone from glycerol with *Gluconobacter oxydans*. Bioprocess Biosyst Eng 26(2):109–116. https://doi.org/10.1007/s00449-003-0338-9

Hentschel E, Will C, Mustafi N, Burkovski A, Rehm N, Frunzke J (2013) Destabilized eYFP variants for dynamic gene expression studies in *Corynebacterium glutamicum*. Microb Biotechnol 6(2):196–201. https://doi.org/10.1111/j.1751-7915.2012.00360.x

Hölscher T, Weinert-Sepalage D, Görisch H (2007) Identification of membrane-bound quinoprotein inositol dehydrogenase in *Gluconobacter oxydans* ATCC 621H. Microbiology 153(Pt 2):499–506. https://doi.org/10.1099/mic.0.2006/002196-0

Jefferson RA, Burgess SM, Hirsh D (1986) Beta-glucuronidase from *Escherichia coli* as a gene-fusion marker. Proc Natl Acad Sci 83(22):8447–8451. https://doi.org/10.1073/pnas.83.22.8447

Kallnik V, Meyer M, Deppenmeier U, Schweiger P (2010) Construction of expression vectors for protein production in *Gluconobacter oxydans*. J Biotechnol 150(4):460–465. https://doi.org/10.1016/j.jbiotec.2010.10.069

Khlebnikov A, Datsenko KA, Skaug T, Wanner BL, Keasling JD (2001) Homogeneous expression of the P(BAD) promoter in *Escherichia coli* by constitutive expression of the low-affinity high-capacity AraE transporter. Microbiology 147(Pt 12):3241–3247. https://doi.org/10.1099/00221287-147-12-3241

Kiefler I, Bringer S, Bott M (2015) SdhE-dependent formation of a functional *Acetobacter pasteurianus* succinate dehydrogenase in *Gluconobacter oxydans*–a first step toward a complete tricarboxylic acid cycle. Appl Microbiol Biotechnol 99(21):9147–9160. https://doi.org/10.1007/s00253-015-6972-8

Kiefler I, Bringer S, Bott M (2017) Metabolic engineering of *Gluconobacter oxydans* 621H for increased biomass yield. Appl Microbiol Biotechnol 101(13):5453–5467. https://doi.org/10.1007/s00253-017-8308-3

Korner H, Sofia HJ, Zumft WG (2003) Phylogeny of the bacterial superfamily of Crp-Fnr transcription regulators: exploiting the metabolic spectrum by controlling alternative gene programs. FEMS Microbiol Rev 27(5):559–592. https://doi.org/10.1016/S0168-6445(03)00066-4

Kovach ME, Elzer PH, Hill DS, Robertson GT, Farris MA, Roop RM 2nd, Peterson KM (1995) Four new derivatives of the broad-host-range cloning vector pBBR1MCS, carrying different antibiotic-resistance cassettes. Gene 166(1):175–176. https://doi.org/10.1016/0378-1119(95)00584-1

Kranz A, Vogel A, Degner U, Kiefler I, Bott M, Usadel B, Polen T (2017) High precision genome sequencing of engineered *Gluconobacter oxydans* 621H by combining long nanopore and short accurate Illumina reads. J Biotechnol 258:197–205. https://doi.org/10.1016/j.jbiotec.2017.04.016

Kranz A, Steinmann A, Degner U, Mengus-Kaya A, Matamouros S, Bott M, Polen T (2018) Global mRNA decay and 23S rRNA fragmentation in *Gluconobacter oxydans* 621H. BMC Genomics 19(1):753. https://doi.org/10.1186/s12864-018-5111-1

Krulwich TA, Sachs G, Padan E (2011) Molecular aspects of bacterial pH sensing and homeostasis. Nat Rev Microbiol 9(5):330–343. https://doi.org/10.1038/nrmicro2549

Mamlouk D, Gullo M (2013) Acetic acid bacteria: physiology and carbon sources oxidation. Indian J Microbiol 53(4):377–384. https://doi.org/10.1007/s12088-013-0414-z

Merfort M, Herrmann U, Bringer-Meyer S, Sahm H (2006a) High-yield 5-keto-D-gluconic acid formation is mediated by soluble and membrane-bound gluconate-5-dehydrogenases of *Gluconobacter oxydans*. Appl Microbiol Biotechnol 73(2):443–451. https://doi.org/10.1007/s00253-006-0467-6

Merfort M, Herrmann U, Ha SW, Elfari M, Bringer-Meyer S, Gorisch H, Sahm H (2006b) Modification of the membrane-bound glucose oxidation system in *Gluconobacter oxydans* significantly increases gluconate and 5-keto-D-gluconic acid accumulation. Biotechnol J 1(5):556–563. https://doi.org/10.1002/biot.200600032

Meyer M, Schweiger P, Deppenmeier U (2013) Effects of membrane-bound glucose dehydrogenase overproduction on the respiratory chain of *Gluconobacter oxydans*. Appl Microbiol Biotechnol 97(8):3457–3466. https://doi.org/10.1007/s00253-012-4265-z

Mientus M, Kostner D, Peters B, Liebl W, Ehrenreich A (2017) Characterization of membrane-bound dehydrogenases of *Gluconobacter oxydans* 621H using a new system for their functional expression. Appl Microbiol Biotechnol 101(8):3189–3200. https://doi.org/10.1007/s00253-016-8069-4

Miller JH (1992) A short course in bacterial genetics. Cold Spring Harbor Laboratory Press, Cold Spring Harbor

Narayanan N, Xu Y, Chou CP (2006) High-level gene expression for recombinant penicillin acylase production using the *araB* promoter system in *Escherichia coli*. Biotechnol Prog 22(6):1518–1523. https://doi.org/10.1021/bp060135u

Paczia N, Nilgen A, Lehmann T, Gatgens J, Wiechert W, Noack S (2012) Extensive exometabolome analysis reveals extended overflow metabolism in various microorganisms. Microb Cell Factories 11:122. https://doi.org/10.1186/1475-2859-11-122

Pappenberger G, Hohmann HP (2014) Industrial production of L-ascorbic acid (vitamin C) and D-isoascorbic acid. Adv Biochem Eng Biotechnol 143:143–188. https://doi.org/10.1007/10_2013_243

Parachin NS, Mulder KC, Viana AAB, Dias SC, Franco OL (2012) Expression systems for heterologous production of antimicrobial peptides. Peptides 38(2):446–456. https://doi.org/10.1016/j.peptides.2012.09.020

Peters B, Mientus M, Kostner D, Junker A, Liebl W, Ehrenreich A (2013) Characterization of membrane-bound dehydrogenases from *Gluconobacter oxydans* 621H *via* whole-cell activity assays using multideletion strains. Appl Microbiol Biotechnol 97(14):6397–6412. https://doi.org/10.1007/s00253-013-4824-y

Prust C, Hoffmeister M, Liesegang H, Wiezer A, Fricke WF, Ehrenreich A, Gottschalk G, Deppenmeier U (2005) Complete genome sequence of the acetic acid bacterium *Gluconobacter oxydans*. Nat Biotechnol 23(2):195–200. https://doi.org/10.1038/nbt1062

Saito Y, Ishii Y, Hayashi H, Imao Y, Akashi T, Yoshikawa K, Noguchi Y, Soeda S, Yoshida M, Niwa M, Hosoda J, Shimomura K (1997) Cloning of genes coding for L-sorbose and L-sorbosone dehydrogenases from *Gluconobacter oxydans* and microbial production of 2-keto-L-gulonate, a precursor of L-ascorbic acid, in a recombinant *G. oxydans* strain. Appl Environ Microbiol 63(2):454–460

Sambrook J, Fritsch EF, Maniatis T (1989) Molecular cloning: a laboratory manual. Cold Spring Harbor Laboratory Press, Cold Spring Harbor

Schleif R (2010) AraC protein, regulation of the L-arabinose operon in *Escherichia coli*, and the light switch mechanism of AraC action. FEMS Microbiol Rev 34(5):779–796. https://doi.org/10.1111/j.1574-6976.2010.00226.x

Schleyer U, Bringer-Meyer S, Sahm H (2008) An easy cloning and expression vector system for *Gluconobacter oxydans*. Int J Food Microbiol 125(1):91–95. https://doi.org/10.1016/j.ijfoodmicro.2007.04.016

Schnappinger D, Ehrt S (2014) Regulated expression systems for mycobacteria and their applications. Microbiol Spectr 2(1). https://doi.org/10.1128/microbiolspec.MGM2-0018-2013

Shaner NC, Lambert GG, Chammas A, Ni Y, Cranfill PJ, Baird MA, Sell BR, Allen JR, Day RN, Israelsson M, Davidson MW, Wang J (2013) A bright monomeric green fluorescent protein derived from *Branchiostoma lanceolatum*. Nat Methods 10(5):407–409. https://doi.org/10.1038/nmeth.2413

Simon R, Priefer U, Pühler A (1983) A broad host range mobilization system for *in vivo* genetic-engineering - Transposon mutagenesis in Gram-negative bacteria. Bioresour Technol 1(9):784–791. https://doi.org/10.1038/nbt1183-784

Soisson SM, MacDougall-Shackleton B, Schleif R, Wolberger C (1997) Structural basis for ligand-regulated oligomerization of AraC. Science 276(5311):421–425. https://doi.org/10.1126/science.276.5311.421

Steiert F, Petrov EP, Schultz P, Schwille P, Weidemann T (2018) Photophysical behavior of mNeonGreen, an evolutionarily distant green fluorescent protein. Biophys J 114(10):2419–2431. https://doi.org/10.1016/j.bpj.2018.04.013

Teh MY, Ooi KH, Teo SXD, Bin Mansoor ME, Lim WZS, Tan MH (2019) An expanded synthetic biology toolkit for gene expression control in *Acetobacteraceae*. ACS Synth Biol 8(4):708–723. https://doi.org/10.1021/j.acssynbio.8b00168

Terpe K (2006) Overview of bacterial expression systems for heterologous protein production: from molecular and biochemical fundamentals to commercial systems. Appl Microbiol Biotechnol 72(2):211–222. https://doi.org/10.1007/s00253-006-0465-8

Tkac J, Navratil M, Sturdik E, Gemeiner P (2001) Monitoring of dihydroxyacetone production during oxidation of glycerol by immobilized *Gluconobacter oxydans* cells with an enzyme biosensor. Enzym Microb Technol 28(4-5):383–388

Tonouchi N, Sugiyama M, Yokozeki K (2003) Construction of a vector plasmid for use in *Gluconobacter oxydans*. Biosci Biotechnol Biochem 67(1):211–213. https://doi.org/10.1271/bbb.67.211

Valero F (2012) Heterologous expression systems for lipases: A review. Methods Mol Biol 861:161–178. https://doi.org/10.1007/978-1-61779-600-5_11

Wang EX, Ding MZ, Ma Q, Dong XT, Yuan YJ (2016) Reorganization of a synthetic microbial consortium for one-step vitamin C fermentation. Microb Cell Factories 15:21. https://doi.org/10.1186/s12934-016-0418-6

Zhang L, Lin JP, Ma YS, Wei DZ, Sun M (2010) Construction of a novel shuttle vector for use in *Gluconobacter oxydans*. Mol Biotechnol 46(3):227–233. https://doi.org/10.1007/s12033-010-9293-2

2.2 Production of L-arabinonic acid from renewable L-arabinose by the acetic acid bacterium *Gluconobacter oxydans*

Fricke, P. M., Hartmann, R., Wirtz, A., Bott, M., & Polen, T. Production of L-arabinonic acid from renewable L-arabinose by the acetic acid bacterium *Gluconobacter oxydans*. **Submitted to Bioresource Technology.**

Authors' contributions:
PMF carried out the production experiments and analyzed the data. RH and AW performed the metabolite analysis. TP designed and supervised the study. PMF, MB and TP wrote and revised the manuscript. All authors read and approved the final version.

Overall contribution PF: 85%

Production of L-arabinonic acid from renewable L-arabinose by the acetic acid bacterium *Gluconobacter oxydans*

Philipp Moritz Fricke[1], Rudolf Hartmann[2], Astrid Wirtz[1], Michael Bott[1] and Tino Polen[1]*

[1] IBG-1: Biotechnology, Institute of Bio- and Geosciences, Forschungszentrum Jülich GmbH, 52425 Jülich, Germany

[2] IBI-7: Structural Biochemistry, Institute of Biological Information Processing, Forschungszentrum Jülich GmbH, 52425 Jülich, Germany

Running title: Production of L-arabinonic acid using *Gluconobacter oxydans*

SUBJECT CLASSIFICATION FOR BIORESOURCE TECHNOLOGY

Subject classification: 60.070 Organic acids

ORCID:	Philipp Moritz Fricke	orcid.org/0000-0002-3507-4881
ORCID:	Rudolf Hartmann	orcid.org/0000-0001-7807-6273
ORCID	Astrid Wirtz	orcid.org/0000-0003-2159-3717
ORCID:	Michael Bott	orcid.org/0000-0002-4701-8254
ORCID:	Tino Polen	orcid.org/0000-0002-0065-3007

*** for correspondence:** Dr. Tino Polen
e-mail: t.polen@fz-juelich.de
phone: +49 (0)2461 61 6205
fax: +49 (0)2461 61 2710

Co-authors email address

Philipp Fricke	p.fricke@fz-juelich.de
Rudolf Hartmann	r.hartmann@fz-juelich.de
Astrid Wirtz	a.wirtz@fz-juelich.de
Michael Bott	m.bott@fz-juelich.de

Keywords: L-arabinonic acid
L-arabonate
L-arabinose
membrane-bound dehydrogenase
glucose dehydrogenase

Abstract

L-Arabinonic acid is a five carbon sugar acid valuable for various potential applications. Based on previous observations that the acetic acid bacterium *Gluconobacter oxydans* oxidizes L-arabinose in the periplasm by the membrane-bound glucose dehydrogenase yielding L-arabinonic acid, we tested the ability of *G. oxydans* for high-level L-arabinonic acid production. In fed-batch shake flasks without pH control, maximal product titers of 17.4 g/L L-arabinonic acid and 5.7 g/L L-arabino-1,4-lactone were obtained, yet a large fraction of L-arabinose remained unused. Strong acidification of the growth medium prevented further substrate oxidation. In contrast, in pH 6-controlled fed-batch bioreactors, up to 120 g/L L-arabinonic acid and 13 g/L of its 1,4-lactone could be obtained with strain 621H after 144 h. This combined high product titer (133 g/L or 814 mM) with a space-time yield of 1.08 g/L/h triples the titers reported before with *Saccharomyces cerevisiae* and *Escherichia coli* and makes *G. oxydans* a very promising host for high-level production of L-arabinonic acid.

1. Introduction

Arabinonic acid (arabonate) is a five carbon sugar acid (predicted pK_a 3.39) that can serve a variety of purposes. In the patent literature, it is described that arabinonic acid or its lactone could be useful for electrolytic decarboxylation to produce erythrose and erythritol (Genders and Stapley 2016; Stapley and Genders 2016; Stapley et al. 2011), for producing polymer variants for different applications (Ohsumi and Fujii 2018; Okawa and Nishijima 2014; Van Es et al. 2017; Weng et al. 2018), for composite cements and semiconductor processing materials (Lee 2013; Yamazaki 2007), for medical applications (Okuda and Shimizu 2016; Sanai and Tanaka 2010; Sanai et al. 2007), and for cosmetics (Hasebe and Yamada 2005; Iwasaki et al. 2004; Kawasaki et al. 2005; Maaß et al. 2013). L-Arabinonic acid can also be used to produce L-1,2,4-butanetriol (Niu et al. 2003), which is a precursor of the propellant 1,2,4-butanetriol trinitrate, an important plasticizer for nitrate ester plasticized polyether and useful to improve mechanical properties and reliability of nitroglycerin (Pei et al. 2017).

Arabinonic acid can be formed chemo-catalytically, *e.g.* by oxidation of arabinose on gold and palladium catalysts, by oxidation of trehalose with *N*-bromoacetamide in the presence of suitable rhodium catalysts, by oxidation of lactose with potassium iodate in the presence of suitable iridium catalysts, or by oxidation of glucose with silver(III) periodate in the presence of suitable ruthenium-osmium catalysts (Correia et al. 2019; Kusema et al. 2010; Singh et al. 2014; Smolentseva et al. 2011).(Kusema et al. 2010; Sataraddi and Nandibewoor 2013).

Enzymatically, arabinonic acid can be formed by arabinose-oxidizing enzymes from L-arabinose-metabolizing bacteria, which typically are intracellular dehydrogenases that use $NAD(P)^+$ as a cofactor. Here, the carbon and energy source L-arabinose is oxidized to L-arabino-1,4-lactone, which then is hydrolyzed in a spontaneous reaction or by a lactonase to yield L-arabinonic acid (Dilworth et al. 1986; Duncan 1979; Johnsen et al. 2013; Mathias et al. 1989; Novick and Tyler 1982; Seiboth and Metz 2011; Watanabe et al. 2006a; Watanabe et al. 2006b; Weimberg 1959; Weimberg and Doudoroff 1955). For the microbial production of L-arabinonic acid from L-arabinose, selected L-arabinose dehydrogenases were tested with *Saccharomyces cerevisiae*. With the L-arabinose / D-galactose 1-dehydrogenase AraDH from *Rhizobium leguminosarum* expressed in *S. cerevisiae*, a titer of 18 g/L L-arabinonic acid corresponding to a yield 86% was achieved within 118 h in a pH 5.5-controlled 0.5 L batch fermenter (Aro-Karkkainen et al. 2014). In an engineered *E. coli* strain with an inactivated L-arabinose metabolism, an L-arabinonic acid titer of 43.9 g/L was achieved with 40 g/L L-arabinose within 36 h in a pH 7-controlled 5 L batch fermenter by expressing the $NAD(P)^+$-dependent L-arabinose dehydrogenase AraDH from *Azospirillum brasilense* (Liu et al. 2014).

In contrast to the intracellular $NAD(P)^+$-dependent oxidation of L-arabinose, the periplasmic oxidation of L-arabinose provides some advantages. Substrate import into the cytoplasm and product export out of the cytoplasm, which may limit the production efficiency,

are not required. Periplasmic enzymes oxidizing sugars including arabinose to the corresponding aldonic acids occur in acetic acid bacteria (AAB), such as *Gluconobacter oxydans* (Matsutani and Yakushi 2018; Peters et al. 2013). *G. oxydans* is well-established in industry for oxidative biotransformations of carbohydrates to produce *e.g.* L-sorbose, a precursor of vitamin C, dihydroxyacetone, a tanning agent, or 6-amino-L-sorbose, a precursor of the antidiabetic drug miglitol (Ameyama et al. 1981; Gupta et al. 2001; Hekmat et al. 2003; Saito et al. 1997; Tkac et al. 2001; Wang et al. 2016). This bacterium catalyzes the regio- and stereoselective periplasmic oxidation of many substrates, including sugars and sugar alcohols, by membrane-bound dehydrogenases with subsequent release of the products into the medium *via* porins in the outer membrane (Mamlouk and Gullo 2013; Mientus et al. 2017; Pappenberger and Hohmann 2014).

For *G. oxydans* 621H, L-arabinose was shown to be oxidized in the periplasm by the membrane-bound glucose dehydrogenase GdhM (GOX0265) yielding L-arabinonic acid, while the cytosolic glucose dehydrogenase GdhS (GOX2015) appeared to be negligible for this reaction (Fricke et al. 2020; Mientus et al. 2017; Peters et al. 2013). Recently, the potential of *G. oxydans* for complete conversion of lignocellulose-derived non-glucose sugars into corresponding sugar acids was reported. A fast and complete conversion of the non-glucose sugars from corn stover, including 10 g/L L-arabinose, into the corresponding sugar acids was observed in pH-controlled bioreactors (Yao et al. 2017).

In this study, we tested the ability of *G. oxydans* 621H to produce L-arabinonic acid at higher levels from pure L-arabinose stock. Control of the medium pH was crucial to achieve long-term formation of L-arabinonic acid, as it caused a strong acidification of the medium. Plasmid-based overexpression of *gdhM*, although having a negative impact on growth and robustness of the cells, improved the biomass-specific production parameters. The highest product titers were obtained with the *G. oxydans* 621H type strain without *gdhM* overexpression. In pH-controlled fed-batch bioreactors, 120 g/L L-arabinonic acid and 13 g/L of its 1,4-lactone were accumulated, which more than tripled the product titers previously reported for *E. coli* and *S. cerevisiae*.

2. Material and methods

2.1. Bacterial strains, plasmids, medium and shake flasks cultivations

Strains and plasmids used in this study are listed in Table 1. *G. oxydans* was cultivated in D-mannitol medium containing 4% (w/v) D-mannitol, 5 g L^{-1} yeast extract, 1 g L^{-1} KH_2PO_4, 1 g L^{-1} $(NH_4)_2SO_4$, 2.5 g L^{-1} $MgSO_4$ x 7 H_2O at 30°C and 180 rpm. As a precaution to prevent bacterial contamination, all media were routinely supplemented with 50 µg mL^{-1} cefoxitin. In cultivations of *G. oxydans* harboring plasmid pMM4a-mGDH, additionally 50 µg mL^{-1} kanamycin was added to the medium (Mientus et al. 2017). For shake flask cultivations, cells

were inoculated from pre-cultures to an initial optical density at 600 nm (OD_{600}) of 0.3 (UV-1800, Shimadzu), and grown in 500 mL shaking flasks with three baffles containing 60 mL D-mannitol medium.

2.2. Quantification of L-arabinose, L-arabinonic acid and L-arabinolacton

For quantification of L-arabinose, L-arabinonic acid, and L-arabino-1,4-lactone by nuclear magnetic resonance (NMR) spectroscopy, supernatant samples were diluted in a 1:10 ratio with miliQ water. Furthermore, 10% (v/v) D_2O was added to generate an NMR lock signal and 5 mM dimethyl sulfoxide (DMSO) as a reference for quantification of reactants. One-dimensional ^1H NMR spectra were acquired with a Bruker AVANCE III HD 600 spectrometer equipped with a 5 mm HCN TCI cryo-probe operating at 599 MHz (14.1 Tesla). The ^1H NMR data were obtained at 25 °C sample temperature and with the following acquisition parameters: presaturation time of 30 seconds for water suppressing, 8 transients, 4800 Hz sweep width corresponding to 4 seconds of acquisition time and 38362 time domain data points. Spectra were processed and analyzed using Bruker Topspin version 3.6.2. After Fourier transformation, zerofilling to 512K data points and baseline correction, the nonoverlapping signals of L-arabinose, L-arabinonic acid and L-arabino-1,4-lactone were integrated. The concentration of the three compounds was calculated by using the 5 mM DMSO reference integral.

2.3. Fed-batch in pH-controlled bioreactor cultivation conditions

DASbox® mini-bioreactors were used for cultivations in D-mannitol medium. Bioreactors controlled by DASware software (Eppendorf) were used in combination with two 6-bladed Rushton-type impellers, pH- (EasyFerm Plus K8 120, Hamilton), O_2- (InPro® 6800 series, Mettler-Toledo) and temperature-sensors. For the cultivations, 385 mL glass vessels were filled with 100 mL 4% (w/v) D-mannitol medium and cells were grown at 30°C from an initial OD_{600} of 0.3. Starting with 500 rpm agitation frequency and a gas flow rate of 6 sl h^{-1} purged directly into the medium, a three step cascade was applied to maintain the dissolved oxygen tension ≥30%. Firstly, agitation was gradually increased to 1,200 rpm. Secondly, the percentage of oxygen in the air supply was up-regulated to a maximum of 80% (v/v), and finally the air flow rate was automatically elevated. During the entire cultivation, pH 6 was maintained by automatic titration with a 3 M KOH solution. Samples for off-line monitoring of growth, substrate consumption and product formation were taken in intervals and treated as described above. Supernatants were stored at -20 °C until the NMR analysis of substrates and products. For the calculations of biomass-specific product titers, a correlation factor of 0.32 g cell dry weight (cdw)/L for a culture with an OD_{600} of 1 was used (Richhardt et al. 2012).

3. Results and discussion

3.1. L-Arabinonic acid formation in shake flasks using simple fed-batch mode is pH-limited

It has already been shown that *G. oxydans* 621H can oxidize L-arabinose to L-arabinonic acid by the membrane-bound glucose dehydrogenase GdhM (GOX0265), while the cytosolic glucose dehydrogenase GdhS (GOX2015) appeared not relevant for this conversion (Fricke et al. 2020; Mientus et al. 2017; Peters et al. 2013). In order to elucidate the potential of *G. oxydans* to form L-arabinonic acid at higher titers from renewable L-arabinose, in first experiments the 621H strain was cultivated in D-mannitol medium supplemented with 10 g/L, 40 g/L, and 80 g/L L-arabinose. After 24 h, a feed of 20 g/L, 40 g/L, and 80 g/L L-arabinose were added using a 50% (w/v) L-arabinose stock solution. Under all conditions, the cells grew very similar as in cultures without L-arabinose supplement. With 80 g/L L-arabinose only a slight growth retardation was observed, demonstrating that the strain is able to grow in the presence of higher L-arabinose concentrations (Fig. 1a). The remaining L-arabinose titers after 24 h before feed and after 48 h indicated that L-arabinose consumption was decreased or even disabled at pH values below 2.7 (Fig. 1a, b). Without a pH control in the shake flasks, the formation of L-arabinonic acid with a pK_a of 3.39 (https://hmdb.ca/metabolites/HMDB0000539) led to a strong acidification of the medium. When grown with initially 10 g/L L-arabinose and fed with 20 g/L L-arabinose after 24 h, the pH was 2.8 (24 h) and finally 2.7 (48 h). Only in this condition the L-arabinonic acid titer further increased in the fed-phase after 24 h. In contrast, in the cultures with 40 g/L and 80 g/L L-arabinose exhibiting pH values close below 2.7, the product titer of L-arabinonic acid showed no further increase after 24 h despite the substrate feed (Fig. 1c). The maximal L-arabinonic acid concentration was 17.4 g/L after 24 h in the cultures with 80 g/L arabinose. The NMR analysis also revealed the presence of L-arabino-1,4-lactone (Fig. 2). The highest titer of the 1,4-lactone was up to 5.7 g/L after 48 h in the cultures with 80 g/L arabinose (Fig. 1d). The somewhat lower L-arabinonic acid titers at 48 h compared to the 24 h value resulted from the 10 mL volume increase due to the feed at 24 h and some acid was likely converted in this acidic conditions to its 1,4-lactone, since these levels were similar at 24 h and 48 h despite the volume increase. Based on the concentrations measured by NMR and the volume changes, the carbon balance sum of the final amounts of residual substrate and the two products corresponded approximately to 120%, 110% and 100% of the amount of substrate provided in total (Fig. 1e). This suggested that the metabolite levels were somewhat overestimated by NMR. Then, the data of the high L-arabinose condition (80+80 g/L) could indicate a carbon gap of 10% to 20% potentially resulting from nonspecific formation of unknown byproducts at higher L-arabinose or L-arabinonic acid titers. However, according to the NMR data no signals suggesting further compounds formed as nonspecific byproducts could be found. At the end of the cultivation (48 h), the molar sum of the two products corresponded to approximately 42%, 19%, and 20% of the amount of 10+20 g/L, 40+40 g/L, and 80+80 g/L L-arabinose provided.

For the D-galactose 1-dehydrogenase annotated in *R. leguminosarum* and later termed L-arabinose / D-galactose 1-dehydrogenase AraDH, the L-arabino-1,4-lactone was reported to be the stable oxidation product, which was assumed to then open slowly at neutral pH to the linear form L-arabonate (Aro-Karkkainen et al. 2014). *Vice versa*, the 1,4-lactone can be formed from the linear form in acidic pH conditions, which we also observed with L-arabinonic acid standard in pH 3 (Fig. 2), and which was reported before (Aro-Karkkainen et al. 2014). In case of GdhM from *G. oxydans*, the 1,4-lactone is unlikely to be the direct oxidation product of the reaction. In the acidic pH conditions of the shake flasks, the 1,4-lactone would not open slowly to the linear form. Therefore, the linear form is likely the direct oxidation product of the GdhM reaction since L-arabinonic acid was the most of the two products in the acidic pH conditions and even increased between 24 h and 48 h in the condition with 10+20 g/L L-arabinose at pH 2.8 to 2.7, yet now below pH 2.7 likely due to the pH-sensitivity of GdhM. The 1,4-lactone was formed rather due to the acidic pH conditions from the linear form.

3.2. Production of L-arabinonic acid in pH-controlled fed-batch bioreactors

As the strong acidification of the medium below pH 2.7 prevented further arabinose oxidation, we next tested L-arabinonic acid production in pH-controlled fed-batch experiments using mannitol medium. pH 6 was reported be optimal for the membrane-bound glucose DH GdhM (Matsushita et al. 1994). Besides *G. oxydans* 621H, we also tested a derivative transformed with plasmid pMM4a-mGDH for constitutive expression of the membrane-bound glucose dehydrogenase gene *gdhM* (Mientus et al. 2017). In pH-controlled bioreactors, strain 621H and strain 621H / pMM4a-mGDH were grown in D-mannitol medium initially supplemented with 40 g/L and 80 g/L L-arabinose. Every 24 h, stock solution with L-arabinose dissolved in D-mannitol-free complex medium was fed to add another 40 g/L or 80 g/L of substrate (corresponding to the initial culture volume). The feed and the KOH titration for keeping the pH at 6 increased the culture volume despite some volume reduction by taking samples for analysis. Overall, due to increased base titration in the cultures with 80 g/L L-arabinose (Table 2), their final culture volume were higher than that of the cultures with 40 g/L L-arabinose (Fig. 3a). As expected for pH-controlled conditions, at the end of the exponential phase strain 621H reached an almost two-fold higher final OD_{600} after 24 h with both 40 g/L (OD_{600} = 7.0 ± 0.3) and 80 g/L L-arabinose (OD_{600} = 7.5 ± 0.3) in D-mannitol medium compared to the shake flask cultivations without pH control (Fig. 3b). In contrast, after 24 h strain 621H / pMM4a-mGDH reached a much lower OD_{600} of 4.8 ± 0.3 with 40 g/L L-arabinose and only 2.3 with 80 g/L L-arabinose. This indicated that the overexpression of *gdhM* and possibly the presence of kanamycin in the medium were detrimental for growth. Kanamycin or the presence of its resistance cassette cause a strong change of the cell morphology of *G. oxydans*, suggesting a kind of stress to the cells (Fricke et al. 2021b). Apparently, the

constitutive overproduction of the membrane-bound GdhM protein in combination with the use of kanamycin was detrimental for cell membrane integrity under osmotic stress conditions. In fact, even without L-arabinose and base titration, we observed differences to the plasmid-free 621H strain when handling the pre-cultures of the pMM4a-mGDH-carrying strain. Notably, sedimentation of the cells by centrifugation was more difficult and the obtained cell pellets were much more loose and slimy compared to the 621H reference strain. In this context and as described above, we frequently observed lower initial OD_{600} values than expected by calculation when inoculating new cultures from resuspended pre-culture pellets suggesting some extent of cell lysis. In the future, conditionally timed and tuned overexpression of *gdhM* could possibly avoid these detrimental effects. Recently, two systems became available for tunable induction of target gene expression in *G. oxydans* (Fricke et al. 2020; Fricke et al. 2021).

When 40 g/L L-arabinose was supplemented, it was always almost fully consumed within 24 h by both strains, while the 80 g/L feed resulted in higher levels of residual substrate at the end of day 3 and later (Fig. 3c). These residual substrate levels in the later stage (≥72 h) were much higher in the cultures of the *gdhM* overexpression strain. Since even with 80 g/L substrate there were no relevant residual L-arabinose titers 24 h after a feed until the end of day 2 (48 h), the much lower biomass (OD_{600}) of the *gdhM* overexpression strain per se was not limiting the L-arabinose oxidation in the first 48 h of the fermentation. Rather, some cell instability and/or (osmotic) stress sensitivity of the *gdhM* overexpression strain was likely limiting the L-arabinose oxidation from 48 h onward and strain 621H without pMM4a-mGDH and with a higher biomass (OD_{600}) finally outperformed the sensitive *gdhM* overexpression strain with respect to the absolute product titers. Generally, for both strains the product titers were higher with 80 g/L compared to 40 g/L L-arabinose feed (Fig. 3d, e). In the 80 g/L condition, the *gdhM* overexpression strain produced a much higher 1,4-lactone level with transiently up to 54 g/L. Since the medium was pH 6-controlled, the much higher transient levels of the 1,4-lactone should have resulted from the open acid form by a lactonizing enzyme activity either released from the more sensitive cells of the overexpression strain upon partial cell lysis or due to increased metabolite exchange through the impaired cell membrane. These 1,4-lactone titers peaking from day 2 to 3 in the 80 g/L feed condition continuously decreased until the end of the fermentation. For the *gdhM* overexpression strain, this decrease cannot be explained alone by increasing culture volumes caused by base titrations and the third substrate feeding. The slow opening of the lactone at close-to-neutral pH could only be effective if the assumed lactonizing activity became more and more inactive. Moreover, in view of the L-arabinose consumption indicated by decreasing residual titers after 72 h, the L-arabinonic acid titer is expected to increase accordingly if L-arabinose is oxidized and if additionally the 1,4-lactone is assumed to open slowly, yet the L-arabinonic acid titer did not increase further.

Thus, the data suggested a loss of substrate or product by nonspecific conversion at higher titers. Balancing the sum of the final amounts of residual L-arabinose substrate and the two products in comparison to the L-arabinose supplied in total revealed a carbon gap of approximately 20% for both strains in the 80 g/L feed conditions while in the 40 g/L conditions the carbon gap was only 4% (Fig. 3f). In the NMR analysis, we did not observe any new signals indicating a nonspecific byproduct. If the carbon gap resulted from nonspecific conversion of L-arabinose, an optimized L-arabinose feeding strategy avoiding too high substrate titers should increase the product formation and reduce the carbon gap. In summary, at the end of the cultivation, the highest combined product titers of L-arabinonic acid plus its 1,4-lactone obtained in pH-controlled bioreactor conditions was approximately 133 g/L for strain 621H, while the *gdhM* overexpression strain showed a higher biomass-specific production (169 g / L / g_{cdw}) compared to strain 621H (131 g / L / g_{cdw}).

4. Conclusion

The results showed that the endogenous capability of *G. oxydans* to oxidize L-arabinose in the periplasm by the membrane-bound glucose dehydrogenase GdhM is highly suitable for one-step production of the valuable five carbon sugar acid L-arabinonic acid from renewable L-arabinose. Uptake of substrate into the cell and export of product out of the cell is not required in this case. Since *G. oxydans* apparently cannot use L-arabinose as a carbon source, inactivation of genes involved in its catabolism to intermediates of the central carbon metabolism is also not required. Without further strain optimization and process improvements, up to 133 g/L L-arabinonic acid and its 1,4-lactone were produced in pH-controlled fed-batch bioreactors. This titer is more than three-fold above those reported for the engineered *S. cerevisiae* and *E. coli* strains described before. The biomass-specific L-arabinonic acid production of the two *G. oxydans* strain tested indicated that additional expression of the *gdhM* has the potential to further increase the space-time yields, yet it seems that *gdhM* overexpression needs to be timed and balanced to avoid detrimental effects on growth and cell physiology and/or stability as observed in this study when *gdhM* was constitutively expressed. Together with an optimized L-arabinose feeding strategy and further process optimizations, a further increase in L-arabinonic acid titers and production rates should be achievable with *G. oxydans*.

Acknowledgements
We are grateful to Armin Ehrenreich for kindly providing the plasmid pMM4a-mGDH. The authors acknowledge access to the Jülich-Düsseldorf Biomolecular NMR Center that is jointly run by Forschungszentrum Jülich and Heinrich-Heine-Universität Düsseldorf.

Availability of data and materials
Data and materials are available upon request.

Funding
We are grateful to the Federal Ministry of Education and Research (BMBF) for financial support of the project IMPRES (031B0370B). The funding organization did not influence the design of the study or collection, analysis, and interpretation of data, or writing the manuscript.

Authors' contributions
PMF carried out the experiments and analyzed the data. RH and AW performed the metabolite analysis. TP designed and supervised the study. PMF, MB and TP wrote and revised the manuscript. All authors read and approved the final version.

Declaration
All authors declare that they have no competing interests.

References

Ameyama M, Shinagawa E, Matsushita K, Adachi O (1981) D-fructose dehydrogenase of *Gluconobacter industrius*: purification, characterization, and application to enzymatic microdetermination of D-fructose. J Bacteriol 145(2):814-23

Aro-Karkkainen N, Toivari M, Maaheimo H, Ylilauri M, Pentikainen OT, Andberg M, Oja M, Penttila M, Wiebe MG, Ruohonen L, Koivula A (2014) L-Arabinose/D-galactose 1-dehydrogenase of *Rhizobium leguminosarum* bv. *trifolii* characterised and applied for bioconversion of L-arabinose to L-arabonate with *Saccharomyces cerevisiae*. Appl Microbiol Biotechnol 98(23):9653-9665 doi:10.1007/s00253-014-6039-2

Correia LS, Grenman H, Warna J, Salmi T, Murzin DY (2019) Catalytic oxidation kinetics of arabinose on supported gold nanoparticles. Chem Eng J 370:952-961 doi:10.1016/j.cej.2019.03.241

Dilworth MJ, Arwas R, Mckay IA, Saroso S, Glenn AR (1986) Pentose metabolism in *Rhizobium leguminosarum* Mnf300 and in cowpea *Rhizobium* Ngr234. J Gen Microbiol 132:2733-2742

Duncan MJ (1979) L-Arabinose metabolism in Rhizobia. J Gen Microbiol 113(Jul):177-179 doi:Doi 10.1099/00221287-113-1-177

Fricke PM, Link T, Gatgens J, Sonntag C, Otto M, Bott M, Polen T (2020) A tunable L-arabinose-inducible expression plasmid for the acetic acid bacterium *Gluconobacter oxydans*. Appl Microbiol Biotechnol 104(21):9267-9282 doi:10.1007/s00253-020-10905-4

Fricke PM, Lürkens M, Hünnefeld M, Sonntag CK, Bott M, Davari MD, Polen T (2021) Highly tunable TetR-dependent target gene expression in the acetic acid bacterium *Gluconobacter oxydans*. Appl Microbiol Biotechnol 105(18):6835-6852 doi:10.1007/s00253-021-11473-x

Genders JD, Stapley JA (2016) Methods for the simultaneous electrolytic decarboxylation and reduction of sugars. EP000003033442B1.

Gupta A, Singh VK, Qazi GN, Kumar A (2001) *Gluconobacter oxydans*: its biotechnological applications. J Mol Microb Biotech 3(3):445-56

Hasebe K, Yamada K (2005) Hair treatment composition and hair cosmetic for damaged hair. EP000001602354A1.

Hekmat D, Bauer R, Fricke J (2003) Optimization of the microbial synthesis of dihydroxyacetone from glycerol with *Gluconobacter oxydans*. Bioproc Biosyst Eng 26(2):109-16 doi:10.1007/s00449-003-0338-9

Iwasaki K, Kitazawa M, Sakamoto (2004) Cosmetics or external preparations for skin. EP000001374831A1.

Johnsen U, Sutter JM, Zaiss H, Schonheit P (2013) L-Arabinose degradation pathway in the haloarchaeon *Haloferax volcanii* involves a novel type of L-arabinose dehydrogenase. Extremophiles 17(6):897-909 doi:10.1007/s00792-013-0572-2

Kawasaki, Y., Hori, M., Yamamoto, Y., Hiraki, J. (2005) Cosmetic composition containing polyorganosiloxane-containing epsilon-polylysine polymer, and polyhydric alcohol, and production thereof. EP000001604647B1.

Kusema BT, Campo BC, Maki-Arvela P, Salmi T, Murzin DY (2010) Selective catalytic oxidation of arabinose - A comparison of gold and palladium catalysts. Appl Catal a-Gen 386(1-2):101-108 doi:10.1016/j.apcata.2010.07.037

Lee W (2013) Novel nitrile and amidoxime compounds and methods of preparation. EP000002207872B1.

Liu H, Valdehuesa KNG, Ramos KRM, Nisola GM, Lee WK, Chung WJ (2014) L-arabonate and D-galactonate production by expressing a versatile sugar dehydrogenase in metabolically engineered *Escherichia coli*. Bioresource Technol 159:455-459 doi:10.1016/j.biortech.2014.03.056

Maaß S, Wagner R, Sockel K-H, Davis M, Schnering A, Streicher K (2013) UV-photo-protecting cosmetic composition. EP000002667947B1.

Mamlouk D, Gullo M (2013) Acetic acid bacteria: physiology and carbon sources oxidation. Indian J Microbiol 53(4):377-84 doi:10.1007/s12088-013-0414-z

Mathias AL, Rigo LU, Funayama S, Pedrosa FO (1989) L-Arabinose metabolism in *Herbaspirillum seropedicae*. J Bacteriol 171(9):5206-5209 doi:DOI 10.1128/jb.171.9.5206-5209.1989

Matsushita K, Toyama H, Adachi O (1994) Respiratory chains and bioenergetics of acetic acid bacteria. Adv Microb Physiol 36:247-301 doi:10.1016/s0065-2911(08)60181-2

Matsutani M, Yakushi T (2018) Pyrroloquinoline quinone-dependent dehydrogenases of acetic acid bacteria. Appl Microbiol Biotechnol 102(22):9531-9540 doi:10.1007/s00253-018-9360-3

Mientus M, Kostner D, Peters B, Liebl W, Ehrenreich A (2017) Characterization of membrane-bound dehydrogenases of *Gluconobacter oxydans* 621H using a new system for their functional expression. Appl Microbiol Biotechnol 101(8):3189-3200 doi:10.1007/s00253-016-8069-4

Niu W, Molefe MN, Frost JW (2003) Microbial synthesis of the energetic material precursor 1,2,4-butanetriol. J Am Chem Soc 125(43):12998-12999 doi:10.1021/ja036391+

Novick NJ, Tyler ME (1982) L-Arabinose metabolism in *Azospirillum brasiliense*. J Bacteriol 149(1):364-367 doi:Doi 10.1128/Jb.149.1.364-367.1982

Ohsumi K, Fujii T (2018) Polymer bead. EP000003584318A1.

Okawa T, Nishijima K (2014) Polysiloxane-n, n-dihydrocarbylene sugar-modified multiblock copolymer and method for producing the same. EP000002655480B1.

Okuda T, Shimizu H (2016) Immunity inducer for saccharide antigens. EP000002993182A1.

Pappenberger G, Hohmann HP (2014) Industrial production of L-ascorbic Acid (vitamin C) and D-isoascorbic acid. Adv Biochem Eng Biotechnol 143:143-88 doi:10.1007/10_2013_243

Pei L, Dong K, Tang Y, Zhang B, Yu C, Li W (2017) Theoretical studies of the decomposition mechanisms of 1,2,4-butanetriol trinitrate. J Mol Model 24(1):6 doi:10.1007/s00894-017-3541-3

Peters B, Mientus M, Kostner D, Junker A, Liebl W, Ehrenreich A (2013) Characterization of membrane-bound dehydrogenases from *Gluconobacter oxydans* 621H *via* whole-cell activity assays using multideletion strains. Appl Microbiol Biotechnol 97(14):6397-412 doi:10.1007/s00253-013-4824-y

Richhardt J, Bringer S, Bott M (2012) Mutational analysis of the pentose phosphate and Entner-Doudoroff pathways in *Gluconobacter oxydans r*eveals improved growth of a Δ*edd* Δ*eda* mutant on mannitol. Appl Environ Microbiol 78(19):6975-6986 doi:10.1128/Aem.01166-12

Saito Y, Ishii Y, Hayashi H, Imao Y, Akashi T, Yoshikawa K, Noguchi Y, Soeda S, Yoshida M, Niwa M, Hosoda J, Shimomura K (1997) Cloning of genes coding for L-sorbose and L-sorbosone dehydrogenases from *Gluconobacter oxydans* and microbial production of 2-keto-L-gulonate, a precursor of L-ascorbic acid, in a recombinant *G. oxydans* strain. Appl Environ Microb 63(2):454-60

Sanai K, Tanaka Y (2010) Preventive/remedy for urinary calculosis. Patent 20100227923.

Sanai K, Tanaka Y, Negishi S, Seri K, Sasaki H (2007) Composition for accelerating calcium absorption. Patent US2007/0293443 A1.

Sataraddi SR, Nandibewoor ST (2013) Oxidation of D-glucose by silver(III) periodate complex in the presence of Ru(III)/Os(VIII) as a homogeneous catalyst: a comparative mechanistic study (stopped flow technique). J Solution Chem 42(5):897-915 doi:10.1007/s10953-013-0002-1

Seiboth B, Metz B (2011) Fungal arabinan and L-arabinose metabolism. Appl Microbiol Biotechnol 89(6):1665-73 doi:10.1007/s00253-010-3071-8

Simon R, Priefer U, Pühler A (1983) A broad host range mobilization system for *in vivo* genetic-engineering - transposon mutagenesis in Gram-negative bacteria. Bio-Technol 1(9):784-791 doi:10.1038/nbt1183-784

Singh AK, Singh RK, Srivastava R, Rahmani S, Srivastava J, Singh M (2014) Rh(III)-catalysed oxidation of D(+) trehalose by *N*-bromoacetamide in acidic medium. a kinetic and mechanistic study. Oxid Commun 37(1):193-208

Smolentseva E, Kusema BT, Beloshapkin S, Estrada M, Vargas E, Murzin DY, Castillon F, Fuentes S, Simakov A (2011) Selective oxidation of arabinose to arabinonic acid over Pd-Au catalysts supported on alumina and ceria. Appl Catal a-Gen 392(1-2):69-79 doi:10.1016/j.apcata.2010.10.021

Stapley JA, Genders JD (2016) Methods for the electrolytic decarboxylation of sugars. EP000002971254B1.

Stapley JA, Genders JD, Atherton DM, Kendall PM (2011) Methods for the electrolytic production of erythrose or erythritol. Patent CA000002642127C.

Tkac J, Navratil M, Sturdik E, Gemeiner P (2001) Monitoring of dihydroxyacetone production during oxidation of glycerol by immobilized *Gluconobacter oxydans* cells with an enzyme biosensor. Enzyme Microb Tech 28(4-5):383-388

Van Es DS, Pazhavelikkakath Purushothaman RK, Frissen AE, Van Haveren J, Van der Klis F (2017) Oxidation of uronic acids to aldaric acids. EP000003204155B1.

Wang EX, Ding MZ, Ma Q, Dong XT, Yuan YJ (2016) Reorganization of a synthetic microbial consortium for one-step vitamin C fermentation. Microb Cell Fact 15:21 doi:10.1186/s12934-016-0418-6

Watanabe S, Kodaki T, Makino K (2006a) Cloning, expression, and characterization of bacterial L-arabinose 1-dehydrogenase involved in an alternative pathway of L-arabinose metabolism. J Biol Chem 281(5):2612-23 doi:10.1074/jbc.M506477200

Watanabe S, Shimada N, Tajima K, Kodaki T, Makino K (2006b) Identification and characterization of L-arabonate dehydratase, L-2-keto-3-deoxyarabonate dehydratase, and L-arabinolactonase involved in an alternative pathway of L-arabinose metabolism. Novel evolutionary insight into sugar metabolism. J Biol Chem 281(44):33521-36 doi:10.1074/jbc.M606727200

Weimberg R (1959) L-2-Keto-4,5-dihydroxyvaleric acid: an intermediate in the oxidation of L-arabinose by *Pseudomonas saccharophila*. J Biol Chem 234(4):727-32

Weimberg R, Doudoroff M (1955) The oxidation of L-arabinose by *Pseudomonas saccharophila*. J Biol Chem 217(2):607-24

Weng W, Liu C, Yan C, Su H, Zhou C (2018) 8-arm polyethylene glycol derivative, manufacturing method and modified bio-related substance thereby. EP000003315531B1.

Yamazaki H (2007) Polycarboxylic acid polymer for cement admixture and cement admixture. EP000001767505A2.

Yao RM, Hou WL, Bao J (2017) Complete oxidative conversion of lignocellulose derived non-glucose sugars to sugar acids by *Gluconobacter oxydans*. Bioresource Technol 244:1188-1192 doi:10.1016/j.biortech.2017.08.078

TABLES

Table 1. Strains and plasmid used in this study.

Strain	Relevant characteristic(s)	Ref. / Source
E. coli S17-1	Δ*recA*, *endA1*, *hsdR17*, *supE44*, *thi*-1, *tra*$^{+}$	(Simon et al. 1983)
G. oxydans 621H	DSM 2343	DSMZ
Plasmid		
pMM4a-mGDH	constitutive expression of the membrane-bound glucose DH gene (GOX0265, *gdhM*)	(Mientus et al. 2017)

Table 2. Calculated concentrations of KOH resulting from base stock titration to maintain pH 6 in bioreactor conditions with complex D-mannitol medium.

Strain and L-arabinose feed	KOH (mM) after 144 h
621H +4% (w/v)	1016
621H +8% (w/v)	1156
621H / pMM4a-mGDH +4% (w/v)	837
621H / pMM4a-mGDH +8% (w/v)	1119

FIGURE LEGENDS

Fig. 1. Shake flasks cultivations of *G. oxydans* 621H grown in D-mannitol medium with supplements of L-arabinose and one feed after 24 h (blue indicator). a) Growth according to OD_{600} and L-arabinose concentrations. b) pH values measured in the culture supernatants after 24 h and 48 h of cultivation. c, d) Concentrations of L-arabinonic acid and L-arabino-γ-1,4-lactone in culture supernatants. e) Carbon balance as stacked relative amounts (%) of the residual substrate L-arabinose and the two formed products L-arabinonic acid and its 1,4-lactone as determined at 48 h and calculated from the concentrations. For each condition, the total amount of the substrate L-arabinose supplied was set to 100%.

Fig. 2. Representative expansions of 599 MHz ^{1}H NMR spectra and colored area indication of signals used for quantification of L-arabinonic acid, its 1,4-lactone and L-arabinose. The signals in samples (A) used for metabolite quantification were selected based on specific nonoverlapping ^{1}H signals obtained with reference samples of L-arabinose (B) using signal 1 (py-H-β1, fu-H-β1 and fu-H-α1), signal 2 (py-H-α1), and signal 3 (py-H-α2), of L-arabinonic acid (C) using signal 4 (H-1), and of the 1,4-lactone (D) using signal 5 (H-3) and 6 (H-2). The chemical shift of the L-arabinonic acid H-1 signal (4) used for the quantification was pH dependent. Sample (D) was a mixture of L-arabinonic acid standard and the 1,4-lactone formed at pH 3. py: pyranose; fu: furanose

Fig. 3. Fed-batch DASbox fermentation of *G. oxydans* 621H without and with plasmid pMM4a-mGDH grown in D-mannitol medium supplemented and fed with L-arabinose as indicated. a) Initial culture volume (100 mL) and volume increase over time due to fed every 24 h (blue arrows and dotted line indicators), withdrawal of samples, and base titration for pH 6 maintenance. b) Biomass formation according to OD_{600}. c, d, e) Concentrations of L-arabinose, L-arabinonic acid, and L-arabino-1,4-lactone according to NMR analysis. Data are based on two independent biological replicates for each strain. For L-arabinose, the largely overlapping data points at a time were somewhat shifted for better visibility.

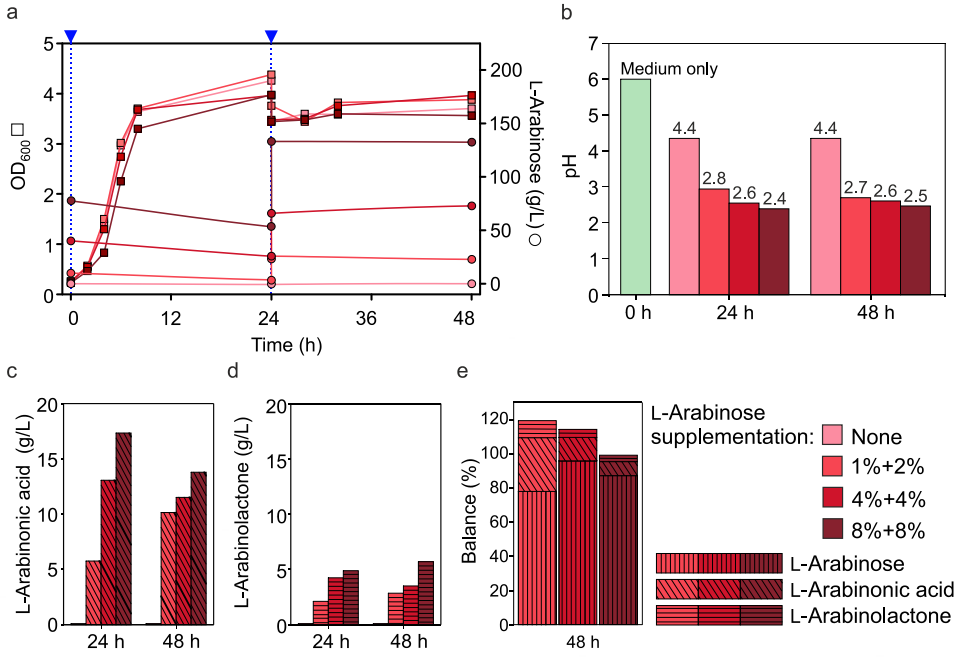
a
b
c
d
e
OD600 □
L-Arabinose (g/L) ○
Time (h)
Medium only
pH
4.4
2.8
2.6
2.4
4.4
2.7
2.6
2.5
0 h
24 h
48 h
L-Arabinonic acid (g/L)
L-Arabinolactone (g/L)
Balance (%)
L-Arabinose supplementation:
None
1%+2%
4%+4%
8%+8%
L-Arabinose
L-Arabinonic acid
L-Arabinolactone

Fig. 1

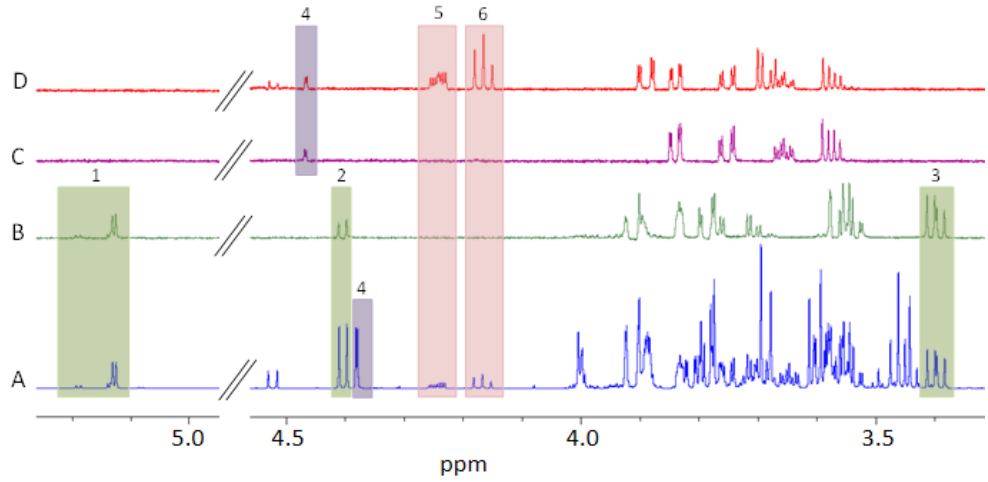

Fig. 2

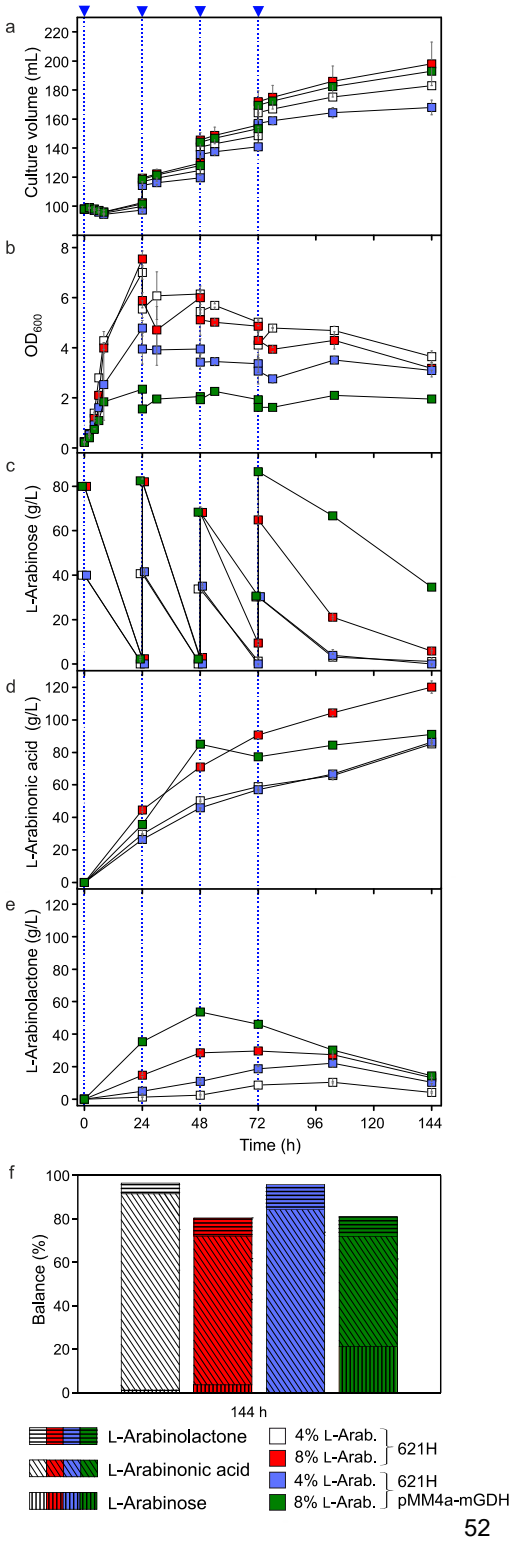
a
Culture volume (mL)
b
OD600
c
L-Arabinose (g/L)
d
L-Arabinonic acid (g/L)
e
L-Arabinolactone (g/L)
Time (h)
f
Balance (%)
144 h
L-Arabinolactone
L-Arabinonic acid
L-Arabinose
4% L-Arab.
8% L-Arab.
621H
4% L-Arab.
8% L-Arab.
621H
pMM4a-mGDH

Fig. 3

2.1 On the way toward regulatable expression systems in acetic acid bacteria: target gene expression and use cases

Fricke, P. M., Klemm, A., Bott, M., & Polen, T. (2021). On the way toward regulatable expression systems in acetic acid bacteria: target gene expression and use cases. **Applied Microbiology and Biotechnology 105:3423–3456.**

doi:10.1007/s00253-021-11269-z

Authors' contributions:
PMF, AK, and TP screened and selected the literature. All authors composed and revised the manuscript and approved the final version.

Overall contribution PF: 25%

Applied Microbiology and Biotechnology
https://doi.org/10.1007/s00253-021-11269-z

MINI-REVIEW

On the way toward regulatable expression systems in acetic acid bacteria: target gene expression and use cases

Philipp Moritz Fricke[1] · Angelika Klemm[1] · Michael Bott[1] · Tino Polen[1]

Received: 5 February 2021 / Revised: 24 March 2021 / Accepted: 4 April 2021

Abstract
Acetic acid bacteria (AAB) are valuable biocatalysts for which there is growing interest in understanding their basics including physiology and biochemistry. This is accompanied by growing demands for metabolic engineering of AAB to take advantage of their properties and to improve their biomanufacturing efficiencies. Controlled expression of target genes is key to fundamental and applied microbiological research. In order to get an overview of expression systems and their applications in AAB, we carried out a comprehensive literature search using the Web of Science Core Collection database. The *Acetobacteraceae* family currently comprises 49 genera. We found overall 6097 publications related to one or more AAB genera since 1973, when the first successful recombinant DNA experiments in *Escherichia coli* have been published. The use of plasmids in AAB began in 1985 and till today was reported for only nine out of the 49 AAB genera currently described. We found at least five major expression plasmid lineages and a multitude of further expression plasmids, almost all enabling only constitutive target gene expression. Only recently, two regulatable expression systems became available for AAB, an *N*-acyl homoserine lactone (AHL)-inducible system for *Komagataeibacter rhaeticus* and an L-arabinose-inducible system for *Gluconobacter oxydans*. Thus, after 35 years of constitutive target gene expression in AAB, we now have the first regulatable expression systems for AAB in hand and further regulatable expression systems for AAB can be expected.

Key points
- *Literature search revealed developments and usage of expression systems in AAB.*
- *Only recently 2 regulatable plasmid systems became available for only 2 AAB genera.*
- *Further regulatable expression systems for AAB are in sight.*

Keywords Acetic acid bacteria · *Acetobacteraceae* · Plasmid · Origin · Promoter · Induction

Introduction

Acetic acid bacteria (AAB) are a group of obligately aerobic Gram-negative bacteria that exhibit a unique form of metabolism by which they typically partially oxidize a variety of substrates such as sugars or ethanol by membrane-bound dehydrogenases (mDHs) and produce acetic acid. AAB are already used for a long time and they are very important for the production of foods and beverages such as vinegar, kombucha, kefir, and other products. Several reviews on AAB are already available that provide overviews, discussions and outlooks on issues related to their taxonomy, physiology and biochemistry, fermentation (foods and beverages), acetic acid resistance, production of exopolysaccharides including bacterial cellulose, pyrroloquinoline quinone (PQQ)-

✉ Tino Polen
t.polen@fz-juelich.de

Philipp Moritz Fricke
p.fricke@fz-juelich.de

Angelika Klemm
a.klemm@fz-juelich.de

Michael Bott
m.bott@fz-juelich.de

[1] IBG-1: Biotechnology, Institute of Bio- and Geosciences, Forschungszentrum Jülich GmbH, 52425 Jülich, Germany

Published online: 15 April 2021

dependent dehydrogenases, oxidation of carbon sources and alcohols, nitrogen fixation, metabolic engineering, biotechnological and industrial applications, as well as their use as microbial biosensors (see, for example, Cleenwerck and De Vos 2008; De Roos and De Vuyst 2018; Gao et al. 2020b; Gomes et al. 2018; Gullo et al. 2018; Kolesovs and Semjonovs 2020; La China et al. 2018; Laureys et al. 2020; Lynch et al. 2019; Mamlouk and Gullo 2013; Matsutani and Yakushi 2018; Trcek et al. 2015; Wang et al. 2015; Zhang et al. 2020). No review is currently available that provides an overview of the expression systems developed, tested and used for target gene expression and their use cases in AAB.

Generally, the expression of target genes to produce proteins in bacterial cell culture for various purposes is a standard method in basic research and biotechnological applications. For constitutive and inducible or regulatable expression, numerous plasmids have already been developed and established in many bacteria, which have been summarized and reviewed in the past for bacteria other than AAB (see, for example, Chen 2012; Connell 2001; Dilworth et al. 2018; Evans and Mizrahi 2015; Forstner et al. 2007; Gruber et al. 2015; Parachin et al. 2012; Schnappinger and Ehrt 2014; Terpe 2006; Valero 2012). In AAB, for a long time, only constitutive target gene expression and in a very few studies only weakly regulatable target gene expression was achieved since, for example, the transfer of heterologous regulatable systems such as the well-known classical examples of the TetR-, AraC-, and LacI-dependent systems and their application was not really successful yet in AAB due to high (leaky) expression already in the absence of the respective inducer (Florea et al. 2016a; Teh et al. 2019). Only two regulatable expression systems, an *N*-acyl homoserine lactone-inducible *luxR*-P_{lux} system for *Komagataeibacter rhaeticus* and an L-arabinose-inducible *araC*-P_{araBAD} system for *Gluconobacter oxydans* with up to 480-fold induction have recently been reported for the two AAB species (Florea et al. 2016a; Fricke et al. 2020). To provide a comprehensive overview of expression systems, their latest developments and the use cases in AAB we have searched and evaluated the literature for relevant AAB studies.

Literature search and updates in the systematics of AAB genera

We carried out a keyword-based literature search using the Web of Science Core Collection (WoSCC) database. Currently, for the *Acetobacteraceae* family there are 49 genera listed in the taxonomy browser of the NCBI website. We assumed that a publication potentially relevant for finding expression plasmids in AAB should contain at least the name of one of these AAB genera in the title, abstract, or keywords, respectively (for *Stella* we used the two full names *Stella humosa* and *Stella vacuolata*). In this first literature filtering step, the single AAB genus word-based searches in the WoSCC database revealed that the top 3 AAB genera with by far the most publications were *Acetobacter* (3,774), *Gluconobacter* (1,446) and *Glucon(o)acetobacter* (1,194), respectively. These top 3 genera were followed by *Acidiphilium* (345), *Komagataeibacter* (229), *Roseomonas* (177), *Asaia* (175), *Acidocella* (62) and *Acidomonas* (33). As outlined below, some genera names were introduced only recently and many of the included species had a different genus name before. Together, these 9 AAB genera already represent 97.6% (6,288) of all (6,440) non-redundant publications somehow related to one or more out of the 49 AAB genera. We then selected the 6097 publications from the year 2020 backward to 1973, the year of the first published successful DNA cloning experiments in *Escherichia coli* (Cohen et al. 1973). Using EndNote, for 3397 publications (55.7%), we could directly get access to the full text (PDF) due to Open Access or journal access via our institutions' central library. To narrow down the AAB-related publication list in a second step, we filtered title, abstract, keywords, and, if available, the full text (PDF) on the one hand by checking for the presence of the text strings *plasmid*, *vector*, *host*, *induction*, *inducer*, *activation*, *activator*, *repression*, *repressor*, *expression*, *promoter*, *regulation* or *terminator*, respectively. On the other hand, we also checked the publications by manual inspection of title, abstract and, if available, full-text PDF in regard to expression systems, the genetic work and the case studies. We finally ended up with a list of 243 publications from 1985 onward representing studies in which plasmids have been created, tested or used in 9 AAB genera. We probably missed a number of studies reporting plasmids for expression in AAB due to missing full-text information.

It should be mentioned that the taxonomy of the AAB has gone through some updates including the creation of new AAB genera and renaming of AAB species already described in the literature. In 1989 the genus *Acidomonas* was proposed to include a group of acidophilic, facultatively methylotrophic bacteria (Urakami et al. 1989). These microorganisms are Gram-negative, non-spore forming, non-motile, and rod-shaped and grow at pH 2.0 to 5.5. These characteristics are unique among the methanol-utilizing bacteria and the typical strain *Acetobacter methanolicus* can be distinguished from the type and representative strains of *Acetobacter*, *Gluconobacter*, and *Acidiphilium*, resulting in the renaming of *Acetobacter methanolicus* to *Acidomonas methanolica*. In 1997 a genus concept of AAB was proposed classifying *Acetobacter*, *Gluconoacetobacter*, *Acidomonas*, and *Gluconobacter* based on partial 16S rRNA sequences (Yamada et al. 1997). In 1998 *Gluconoacetobacter* was changed to *Gluconacetobacter* (International Committee on Systematic Bacteriology). As a consequence of these changes and updates, *Acetobacter diazotrophicus*, *A. europaeus*,

A. hansenii, *A. liquefaciens*, and *A. xylinum* (alias *A. xylinus*) were included in the genus *Gluconacetobacter* with the respective changes in nomenclature: *Gluconacetobacter diazotrophicus*, *Ga. europaeus*, *Ga. hansenii*, *Ga. liquefaciens*, and *Ga. xylinus*, respectively. Furthermore, in the following years, a phylogenetic duality in the new genus *Gluconacetobacter* was found. The *Ga. liquefaciens* group and the *Ga. xylinus* group could be phylogenetically, phenotypically and ecologically distinguished from each other at the generic level. This resulted in the creation of the new AAB genus *Komagataeibacter* based on 16S rRNA gene sequences and the transfer of several new combinations including *Ga. xylinus* (formerly *A. xylinus* alias *A. xylinum*) to *Komagataeibacter xylinus* on the basis of taxonomic characteristics (Yamada 2014; Yamada et al. 2012). Taking these AAB genera updates and renaming of AAB species into account for the publications before 1989, 1998, and 2014 (and after), we found in our final list 101 publications related to *Gluconobacter*, 61 to *Komagataeibacter*, 41 to *Acetobacter*, 20 to *Gluconacetobacter*, 8 to *Acidiphilium*, 6 to *Acidomonas*, 4 to *Asaia*, 1 to *Kozakia*, and 1 to *Roseomonas*, respectively. Among these 243 publications, in 59 studies genomic allele replacements and transposon- or plasmid-based gene inactivation screenings requiring the functional expression of transposases or resistance genes as well as homologous recombination were carried out using a few strategies without further recombinant target gene expression. These studies were excluded from our review which removed the genera *Kozakia* and *Roseomonas* from our list. The remaining 184 publications were organized according to the expression plasmids used, the case studies or their timelines, and are presented for the seven remaining AAB genera according to the number of publications (Fig. 1).

Target gene expression in *Gluconobacter*

Most studies reporting on the construction and usage of expression plasmids in AAB were found for the genus *Gluconobacter* (81). Initially, in 11 studies, several plasmids were constructed and tested before a major expression plasmid family was established in *Gluconobacter* in 2006.

Plasmid diversity before establishing the major expression plasmid lineage

The first study reporting an *E. coli* / *Gluconobacter* shuttle vector was published in 1985 by Teruhiko Beppu and coworkers, who in parallel were also working on shuttle vectors for *Acetobacter* (see *Acetobacter* section). This first shuttle vector for *Gluconobacter* was constructed by ligation of cryptic plasmid pMV201 (2.5 kb) found in *G. suboxydans* IFO 3130 with the *E. coli* plasmid pACYC177 (3.9 kb) carrying the p15A *ori*. The resulting chimeric plasmid pMG101 (6.2 kb) carries an ampicillin (Amp) resistance gene and replicates in *G. suboxydans* as well as in *E. coli* (Fukaya et al. 1985b). Later, conjugal transfer of a series of plasmids of the incompatibility group P (RP4, RP1::Tn*951*, pRK290 and derivatives thereof) and Q (pKT230/231) was studied. A gentamycin (Gm) resistance-encoding pRK290 derivative (20 kb, minimal replicon derivative of RK2) was constructed and suggested to offer considerable potential as a versatile gene delivery system for *Gluconobacter* (Condon et al. 1991). The promoter of the Gm resistance gene is functional since pRK290::Gm increased the minimal inhibitory concentration for gentamycin from 80 μg/mL to more than 2 mg/mL. With plasmid RP1::Tn*951* carrying the lactose transposon, heterologous gene expression and regulation was tested in *Gluconobacter*. Tn*951* contains IPTG-inducible and cAMP receptor protein (CRP)-dependent genes homologous to the *E. coli lacI*, *lacZ*, and *lacY* genes. The Tn*951*-based β-galactosidase activity was found to be induced 4-fold to 6-fold by IPTG in *Gluconobacter*, which suggested the synthesis of a functional LacI repressor in *Gluconobacter*, yet the repression was leaky in the absence of IPTG and the induced LacZ activity less than 5% compared to fully induced levels in *E. coli*. Since in *E. coli* the *lac* operon displays reversible cAMP-dependent catabolite repression with glucose, cAMP was exogenously added (100 μM) to the *Gluconobacter* culture. cAMP did not result in any detectable increase in LacZ activity, suggesting that a catabolite repression-like phenomenon was unlikely to be the cause of the poor LacZ activity in *Gluconobacter* if the assumption holds true that cAMP can be transported into the cell at levels sufficient for physiological effects to be observed. With the genome sequences available today we know that a CRP gene appears to be absent in *Gluconobacter*. The low levels of LacZ activity could be explained by inefficient recognition of the heterologous Tn*951* promoter in *Gluconobacter* (Condon et al. 1991).

Generally, RK2-based vectors such as the broad host range vector pRK293 (21.4 kb) can be transferred to *G. oxydans* by bacterial mating, yet efforts to use this cloning vehicle were unsuccessful, since the transfer of pRK293 occurred only with very low efficiency and with pRK293 containing a 4.7 kb insert of interest no clones could be obtained (Cleton-Jansen et al. 1991). In another attempt to construct and test a suitable shuttle vector, the small cryptic plasmid pGY1 (2.7 kb) also detected in *G. suboxydans* IFO 3130 was cleaved and ligated with cleaved pUC18 (Takeda and Shimizu 1992). The resulting chimeric vector pGEA1 (5.4 kb) carries ampicillin resistance and was used to express the cytochrome *c*-553 gene of *G. suboxydans* IFO 12528 from its native promoter region in *G. suboxydans* IFO 3254, which oxidizes ethanol poorly because of a deficiency of the second subunit of the membrane-bound alcohol dehydrogenase. Transformants of IFO 3254 exhibited ethanol oxidation activity and increased

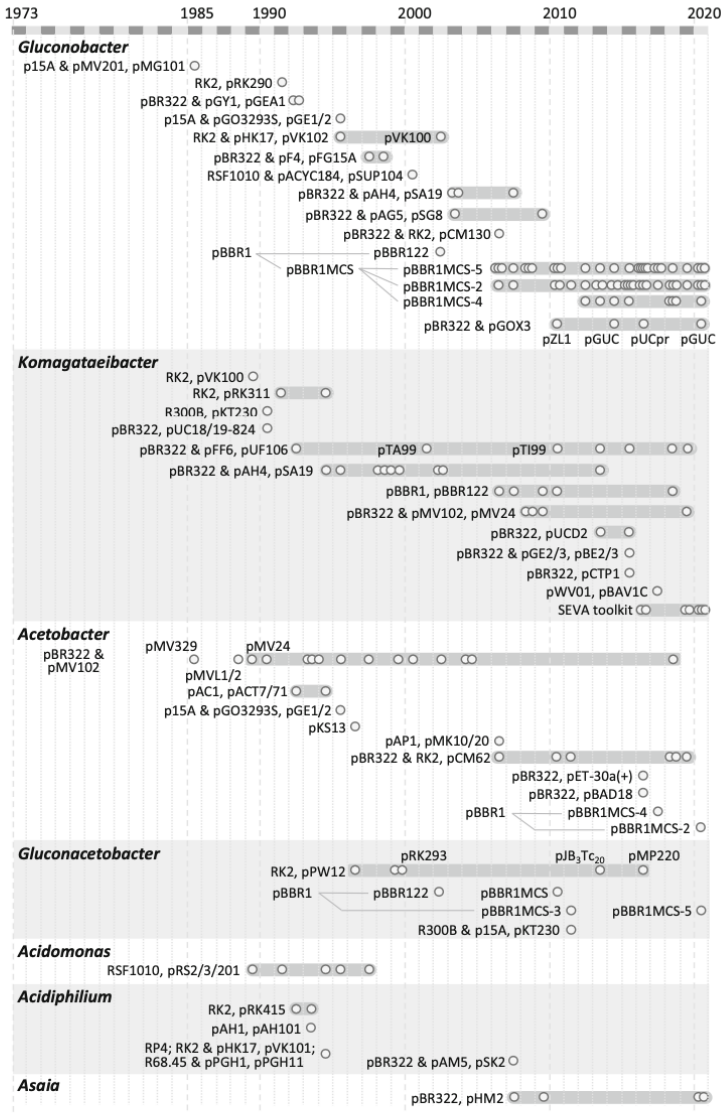

Fig. 1 Time plot illustrating major lineages and diversity of expression plasmids and their origins of replication hitherto used in AAB and found for seven out of 49 AAB genera according to the publications (o) in the WoSCC database

dehydrogenase activities for D-glucose, D-sorbitol and glycerol. Furthermore, azide insensitivity of the respiratory chain was restored, which indicated that cytochrome *c*-553 is in the pathway of the azide-insensitive respiratory chain bypass of *G. suboxydans* (Takeda and Shimizu 1992; Takeda et al. 1992). While in these early *Gluconobacter* studies chemically competent cells or conjugation were used to transfer plasmids, electroporation was also established for *Gluconobacter* and enabled transformation frequencies of up to 10^5 transformants /μg of DNA (Creaven et al. 1994). In the following, conjugation and electroporation were used for *Gluconobacter* almost equally often.

In a further attempt to construct, test, and establish a suitable shuttle vector, the chimeric plasmid pGE1 (11.9 kb) was constructed from the endogenous cryptic plasmid pGO3293S (9.9 kb) found in *G. oxydans* IFO 3293 and plasmid pSUP301 (5 kb) from *E. coli* (Shinjoh and Hoshino 1995). The plasmid pGO3293S encodes enzyme activities that converts L-sorbose to 2-keto-L-gulonic acid, the non-lactonized precursor of vitamin C. Plasmid pSUP301 contains pACYC177 introduced above. The plasmid pGE1 could be transferred into *G. oxydans* IFO 3293 with a high frequency (10^{-1} transconjugants per recipient) by conjugal transfer, maintained very stably without antibiotic selection, and did not inhibit the growth or 2-keto-L-gulonic acid productivity of producer strains derived from *G. oxydans* IFO 3293. pGE1 could also be shortened to a 9.8-kb plasmid termed pGE2. pGE1 could be introduced in 6 *Gluconobacter* and 4 *Acetobacter* strains out of 6 and 28 strains tested. Thus, it showed a broader host-range than the shuttle vector pMG101 introduced above, which showed a limited host-range even in *Gluconobacter*. pGE1 was considerably stable in the transconjugants after two cycles of cultivation without kanamycin, except in *G. frateurii* IFO 3271. The usefulness of pGE1 as an expression vector was confirmed by subcloning the membrane-bound L-sorbosone dehydrogenase (SNDH) gene of *A. liquefaciens* IFO 12258 and its expression in *G. oxydans* IFO 3293 derivatives. Using resting cells, pGE1 derivatives with the SNDH gene, however, did not lead to a higher 2-keto-L-gulonic acid production than the pVK102 derivative with the SNDH gene (Shinjoh and Hoshino 1995). Already beforehand, plasmid pVK102 (23 kb), a mobilizable broad-host-range cosmid vector constructed from pRK290 and pHK17 via the intermediate pVK100 originally used in *Agrobacterium* and providing kanamycin and tetracycline resistance, was used to construct a genomic library of *A. liquefaciens* IFO 12258 for a SNDH activity screening in a *G. oxydans* IFO 3293 mutant that accumulates L-sorbosone in the presence of L-sorbose (Shinjoh et al. 1995). Plasmid pVK100 was used in a check of the biological functions of the polyol dehydrogenase genes *sldAB* to complement mutants of *G. oxydans* DSM 4025 disrupted in the *sldAB* genes by expressing *sldA*, *sldB*, or both genes from *G. oxydans* promoter P_A (Shinjoh et al. 2002).

In another attempt to create a shuttle vector, the endogenous plasmid pF4 (4.4 kb) extracted from *G. oxydans* T-100 was ligated with plasmid pHSG298 (2.7 kb) carrying pBR322 *ori* and the resulting chimeric plasmid pFG15A (7.3 kb) was confirmed to be also stable in *G. oxydans* G624 across several passages in a broth without kanamycin and had no effects on the L-sorbose production by the host (Saito et al. 1997). Plasmid pFG15A was used to express L-sorbose and L-sorbosone dehydrogenase genes of *G. oxydans* T-100 from their native promoter regions. *G. oxydans* G624, which is unable to produce 2-keto-L-gulonic acid endogenously, cultivated in the presence of D-sorbitol and with the expression plasmid reached a 2-keto-L-gulonic acid titer 2.3-fold higher than the titer obtained by *G. oxydans* T-100, yet the yield was still insufficient (Saito et al. 1997). Therefore, to improve the expression of the dehydrogenase genes, the native promoter region was replaced with that of *E. coli* P_{tufB1}, P_{lac}, or P_L, which all were active. In combination with chemical mutagenesis of the strain, the 2-keto-L-gulonic acid production level was further increased 3-fold (Saito et al. 1998).

In another study, the broad-host-range vector pSUP104, which includes the mobilization and replication functions of the IncQ plasmid RSF1010 and was originally tested in *Rhizobium*, *Agrobacterium*, and *Pseudomonas* species, respectively, was used in *Gluconobacter* to complement a Tn*5*-based *pqqE*-deficient mutant by expressing a genomic library fragment containing the *pqqE* gene of the PQQ coenzyme biosynthesis gene cluster *pqqBCDE* of *G. oxydans* ATCC 9937 (Felder et al. 2000). RSF1010 was used otherwise in some *Acidomonas* studies and in an *ori* test using the pSEVA tool kit in *Komagataeibacter* (see sections below).

Another expression plasmid used in *Gluconobacter* is the shuttle vector pSA19 already developed and introduced for use in *Komagataeibacter* in 1994 (see *Komagataeibacter* section). The feasibility of using pSA19 was also demonstrated for *Gluconobacter* by expressing the xylitol dehydrogenase (XDH) gene of *Morganella morganii* from the promoter P_{lac} (Tonouchi et al. 2003). In the recombinant *G. oxydans* ATCC 621 strain, the XDH activity was increased 4-fold. To develop an improved production process for the alternative sweetener xylitol, also the endogenous XDH gene from *G. oxydans* ATCC 621 was cloned with and without its native promoter region into pSA19 (Sugiyama et al. 2003). Expression from P_{lac} alone increased the XDH activity 5-fold in the recombinant *G. oxydans* strain, while XDH activity was 11-fold higher when the gene was expressed from both P_{lac} and its native promoter. The latter construct increased the xylitol titer obtained by conversion of D-arabitol to xylulose with arabitol dehydrogenase followed by reduction to xylitol 2-fold within 48 h when ethanol was added. Later pSA19 was used to express the *sboA* and *sboR* genes both located upstream of the FAD-dependent D-sorbitol dehydrogenase (SLDH) genes *sldSLC* in *G. frateurii* THD32 to analyze SboA enzyme activity and the role of the putative transcriptional regulator SboR in the regulation of *sldSLC* expression (Soemphol et al. 2007). The SboA enzyme showed NADPH-dependent L-sorbose reductase activity. The predicted transcriptional regulator SboR was suggested to be a repressor of *sboA* expression while another regulator was assumed to be required for the induction of *sldSLC* by D-sorbitol or L-sorbose. When *sboR* was disrupted in *G. frateurii*, the SboA activity was increased 1.5-fold and 2-fold when grown on D-sorbitol and L-sorbose, respectively. Since the basal expression in the parental strain was already relatively high according to the activities in the

cytosolic fraction (0.6 to 0.9 U/mg) the SboR-repressed promoter of the *sboRA* operon seems not suitable to be used for a regulatable expression system in *Gluconobacter*.

In parallel to the test and usage of pSA19 in *Gluconobacter*, another shuttle plasmid was created and tested. The cryptic endogenous plasmid pAG5 (5.6 kb) found in *G. oxydans* IFO 3171 was ligated with pUC18 and the chimeric vector was termed pSG8 (Tonouchi et al. 2003). Additionally, the 2 kb smaller plasmid pSG6 was created by *Eco*RI digestion of pSG8 and self-ligation of the 3.6 kb fragment. The copy numbers of pSG8/6 were estimated to be 10 per genome and both were found to be stable in *G. oxydans* ATCC 621 after 10 days of repeated cultivation (50 generations) in the absence of ampicillin. Plasmid pSG6 was used for expression of the endogenous cyanide-insensitive quinol oxidase genes *cioAB* in the wild type *G. suboxydans* IFO 12528 (Mogi et al. 2009). Additional plasmid-based expression was required for the biochemical characterization of the membrane-bound enzyme, as it was difficult without due to the low native expression level and the enzyme instability in detergent solution.

pBBR1MCS derivatives—the major plasmid family used in *Gluconobacter*

Besides testing the various plasmids described above for recombinant expression, in 2002, the plasmid pBBR122 was used to test whether lactose metabolism could be established in *G. oxydans* by cloning and expressing the *E. coli lacZY* genes from P_{lac} in five *G. oxydans* strains and one *Ga. liquefaciens* strain (Mostafa et al. 2002). In three *G. oxydans* strains the LacZ activities were similarly high as the LacZ activity in induced *E. coli* XL1-Blue cells, while on other *G. oxydans* strains and in *Ga. liquefaciens* the LacZ activities were much lower. Albeit for unknown reasons only a few transformants of *G. oxydans* were able to grow on lactose, these results demonstrated that active β-galactosidase can be produced in *G. oxydans* at levels much higher than the LacZ activities obtained with Tn*951* mentioned above. This also suggested that the Tn*951* promoter is very weak in *Gluconobacter* which could be useful when very low target gene expression levels are required.

The plasmid pBBR122 is based on the very small endogenous plasmid pBBR1 (2.6 kb) isolated from *Bordetella bronchiseptica* (Antoine and Locht 1992). pBBR122 was commercialized by MoBiTec and exhibits a broad-host-range compatible with IncP, IncQ, and IncW group plasmids as well as with ColE1- and p15A-based replicons. The pBBR1 derivative pBBR1MCS carrying pBBR1 *ori*, a MCS and a chloramphenicol resistance cassette was used to create four new derivatives each with a different antibiotic resistance cassette: pBBR1MCS-2 confers kanamycin resistance, pBBR1MCS-3 tetracycline resistance, pBBR1MCS-4 ampicillin resistance, and pBBR1MCS-5 gentamicin resistance (Kovach et al. 1995; Kovach et al. 1994). The family members exhibit several advantages in that they are relatively small (<5.3 kb), possess an extended MCS, allow direct selection of recombinant plasmids in *E. coli* via disruption of the LacZα peptide, and are mobilizable when the RK2 transfer functions are provided in *trans*, yet can also be introduced by electroporation.

Since 2006, the pBBR1MCS-based plasmids have been used in most *Gluconobacter* studies reporting recombinant gene expression; thus, it is the major expression plasmid lineage used in *Gluconobacter* and it also exhibits the most use cases in AAB in general (Table 1). While pBBR1MCS-3 providing tetracycline resistance was apparently not used in *Gluconobacter*, pBBR1MCS-5 has been used in 27 studies, pBBR1MCS-2 in 25 studies, and pBBR1MCS-4 in 8 studies. In 51 cases *Gluconobacter* genes, in 5 cases genes from other AAB genera, and in 13 cases genes from bacteria other than AAB, were expressed from P_{lac} or selected promoters (Table 2). In a few studies, fusion proteins with signal peptides for export or for surface display and a tagged protein for one-step membrane protein purification from *Gluconobacter* cells were produced.

Other expression plasmids recently used in *Gluconobacter*

In parallel to the use of the very successful pBBR1MCS-based plasmid family in *Gluconobacter*, further plasmids have been constructed based on the two homologous cryptic plasmids pGOX3 (14.5 kb) found in two *G. oxydans* strains and pUC18 or pUC19 carrying pBR322 *ori*. The chimeric plasmids are selectable by conferring ampicillin resistance, are compatible with the pBBR1MCS family and double selectable except with pBBR1MCS-4 also carrying ampicillin resistance. In the first case, the *par* and *rep* loci of pGOX3 from *G. oxydans* DSM 2003 were amplified as a 2.3-kb fragment and cloned into pUC18, resulting in the 5 kb shuttle vector pZL1 (Zhang et al. 2010). Plasmid pZL1 was found to replicate in both *E. coli* and *G. oxydans* DSM 2003 and was maintained for 144 h during serial subcultures in the absence of selective pressure in 80% of the DSM 2003 cells, while pUC18 was almost completely lost already after 48 h. The relative plasmid copy number of pZL1 in DSM 2003 was found to be 13 times higher than that of the endogenous pGOX3. The capability of pZL1 to express heterologous genes in DSM 2003 was shown by using the fluorescence reporter gene *wasabi*. When expressed in DSM 2003 from the strong promoter P_{tufB}, the fluorescence signal with the reporter plasmid pZL1-tufB-wasabi was almost as high as with pBBR1MCS-5-tufB-wasabi.

A comparable assembly process as for pZL1 was used to construct the shuttle vector pGUC based on the *par* and *rep*

Table 1 The five most frequently used plasmid lineages for recombinant target gene expression in AAB and the flexible SEVA plasmid toolkit

Backbone	Plasmid/Derivative	Reference	AAB genera use	#	AAB references
pBBR1	pBBR122, Cm^R, Km^R	Antoine and Locht 1992	*Komagataeibacter*	5	[a] pBBR122 *K.* ref.
			Gluconobacter	1	Mostafa et al. 2002
			Gluconacetobacter	1	Mostafa et al. 2002
	pBBR1MCS, Cm^R, P_{lac}, P_{T3}, P_{T7}	Kovach et al. 1994	*Gluconacetobacter*	1	Rouws et al. 2010
	pBBR1MCS-5, Gm^R, P_{lac}, P_{T3}, P_{T7}	Kovach et al. 1995	*Gluconobacter*	27	Table 2
			Gluconacetobacter	1	Camelo et al. 2020
	pBBR1MCS-2, Km^R, P_{lac}, P_{T3}, P_{T7}	Kovach et al. 1995	*Gluconobacter*	25	Table 2
			Acetobacter	1	Gao et al. 2020a
	pBBR1MCS-4, Ap^R, P_{lac}, P_{T3}, P_{T7}	Kovach et al. 1995	*Gluconobacter*	8	Table 2
			Acetobacter	1	Wu et al. 2017
	pBBR1MCS-3, Tc^R, P_{lac}, P_{T3}, P_{T7}	Kovach et al. 1995	*Gluconacetobacter*	1	Velazquez-Hernandez et al. 2011
pUC18 & pMV329	pMV24, Ap^R, P_{lac}	Fukaya et al. 1989	*Acetobacter*	13	[b] pMV24 *A.* ref.
			Komagataeibacter	4	[c] pMV24 *K.* ref.
pUC18 & pAH4	pSA19, Ap^R, P_{lac}	Tonouchi et al. 1994	*Komagataeibacter*	8	[d] pSA19 ref.
pTrc99A & pFF6	pTA99, Ap^R, P_{trc} pTI99, Km^R, P_{trc}	Tajima et al. 2001 Hu et al. 2010	*Komagataeibacter*	6	[e] pTA99 / pTI99 ref.
pUC19 & pDN19	pCM62, Tc^R , P_{lac}	Marx and Lidstrom 2001	*Acetobacter*	6	[f] pCM62 ref.
pSEVA	flexible design	Durante-Rodriguez et al. 2014	*Komagataeibacter*	7	[g] pSEVA ref.

[a] pBBR122 *K.* ref.: Chien et al. 2006; Setyawati et al. 2007; Setyawati et al. 2009; Yadav et al. 2010; Liu et al. 2018

[b] pMV24 *A.* ref.: Fukaya et al. 1989; Fukaya et al. 1990; Fukaya et al. 1993; Takemura et al. 1993b; Takemura et al. 1993a; Kondo et al. 1995; Kondo and Horinouchi 1997; Kashima et al. 1999; Kashima et al. 2000; Okamoto-Kainuma et al. 2002; Okamoto-Kainuma et al. 2004; Nakano et al. 2004; Zheng et al. 2018

[c] pMV24 *K.* ref.: Iida et al. 2008a; Iida et al. 2008b; Iida et al. 2009; Konjanda et al. 2019

[d] pSA19 ref.: Tonouchi et al. 1995; Tonouchi et al. 1998b; Tonouchi et al. 1998a; Nakai et al. 1998; Nakai et al. 1999; Nakai et al. 2002; Ishida et al. 2002; Nakai et al. 2013

[e] pTA99 / pTI99 ref.: Fujiwara et al. 1992; Hu et al. 2010; Sunagawa et al. 2013; Fang et al. 2015; Jacek et al. 2018; Jacek et al. 2019

[f] pCM62 ref.: Deeraksa et al. 2006; Masud et al. 2010; Soemphol et al. 2011; Theeragool et al. 2018; Yakushi et al. 2018a; Phathanathavorn et al. 2019

[g] pSEVA ref.: Florea et al. 2016a; Florea et al. 2016b; Walker et al. 2019; Teh et al. 2019; Huang et al. 2020; Hur et al. 2020; Liu et al. 2020b

loci of pGOX3 from *G. oxydans* 621H and pUC18 (Gao et al. 2014). Plasmid pGUC and again the strong promoter P_{tufB} were used to express and test different combinations of five L-sorbose dehydrogenase (SDH) genes and two L-sorbosone dehydrogenase (SNDH) genes from *Ketogulonicigenium vulgare* in *G. oxydans* WSH-003, an industrial strain used for the conversion of D-sorbitol to L-sorbose. As the production of the vitamin C precursor 2-keto-L-gulonic acid from D-sorbitol involves three sequential oxidation reactions, the spatial proximity of the corresponding dehydrogenases appeared to be useful to enhance the production. Therefore, with a series of linker peptides, SDH-SNDH fusion enzymes were tested and for a selected SDH-SNDH fusion the *pqqA* gene alone or the *pqqABCDE* gene cluster for PQQ biosynthesis was additionally included on the pGUC plasmid. Additional expression of the PQQ biosynthesis gene(s) enhanced cell growth and with the stepwise metabolic engineering of *G. oxydans*, the final 2-keto-L-gulonic acid titer was improved 8-fold (39 g/L) compared to that obtained with the independent expression of the dehydrogenase genes (Gao et al. 2014). In further work, the adaptor protein SH3 gene sequence was fused via a linker sequence to the SDH gene of the SDH-linker-SNDH construct and co-expressed with the gene of the small trimeric protein CutA from *Pyrococcus horikoshii* fused to the SH3lig gene sequence, all present on pGUC and each expressed from P_{tufB} (Gao et al. 2020c). The adaptor protein SH3 as docking protein and its ligand SH3lig as docking station peptide improved the chemical structure stability of fused SDH-SNDH complexes surrounding the trimeric CutA protein. The recombinant strain *G. oxydans* WSH-003 with the pGUC-based expression plasmid produced 40 g/L of 2-keto-L-gulonic acid after 168 h. Additionally, co-expression of the *pqqABCDE* operon from P_{tufB} on pGUC increased the 2-keto-L-gulonic acid titer to 43 g/L, demonstrating an efficient conversion of D-sorbitol to 2-keto-L-gulonic acid with a single strain (Gao et al. 2020c).

Table 2 Use of the pBBR1MCS-based plasmid family in *Gluconobacter*. The studies are grouped by the pBBR1MCS derivative and ordered by the year of publication. *cyt.* cytochrome; *DH* dehydrogenase; *DHA* dihydroxyacetone; *GFP* green fluorescent protein; *P* promoter; *PPP* pentose phosphate pathway; *PQQ* pyrroloquinoline quinone; *SNP* single nucleotide polymorphism; *SP* signal peptide

Expressed genes	Encoded activity/function	P [a]	Context	Reference
pBBR1MCS-5				
tldD, *pqqA*, *pqqABCDE* from *G. oxydans* 621H	PQQ biosynthesis-related enzymes	P_{tufB}, P_{pqqA}, $P_{pqqBCDE}$	analysis of PQQ biosynthesis genes in *G. oxydans*	Hölscher and Görisch 2006
gdh, ga5dh from *G. oxydans* 621H	membrane-bound PQQ-dependent glucose DH and gluconate-5-DH	P_{lac}	increase of gluconate and 5-keto-D-gluconic acid production by *G. oxydans* strains	Merfort et al. 2006b
ga5dh from *G. oxydans* 621H	membrane-bound PQQ-dependent gluconate-5-DH	P_{tufB}, P_{gdh}	increase of 5-keto-D-gluconic acid production by *G. oxydans* mutant strain	Merfort et al. 2006a
sldAB from *G. oxydans* 621H	membrane-bound PQQ-dependent polyol DH	P_{tufB}, P_{gdh}	increase of DHA production from glycerol by *G. oxydans* mutant	Gätgens et al. 2007
sldAB from *G. oxydans* M5	membrane-bound PQQ-dependent D-sorbitol DH	P_{lac}	characterization of the enzyme in *G. oxydans* M5 and role in miglitol precursor production	Yang et al. 2008
sldBA from *G. suboxydans* IFO 3255	membrane-bound PQQ-dependent D-sorbitol DH	P_{lac}, P_{sldBA}	characterization of two membrane-bound D-sorbitol DHs and complementation in *G. frateurii*	Soemphol et al. 2008
sldA'B' from *G. oxydans* 621H	N-terminal fragments of membrane-bound PQQ-dependent polyol DH	P_{tufB}	construction of the pEXGOX family; a cloning and expression vector system with P_{tufB} from *G. oxydans*	Schleyer et al. 2008
adhAB from *G. oxydans* DSM 2003	membrane-bound PQQ-dependent alcohol DH (mADH)	P_{lac}	enzyme characterization; mADH mutant complementation; lactic acid production from 1,2-propanediol	Wei et al. 2010
gdh from G. oxydans M5	membrane-bound PQQ-dependent glycerol DH	P_{lac}	enhanced production of DHA by *G. oxydans* mADH mutant	Li et al. 2010b
vgb from Vitreoscilla	*Vitreoscilla* hemoglobin	P_{tufB}	improvement of cell growth and DHA production by *G. oxydans* M5	Li et al. 2010a
adhAB from *G. oxydans* DSM 2003	membrane-bound PQQ-dependent alcohol DH (mADH)	P_{adh}	characterization of mADH and complementation in *G. oxydans* DSM 2003 mADH mutant	Wei et al. 2012
xdh from *G. oxydans* NH-10; *gdh* from *B. subtilis*	xylitol DH (XDH) and glucose DH (GDH)	P_{tufB}	improvement of xylitol production by construction of a *xdh* and *gdh* co-expressing *G. oxydans* strain	Zhang et al. 2013
ndh and *ga2dh* from *G. oxydans* DSM 2003; *gfp*	membrane-bound type II NADH DH; FAD-dependent gluconate-2-DH; GFP	$P_{gHp0169}$, P_{tufB}	evaluation of promoter gHp0169 and improvement of 2-keto-D-gluconic acid production by *G. oxydans* DSM 2003	Shi et al. 2014
ga2dh from *G. oxydans* DSM 2003	FAD-dependent gluconate-2-DH	P_{tufB}	rational mutagenesis to increase the pBBR1MCS-5 copy number; 2-keto-D-gluconic acid production	Shi et al. 2015
sldAB from *G. oxydans* 621H; *gfp*	membrane-bound PQQ-dependent polyol DH; green fluorescent protein	$P_{GOX0169}$, $P_{GOX0264}$, $P_{GOX0452}$, P_{tufB}	promoter strength analysis and 5-keto-D-gluconate accumulation using combinatorial metabolic engineering strategies in industrial strain *G. oxydans* ZJU2	Yuan et al. 2016a
ga2dh from G. oxydans DSM 2003	FAD-dependent gluconate-2-DH	P_{tufB}, P_{ga2dh}, $P_{gHp0169}$	improvement of 2-keto-D-gluconic acid production by *G. oxydans* DSM 2003	Li et al. 2016a
adhS and *adhABS* from *G. oxydans* DSM 2003	membrane-bound PQQ-dependent alcohol DH (mADH)	P_{adhS}, P_{adhAB}	study of the AdhS subunit and effect on mADH activity in *G. oxydans* DSM 2003; hydroxy acid production	Zhang et al. 2016
gcd from *X. campestris* DSM 3586	alcohol DH	$P_{GOX0169}$	improvement of 5-keto-D-gluconate production by *G. oxydans* ZJU2 mutant strain	Yuan et al. 2016b
zwf, *gnd* from *G. oxydans* NH-10	glucose-6-phosphate DH and 6-phospho-gluconate DH	P_{tufB}	improvement of xylitol production by *G. oxydans* NH-10; coenzyme regeneration efficiency of the PPP	Li et al. 2016b
fusion of L-RI gene from *Acinetobacter* sp.	L-ribose isomerase (L-RI) C-terminally fused to PDZ ligand; membrane-bound	P_{tufB}	protein localization; novel strategy for the production of L-erythrose by localizing	Zou et al. 2017

Table 2 (continued)

Expressed genes	Encoded activity/function	P [a]	Context	Reference
DL-28; *sdh* from *G. oxydans* DSM 2003; *gfp*	PQQ-dependent D-sorbitol DH (SDH) N-terminally fused to PDZ domain; GFP fusion protein		the assembly of L-RI to SDH *via* protein-peptide interaction of PDZ ligand and PDZ domain	
adh, *idh*, *aldh*, *gidh*, *gdh*, *pqq3*, *pqq4*, *sldAB* from *G. oxydans* 621H	membrane-bound DHs (mDHs)	$P_{GOX1067\text{-}68}$, $P_{GOX1857}$,	test of promoter strength and enzymatic characterization of mDHs in *G. oxydans* multi-deletion strain BP.9	Mientus et al. 2017
genes of putative membrane-bound DHs from mother of vinegar DNA	glucose DH like DH; alcohol DH like DH; polyol DH like DH; aldehyde DH like DH; D-lactate DH like DH	P_{adh} ($P_{GOX1067\text{-}68}$)	heterologous expression of metagenomic mDHs in *G. oxydans* BP.9 and identification of new substrate specificities	Peters et al. 2017
adhA, *adhAB*, *aldh* from *G. oxydans* DSM 2003	membrane-bound alcohol DH (mADH) and aldehyde DH (mALDH)	P_{tufB}	characterization of mADH and mALDH; 3-hydroxypropionic acid production	Zhu et al. 2018
sldAB from *G. oxydans* ZJB-605	membrane-bound PQQ-dependent D-sorbitol DH	$P_{gHp0169}$	improvement of miglitol precursor production by industrial strain *G. oxydans* ZJB-605	Ke et al. 2019
trx from *G. oxydans* NL71	thioredoxin	P_{lac}	enhancement of *G. oxydans* resistance to lignocellulosic-derived inhibitors; xylonic acid production	Shen et al. 2020
araC, *araE* from *E. coli* MC4100	transcriptional regulator AraC; L-arabinose-transporter AraE	P_{araBAD}	plasmid-based tunable L-arabinose-inducible expression system for *G. oxydans*	Fricke et al. 2020
pqqABCDE and *tldD* from *G. oxydans* H-8	PQQ biosynthesis-related enzymes	$P_{gHp0169}$	increase PQQ biosynthesis in repeated batch biotransformation for miglitol precursor production by mutant strain *G. oxydans* H-8	Liu et al. 2020a
pBBR1MCS-2				
gdh from *G. oxydans* 621H	membrane-bound PQQ-dependent glucose DH	P_{lac}	gluconate and 5-keto-D-gluconic acid accumulation by *G. oxydans*	Merfort et al. 2006b
GOX1857 from *G. oxydans* 621H	membrane-bound PQQ-dependent inositol DH	$P_{GOX1857}$	substrate and co-factor analysis of GOX1857 in *G. oxydans* 621H	Hölscher et al. 2007
uidA from *E. coli* DH5α	β-D-glucuronidase UidA	P_{lac}, $P_{GOX0254}$, $P_{GOX0452}$	characterization of constitutive *G. oxydans* promoter strength	Kallnik et al. 2010
sldA from *G. oxydans* DSM 7145	membrane-bound PQQ-dependent polyol / glycerol DH	P_{sldB}	characterization of *sldA* disruptant mutant and substrate analysis of the enzyme	Voss et al. 2010
mgdh from *G. oxydans* 621H	membrane-bound PQQ-dependent glucose DH	P_{mgdh}	evolution for enhanced growth and biotransformations by *G. oxydans* at low glucose concentration	Zhu et al. 2011
edd-eda and *gnd* from *G. oxydans* 621H	6-phosphogluconate dehydratase; 2-keto-3-deoxy-6-phospho-gluconate aldolase; 6-phosphogluconate DH	$P_{GOX0384}$	analysis of cytoplasmic fructose catabolism in a Δ*gnd* mutant lacking the oxidative PPP and Δ*edd* Δ*eda* mutant lacking the Entner-Doudoroff pathway	Richhardt et al. 2012
cyoBACD, *cydAB* and *cydABCD* of *G. oxydans* 621H	quinol terminal oxidases cytochrome bo_3 and cytochrome *bd*	$P_{GOX0384}$	influence of terminal oxidases on growth and yield of *G. oxydans* 621H	Richhardt et al. 2013
GOX0265 of *G. oxydans* 621H	membrane-bound PQQ-dependent glucose DH (mGHD) with C-terminal Strep-tag	$P_{GOX0452}$	gluconate production; influence of mGDH on O_2 consumption rate; membrane protein purification by Strep-tactin affinity chromatography	Meyer et al. 2013
phoA and *treA* from *E. coli* DH5α	alkaline phosphatase and trehalase fused to selected SPs	$P_{GOX0264}$	SP screening in *G. oxydans* and broadening the substrate range of *G. oxydans* for growth on trehalose	Kosciow et al. 2014
sldhAB from *G. oxydans* WSH-003	membrane-bound PQQ-dependent sorbitol DH (SLDH)	P_{tufB}	enhancing production of L-sorbose from D-sorbitol; increase *sldhAB* mRNA level by artificial poly-A/T tail	Xu et al. 2014
ndh from *G. oxydans* DSM 3504	type II NADH DH (NDH-2)	P_{ndh}	consequence of an additional NADH DH paralog on growth of *G. oxydans* 621H	Kostner et al. 2015
sdhCDAB, *sdhE A. pasteurianus; sdhE* from *Serratia sp.*	succinate DH (SDH) and assembly factor SdhE for attachment of FAD to SdhA	$P_{GOX0384}$, $P_{sdhE\text{-}Ace}$, $P_{sdhE\text{-}Ser}$	SdhE-dependent formation of a functional *A. pasteurianus* SDH in *G. oxydans* 621H	Kiefler et al. 2015

Table 2 (continued)

Expressed genes	Encoded activity/function	P [a]	Context	Reference
GOX1801 from *G. oxydans* 621H	succinic semialdehyde reductase (SSR) fused C-terminally to Strep-tag	$P_{GOX0264}$	characterization of GOX1801 enzyme activities; the first SSR from an aerobic bacterium with high catalytic efficiency	Meyer et al. 2015
sldh from *G. oxydans* WSH-003; *egfp*	D-sorbitol DH; enhanced GFP (eGFP),	P_{B932_2000}, P_{tufB}	identification of strong promoters; comparison of P_{B932_2000} with P_{tufB} form *E. coli* and from *G. oxydans*; enhancing production of L-sorbose	Hu et al. 2015
GOX1432 from *G. oxydans* 621H	cytoplasmic $NADP^+$-dependent mannitol DH fused C-terminally to Strep-tag II	$P_{GOX0264}$	role of mannitol DHs in osmoprotection of *G. oxydans* 621H	Zahid and Deppenmeier 2016
xynA from B. subtilis	endo-1,4-β-xylanase fused N-terminally to the PelB SP	$P_{GOX0264}$	xylan utilization; degradation of renewable organic materials and incomplete oxidation for production of value-added products	Kosciow et al. 2016
pqqA, *pqqB*, *pqqC*, *pqqD*, *pqqE*, *tldD* from *G. oxydans* WSH-003	PQQ biosynthesis proteins	P_{pqqA}, P_{tufB}	analysis of PQQ levels in *G. oxydans* WSH-003 and related conversion of D-sorbitol to L-sorbose	Wang et al. 2016
sdhCDAB and *sdhE* from *A. pasteurianus*; *sucCD* from *Ga. diazotrophicus*	succinate DH (SDH) and assembly factor SdhE for attachment of FAD to SdhA; succinyl-CoA synthetase	$P_{GOX0264}$, P_{sdhE}	used for fragment construction for chromosomal insertion of genes to obtain *G. oxydans* 621H with completed TCA cycle for increased biomass yield from glucose	Kiefler et al. 2017
fdhSCL from *G. japonicus*; *sacC* from *Z. mobilis* ZM4	membrane-bound fructose DH; extracellular sucrase SacC fused N-terminally to the PelB SP	$P_{GOX0264}$	production of 5-ketofructose from fructose or sucrose using genetically modified *G. oxydans* strains	Siemen et al. 2018
fdhSCL from *G. japonicus* NBRC3260	membrane-bound fructose DH (Fdh)	$P_{GOX0264}$	production of 5-ketofructose; online monitoring of the respiration activity; pulsed and continuous fructose feed	Herweg et al. 2018
phoA from *E. coli*; *oprF* from *P. aeruginosa* PAO1	alkaline phosphatase PhoA; first 188 aa of outer membrane porin OprF fused C-terminally to Strep-tag; OprF-PhoA fusion protein	$P_{GOX0264}$, $P_{GOX0452}$	surface display of PhoA in *G. oxydans* using OprF for delivery and test of linker regions in OprF-PhoA fusion proteins	Blank and Schweiger 2018
codon-optimized *sldh* from *G. oxydans* G624; *lrenox* from *Lactobacillus reuteri*	sorbitol DH; NAD(P)H oxidase	P_{adh}	overcoming inhibitory effect of NADPH formation during conversion of D-sorbitol to L-sorbose in *G. oxydans* KCTC 1091	Kim et al. 2019
fdhSCL from *G. japonicus* NBRC3260; *inv1417* from *G. japonicus* LMG 1417	membrane-bound fructose DH (Fdh); β-fructofuranosidase / invertase	$P_{GOX0264}$	production of 5-ketofructose (5-KF) by *G. oxydans* and *G. japonicus*; production of 5-KF from sucrose by invertase and Fdh with recombinant *G. oxydans* strains	Hoffmann et al. 2020
fdhSCL from *G. japonicus* NBRC3260	membrane-bound fructose DH (Fdh)	$P_{GOX0264}$	production of 5-ketofructose from sucrose by fructose DH and invertase with *G. oxydans* IK003.1	Battling et al. 2020
levS1417 from *G. japonicus* LMG 1417 pBBR1MCS-4	levansucrase	$P_{GOX0264}$	high yield production of levan-type fructans by *G. japonicus* LMG 1417	Hövels et al. 2020
sldAB from *G. oxydans* 621H	membrane-bound sorbitol DH (mSLDH)	P_{tufB}, P_{sldAB}	growth performance and DHA production by engineered *G. oxydans* 621H	Lu et al. 2012
fdhSCL from *G. japonicus* NBRC3260	flavoprotein-cyt. c complex fructose DH (FDH)	P_{adhAB}	production of FDH in *G. oxydans* NBRC12528 strains; 5-keto-D-fructose formation	Kawai et al. 2013
aroQ from *G. oxydans* NBRC3244	type II 3-dehydroquinate dehydratase	P_{lac}, P_{aroQ}	biotransformation of quinate to 3-dehydroshikimate by *G. oxydans* NBRC3244	Nishikura-Imamura et al. 2014
	2-ketogluconate DH	P_{adhAB}		Kataoka et al. 2015

Table 2 (continued)

Expressed genes	Encoded activity/function	P [a]	Context	Reference
kgdSLC from *G. oxydans* NBRC3293			production of 2,5-diketo-D-gluconate by *G. japonicus* NBRC3271	
sldBA from *G. frateurii* NBRC101659	membrane-bound PQQ-dependent glycerol / polyol DH (GLDH)	P_{lac}	sugar oxidase activities of GLDH in *G. frateurii* NBRC101659 strains	Yakushi et al. 2018c
steP from *G. frateurii* NBRC101659	sugar-transporting / exporting permease	none, P_{lac}, $P_{GOX0284}$, $P_{GOX0452}$	SNP in *steP* affects trehalose efflux / sorbose uptake; NADPH/$NADP^+$ ratio and thermotolerance of *G. frateurii*	Matsumoto et al. 2018
quiA from *G. oxydans* NBRC3292 and NBRC3244	membrane-bound PQQ-dependent quinate DH (QDH)	P_{lac}, P_{adhAB}, P_{quiA}	improving QDH activities, tested in *G. oxydans* NBRC12528 and *G. frateurii* NBRC101659 strains	Yakushi et al. 2018b
sndh from *Ga. liquefaciens* RCTMR10	membrane-bound sorbosone DH (SNDH)	P_{adhAB}	expression in *G. oxydans* NBRC12528 and identification of the prosthetic group of SNDH	Yakushi et al. 2020

[a] If no promoter or no native upstream region of the cloned gene(s) is mentioned in the publication, promoter P_{lac} present on the pBBR1MSC-based plasmids was assumed to be responsible for target gene expression

In another study, the amplified *par-rep* fragment of pGOX3 from *G. oxydans* 621H was ligated with pUC19 and shuttle vector pUCpr was obtained (Yuan et al. 2016a). In this work two compatible plasmids, pBBR1MCS-5 and pUCpr have been applied simultaneously in the same strain for target gene expression. Plasmid pBBR1MCS-5 was used to express the membrane-bound PQQ-dependent sorbitol dehydrogenase genes *sldAB* from the strong promoter $P_{GOX0169}$ in different combination with pUCpr derivatives carrying either the PQQ biosynthesis genes *pqqABCDE* or *pqqABCDE-tldD* under control of $P_{GOX0169}$ alone, or each in combination with the cytochrome bo_3 oxidase genes *cyoBACD* expressed from a separate copy of the $P_{GOX0169}$ promoter. In fed-batch cultivation with pH and dissolved oxygen tension control, 5-keto-D-gluconate production could be significantly enhanced with the combinatorial metabolic engineering strategy to 162 g/L based on the two-plasmid-system in the recombinant industrial *G. oxydans* strain ZJU2 (Yuan et al. 2016a).

Plasmid-based promoter analysis in *Gluconobacter*

Besides the expression of target genes in screening, complementation, functional, or metabolic engineering studies, plasmids have also been used in *Gluconobacter* to analyze and compare relative promoter strength using selected reporter genes. The promoter probe vector pCM130 is a derivative of the P_{lac} expression plasmid pCM62 introduced below in the *Acetobacter* section and carries the reporter gene *xylE* encoding catechol 2,3-dioxygenase from *Pseudomonas* in place of P_{lac}. It was used to compare the strength of the promoter P_{pqqA} and a potential intrinsic promoter $P_{pqqBCDE}$ of the *pqqABCDE* operon from *G. oxydans* 621H (Hölscher and Görisch 2006). With both D-mannitol or D-gluconate as a growth substrate, the reporter activities of $P_{pqqBCDE}$ were below the activity found for the pCM130 empty vector, while with P_{pqqA} the reporter activities were at least 3.5-fold higher than with the empty vector. Therefore, the reporter assay results suggested that P_{pqqA} represents the only promoter of the *pqqABCDE* operon in *G. oxydans* 621H, a situation similar to that found for other PQQ-synthesizing bacteria.

With the aim to provide effective P_{lac}-independent expression vectors for gene expression in *G. oxydans*, constitutive promoters were selected to determine their relative strength using pBBR1MCS-2 and the β-D-glucuronidase gene *uidA* from *E. coli* as a reporter (Kallnik et al. 2010). The promoters of GOX0264 and GOX0452 encoding the ribosomal proteins L35 and L13, respectively, were found to be strong ($P_{GOX0264}$) and moderate ($P_{GOX0452}$), while the intrinsic promoter P_{lac} of pBBR1MCS-2 appeared rather weak in *G. oxydans* 621H. In another approach to identify strong promoters, chromosomal DNA of *G. oxydans* DSM 2003 was randomly digested and DNA fragments were inserted into pBBR1MCS-5-gfp carrying the promoterless green fluorescent protein gene as a reporter (Shi et al. 2014). After screening the GFP fluorescence signals of 710 transformants, the one with the highest fluorescence intensity was selected and a 261-bp DNA fragment was obtained that exhibited promoter activity and was homologous to the *G. oxydans* 621H intergenic region between GOX0168 encoding an NAD-dependent DNA ligase and GOX0169 encoding a hypothetical protein. The promoter region was termed gHp0169 and $P_{gHp0169}$ activity was determined to be almost 2-fold stronger (2.47 U/mg) than

P_{tufB} from *G. oxydans* (1.39 U/mg) when assayed with pBBR1MCS-5 and the *ndh* gene encoding the type II NADH dehydrogenase as a reporter.

Since strong promoters are one of the essential factors that can improve strain performance by overexpression of specific genes, a pipeline for screening strong promoters by proteomics analysis and promoter assays was also established (Hu et al. 2015). Using this approach, the strong promoter P_{B932_2000} was identified in *G. oxydans* WSH-003. As assessed by analysis of pBBR1MCS-2-based *egfp* expression and qRT-PCR analysis of *egfp* mRNA, the strength of P_{B932_2000} in *G. oxydans* WSH-003 was at least 2-fold higher than that of P_{tufB} from *G. oxydans* and at least 4-fold higher than that of P_{tufB} from *E. coli*. In a further study the aforementioned *G. oxydans* promoters P_{tufB}, $P_{GOX0169}$, $P_{GOX0264}$, and $P_{GOX0452}$ were assayed for their relative strength in *G. oxydans* 621H using pBBR1MCS-5 and *gfp* as reporter gene (Yuan et al. 2016a). In this assay, $P_{GOX0169}$ was found to be the strongest one, followed by $P_{GOX0264}$, P_{tufB}, and $P_{GOX0452}$, respectively.

In contrast to the previous studies searching mainly for strongest promoters, another study aimed to develop a new vector for successful expression of genes encoding membrane-bound dehydrogenases in *G. oxydans*, which typically requires intermediate or even low expression levels to obtain functional enzymes (Mientus et al. 2017). In this study, the strength and the regulation of the promoters of the alcohol dehydrogenase gene (P_{adh}) and the inositol dehydrogenase gene (P_{idh}) were analyzed using pBBR1MCS-5-based pJV17 derivatives carrying the *E. coli lacZ* reporter gene. According to the β-galactosidase assays, both promoters were practically not active in *E. coli*, while they showed good activity in *G. oxydans* grown on D-mannitol, D-sorbitol or D-glucose as carbon source. P_{adh} led to similar LacZ activities with all three substrates and was generally more active than P_{idh}, which led to weak LacZ activity on D-mannitol and appeared to be repressed 100-fold in the presence of D-glucose when compared to D-sorbitol.

Chromosomal integrations and intergenic regions suitable for target gene expression

Besides plasmid-based expression, chromosomally integrated expression cassettes using either the native promoter or selected endogenous or heterologous promoters have also been applied for target gene expression in *Gluconobacter*. In an early study analyzing the maltose-oxidizing ability of a *G. oxydans* strain, the effect of a single amino acid substitution on the substrate specificity of the PQQ-dependent glucose dehydrogenase (mGDH) was tested by chromosomal insertion due to the lack of a suitable expression plasmid for *Gluconobacter* at that time (Cleton-Jansen et al. 1991). A *G. oxydans* strain with an endogenous mGDH not capable of oxidizing maltose was transformed with the non-replicable pGP173 plasmid backbone, which carried the mGDH gene of the maltose-oxidizing strain under control of its native promoter region and a kanamycin resistance cassette. Recombinant cells formed by homologous recombination were selected by growth on maltose. Further analysis revealed that the exchange H787N broadened the substrate spectrum of the mGDH and enabled the oxidation of the disaccharide maltose.

Later, chromosomal integrations for target gene expression have been used in combinatorial metabolic engineering studies for which suitable integration sites had to be selected. For example, to increase the biomass yield of *G. oxydans* 621H on glucose, of which 90% is typically oxidized already in the periplasm to gluconate and 2-ketogluconate accumulating unused in the medium, the carbon flux into the central carbon metabolism needs to be increased and additionally, the incomplete tricarboxylic acid (TCA) cycle of *G. oxydans* 621H needs to be completed by a succinate dehydrogenase and a succinyl-CoA synthetase, since these two TCA cycle enzymes are absent. These requirements were addressed by combining the chromosomal insertion of several heterologous genes and deletion of the two glucose dehydrogenase genes to eliminate the periplasmic and cytosolic oxidation of glucose to gluconate (Kiefler et al. 2017). In detail, the cytoplasmic NADP-dependent glucose dehydrogenase gene *gdhS* was replaced by the succinate dehydrogenase genes *sdhCDAB* and the flavinylation factor gene *sdhE* from *A. pasteurianus* with the *sdhCDAB* operon under the control of strong $P_{GOX0264}$ and *sdhE* under the control of its native promoter. The membrane-bound PQQ-dependent glucose dehydrogenase gene *gdhM* was replaced by the succinyl-CoA synthetase genes *sucCD* from *Ga. diazotrophicus* again using the strong promoter $P_{GOX0264}$. Furthermore, the pyruvate decarboxylase gene *pdc* was replaced by a second *ndh* gene for a type II NADH dehydrogenase with its native promoter from *G. oxydans* DSM 3504 to eliminate acetate formation from pyruvate and to increase the overall NADH oxidation capacity. Together, the biomass yield of the engineered plasmid-free *G. oxydans* strain IK003.1 was increased by 60% and the strain was stable for more than 70 generations, making it very interesting as a host for oxidative biotransformations and further metabolic engineering approaches (Kiefler et al. 2017; Kranz et al. 2017).

Generally, for successful expression of chromosomally integrated recombinant genes, suitable intergenic regions need to be identified. Consequently, *G. oxydans* IK003.1 was used to test different intergenic regions (IGRs) selected on the basis of RNAseq data for their suitability to integrate and express the fructose dehydrogenase (FDH) genes *fdhSCL* from *G. japonicus* under the control of the strong promoter $P_{GOX0264}$ for the oxidative biotransformation of fructose to 5-ketofructose (5-KF) (Battling et al. 2020; Kranz et al. 2018). 5-KF is a promising non-nutritive natural sweetener

for which high-titer production was achieved already before in plasmid-based approaches (Kawai et al. 2013; Siemen et al. 2018). In the chromosome-based approach, four IGRs have been identified in the *G. oxydans* 621H genome suitable for expression of heterologous genes. That is the IGR of the genes GOX0013-GOX0014, GOX0028-GOX0089; GOX0038-GOX0039 and GOX2095-GOX2096, respectively, all located close to the genomic *ori* to take advantage of the increased average DNA copy number during chromosome replication in the exponential growth phase. Finding more than one suitable integration site allowed independent double-integration of the *fdhSCL* operon associated with a strong increase in the 5-KF production rate compared to the single integration strains. Therefore, more integrated copies of the *fdhSCL* operon are expected to further increase the 5-KF production rate by plasmid-free strains. Additionally, the use of a promoter stronger than $P_{GOX0264}$ could enhance *fdhSCL* expression and thereby 5-KF production. Besides fructose as substrate, 5-KF could also be produced from the cost-efficient and renewable feedstock sucrose when applying a sucrose-hydrolyzing enzyme and FDH (Hoffmann et al. 2020). The *fdhSCL* genes were disruptively integrated into the mGDH gene locus under the control of the strong promoter $P_{GOX0264}$ and the invertase Inv1417 gene was expressed under the control of the same promoter on a pBBR1MCS-2-based plasmid. The average yield of 5-KF formation from sucrose was 90 mM 5-KF, which is 84% in relation to the fructose released from 105 mM sucrose almost completely hydrolyzed. The invertase contains a Tat-signal peptide for secretion into the periplasm, but only 40% of the total invertase activity was found in the periplasm and 60% in the cytoplasm. This suggested that plasmid-based expression of the Inv1417 gene using the strong promoter $P_{GOX0264}$ possibly caused an overload of the Tat export machinery. Chromosomal integration of the invertase gene into one of the suitable *G. oxydans* IGRs mentioned above might solve this limitation.

The same principle of combining gene deletion to eliminate undesired enzyme activity and inserting an expression cassette into the disrupted gene locus was applied for biotransformation of glucose to 2-keto-D-gluconic acid via intermediate D-gluconic acid by recombinant *G. japonicus*. The gene for a subunit of gluconate-5-dehydrogenase producing the unwanted by-product 5-keto-D-gluconic acid from D-gluconic acid was deleted and in this locus a cassette for the expression of a gluconate-2-dehydrogenase gene was inserted to increase 2-keto-D-gluconic acid formation from D-gluconic acid produced from glucose (Zeng et al. 2019).

L-Arabinose-induced AraC-dependent regulatable expression

Until now, an L-arabinose-inducible *araC*-P_{araBAD} system on the pBBR1MCS-5 backbone is the only regulatable system available for *Gluconobacter* (Fricke et al. 2020). The mechanism of transcriptional gene regulation by AraC is different compared to those of the pure repressor proteins TetR and LacI, which just dissociate from their operator DNA when their respective inducer is bound to the protein. In *E. coli* AraC does not only repress P_{araBAD} by looping the DNA when bound to specific target sequences in the absence of L-arabinose, but also is essential for activation of P_{araBAD} (Fig. 2a). In the presence of L-arabinose, a modified binding of AraC to target sequences causes unlooping of the promoter DNA and stimulation of both the binding of RNA polymerase and the transition from the closed to the open promoter complex (Schleif 2010; Soisson et al. 1997). Additionally, in *E. coli*, the cAMP receptor protein (CRP) also plays an important role. According to the *G. oxydans* 621H genome sequences, a CRP appears to be absent (Kranz et al. 2017; Prust et al. 2005). The heterologous *araC*-P_{araBAD} system of *E. coli* MC4100 is very tight in *G. oxydans* even in the absence of AraC, indicating that promoter P_{araBAD} is not active in *G. oxydans* without AraC. The system is also well-tunable with up to 480-fold induction by L-arabinose concentrations up to 1% (w/v) (Fig. 2b). Unexpectedly, the performance of this system was strongly affected by only one or two small sequence alterations in the constructed plasmids. A single G to C exchange between the RBS and the ATG start codon of the reporter gene to create a *Nde*I cloning site in the MCS region of the *araC*-P_{araBAD} empty vector and/or the short remaining sequence of the *Xho*I site (CTCGAG) after the stop codon of the reporter gene, strongly reduced the maximum of the resulting reporter activity. In future studies, systematic analysis of such and other sequence alterations including terminators and orientations of neighboring genes (for example, target gene and the plasmid resistance cassette) may reveal specific rules that should be considered for successful construction and establishment of tight and regulatable heterologous expression systems in *Gluconobacter* or in AAB.

The L-arabinose concentrations required for highest induction in *G. oxydans* were much higher than the ones typically used for *E. coli*. Attempts to increase the arabinose sensitivity of the *araC*-P_{araBAD} system by expression of the L-arabinose transporter gene *araE* in tandem with *araC* from the promoter of *araC* had a strong negative effect on the growth of *G. oxydans* and the expression performance (Fricke et al. 2020). With a pBBR1MCS-5 derivative carrying *araE* separately under control of the weak constitutive *G. oxydans* promoter $P_{GOX0384}$ no *G. oxydans* 621H transformants could be obtained yet, suggesting a severe growth defect upon *araE* expression in *G. oxydans*, even in the absence of L-arabinose (our unpublished results). Thus, before using AraE to hopefully increase the sensitivity of the *araC*-P_{araBAD} system toward L-arabinose, the strong negative effect of *araE* expression should be understood and overcome. Therefore, conditional and tuned expression of *araE* using the *araC*-P_{araBAD}

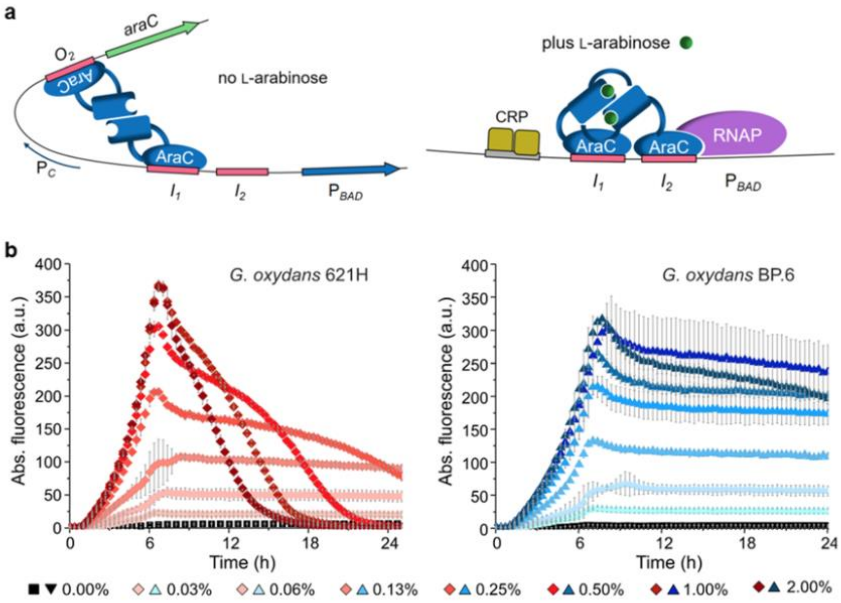

Fig. 2 **a** The region of the P_{araBAD} promoter between the *araC* and *araBAD* genes illustrating the regulatory mode of action by the AraC regulator protein according to Schleif 2010. **b** AraC-dependent induction of mNeonGreen (mNG) expression up to 480-fold in *G. oxydans* 621H and mutant strain BP.6 both with plasmid pBBR1MCS-5-*araC*-P_{BAD}-*mNG* induced by concentrations of L-arabinose (Fricke et al. 2020). As further analyzed and discussed in the study, the decrease of the mNG fluorescence in strain 621H at stronger induction is pH-dependent due to enzymatic oxidation of L-arabinose forming L-arabinonic acid and can be avoided by either using the multi-deletion strain BP.6 or pH-controlled condition

system itself could help to clarify the negative effects of *araE* expression in *G. oxydans*. Likewise, *araC*-P_{araBAD}-dependent conditional expression could also help to express genes for other "difficult" transporters and (membrane-bound) enzymes in AAB.

Target gene expression in *Komagataeibacter*

Taken into account the changes in the AAB genera systematics and the associated transfers of species as described before, we found 42 studies for *Komagataeibacter* reporting on expression plasmids, among which 5 major lineages can be identified. Almost all studies employed electroporation as the method of choice for transfer of plasmids into *Komagataeibacter*, whereas conjugation was rarely used (Hall et al. 1992; Zhu et al. 2012).

Early plasmid studies in *Komagataeibacter*

Initial work on the genetics to provide a gene transfer system was published by Johs Kjosbakken and co-workers in 1986 when studying the conjugative transfer of broad-host-range plasmids and cloning vectors (RP1, pKT210, pRK290, pBR322) with several antibiotic resistances into bacterial cellulose-producing *K. xylinus* (alias *Ga. xylinus* alias *A. xylinum*) and analyzing the number of transconjugants (Valla et al. 1986; Valla et al. 1987). The plasmid RP4::Mu *c*ts61 was used for the insertion of Tn*1* into the endogenous and conjugatively mobilizable 16-, 44-, and 64-kb plasmids of *K. xylinus*. Many of the Tn*1* insertions affected the copy number of the plasmids, yet it provided a selectable marker for the potential use of the plasmids in gene transfer experiments. In follow-up studies on cellulose-forming (Cel^+) and cellulose-negative (Cel^-) mutants of *K. xylinus* the broad-host-range cloning vector pVK100 and cosmid vector pRK311 were used to prepare gene libraries of *K. xylinus* to search for genes expressed from their native promoters and complementing the Cel^- phenotype (Fjaervik et al. 1991; Valla et al. 1989). The screenings revealed a uridine 5'-diphosphoglucose (UDPG) pyrophosphorylase gene designated *celA* involved in cellulose biosynthesis for which UDPG is the precursor, and a gene encoding phosphoglucomutase activity, which

catalyzes the second step of UDPG synthesis from glucose by isomerization of glucose-6-phosphate to glucose-1-phosphate.

In a similar complementation screening, a cosmid vector derived from the high copy number, double-replicon vector pKT230, exhibiting a broad host range and found to be stably maintained in *K. xylinus*, was used for the construction of a genomic library (Wong et al. 1990). Four genes designated *bcsA*, *bcsB*, *bcsC*, and *bcsD*, which form the cellulose synthase operon, were found to complement the Cel^- phenotype caused by a cellulose synthase deficiency. In this study, it was also discovered that *K. xylinus* could be transformed by DNA via electroporation and a small endogenous cryptic plasmid (3.6 kb) was found. The latter was used to construct two shuttle plasmids by ligating the small cryptic plasmid with the *E. coli* plasmids pUC18 and pUC19 at the *Sst*I sites to obtain pUC18-824 and pUC19-824. These shuttle plasmids confer ampicillin resistance and also serve as expression vectors due to the presence of P_{lac} from *E. coli* which is actively transcribed in *K. xylinus*. Cloning of the single *bcs* genes expressed from P_{lac} allowed specific complementation of different Cel^- mutants. Additionally, replacing the native *bcs* promoter P_{bcs} on the chromosome with the heterologous promoters P_{lac} or P_{tac} reduced the cellulose synthase activities of cells to ~60% and ~85% of the level of the parental strain, demonstrating that the promoter P_{bcs} is quite strong and useful for high expression of desired target genes. In a later study on the cellulose-synthesizing operon *acs* in another *K. xylinus* strain, the cosmid vector pRK311 already mentioned above was used to express the single gene *acsD* from P_{tac} for recovery of normal cellulose production in an *acsD* mutant (Saxena et al. 1994).

pUF106, pTA99, and pTI99—a first major expression plasmid lineage

The principle of fusing endogenous cryptic plasmids derived from *K. xylinus* strains with well-characterized *E. coli* plasmids to obtain shuttle vectors was also tested and applied in further studies using pUC18, pBR322 or the pBR322-based plasmid pTrc99A. Based on the endogenous *K. xylinus* plasmid pFF6 (2.72 kb) fused with pUC18 or with pTrc99A, the plasmids pUF106 and pTA99 were constructed to obtain shuttle vectors (Fujiwara et al. 1992; Tajima et al. 2001). Plasmid pTA99 was used to express the (exo)polysaccharide metabolism-related β-glucosidase gene *bglxA* from a *K. xylinus* strain driven by the strong *E. coli* P_{lac}-P_{trp} hybrid promoter P_{trc}. Analysis of culture supernatants demonstrated an approximately tenfold higher specific β-glucosidase activity compared to *K. xylinus* cells carrying the empty vector as a control. Similar to pTA99, shuttle vector pTI99 was also obtained by fusion of pFF6 with pTrc99A (Hu et al. 2010). It was used to clone various gene variants encoding N-terminally truncated AxCeSD proteins that form subunit D of the cellulose-synthesizing terminal complex in *K. xylinus* (Hu et al. 2010). Thereby, the N-terminal loop of subunit D, especially residue Lys6, turned out to be important for cellulose production. The AxCeSD and CcpAx proteins of the cellulose-synthesizing terminal complex were also expressed as fusion proteins with an enhanced green fluorescent protein (EGFP) using pTI99 (Sunagawa et al. 2013). In fluorescence microscopy analysis, the AxCeSD-EGFP fusion protein showed a cellular localization similar to the CcpAx fusion protein. Together with other data, AxCeSD and CcpAx showed significant interaction and were suggested to function as members of the terminal complex in *K. xylinus*.

To obtain modified bacterial cellulose with altered mechanical strength, biodegradability, and bioactivity for biomedical use, the curdlan synthase gene *crdS* from *Agrobacterium* was expressed in *K. xylinus* using pTI99 (Fang et al. 2015). It enabled curdlan (β-1,3-glucan) to be synthesized in *K. xylinus* simultaneously with cellulose nanofibers in vivo for biopreparation of nanocomposites. Production of bacterial cellulose with altered and advantageous properties could also be obtained without chemical modifications solely through altering the tight spatial organization of the cellulose fibers using a non-motile cellulose-producing *K. hansenii* with increased cell length and the ability to move on the surface of the medium (Jacek et al. 2019; Jacek et al. 2018). Therefore, the *motAB* genes encoding motor and stator proteins essential for flagellum rotation in numerous bacterial species were expressed either as an operon, or alone, or each gene as a translational fusion with *gfp* using the pTI99 vector backbone. It was assumed that probably the torque produced by the MotAB proton pump could affect other yet unknown motility mechanisms, cell division, filamentation or transport, thereby affecting the structure of the cellulose. Indeed, *K. hansenii* mutants with increased cell length and motility were shown to produce altered cellulose membranes with increased pore sizes and a relaxed fiber structure, which supported chondritic cell proliferation important for potential future application in tissue engineering.

pSA19—a second major expression plasmid development

In parallel to the pFF6-based plasmid lineage, another endogenous cryptic plasmid termed pAH4 (4 kb) from a cellulose-producing *K. xylinus* strain was used for construction of a shuttle vector and established pSA19 as another major expression plasmid. *Hind*III-linearized pAH4 and pUC18 were fused to obtain the shuttle vector pSA19, which contains several pUC18 cloning sites and the promoter P_{lac} for expression of cloned genes (Tonouchi et al. 1994). The copy number of pSA19 in *K. xylinus* is roughly ten per genome and transformation efficiency was strongly increased when recombinant

pSA19 plasmids were propagated in *K. xylinus* instead of *E. coli*, suggesting the presence of an effective restriction-modification system in *K. xylinus*. Later, restriction data obtained from two cryptic plasmids discovered in *K. xylinus* B42 showed that these plasmids contain protected *Eco*RI and *Apo*I sites. The protection was also present in the chromosomal DNA and the results suggest the presence of a modification system in *K. xylinus* that recognizes the tetranucleotide 5'-AATT (Petroni et al. 1996). However, plasmid pSA19 was successfully used in 8 further studies on cellulose-producing *K. xylinus* strains:

(i) pSA19 was used to express a wild-type endo-β-1,4-glucanase from *Bacillus* and a mutated variant (H131F), which is inactive but still binds to cellulose, to study their effects on cellulose production by *K. xylinus* (Tonouchi et al. 1995). The native glucanase enzyme enhanced cellulose production and reduced the amount of a polysaccharide called acetan, while the inactive variant did not affect cellulose production. It was concluded, therefore, that the endoglucanase activity itself, but not the cellulose-binding ability, was essential for the enhancement of cellulose production.

(ii) The extracellular sucrase gene *sucZE3* from *Zymomonas mobilis* together with the secretion-activating factor gene *zliS* and the *B. subtilis* levansucrase gene *sacB* containing a mutation causing decreased levan-forming activity were cloned into pSA19 under the control of P_{lac} to study cellulose production by *Komagataeibacter* from sucrose, which is the most suitable carbon source for the economical production of bacterial cellulose (Tonouchi et al. 1998b). The gene expression resulted in increased cellulose production and reduced levan accumulation.

(iii) A sucrose phosphorylase (SPase) gene from *Leuconostoc mesenteroides* was expressed with pSA19 using several promoters (P_{lac}, P_{tac}, P_{ugp} from *K. xylinus*, P_{gdh} from *G. oxydans*) to improve cellulose production in *K. xylinus* (Tonouchi et al. 1998a). Compared to expression from P_{lac}, the SPase expression level was 78% with P_{tac}, 37% with P_{ugp}, and only 13% with P_{gdh}. Interestingly, a small increase of the 5'-UTR length with a modified P_{lac} region increased the SPase expression level 3-fold.

(iv) pSA19 was used to express a sucrose synthase gene with the 5'-upstream region (~3.1 kb) of the cellulose synthase operon *bcs* from a *K. xylinus* strain instead of P_{lac} to study this *bcs* promoter region (Nakai et al. 1998). In *K. xylinus*, the expression occurred more than 241 bp upstream from the ATG start codon within the 1.1 kb upstream region. In *A. aceti* the expression was 75% of that in *K. xylinus*, while in *E. coli* no expression at all was detected, suggesting that the *bcs* upstream region studied may function as an ABB-specific promoter.

(v) To make use of the free energy of the glycosidic bond in sucrose for cellulose biosynthesis, the gene encoding native sucrose synthase from mung bean or a variant with a S11E mutation mimicking phosphorylation were cloned and expressed with pSA19 in *K. xylinus* under control of P_{lac} (Nakai et al. 1999). Sucrose synthase reversibly converts sucrose and UDP to fructose and UDP-glucose, the substrate of cellulose synthase. Expression of sucrose synthase in *K. xylinus* enhanced cellulose production from sucrose and the S11E variant with an increased sucrose affinity had an even stronger stimulating effect on cellulose synthesis.

(vi) For complementation of an ORF2 disruptant mutant of *K. xylinus* and functional analysis of the ORF2 polypeptide involved in cellulose synthesis, the ORF2 sequence plus a kanamycin resistance cassette was cloned into pSA19 (Nakai et al. 2002). The parental strain produced tough, colorless, and insoluble cellulose pellicles, whereas the ORF2 mutant produced thin, yellow, and fragile pellicles. The ORF2 polypeptide was suggested to be involved in the assembly of glucan chains into crystalline cellulose I microfibrils.

(vii) For complementation of *K. xylinus* mutants with disrupted *aceR* and *aceQ*, these genes involved in acetan biosynthesis were cloned into pSA19 for expression (Ishida et al. 2002). NMR and ESI-MS analyses of the produced water-soluble polysaccharides suggested that *aceQ* and *aceR* encode a glucosyltransferase and a rhamnosyltransferase, respectively.

(viii) In a mutant of *K. xylinus* in which the carboxymethylcellulase gene *cmcax* was disrupted by an ampicillin resistance cassette, the *cmcax* gene was expressed in *trans* using the pSA19 backbone carrying a kanamycin resistance cassette as an additional selection marker (Nakai et al. 2013).

pBBR122 and pMV24—two other major expression plasmids used in *Komagataeibacter*

Another expression plasmid stably used in *Komagataeibacter* is the broad-host-range plasmid pBBR122 introduced above in the *Gluconobacter* section. With this plasmid, the gene of the bacterial hemoglobin from *Vitreoscilla* (VHb) was expressed driven by the constitutive *bla* promoter in cellulose-producing *K. xylinus* (Chien et al. 2006; Liu et al. 2018; Setyawati et al. 2007). VHb has been widely applied to improve cell survival during hypoxia. The hemoglobin was biochemically active also in *K. xylinus* and enhanced both the growth rate in shaken cultures by 50% and the cellulose titers. VHb allowed growth or survival of *K. xylinus* at lower oxygen tension and facilitated cellulose production in static culture, in

which the polysaccharide exhibited interesting altered material properties. Cellulose nanofibers can also be used to self-immobilize *K. xylinus* in a biofilm, with the advantage of better resistance toward harsh biotransformation reaction conditions. This was tested for the production of α-ketoacids by a heterologous D-amino acid oxidase (DAAO), the gene of which was constitutively expressed from P_{lac} using pBBR122 (Setyawati et al. 2009). In the DAAO-catalyzed reaction toxic H_2O_2 is formed as a product. With self-immobilized *K. xylinus* cells expressing the DAAO gene, the system exhibited improved thermal and operational stability, as well as easy retrieval for repeated use. In contrast, for biomedical and biomass conversion applications, degradability of bacterial cellulose is important. To improve the poor in vitro and in vivo degradability of bacterial cellulose, a three-gene operon from *Candida albicans* for UDP-*N*-acetylglucosamine (UDP-GlcNAc) synthesis was expressed from the constitutive promoter P_{bla} in *K. xylinus* with the aim to introduce GlcNAc residues by cellulose synthase and produce a chimeric polymer (Yadav et al. 2010). The modified bacterial cellulose exhibited a high GlcNAc content and lower crystallinity, making it a multifunctional bioengineered polymer susceptible to lysozyme, an enzyme widespread in the human body, and to rapid hydrolysis by cellulase, an enzyme commonly used in biomass conversion.

Another shuttle vector used in *Komagataeibacter* studies from 2008 onward is pMV24 already constructed and introduced in 1989 for expression in *Acetobacter* (see *Acetobacter* section below). pMV24 was used to study the regulation and function of the genes *ginI*, *ginA* and *ginR* of a quorum-sensing system from a *K. intermedius* strain producing three different *N*-acylhomoserine lactones (Iida et al. 2008a). The data demonstrated that the GinI/GinR quorum-sensing system controls the expression of *ginA*, which in turn inhibits oxidative fermentation, including acetic acid and gluconic acid fermentation by an unknown mechanism. In a further study, it was discovered that expression of the outer membrane protein gene *gmpA* is positively controlled by the GinA protein in an unknown manner (Iida et al. 2008b). Complementation studies with the expression of *gmpA* using pMV24 demonstrated that GmpA plays a role in inhibiting the formation of oxidized products, including acetic acid and gluconic acid. Transcriptome analysis revealed *gltA* encoding a putative glycosyltransferase, *pdeA* encoding a putative cyclic-di-GMP phosphodiesterase, and *nagA* encoding a putative N-acetylglucosamine-6-phosphate deacetylase as further target genes whose expression is influenced by the GinA protein. For functional and phenotypic analysis *gltA* and *nagA* were expressed under the control of both their own promoter as well as the promoter P_{lac} of pMV24 and *pdeA* was expressed from P_{lac} in *K. intermedius* (Iida et al. 2009). Recently, pMV24 was used to express the acyl-CoA dehydrogenase (ACAD) gene *caiA* from a thermotolerant *K. intermedius* in a non-thermotolerant *K. medellinensis* strain (Konjanda et al. 2019). It improved growth, acetic acid tolerance and ethanol oxidation even at higher temperature.

Other pBR322-based expression plasmids used in *Komagataeibacter*

Another pBR322-based plasmid is pUCD2 originally developed for *Agrobacterium* and exhibiting autonomous replication and an active P_{tet} promoter of the *tetC* gene for tetracycline resistance in *K. hansenii* (Deng et al. 2013). pUCD2 was used to test the complementation of *K. hansenii* Cel^- mutants by expressing the cellulose synthase complex gene *acsA*, the guanylate dicyclase gene *dgc1*, and the putative transcriptional regulator gene *crp-fnr* (*ccp*) from their native promoters (Deng et al. 2013). In this study, pUCD2 with a promoterless *tetC* gene was also used to test promoter activities in *E. coli* and *K. hansenii* to study the *acs* operon and *ccp* promoter regions. pUCD2 was also used for complementation by expressing lysine decarboxylase and alanine racemase genes fused at the 3' ends (C-terminally) with the sequence for an octapeptide FLAG epitope tag allowing detection via immunoblotting (Deng et al. 2015). Furthermore, pBR322 was used to create the shuttle vectors pBE2 and pBE3 by ligating linearized native pGE2 and pGE3 plasmids from *K. europaeus* with pBR322 (Akasaka et al. 2015). pBE2 and pBE3 can replicate in *K. europaeus*, but were not used further. Another pBR322-based vector is pCTP1 containing a chlamydial plasmid cloned into pBR322 and used to express *acsD* of the cellulose synthesizing operon *acs* in fusion with *gfp* from P_{lac} to produce N-terminal and C-terminal fusion proteins in complementation studies of a *K. xylinus acsD* disruption mutant (Mehta et al. 2015). The data obtained suggested that the AcsD protein aids in the proper orientation of the linear terminal complexes along the longitudinal axis of the cell, thus AcsD is involved in the final stage of the hierarchical assembly of cellulose.

pSEVA plasmids and regulatable expression in *Komagataeibacter*

The most recent lineage of expression plasmids used in *Komagateibacter* is based on the *Standard European Vector Architecture* (SEVA) toolkit, a resource for constructing optimal plasmid vectors based on a minimized backbone and three interchangeable modules to design a compilation from several origins of replication, diverse antibiotic resistance markers, and a cargo of interest, flanked by uncommon restriction sites (Durante-Rodriguez et al. 2014). Based on SEVA, a complete set of tools was developed for engineering *Komagataeibacter* that consists of protocols, modular plasmids, promoters, reporter proteins, and inducible constructs that should enable external control of gene expression (Florea et al. 2016a).

Eight SEVA-based plasmids with different *ori* and low, medium or high expected copy number were assessed for propagation in *K. rhaeticus* iGEM. With *ori* RK2, pBBR1, and RSF1010 also mentioned above or below and pWV01, the respective SEVA plasmids were found to show replication, while with *ori* R6K, pRO1600/ColE1, pMB1 and ColE1/pBR322 the SEVA constructs tested did not show replication. The latter, *ori* pBR322 could be used in *Komagataeibacter* at least in other plasmids as mentioned above. From seven reporter proteins tested, mRFP1, GFPmut3, and sfGFP showed visually detectable expression. With mRFP1 as reporter 10 promoters from an open-access collection of synthetic minimal *E. coli* promoters were tested for their promoter strength in *K. rhaeticus* iGEM. For inducible gene expression, four constructs expected to be induced externally by anhydrotetracycline (ATc) or *N*-acyl homoserine lactone (AHL) were tested. From these, the AHL-inducible constructs showed higher induction and lower leakiness than the ATc-induced constructs, yet the induction fold-changes were only up to 5-fold under the conditions tested (Florea et al. 2016a). Interestingly, the LuxR-dependent AHL-inducible system showed a much better induction performance due to a very low basal mRFP1 signal when non-induced and a very strong mRFP1 signal when cells were induced inside cellulose pellicles. Furthermore, the *E. coli* Hfq protein that binds small regulatory RNAs (sRNAs) and mRNAs to facilitate mRNA translational regulation and a sRNA targeting UDP-glucose pyrophosphorylase (UGPase) mRNA were co-expressed from a SEVA plasmid with pBBR1 *ori* in response to the AHL inducer to inhibit UGPase mRNA translation. UGPase catalyzes the production of UDP-glucose, the substrate for cellulose synthesis, and is encoded by a single gene in the genome, allowing knockdown by a single sRNA. This system was found to be highly efficient, as cellulose production was suppressed completely upon full induction and could be fine-tuned using different concentrations of AHL. With *E. coli* Hfq and broad-host-range backbone, the system was engineered to be a general platform for targeted knockdowns in *Komagataeibacter* and other bacterial species independent from the host Hfq by adding new sRNA sequences to the plasmid making the construct easily modifiable for other mRNA targets (Florea et al. 2016a).

The pWV01 *ori* found to be functional in the above study with a SEVA backbone is also present in the non-SEVA plasmid backbone pBAV1C containing the L-arabinose-inducible *araC*-P_{araBAD} system, which was used to induce expression of the *bcs* operon genes *bcsA*, *bcsAB*, and *bcsABCD* in *K. xylinus* for engineering and characterization of bacterial nanocellulose films as low cost and flexible sensor material (Mangayil et al. 2017). Despite several attempts, the pBAV1C derivative with pWV01 *ori* could not be isolated from the transformed *K. xylinus* cells suggesting instability, although clear phenotypic differences were detected in growth curves and cellulose production in the presence of the plasmid.

The SEVA-based *luxR*-P_{lux} system mentioned above was extended by including the AHL-synthesis gene *luxI* downstream of the synthetic constitutive promoter J23104 on a separate plasmid to establish synthetic cell-to-cell communication in *K. rhaeticus* (Walker et al. 2019). Expression of *luxI* allowed the production of the diffusible AHL molecule N-(3-oxohexanoyl) homoserine lactone in the transformed *K. rhaeticus* strain (sender). In another *K. rhaeticus* strain carrying the *luxR*-P_{lux} system (receiver), the signal molecule was sensed, affecting the expression of the *mRFP* gene encoding the fluorescence reporter protein. It was demonstrated that communication can occur both within and between growing pellicles in mixed cultures of the two strains.

SEVA-based plasmids were also used to characterize 11 constitutive promoters, 3 inducible promoters (P_{lux}, P_{tet}, P_{araBAD}), natural and synthetic terminators and ribosome binding sites as well as protein degradation tags in *K. xylinus*, *K. hansenii*, and *K. rhaeticus* iGEM (Teh et al. 2019). P_{lux} was found to be stronger and less leaky than P_{tet} and P_{araBAD}. Due to the high leakiness, induction fold changes of P_{tet} and P_{araBAD} were rather small and in the case of P_{araBAD} depended on the carbon source supplemented for growth. In this study, CRISPR interference (CRISPRi) with a catalytically inactive *Streptococcus pyogenes* Cas9 protein (dCas9) was also tested as a tool to readily knock down the expression of a target gene by blocking transcription. Therefore, the dCas9 gene fused to a 3xFLAG tag DNA sequence was expressed by the strong promoter J23104 together with a single guide RNA (sgRNA) gene under the control of the native tracrRNA promoter from *S. pyogenes*. Alternatively, the sgRNA gene was positioned without promoter just downstream of the *dCas9*-3xFLAG gene, thus forming an operon. The mentioned constructs were cloned into a single pSEVA331Bb plasmid backbone. When targeting the 5'-ends of the *acsAB* gene and of the *acsD* gene of the endogenous *acs* operon for cellulose synthesis in *K. hansenii* by two different sgRNAs, a more than 2-fold decrease in *acsAB* expression and 15% reduced cellulose yield were observed, while for *acsD* no significant change in expression was observed.

pSEVA-based CRISPRi was also used in *K. xylinus* to control the expression level of *galU* encoding UGPase controlling the metabolic carbon flux between the cellulose synthesis pathway and the pentose phosphate pathway (Huang et al. 2020). By overexpression of *galU* and interfering with different sites of the *galU* sequence using CRISPRi, varying expression levels of *galU* from 3 to 3000% were obtained. Analysis of the cellulose characteristics showed that porosity was negatively and crystallinity was positively correlated with increasing *galU* expression levels. This results also confirmed that the properties of the bacterial cellulose can be altered without chemical modifications to increase the application

potential in different fields. Furthermore, these studies showed that CRISPRi as well as Hfq-mediated RNA interference can be used to modulate target gene expression in *Komagataeibacter* and potentially also in other AAB.

To enhance bacterial cellulose production by *K. xylinus*, the effect of the expression levels of the UGPase gene *galU*, the phosphoglucomutase gene *pgm*, and the nucleoside-diphosphate kinase gene *ndp* were analyzed using pSEVA331 derivatives and synthetic RBSs exhibiting different strength identified via fluorescence-activated cell sorting (FACS) in a GFP reporter library (Hur et al. 2020). With pSEVA331-based expression of all mentioned genes under the control of P_{J23104} and with a selected synthetic RBS, the bacterial cellulose titer was 4-fold higher under shaking conditions (3.7 g/L) than that of wild-type *K. xylinus*. In static conditions 5.3 g/L cellulose was reached, demonstrating that reinforced metabolic flux toward bacterial cellulose through modified gene expression represents a practical approach for the improvement of bacterial cellulose production. By another strategy, which included the deletion of a PQQ-dependent glucose dehydrogenase gene and co-expression of the glucose facilitator gene *glf* from *Zymomonas mobilis* and the endogenous glucokinase gene *glk* from *K. xylinus*, a somewhat higher cellulose titer (5.9 g/L) was obtained with *K. xylinus* in a specific growth condition (Liu et al. 2020b). In this study, expression plasmid pRedGX with a pBBR1 *ori*, a kanamycin resistance gene *kanR*, *lacI*^{q}, and the λ-*red* gene controlled by LacI^q-dependent P_{trc} was constructed via Gibson assembly in a SEVA-like manner. This plasmid was used for the IPTG-induced expression of λ-Red recombinase gene in order to increase the efficiency of homologous recombination between the targeted chromosomal gene-flanking regions and a linear PCR product consisting of the in-frame deleted gene and chloromycetin resistance gene with flanking FLP recognition target (FRT) sites, all flanked by the targeted gene-flanking regions. A second expression plasmid, pFLPGX, containing *lacI*^{q}, a pBBR1 *ori* flanked by FRT sites, a spectinomycin resistance gene, and the FLP recombinase gene *flp* controlled by LacI^q-dependent P_{trc}, was also constructed via Gibson assembly. pFLPGX with the same *ori* as pRedGX but a different resistance gene was used to eliminate the λ-*red* plasmid by antibiotics selection and to produce FLP recombinase, which catalyzes the reciprocal recombination between the FRT sites introduced into the chromosome for in-frame gene deletion and also between the FRT sites in the *flp* plasmid (FRT-pBBR1 *ori*-FRT) for self-elimination of the *flp* plasmid. Using the λ-*red* and the *flp* expression plasmids, four putative glucose dehydrogenase genes were deleted in *K. xylinus*, resulting in the identification of one of these genes as being responsible for gluconate formation from glucose. In the respective mutant, the *glf* and *glk* genes were constitutively co-expressed from a plasmid with a pBBR1 *ori* and a kanamycin resistance gene. The results obtained indicated that glucose was transported into the cell by the facilitator protein and glucokinase further increased the production of cellulose (Liu et al. 2020b). In contrast, the constitutive expression of the glucose phosphotransferase system genes *ptsG* and *ptsHIcrr* from *E. coli* did not significantly increase the efficiency of glucose utilization, likely because of limited availability of PEP, which is the donor of the phosphate group during PTS-catalyzed glucose uptake.

Genomic integrations for target gene expression in *Komagataeibacter*

In two studies, genomic integrations instead of plasmids have been used for the expression of target genes in *Komagataeibacter*. A wild-type *K. xylinus* strain was modified by random transposon mutagenesis to insert the *E. coli* β-galactosidase gene *lacZ* generating a lactose-utilizing and cellulose-producing mutant strain (Battad-Bernardo et al. 2004). The promoterless *lacZ* gene expressed from the Tn*10* cassette inserted once into the chromosome was constitutively expressed, alleviated the growth retardation in lactose medium and was stably maintained in a non-selective medium for more than 60 generations. The modified strain showed a 28-fold increase in cellulose production when grown in lactose medium and could utilize 17 g/L of lactose in whey substrate within 4 days. In a genomic and metabolic analysis of a *K. xylinus* strain producing bacterial cellulose nanofiber (CNF), glucose-6-phosphate isomerase and 6-phosphogluconate dehydrogenase encoded by *pgi* and *gnd* have been predicted as novel overexpression targets for the enhanced CNF production (Jang et al. 2019). Therefore, the heterologous *pgi* and *gnd* genes from *E. coli* and *Corynebacterium glutamicum* were individually constitutively overexpressed from the chromosomal *sacB* locus under the control of P_{tac}. By this approach, the amount of CNF produced in a complex medium containing glucose was doubled compared to that obtained with the control strain.

Target gene expression in *Acetobacter*

For *Acetobacter*, we found 30 publications reporting on recombinant DNA work with expression plasmids and 2 major lineages can be seen. The first studies were published in 1985 by Teruhiko Beppu and co-workers. Here, the first chimeric shuttle vectors for *E. coli* / *A. aceti* (*Acetobacter* subgenus *Acetobacter*) have been constructed by ligation of cryptic plasmid pMV102 endogenously present in *A. aceti* subsp. *xylinum* NBI 1002 with the *E. coli* plasmids pACYC177, pBR322, or pBR325. The initial size of chimeric plasmids (>6 kb) was reduced by a series of consecutive digestion and ligation steps delivering pMV329 with only 3.4 kb as the smallest vector (Fukaya et al. 1985a). Most of the constructed

shuttle vectors were stably maintained in *Acetobacter*. In parallel, improvements in the chemically induced competence for the transformation of *Acetobacter* were reported (Fukaya et al. 1985c; Okumura et al. 1985). Furthermore, shuttle vectors pMVL1 and pMVL2 were constructed by ligation of the pMV102 plasmid with a pBR322 derivative containing the β-isopropylmalate dehydrogenase gene *leuB* from *A. aceti* under control of its native promoter (Okumura et al. 1988). Therefore, pMVL1 and pMVL2 carrying an ampicillin resistance cassette were the first *A. aceti* / *E. coli* shuttle vectors with double selection markers as the *leuA* gene allowed selection of *leu*$^+$ transformants in an *A. aceti leuA*$^-$ host. Both pMVL1 and pMVL2 appeared to be stably maintained in *A. aceti* as plasmids after 4 times of successive inoculation and cultivation.

pMV24—the first major expression plasmid used in *Acetobacter*

The smallest plasmid of the pMV series described above (pMV329; 3.4 kb) was used to construct the shuttle vector pMV24 by inserting pMV329 between the *Aat*II and *Nde*I sites of pUC18 (Fukaya et al. 1989). Plasmid pMV24 exhibits an estimated copy number of 10 in *A. pasteurianus*, promoter P_{lac}, and allows translational fusion of the target protein with the 10 N-terminal amino acids of the *E. coli* β-galactosidase. pMV24 was used for recombinant DNA work in 13 *Acetobacter* studies for expression of various genes from the P_{lac} promoter present on the plasmid and additionally from the native gene promoter, if present on the cloned insert:

(i) A membrane-bound aldehyde dehydrogenase ALDH from *A. polyoxogenes* fused to the short N-terminal β-galactosidase peptide was produced in an *A. aceti* mutant lacking the enzyme activity (Fukaya et al. 1989). In submerged fermentation, expression of the ALDH-encoding gene caused an approximately 2-fold increase of the production rate and the maximum concentration of acetic acid.

(ii) Complementation studies with acetic acid-sensitive mutants of *A. aceti* obtained by chemical mutagenesis revealed three genes termed *aarA*, *aarB*, and *aarC* responsible for acetic acid resistance. Gene *aarA* was identified to encode a citrate synthase (Fukaya et al. 1990).

(iii) The *aarC* gene expressed from the pMV24 backbone was found to functionally complement an *aarC* gene disruptant mutant of *A. aceti*, which is defective in acetate assimilation (Fukaya et al. 1993).

(iv) A part of the promoter region of the membrane-bound alcohol dehydrogenase (ADH) gene of *A. pasteurianus* was cloned into pMV24 to corroborate a second transcriptional start by primer extension analysis (Takemura et al. 1993b). Furthermore, a promoterless chloramphenicol acetyltransferase (CAT) gene was cloned into pMV24 resulting in pMVC18 usable for promoter analysis by CAT activity assays. It was shown that the more than 10-fold increased ADH activity caused by ethanol was not due to increased transcription of the *adh* gene, suggesting a mechanism involving translational or posttranslational regulation.

(v) In a search for genes conferring ethanol resistance, an ethanol-sensitive *A. pasteurianus* mutant was transformed with a pMV24-based genomic library and the recombinants were screened for ethanol resistance. The *his1* gene encoding histidinol phosphate aminotransferase was shown to be responsible for the suppression of the ethanol sensitivity of the mutant. This effect was dependent on the higher copy number of *his1* obtained with plasmid pMV24, as the single genomic *his1* copy was not sufficient to enable ethanol resistance (Takemura et al. 1993a).

(vi) The *adhS* gene encoding subunit III of the three-component membrane-bound alcohol dehydrogenase (ADH) from *A. pasteurianus* was expressed from pMV24 and restored the ADH activity of an *adhS* mutant deficient in subunit III (Kondo et al. 1995).

(vii) In a follow-up study, the *gdhS* gene for subunit III of the ADH from *G. suboxydans*, which strongly differs in its amino acid sequence from GdhS of *A. pasteurianus*, was expressed in the *A. pasteurianus adhS* mutant and could not restore the ADH activity (Kondo and Horinouchi 1997). (viii) A study on the esterase-encoding genes *est1*, which is induced only in the presence of ethanol, and *est2*, which is repressed in the presence of ethanol, suggested a *cis*-acting domain exerting transcriptional regulation in the 5'-region of *est2* mRNA (Kashima et al. 1999). Furthermore, the *est1* promoter activity was analyzed using the CAT reporter plasmid pMVC18 introduced above to demonstrate the in vivo effect of ethanol on the transcription of *est1*.

(viii) In a follow-up study, *est1* was shown to play a major role in ethyl acetate formation and its production was fully recovered in an *A. pasteurianus est1* mutant by expressing an *est1*-containing DNA fragment from pMV24 (Kashima et al. 2000).

(ix) In *A. aceti*, pMV24-based overexpression of *groESL* encoding the chaperones GroEL and GroES, which are induced not only by temperature shifts but also by other stresses such as exposure to ethanol, conferred improved growth of *A. aceti* at increased temperature (42°C) and also supported the resistance against ethanol stress (Okamoto-Kainuma et al. 2002).

(x) Similarly, pMV24-based overexpression of the molecular chaperone operon *dnaKJ* with its heat-shock promoter resulted in improved growth of *A. aceti* compared to

the control strain at high temperature or in the presence of ethanol, suggesting a correlation to resistance against various stressors present during fermentation, although it did not increase the resistance to acetic acid (Okamoto-Kainuma et al. 2004).

(xi) Acetic acid resistance of *A. aceti* was increased when the aconitase gene was overexpressed from P_{lac} using pMV24, showing that multiple copies of the aconitase gene, and accordingly an increase in aconitase activity, conferred acetic acid resistance (Nakano et al. 2004).

(xii) In *A. pasteurianus*, pMV24-based overexpression of the *uvrA* gene, whose product is involved in recognition and processing of DNA lesions, resulted in increased biomass formation in the presence of high acetic acid concentrations and resulted in upregulation of enzymes involved in ethanol oxidation and acetic acid tolerance. UvrA thus contributes to acetic acid tolerance by protecting genome integrity, thereby ensuring gene expression and metabolism (Zheng et al. 2018).

pCM62—the second major expression plasmid used in *Acetobacter*

In other studies with *Acetobacter*, the improved broad-host-range cloning vector pCM62 was used as an expression plasmid. It was originally developed for use in methylotrophs and other Gram-negative bacteria by combining the functions present in the minimal transferable and selectable RK2 replicon of the pTJS75 derivative pCM51 with the polylinker and pBR322 *ori* of pUC19 (Marx and Lidstrom 2001). pCM62 was used to express from the promoter P_{lac} or the native promoter, if present on the inserted fragment, a number of different genes:

(i) The UDP-galactose synthesis gene *galE* was expressed for complementation of a *galE* mutant of *A. tropicalis*, which was found to produce extracellular polysaccharide secreted into the medium instead of forming capsular polysaccharide involved in pellicle formation (Deeraksa et al. 2006).

(ii) The subunit III gene *adhS* of the PQQ-dependent alcohol dehydrogenase (ADH) from *A. pasteurianus* was expressed to complement an *adhS* disruptant mutant, which revealed that subunit III is essential for the formation of the active ADH complex besides subunit I and II (Masud et al. 2010).

(iii) Several selected genes identified to support growth of *A. tropicalis* at higher temperatures were expressed to complement gene disruptant mutants obtained by transposon mutagenesis (Soemphol et al. 2011). The study revealed a serine protease, glutamine synthetase, lysyl-tRNA synthetase, 3-phosphoglycerate dehydrogenase, and a few other proteins to rescue the growth defect of the respective mutant strain at higher temperature (42°C).

(iv) The chaperone genes *groESL* were expressed in an *A. pasteurianus groEL* disruptant mutant for complementation and in the parental strain, which enhanced the resistance against 4% acetic acid and 5% ethanol (Theeragool et al. 2018).

(v) The membrane-bound aldehyde dehydrogenase genes *aldFGH*, which are indispensable for acetic acid formation from ethanol, and the isozyme genes *aldSLC*, whose mRNA levels were 10-fold lower during growth on ethanol compared to growth without ethanol, were expressed in *A. pasteurianus* (Yakushi et al. 2018a).

(vi) A mutated oxidoreductase gene *fabG* that may change the fatty acid composition and supports growth of *A. pasteurianus* in a low-nutrient environment were expressed. It enhanced growth of *A. pasteurianus* and the acetic acid production useful for cost-effective manufacturing of rice vinegar (Phathanathavorn et al. 2019).

Other expression plasmids used in *Acetobacter*

Other shuttle vectors for cloning were prepared using the replication region of the large native ~19 kb plasmid pAC1 from *A. pasteurianus* and the kanamycin or tetracycline resistance markers obtained from pUC4-KAPA and pBR322 fragments to yield pACK1 (4.5 kb), pACT7 (3.9 kb) and its smaller *Bal*I / *Pvu*II-digested and self-ligated derivative pACT71 (3.3 kb) (Grones and Turna 1992). Plasmid pACT7 was further modified to include a kanamycin resistance cassette enabling double selection, resulting in plasmid pACG3 (4.8 kb). These shuttle vectors for *E. coli* / *A. pasteurianus* exhibit only the replication region from pAC1, yet possess a similar ability to replicate in *E. coli* and *A. pasteurianus* as the shuttle vectors of the pMV series developed for *A. aceti* mentioned above. The plasmids with pAC1 replicon only were successfully expressed in twelve *Acetobacter* species and transfer of plasmid DNA was optimized for *A. pasteurianus* (Bilska and Grones 2003; Grones and Turna 1995). The pAC1 replicon only plasmid pACT71 was used to express the *E. coli* β-galactosidase gene from P_{lac} in *A. pasteurianus* to analyze its production and release of the protein through the outer membrane in dependence of the medium composition (Grones and Bencova 1994).

In a study on the functions of the multiple heme *c* moieties in intramolecular electron transport and ubiquinone reduction by ADH, the expression plasmid pKS13 providing tetracycline resistance was used to express the alcohol dehydrogenase (ADH) genes *adhAB* from *A. aceti* in *A. pasteurianus* NP 2503 deficient in ADH (Matsushita et al. 1996). Later, the two

cloning and expression vectors pMK10 and pMK20 were constructed from the small *A. pasteurianus* plasmid pAP1 (3 kb) conferring kanamycin resistance, which can also replicate in *E. coli* (Kretova and Grones 2006). Plasmid pMK10 was constructed from a pAP1 fragment containing the origin and the *Hae*II fragment of pUC19 carrying the *lacZ*' gene. Plasmid pMK20 was constructed from another pAP1 fragment with the origin fused with the *Eco*RI-*Pst*I fragment of plasmid pCE30 carrying the P_L and P_R promoters and the gene encoding the temperature-sensitive repressor cI^{857} from bacteriophage lambda. The plasmids pMK10 and pMK20 were stable 96–98% both in *A. pasteurianus* and *E. coli* after 250 generations in the absence of kanamycin. Plasmid pMK20 was successfully used for cloning and expression of a membrane protein from *Salmonella* (unpublished), but no further work based on these plasmids was reported.

In one *Acetobacter* study, the IPTG-inducible P_{T7}-based Novagen vector pET-30a(+) with pBR322 origin was described to have been used in *A. pasteurianus* for inducible expression of the endogenous genes of DnaA- and DnaB-like proteins as well as the *dnaA* and *dnaB* genes from *E. coli* to study the replacement of the corresponding endogenous proteins expressed from the chromosome (Bugala et al. 2016). A strong induction of the plasmid-based gene expression in *A. orleanensis* was reported, yet it was not explained whether it resulted from the T7 promoter present on pET-30a(+) or from another promoter included by the cloning procedure. Furthermore, plasmid backbone pBAD18 carrying pBR322 origin, the classical L-arabinose-dependent AraC regulator gene *araC* and the P_{araBAD} target promoter of AraC have been used in *A. orleanensis* for arabinose-inducible expression of asRNA fragments (121 nucleotides) which are antisense to the C-terminal coding sequence of the *dnaA* and *dnaB* gene sequences studied (Bugala et al. 2016). The data of the asRNA induction by arabinose have not been shown, thus a conclusion about leakiness and induction performance is not possible yet.

In two recent *Acetobacter* studies, the pBBR1-based broad-host-range cloning vectors pBBR1MCS-4 and pBBR1MCS-2 already introduced above in the *Gluconobacter* section were used. pBBR1MCS-4 was used to express in *A. pasteurianus* the *adhAB* operon of the endogenous PQQ-dependent alcohol dehydrogenase (ADH) from its native promoter P_{adh} (Wu et al. 2017). By this, the acetic acid production was improved while the residual ethanol content was decreased. 2D proteomic analysis indicated that 19 proteins with several functional classifications were differently expressed more than 2-fold upon *adhAB* overexpression. Metabolic flux analysis of the pathway from ethanol and glucose revealed that overproduction of the PQQ-dependent ADH is an effective way to improve the ethanol-oxidizing respiratory chain. pBBR1MCS-2 was used in *A. pasteurianus* to express genes of the membrane-bound alcohol dehydrogenase (*adhA*) and aldehyde dehydrogenase (*aldH*), PQQ biosynthesis genes (*pqqAB* or *pqqABCDE*), and combinations thereof, each under the control of the promoter P_{tuf} that was 1.8-fold stronger than P_{adhA} in GFP reporter assays (Gao et al. 2020a). Synergistic expression of these genes could not only efficiently relieve the conflict between increased acetic acid production (69 g/L in semi-continuous cultivation) and compromised cell fitness, but also enhanced the acetic acid tolerance of *A. pasteurianus* to a high initial concentration of 3% (v/v) thereby shortening the duration of the starting-up process from 116 to 99 h. This strategy is of significance for decreasing costs for producing high-strength acetic acid industrially and will also be useful for the production of other desired organic acids, especially those involving PQQ-dependent enzymes.

Target gene expression in *Gluconacetobacter*

Plasmid diversity in *Gluconacetobacter*

Taking into account the AAB genera and strain updates, as well as our exclusion criteria mentioned before, we found 10 studies using diverse plasmids for gene expression in *Ga. diazotrophicus*. Mostly, electroporation was used to transfer the recombinant DNA, yet conjugation was also used in some cases. The first recombinant DNA study in *Gluconacetobacter* was a complementation experiment in a levan synthesis-deficient mutant of the renamed *A. diazotrophicus* (Arrieta et al. 1996). Here, the plasmid pPW12, a derivative of the broad-host-range cosmid cloning vector pLAFR1 conferring tetracycline resistance and derived from pRK290 with RK2 *ori*, was used to construct a cosmid library from total genomic DNA of the parental strain to express endogenous complementing genes from their native promoters. This approach revealed a gene termed *lsdA* encoding a levansucrase potentially interesting for the production of the trisaccharide kestose from sucrose. The isolated complementing cosmid termed p21R1 was mobilized into the parental strain by conjugal mating to increase the gene copy number and thereby the levansucrase yield, finally resulting in 189 units mL^{-1} representing more than 95% of the total proteins secreted under selected culture conditions (Hernandez et al. 1999). In a further study, this levansucrase and its D309N derivative were enzymatically characterized after cloning their genes into broad-host-range cloning vector pRK293 and expression from the native *lsdA* promoter (Batista et al. 1999). A later study demonstrated the importance of *lsdA* for adaptation to high osmotic stress and for biofilm formation (Velazquez-Hernandez et al. 2011). The *lsdA* mutant showed a decreased tolerance to 50–150 mM NaCl, a 99% reduced tolerance to desiccation, and a decrease in the ability to form cell aggregates on abiotic surfaces. Complementation of the mutant by expressing *lsdA* again

from its native promoter, both cloned as a fragment into broad-host-range plasmid pBBR1MCS-3 (see *Gluconobacter* section), recovered the abilities of the parental strain in the *lsdA* disruptant mutant.

Ga. diazotrophicus as an endophytic nitrogen-fixing plant-associated microbe is generally also interesting as a host to express genes encoding proteins that could enable control of pests attacking agricultural plants. In this context, the *Bacillus thuringiensis cry* genes are interesting since they encode δ-endotoxins exhibiting entomopathogenic activity. To test the control of coleopteran pests in sugarcane, the *cry3A* gene hooked in the transposon Tn*5* was introduced into *Ga. diazotrophicus* by conjugation on the narrow-host-range suicide plasmid backbone pSUP1021 carrying the transfer origin *oriT* of plasmid RP4 and integrating into the genome (Salles et al. 2000). The *cry3A* gene was successfully expressed in nitrogen-fixing conditions when fused to the promoter of the *nifHDK* operon from *Rhizobium leguminosarum* biovar *trifolii*. The use of regulated promoters activated only under specific conditions may avoid the problem of insect resistance caused by constant production of the δ-endotoxin. Later, the *Cry1Ac* gene from *B. thuringiensis* var. *kurstaki* was introduced into *Ga. diazotrophicus* after cloning into the double replicon shuttle vector pKT230 (Subashini et al. 2011). Clones containing the *Cry1Ac* gene produced the 130 kDa toxin protein both when present inside the sugarcane tissue as well as *ex planta*, and it did not impair the process of nitrogen fixation. To evaluate the colonization process of sugarcane plantlets and hydroponically grown rice seedlings by *Ga. diazotrophicus*, strain PAL5 was marked with *gusA* encoding β-glucuronidase and *gfp* encoding green fluorescent protein (Rouws et al. 2010). The *gusA* and *gfp* reporter genes were constitutively expressed under the control of the gentamicin resistance gene promoter on the broad-host-range plasmid backbone pBBR1. The reporter plasmids were shown to be valid tools to detect strain PAL5 and monitor colonization.

Recently, pBBR1MCS-5 (see *Gluconobacter* section) containing the mCherry gene under control of the promoter P_{tac} was used to analyze the colonization of *Ga. diazotrophicus* on two genotypes of elephant grass (*Pennisetum purpureum*), a perennial C4-plant employed for grazing, silage production or bioenergy, via seed coat and leaf spray (Camelo et al. 2020). The results showed that one elephant grass genotype produced a higher amount of biomass and total nitrogen than the other when *Ga. diazotrophicus* was sprayed on leaves. When colonizing plants and performing nitrogen fixation, the limited availability of iron might impose restrictions on the expression, assembly, and function of the nitrogenase complex. To better understand the iron uptake mechanisms in *Ga. diazotrophicus*, an ATP-binding cassette (ABC) transport system comprising the three genes *feuABC* encoding a periplasmic-binding protein, a permease, and a traffic ATPase was analyzed earlier (Urzua et al. 2013). In this study, the *feuABC* operon was expressed from its native promoter on a pJB_3Tc_{20}-based plasmid backbone with the RK2 replicon in a *Ga. diazotrophicus* parental strain and its *feuAB* disruptant mutant under iron-replete and iron-depleted conditions. The complementation of the mutant with the plasmid carrying the *feuABC* operon restored growth under iron-restricted conditions to the level seen for the parental strain, indicating that *feuABC* is needed for iron uptake.

Promoter screening in *Ga. diazotrophicus*

For *Ga. diazotrophicus*, a promoter library was constructed using the promoter probe vector pPW452, a derivative of the broad-host-range vector pMP220 obtained from pTJS75 with an RK2 replicon and containing a multiple cloning site upstream of a promoterless *lacZ* reporter gene (Schwab et al. 2016). With the library prepared from total *Ga. diazotrophicus* DNA, 480 clones were screened and six promoters were isolated and characterized further. They showed variable expression strengths in the presence of organic acids and polyalcohols, or glucose and sugarcane juices. The characterized promoters might be used in the future for the expression of genes of interest in *Ga. diazotrophicus*. Interestingly, three out of the six characterized promoters are probably involved in the transcription of antisense RNA, including the one showing the highest expression strength. However, a tight and strongly conditionally regulated promoter was not revealed in this study.

Target gene expression in *Acidomonas*

As described before, the AAB genus *Acidomonas* was established since several characteristics of the former species *Acetobacter methanolicus* could be distinguished from other type and representative AAB including *Acetobacter* strains, resulting in the renaming of *A. methanolicus* to *Acidomonas methanolica* (Urakami et al. 1989). For *Acidomonas* expression vectors including a basic promoter probe vector have been created based on the popular broad-host-range multicopy plasmid RSF1010 (Schröder et al. 1989; Schröder et al. 1991). In *A. methanolica*, a RSF1010-based derivative was used to express the core antigen gene of hepatitis B virus subtype ayw under control of the *E. coli* P_{lac} promoter alone and under tandem control of the strong promoter P_{acm} from the *Acetobacter* phage *Acm*I and from P_{lac}. When produced from the tandem promoters, the core antigen detected in lysates of *A. methanolica* was about 7-fold higher than in *E. coli* (Schröder et al. 1991).

The P_{acm} promoter and the *E. coli* promoters P_{lac} and the temperature-dependent phage lambda P_R promoter were tested in a RSF1010-based vector for expression of the pectate lyase gene *pltB* from *Erwinia carotovora* and the

aspartokinase/homoserine dehydrogenase genes *thrAB* from *E. coli* in *A. methanolica* (Föllner et al. 1994). The highest specific activities of the enzymes were detected with P_R in tandem arrangement with *ptlB* and its native promoter and with P_{acm} in tandem with *thrAB* and its native promoter. A temperature shift to activate the P_r promoter was not needed in *A. methanolica* and was even disadvantageous, since it drastically lowered the resulting specific enzyme activity. The created vector system was also stable in *A. methanolica* in antibiotics-free media.

The RSF1010-based promoter probe vector pRS201 carrying a promoterless *lacZ* gene as a reporter was used to analyze the induction of the stationary growth phase promoters P_{bolAP1} and P_{fic} from *E. coli* in Gram-negative bacteria including *A. methanolica* (Miksch and Dobrowolski 1995). Transcriptional activation of P_{fic} in *A. methanolica* was growth phase-dependent as in *E. coli* and was increased 6- to 7-fold during the transition to the stationary phase. Subsequently, P_{fic} was used to test growth phase-dependent expression and production of a secreted hybrid β-glucanase consisting of 107 amino-terminal residues of *Bacillus amyloliquefaciens* β-glucanase and 107 carboxy-terminal residues of *B. macerans* β-glucanase in *A. methanolica* using a Tn*5*-based transposon cassette non-specifically integrating into the chromosome (Miksch et al. 1997). Due to P_{fic}, the β-glucanase was highly overexpressed and secreted into the medium during the stationary phase, while total and extracellular production of β-glucanase varied depending on the transposon integration site. The viability of the bacterial cells was not affected and cell lysis did not occur.

Target gene expression in *Acidiphilium*

The transfer of genetic information into *Acidiphilium* and the construction of suitable vectors started about 30 years ago (Roberto et al. 1991). Plasmids from different incompatibility groups have been tested to determine the frequency with which they are transferred from *E. coli* to *Acidiphilium* strains. During these studies, a conjugative function has been discovered in *Acidiphilium* strains by observing the transfer of mobilizable, but not self-transmissible plasmids between *Acidiphilium* cells (Roberto et al. 1991). In following studies, DNA transfer into *Acidiphilium* by conjugation but also by electroporation was established and improved (Glenn et al. 1992; Inagaki et al. 1993). The pRK2 replicon-based broad-host-range plasmids pRK415 and pLAFR3 were used to analyze transformation efficiencies, which turned out to depend on the recipient strains (Glenn et al. 1992). Also, the *E. coli* / *Acidiphilium* shuttle vector pAH101 was constructed by fusing a restriction fragment from the native pAH1 plasmid from *Acidiphilium* sp. 42H with a fragment carrying the β-lactamase gene from pUC19 as resistance marker. Transformants of *A. facilis* could grow in ampicillin-containing medium only with pAH101, showing that the β-lactamase gene was efficiently expressed from the native Tn*3* promoter region also in *A. facilis* (Inagaki et al. 1993). However, the pAH101 plasmid appeared to be unstable in *A. facilis* in the stationary phase.

In further work, the plasmid pRK415 conferring tetracycline resistance was used to express the arsenic resistance genes *arsABC* from a natural *E. coli* isolate in *Acidiphilium* (Bruhn and Roberto 1993). After conjugal transfer of the constructed plasmid pIRC107 from *E. coli* to *Acidiphilium*, the plasmid was stable for at least one week with and without tetracycline selection. Also, the transformed *Acidiphilium* strain survived longer and in higher numbers in cultures with arsenopyrite ore than the parental strain did, suggesting a functional expression of the *arsABC* operon from its native *E. coli* promoter. Genetically improved strains of acidophilic bacteria were considered to have the potential to optimize microbial leaching of metals from ores. Enhancing their resistance to toxic metals is one option for strain improvement.

Acidiphilium could also be used to degrade organic pollutants in acidic wastewaters, provided they harbor the required genes. To evaluate the potential of *Acidiphilium* for biodegradation in acidic environments, gene transfer systems were tested by using the IncP1 antibiotic resistance plasmids RP4 and pVK101 and the phenol degradation-encoding plasmid pPGH11 (Quentmeier and Friedrich 1994). The plasmids RP4 from *Pseudomonas*, pVK101 (RK2 and pHK17, see *Gluconobacter* section for pVK) and pPGH11 (R68.45 and pPGH1 from *Pseudomonas*) could be transferred into *A. cryptum* with frequencies of 1.8×10^{-2} to 9.8×10^{-4} transconjugants per recipient cell. In the transconjugants, the antibiotic resistances and the ability to degrade phenol were expressed. *A. cryptum* with pPGH11 grew with 2.5 mM phenol at a doubling time of 12 h and a yield of 0.52 g dry cell weight per g of phenol.

In a later study, the native pAM5 plasmid from *A. multivorum* was sequenced and analyzed to use its characteristics for the construction of a shuttle vector (Singh and Banerjee 2007). The plasmid pSK2 containing the pAM5 *rep* region, the pBR322 *ori* and the ampicillin resistance gene *ampR* from pUC19, and a multiple cloning site, was able to replicate and stably maintained in *E. coli*, *Acidiphilium* as well as in *Acidocella*. The plasmid copy number of pAM5 and pSK2 in *A. multivorum* was determined to be 50-60. Apparently, no further study was published yet demonstrating the functional expression of target genes in *Acidiphilium* strains with pSK2.

Target gene expression in *Asaia*

Representatives from AAB genera have been demonstrated to be naturally associated not only with plants (e.g., *Acetobacter*, *Asaia*, *Gluconacetobacter*, *Gluconobacter*), but also with insects. The presence of AAB genera in insects (e.g., the fruit fly *Drosophila melanogaster* and the honeybee *Apis mellifera*), that typically use plant materials and sugar-rich matrices as food sources, is seen as roles of these AAB in exploitation of the food. *Asaia* was also found in the malaria mosquito vector *Anopheles stephensi* and is also present in and cross-colonizing other sugar-feeding insects of phylogenetically distant genera and orders (Crotti et al. 2009; Favia et al. 2007). In these studies, for tracking one *Asaia* strain was constructed by tagging it with a plasmid derivative of pHM2 carrying the pBR322 *ori*. The plasmid pHM2-Gfp was used to functionally express the green fluorescent protein Gfp under control of the neomycin phosphotransferase promoter $P_{npt\ II}$ found to be active in a broader range of species. Cross-colonization patterns of the body of the mosquitos *An. stephensi, Aedes aegypti* and the leafhopper *Scaphoideus titanus* have been documented with *Asaia* strains labeled with a chromosome- and a plasmid-encoded fluorescent protein. Another *Asaia* strain was constructed by the insertion of a mini-Tn*5* gene cassette into the chromosome. This cassette contained the *dsRed* gene encoding a red fluorescent protein under control of the ribosomal promoter P_{rrnBP1} from *E. coli*. Fluorescence and confocal microscopy analysis showed that the labeled *Asaia* strains efficiently colonized guts, male and female reproductive systems and the salivary glands.

The ability to cross-colonize insects of phylogenetically distant orders is an important property for the development of symbiont-based control of different vector-borne diseases. To test the potential of such a control by activation of insect immunity, the pHM2 backbone was used in *Asaia* to express the *Wolbachia* surface protein (WSP) gene with its signal peptide sequence under the control of $P_{npt\ II}$ that was derived from a *Wolbachia* strain isolated from the nematode *Dirofilaria immitis* (Epis et al. 2020). The recombinant strain $Asaia^{WSP}$ induced the activation of the host immune response in *An. stephensi* and *Ae. aegypti* mosquitos and it inhibited the development of the heartworm parasite *D. immitis* in *Ae. aegypti*. The recombinant $Asaia^{WSP}$ was also found to activate macrophages and *Leishmania* killing stronger than the empty vector control strain did (Varotto-Boccazzi et al. 2020). These results consolidated the immune-stimulating property of WSP and make $Asaia^{WSP}$ worth of further investigations as a potential tool for the control of mosquito-borne diseases and for immune prophylaxis and therapy of leishmaniases and other diseases that could be inhibited by macrophage activation.

Outlook

For AAB a diversity of expression plasmids has been developed and tested for expression of target genes and major plasmid lineages can be identified that are applied most often in AAB, although hitherto in only seven out of 49 AAB genera. Expression of target genes was achieved using the corresponding native promoter region or using a limited number of characterized promoters. Apparently, P_{lac} allowing LacI-dependent induction of expression in *E. coli* is the most used heterologous promoter for expression in AAB. Varying the length of the P_{lac} region can increase or decrease target gene expression in *Acetobacter* likely due to 5'-UTR effects in the mRNA (Tonouchi et al. 1998a). Only two studies reported to have used LacI-dependent IPTG-induced target gene expression (Bugala et al. 2016; Liu et al. 2020b). Only in one study the LacI-dependent IPTG-induced expression performance has been reported (Liu et al. 2020b). By using the fluorescence reporter gene *mRFP1*, the results showed that according to fluorescence microscope analysis, only a fraction of *K. xylinus* cells showed mRFP1 fluorescence; thus, cell heterogeneity was observed. Furthermore, only 3-fold induction by IPTG was observed from 0.1 mM to 0.5 mM reaching a saturation level of mRFP1 signals at 0.4 mM and 0.5 mM, while the 0 mM condition was not reported yet. Thus, the performance of IPTG-induced expression in AAB still remains to be solved or at least to be improved for tight and homogenous LacI-dependent target gene expression.

Due to a deficiency in regulatable promoters, almost only constitutive promoters have been used in AAB. The greatest variety of endogenous, heterologous, and synthetic promoters functional in AAB and exhibiting weak, moderate, strong, or very strong activity is known for *Gluconobacter* and *Komagataeibacter* (Florea et al. 2016a; Hölscher and Görisch 2006; Hu et al. 2015; Kallnik et al. 2010; Mientus et al. 2017; Shi et al. 2014; Teh et al. 2019; Yuan et al. 2016a). These data will be helpful to test and broaden the range of usable promoters in other AAB genera. For *Gluconobacter*, the highest change of a promoter activity according to plasmid-based LacZ activities was reported for the promoter P_{idh} of the inositol dehydrogenase gene GOX1857 from *G. oxydans* 621H (Mientus et al. 2017). Depending on the carbon source, P_{idh} activity was very low on mannitol and even lower on glucose, while P_{idh} activity on sorbitol was 100-fold higher than on glucose. This probably is the highest fold-change difference reported so far for *Gluconobacter* or AAB in general. However, the molecular mechanism of P_{idh} regulation and the transcriptional regulator(s) of P_{idh} involved need to be unraveled as well as the performance and the suitability of P_{idh} for use in a regulatable endogenous expression system. The *R. leguminosarum* promoter of the *nifHDK* operon, which is activated under nitrogen-fixing conditions, was functional in plant-associated *Ga. diazotrophicus in planta*.

Therefore, P_{nifHDK} might also be used in nitrogen-fixing AAB *ex planta* to control gene expression in dependence of the available nitrogen sources (Salles et al. 2000). The basal expression (tightness), induction performance and relative induced expression strength of the heterologous P_{nifHDK} promoter applied in AAB were not reported yet. Likewise, endogenous *nif* promoters from nitrogen-fixing AAB strains could be characterized and, if suitable, used to construct regulatable expression systems in nitrogen-fixing AAB. The system(s) could possibly be transferred with all regulatory requirements to non-nitrogen-fixing AAB.

Until now, for AAB only two well-documented inducible heterologous expression systems are available for only two species from different genera. As described above, one is based on an AHL-inducible *luxR*-P_{lux} system and the other one is a well-tunable L-arabinose-inducible *araC*-P_{araBAD} system with up to 480-fold induction (Florea et al. 2016a; Fricke et al. 2020). The AHL-inducible *luxR*-P_{lux} system was reported to enable strong induction in *Komagataeibacter*, yet the strength of the induction appeared to depend on the growth conditions. Induction ranged from only up to 5-fold due to high leakiness in the absence of the inducer to a very much better induction performance in cells inside cellulose pellicles (Florea et al. 2016a). Understanding the reason for this difference in induction performance may help to further improve the *luxR*-P_{lux} system and possibly other heterologous expression systems (e.g., TetR) still leaky in *Komagataeibacter* for full functionality in any growth condition. In *Komagataeibacter*, an L-arabinose-inducible *araC*-P_{araBAD} system was also very leaky and thus induction fold-change was very low (Teh et al. 2019). In contrast, in *G. oxydans* 621H, the heterologous *araC*-P_{araBAD} system from *E. coli* MC4100 was very tight and tunable by L-arabinose concentrations up to 1% (w/v) (Fricke et al. 2020). However, in *G. oxydans* 621H, the L-arabinose oxidation activity is high and contributes to the strong acidification of the growth medium by forming arabinonic acid causing a severe loss of reporter activities, while the D-arabinose oxidation activity is low (Fricke et al. 2020; Mientus et al. 2017; Peters et al. 2017). Thus, using D-arabinose-responsive AraC derivatives could circumvent the pH issue of L-arabinose induction and might probably also result in increased sensitivity toward arabinose concentrations. Therefore, engineered AraC mutant proteins with altered binding pockets which activate transcription in response to D-arabinose and not in response to L-arabinose could be tested (Tang et al. 2008). The AraC protein was also engineered to specifically respond to triacetic acid lactone, vanillin and salicylic acid (Frei et al. 2018). The new phenolic-sensing variants of AraC showed responses of more than 100-fold over the background in *E. coli* and were highly specific toward their target compound. That illustrates the potential of the AraC transcriptional regulatory protein for molecular sensing, reporting and target gene expression, which could possibly also be achieved and used in AAB.

In summary, after 35 years of constitutive target gene expression in AAB, we now have the first regulatable expression systems for AAB in hand. Further promising candidates are in sight for both heterologous and endogenous regulatable expression systems and future studies certainly will reveal more regulated AAB promoters. Additionally, the flexible SEVA toolkit, used within the AAB hitherto only in *Komagataeibacter*, is expected to speed up expression system development and testing or screening of such systems in even more AAB genera.

Acknowledgements The authors would like to thank the central library of the Forschungszentrum Jülich for their support.

Authors' contributions PMF, AK, and TP screened and selected the literature. All authors developed the manuscript, revised the manuscript, and read and approved the final version.

Funding Open Access funding enabled and organized by Projekt DEAL. We are grateful to the Federal Ministry of Education and Research (BMBF) for the financial support of PF within the project IMPRES (031B0370B). The funding organization did not influence the writing of the manuscript.

Declarations

Ethics approval This article does not contain any studies with human participants or animals performed by any of the authors.

Competing interests The authors declare no competing interests.

References

Akasaka N, Astuti W, Ishii Y, Hidese R, Sakoda H, Fujiwara S (2015) Change in the plasmid copy number in acetic acid bacteria in response to growth phase and acetic acid concentration. J Biosci Bioeng 119(6):661–668. https://doi.org/10.1016/j.jbiosc.2014.11.003

Antoine R, Locht C (1992) Isolation and molecular characterization of a novel broad-host-range plasmid from *Bordetella bronchiseptica* with sequence similarities to plasmids from gram-positive organisms. Mol Microbiol 6(13):1785–1799. https://doi.org/10.1111/j.1365-2958.1992.tb01351.x

Arrieta J, Hernandez L, Coego A, Suarez V, Balmori E, Menendez C, PetitGlatron MF, Chambert R, SelmanHousein G (1996) Molecular

characterization of the levansucrase gene from the endophytic sugarcane bacterium *Acetobacter diazotrophicus* SRT4. Microbiol 142: 1077–1085. https://doi.org/10.1099/13500872-142-5-1077

Batista FR, Hernandez L, Fernandez JR, Arrieta J, Menendez C, Gomez R, Tambara Y, Pons T (1999) Substitution of Asp-309 by Asn in the Arg-Asp-Pro (RDP) motif of *Acetobacter diazotrophicus* levansucrase affects sucrose hydrolysis, but not enzyme specificity. Biochem J 337:503–506. https://doi.org/10.1042/0264-6021:3370503

Battad-Bernardo E, McCrindle SL, Couperwhite I, Neilan BA (2004) Insertion of an *E. coli lacZ* gene in *Acetobacter xylinus* for the production of cellulose in whey. FEMS Microbiol Lett 231(2): 253–260. https://doi.org/10.1016/S0378-1097(04)00007-2

Battling S, Wohlers K, Igwe C, Kranz A, Pesch M, Wirtz A, Baumgart M, Büchs J, Bott M (2020) Novel plasmid-free *Gluconobacter oxydans* strains for production of the natural sweetener 5-ketofructose. Microbiol Cell Fact 19(1) ARTN 54. https://doi.org/10.1186/s12934-020-01310-7

Bilska V, Grones J (2003) Optimization of transformation and electroporation of plasmid DNA with pAC1 replicon into *Acetobacter pasteurianus*. Biologia 58(6):1029–1035

Blank M, Schweiger P (2018) Surface display for metabolic engineering of industrially important acetic acid bacteria. PeerJ 6. ARTN e4626. https://doi.org/10.7717/peerj.4626

Bruhn DF, Roberto FF (1993) Maintenance and expression of enteric arsenic resistance genes in *Acidiphilium*. Biohydrometallurgical Technologies 2:745–754

Bugala J, Cimova V, Grones P, Grones J (2016) Characterization of newly identified DnaA and DnaB proteins from *Acetobacter*. Res Microbiol 167(8):655–668. https://doi.org/10.1016/j.resmic.2016.06.010

Camelo A, Barreto CP, Vidal MS, Rouws JRC, Ledo FJD, Schwab S, Baldani JI (2020) Field response of two seed propagated elephant grass genotypes to diazotrophic bacterial inoculation and in situ confocal microscopy colonization analyses. Symbiosis. https://doi.org/10.1007/s13199-020-00730-8

Chen R (2012) Bacterial expression systems for recombinant protein production: *E. coli* and beyond. Biotechnol Adv 30(5):1102–1107. https://doi.org/10.1016/j.biotechadv.2011.09.013

Chien LJ, Chen HT, Yang PF, Lee CK (2006) Enhancement of cellulose pellicle production by constitutively expressing *Vitreoscilla* hemoglobin in *Acetobacter xylinum*. Biotechnol Progr 22(6):1598–1603. https://doi.org/10.1021/bp060157g

Cleenwerck I, De Vos P (2008) Polyphasic taxonomy of acetic acid bacteria: An overview of the currently applied methodology. Int J Food Microbiol 125(1):2–14. https://doi.org/10.1016/j.ijfoodmicro.2007.04.017

Cleton-Jansen AM, Dekker S, Vandeputte P, Goosen N (1991) A single amino acid substitution changes the substrate specificity of quinoprotein glucose dehydrogenase in *Gluconobacter oxydans*. Mol Gen Genet 229(2):206–212. https://doi.org/10.1007/Bf00272157

Cohen SN, Chang ACY, Boyer HW, Helling RB (1973) Construction of biologically functional bacterial plasmids *in vitro*. P Natl Acad Sci USA 70(11):3240–3244. https://doi.org/10.1073/pnas.70.11.3240

Condon C, Fitzgerald RJ, Ogara F (1991) Conjugation and heterologous gene expression in *Gluconobacter oxydans* ssp *suboxydans*. FEMS Microbiol Lett 80(2-3):173–178. https://doi.org/10.1016/0378-1097(91)90590-7

Connell ND (2001) Expression systems for use in actinomycetes and related organisms. Curr Opin Biotechnol 12(5):446–449. https://doi.org/10.1016/S0958-1669(00)00243-3

Creaven M, Fitzgerald RJ, Ogara F (1994) Transformation of *Gluconobacter oxydans* subsp. *suboxydans* by electroporation. Can J Microbiol 40(6):491–494. https://doi.org/10.1139/m94-079

Crotti E, Damiani C, Pajoro M, Gonella E, Rizzi A, Ricci I, Negri I, Scuppa P, Rossi P, Ballarini P, Raddadi N, Marzorati M, Sacchi L, Clementi E, Genchi M, Mandrioli M, Bandi C, Favia G, Alma A, Daffonchio D (2009) *Asaia*, a versatile acetic acid bacterial symbiont, capable of cross-colonizing insects of phylogenetically distant genera and orders. Environ Microbiol 11(12):3252–3264. https://doi.org/10.1111/j.1462-2920.2009.02048.x

De Roos J, De Vuyst L (2018) Acetic acid bacteria in fermented foods and beverages. Curr Opin Biotechnol 49:115–119. https://doi.org/10.1016/j.copbio.2017.08.007

Deeraksa A, Moonmangmee S, Toyama H, Adachi O, Matsushita K (2006) Conversion of capsular polysaccharide, involved in pellicle formation, to extracellular polysaccharide by *galE* deletion in *Acetobacter tropicalis*. Biosci Biotechnol Biochem 70(10):2536–2539. https://doi.org/10.1271/bbb.60143

Deng Y, Nagachar N, Fang L, Luan X, Catchmark JM, Tien M, Kao TH (2015) Isolation and characterization of two cellulose morphology mutants of *Gluconacetobacter hansenii* ATCC23769 producing cellulose with lower crystallinity. PLOS One 10(3) ARTN e0119504. https://doi.org/10.1371/journal.pone.0119504

Deng Y, Nagachar N, Xiao CW, Tien M, Kao TH (2013) Identification and characterization of non-cellulose-producing mutants of *Gluconacetobacter hansenii* generated by Tn*5* transposon mutagenesis. J Bacteriol 195(22):5072–5083. https://doi.org/10.1128/Jb.00767-13

Dilworth MV, Piel MS, Bettaney KE, Ma P, Luo J, Sharples D, Poyner DR, Gross SR, Moncoq K, Henderson PJF, Miroux B, Bill RM (2018) Microbial expression systems for membrane proteins. Methods 147:3–39. https://doi.org/10.1016/j.ymeth.2018.04.009

Durante-Rodriguez G, de Lorenzo V, Martinez-Garcia E (2014) The *Standard European Vector Architecture* (SEVA) plasmid toolkit. Pseudomonas: Methods and Protocols 1149:469–478. https://doi.org/10.1007/978-1-4939-0473-0_36

Epis S, Varotto-Boccazzi I, Crotti E, Damiani C, Giovati L, Mandrioli M, Biggiogera M, Gabrieli P, Genchi M, Polonelli L, Daffonchio D, Favia G, Bandi C (2020) Chimeric symbionts expressing a *Wolbachia* protein stimulate mosquito immunity and inhibit filarial parasite development. Commun Biol 3(1) ARTN 105. https://doi.org/10.1038/s42003-020-0835-2

Evans JC, Mizrahi V (2015) The application of tetracyclineregulated gene expression systems in the validation of novel drug targets in *Mycobacterium tuberculosis*. Front Microbiol 6:812. https://doi.org/10.3389/fmicb.2015.00812

Fang J, Kawano S, Tajima K, Kondo T (2015) *In vivo* curdlan/cellulose bionanocomposite synthesis by genetically modified *Gluconacetobacter xylinus*. Biomacromolecules 16(10):3154–3160. https://doi.org/10.1021/acs.biomac.5b01075

Favia G, Ricci I, Damiani C, Raddadi N, Crotti E, Marzorati M, Rizzi A, Urso R, Brusetti L, Borin S, Mora D, Scuppa P, Pasqualini L, Clementi E, Genchi M, Corona S, Negri I, Grandi G, Alma A, Kramer L, Esposito F, Bandi C, Sacchi L, Daffonchio D (2007) Bacteria of the genus *Asaia* stably associate with *Anopheles stephensi*, an Asian malarial mosquito vector. P Natl Acad Sci USA 104(21):9047–9051. https://doi.org/10.1073/pnas.0610451104

Felder M, Gupta A, Verma V, Kumar A, Qazi GN, Callum J (2000) The pyrroloquinoline quinone synthesis genes of *Gluconobacter oxydans*. FEMS Microbiol Lett 193(2):231–236. https://doi.org/10.1016/S0378-1097(00)00487-0

Fjaervik E, Frydenlund K, Valla S, Huggirat Y, Benziman M (1991) Complementation of cellulose-negative mutants of *Acetobacter xylinum* by the cloned structural gene for phosphoglucomutase. FEMS Microbiol Lett 77(2-3):325–330. https://doi.org/10.1111/j.1574-6968.1991.tb04370.x

Florea M, Hagemann H, Santosa G, Abbott J, Micklem CN, Spencer-Milnes X, Garcia LD, Paschou D, Lazenbatt C, Kong DZ, Chughtai

H, Jensen K, Freemont PS, Kitney R, Reeve B, Ellis T (2016a) Engineering control of bacterial cellulose production using a genetic toolkit and a new cellulose-producing strain. P Natl Acad Sci USA 113(24):E3431–E3440. https://doi.org/10.1073/pnas.1522985113

Florea M, Reeve B, Abbott J, Freemont PS, Ellis T (2016b) Genome sequence and plasmid transformation of the model high-yield bacterial cellulose producer *Gluconacetobacter hansenii* ATCC 53582. Sci Rep 6. ARTN 23635. https://doi.org/10.1038/srep23635

Föllner CG, Schröder R, Babel W (1994) Construction of broad-host-range plasmids for the expression of heterologous genes in *Acetobacter methanolicus* B58. Acta Biotechnol 14(2):141–151. https://doi.org/10.1002/abio.370140205

Forstner M, Leder L, Mayr LM (2007) Optimization of protein expression systems for modern drug discovery. Expert Rev Prot 4(1):67–78. https://doi.org/10.1586/14789450.4.1.67

Frei CS, Qian S, Cirino PC (2018) New engineered phenolic biosensors based on the AraC regulatory protein. Protein Eng Des Sel 31(6): 213–220. https://doi.org/10.1093/protein/gzy024

Fricke PM, Link T, Gätgens J, Sonntag C, Otto M, Bott M, Polen T (2020) A tunable L-arabinose-inducible expression plasmid for the acetic acid bacterium *Gluconobacter oxydans*. Appl Microbiol Biotechnol. https://doi.org/10.1007/s00253-020-10905-4

Fujiwara M, Fukushi K, Takai M, Hayashi J, Fukaya M, Okumura H, Kawamura Y (1992) Construction of shuttle vectors derived from *Acetobacter xylinum* for cellulose-producing bacterium *Acetobacter xylinum*. Biotechnol Lett 14(7):539–542. https://doi.org/10.1007/Bf01023936

Fukaya M, Okumura H, Masai H, Uozumi T, Beppu T (1985a) Construction of new shuttle vectors for *Acetobacter*. Agr Biol Chem 49(7):2083–2090. https://doi.org/10.1080/00021369.1985.10867038

Fukaya M, Okumura H, Masai H, Uozumi T, Beppu T (1985b) Development of a host-vector system for *Gluconobacter suboxydans*. Agr Biol Chem 49(8):2407–2411. https://doi.org/10.1080/00021369.1985.10867095

Fukaya M, Takemura H, Okumura H, Kawamura Y, Horinouchi S, Beppu T (1990) Cloning of genes responsible for acetic acid resistance in *Acetobacter aceti*. J Bacteriol 172(4):2096–2104. https://doi.org/10.1128/jb.172.4.2096-2104.1990

Fukaya M, Takemura H, Tayama K, Okumura H, Kawamura Y, Horinouchi S, Beppu T (1993) The *aarC* gene responsible for acetic acid assimilation confers acetic acid resistance on *Acetobacter aceti*. J Ferment Bioeng 76(4):270–275. https://doi.org/10.1016/0922-338x(93)90192-B

Fukaya M, Tayama K, Okumura H, Masai H, Uozumi T, Beppu T (1985c) Improved transformation method for *Acetobacter* with plasmid DNA. Agr Biol Chem 49(7):2091–2097. https://doi.org/10.1080/00021369.1985.10867039

Fukaya M, Tayama K, Tamaki T, Tagami H, Okumura H, Kawamura Y, Beppu T (1989) Cloning of the membrane-bound aldehyde dehydrogenase gene of *Acetobacter polyoxogenes* and improvement of acetic acid production by use of the cloned gene. Appl Environ Microbiol 55(1):171–176. https://doi.org/10.1128/Aem.55.1.171-176.1989

Gao L, Wu XD, Xia XL, Jin ZY (2020a) Fine-tuning ethanol oxidation pathway enzymes and cofactor PQQ coordinates the conflict between fitness and acetic acid production by *Acetobacter pasteurianus*. Microbiol Biotechnol. https://doi.org/10.1111/1751-7915.13703

Gao L, Wu XD, Zhu CL, Jin ZY, Wang W, Xia XL (2020b) Metabolic engineering to improve the biomanufacturing efficiency of acetic acid bacteria: advances and prospects. Crit Rev Biotechnol 40(4): 522–538. https://doi.org/10.1080/07388551.2020.1743231

Gao LL, Hu YD, Liu J, Du GC, Zhou JW, Chen J (2014) Stepwise metabolic engineering of *Gluconobacter oxydans* WSH-003 for the direct production of 2-keto-L-gulonic acid from D-sorbitol. Metab Eng 24:30–37. https://doi.org/10.1016/j.ymben.2014.04.003

Gao LL, Liu YF, Zhang XY, Zhang HS (2020c) Efficient optimization of *Gluconobacter oxydans* based on protein scaffold-trimeric CutA to enhance the chemical structure stability of enzymes for the direct production of 2-keto-L-gulonic acid. J Chem 2020. ARTN 5429409. https://doi.org/10.1155/2020/5429409

Gätgens C, Degner U, Bringer-Meyer S, Herrmann U (2007) Biotransformation of glycerol to dihydroxyacetone by recombinant *Gluconobacter oxydans* DSM 2343. Appl Microbiol Biotechnol 76(3):553–559. https://doi.org/10.1007/s00253-007-1003-z

Glenn AW, Roberto FF, Ward TE (1992) Transformation of *Acidiphilium* by electroporation and conjugation. Can J Microbiol 38(5):387–393. https://doi.org/10.1139/m92-065

Gomes RJ, Borges MD, Rosa MD, Castro-Gomez RJH, Spinosa WA (2018) Acetic acid bacteria in the food Industry: Systematics, characteristics and applications. Food Technol Biotechnol 56(2):139–151. https://doi.org/10.17113/ftb.56.02.18.5593

Grones J, Bencova K (1994) Cloning, Production and Secretion of Beta-Galactosidase in Acetobacter-Pasteurianus. Folia Microbiol 39(2): 99–104. https://doi.org/10.1007/Bf02906802

Grones J, Turna J (1992) Construction of shuttle vectors for cloning in *Escherichia coli* and *Acetobacter pasteurianus*. Folia Microbiol 37(6):395–400. https://doi.org/10.1007/Bf02899895

Grones J, Turna J (1995) Transformation of microorganisms with the plasmid vector with the replicon from pAC1 from *Acetobacter pasteurianus*. Biochem Bioph Res Co 206(3):942–947. https://doi.org/10.1006/bbrc.1995.1133

Gruber S, Schwab H, Koefinger P (2015) Versatile plasmid-based expression systems for Gram-negative bacteria - General essentials exemplified with the bacterium *Ralstonia eutropha* H16. New Biotechnol 32(6):552–558. https://doi.org/10.1016/j.nbt.2015.03.015

Gullo M, La China S, Falcone PM, Giudici P (2018) Biotechnological production of cellulose by acetic acid bacteria: Current state and perspectives. Appl Microbiol Biotechnol 102(16):6885–6898. https://doi.org/10.1007/s00253-018-9164-5

Hall PE, Anderson SM, Johnston DM, Cannon RE (1992) Transformation of *Acetobacter xylinum* with plasmid DNA by electroporation. Plasmid 28(3):194–200. https://doi.org/10.1016/0147-619x(92)90051-B

Hernandez L, Ramirez R, Hormaza JV, Madrazo J, Arrieta J (1999) Increased levansucrase production by a genetically modified *Acetobacter diazotrophicus* strain in shaking batch cultures. Lett Appl Microbiol 28(1):41–44. https://doi.org/10.1046/j.1365-2672.1999.00470.x

Herweg E, Schopping M, Rohr K, Siemen A, Frank O, Hofmann T, Deppenmeier U, Büchs J (2018) Production of the potential sweetener 5-ketofructose from fructose in fed-batch cultivation with *Gluconobacter oxydans*. Bioresource Technol 259:164–172. https://doi.org/10.1016/j.biortech.2018.03.038

Hoffmann JJ, Hövels M, Kosciow K, Deppenmeier U (2020) Synthesis of the alternative sweetener 5-ketofructose from sucrose by fructose dehydrogenase and invertase producing *Gluconobacter* strains. J Biotechnol 307:164–174. https://doi.org/10.1016/j.jbiotec.2019.11.001

Hölscher T, Görisch H (2006) Knockout and overexpression of pyrroloquinoline quinone biosynthetic genes in *Gluconobacter oxydans* 621H. J Bacteriol 188(21):7668–7676. https://doi.org/10.1128/Jb.01009-06

Hölscher T, Weinert-Sepalage D, Görisch H (2007) Identification of membrane-bound quinoprotein inositol dehydrogenase in *Gluconobacter oxydans* ATCC 621H. Microbiol 153:499–506. https://doi.org/10.1099/mic.0.2006/002196-0

Hövels M, Kosciow K, Kniewel J, Jakob F, Deppenmeier U (2020) High yield production of levan-type fructans by *Gluconobacter japonicus*

LMG 1417. Int J Biol Macromol 164:295–303. https://doi.org/10.1016/j.ijbiomac.2020.07.105

Hu SQ, Gao YG, Tajima K, Sunagawa N, Zhou Y, Kawano S, Fujiwara T, Yoda T, Shimura D, Satoh Y, Munekata M, Tanaka I, Yao M (2010) Structure of bacterial cellulose synthase subunit D octamer with four inner passageways. P Natl Acad Sci USA 107(42):17957–17961. https://doi.org/10.1073/pnas.1000601107

Hu YD, Wan H, Li JG, Zhou JW (2015) Enhanced production of L-sorbose in an industrial *Gluconobacter oxydans* strain by identification of a strong promoter based on proteomics analysis. J Ind Microbiol Biotechnol 42(7):1039–1047. https://doi.org/10.1007/s10295-015-1624-7

Huang LH, Liu QJ, Sun XW, Li XJ, Liu M, Jia SR, Xie YY, Zhong C (2020) Tailoring bacterial cellulose structure through CRISPR interference-mediated downregulation of *galU* in *Komagataeibacter xylinus* CGMCC 2955. Biotechnol Bioeng 117(7):2165–2176. https://doi.org/10.1002/bit.27351

Hur DH, Choi WS, Kim TY, Lee SY, Park JH, Jeong KJ (2020) Enhanced production of bacterial cellulose in *Komagataeibacter xylinus via* tuning of biosynthesis genes with synthetic RBS. J Microbiol Biotechnol 30(9):1430–1435. https://doi.org/10.4014/jmb.2006.06026

Iida A, Ohnishi Y, Horinouchi S (2008a) Control of acetic acid fermentation by quorum sensing *via* N-acylhomoserine lactones in *Gluconacetobacter intermedius*. J Bacteriol 190(7):2546–2555. https://doi.org/10.1128/Jb.01698-07

Iida A, Ohnishi Y, Horinouchi S (2008b) An OmpA family protein, a target of the GinI/GinR quorum-sensing system in *Gluconacetobacter intermedius*, controls acetic acid fermentation. J Bacteriol 190(14):5009–5019. https://doi.org/10.1128/Jb.00378-08

Iida A, Ohnishi Y, Horinouchi S (2009) Identification and characterization of target genes of the GinI/GinR quorum-sensing system in *Gluconacetobacter intermedius*. Microbiol 155:3021–3032. https://doi.org/10.1099/mic.0.028613-0

Inagaki K, Tomono J, Kishimoto N, Tano T, Tanaka H (1993) Transformation of the acidophilic heterotroph *Acidiphilium facilis* by electroporation. Biosci Biotechnol Biochem 57(10):1770–1771. https://doi.org/10.1271/bbb.57.1770

Ishida T, Sugano Y, Shoda M (2002) Novel glycosyltransferase genes involved in the acetan biosynthesis of *Acetobacter xylinum*. Biochem Bioph Res Co 295(2):230–235. Pii S0006-291x(02)00663-0. https://doi.org/10.1016/S0006-291x(02)00663-0

Jacek P, Ryngajllo M, Bielecki S (2019) Structural changes of bacterial nanocellulose pellicles induced by genetic modification of *Komagataeibacter hansenii* ATCC 23769. Appl Microbiol Biotechnol 103(13):5339–5353. https://doi.org/10.1007/s00253-019-09846-4

Jacek P, Szustak M, Kubiak K, Gendaszewska-Darmach E, Ludwicka K, Bielecki S (2018) Scaffolds for chondrogenic cells cultivation prepared from bacterial cellulose with relaxed fibers structure induced genetically. Nanomaterials 8(12) ARTN 1066. https://doi.org/10.3390/nano8121066

Jang WD, Kim TY, Kim HU, Shim WY, Ryu JY, Park JH, Lee SY (2019) Genomic and metabolic analysis of *Komagataeibacter xylinus* DSM 2325 producing bacterial cellulose nanofiber. Biotechnol Bioeng 116(12):3372–3381. https://doi.org/10.1002/bit.27150

Kallnik V, Meyer M, Deppenmeier U, Schweiger P (2010) Construction of expression vectors for protein production in *Gluconobacter oxydans*. J Biotechnol 150(4):460–465. https://doi.org/10.1016/j.jbiotec.2010.10.069

Kashima Y, Iijima M, Nakano T, Tayama K, Koizumi W, Udaka S, Yanagida F (2000) Role of intracellular esterases in the production of esters by *Acetobacter pasteurianus*. J Biosci Bioeng 89(1):81–83. https://doi.org/10.1016/S1389-1723(00)88055-X

Kashima Y, Nakajima W, Nakano T, Tayama K, Koizumi Y, Udaka S, Yanagida F (1999) Cloning and characterization of ethanol-regulated esterase genes in *Acetobacter pasteurianus*. J Biosci Bioeng 87(1):19–27. https://doi.org/10.1016/S1389-1723(99)80003-6

Kataoka N, Matsutani M, Yakushi T, Matsushita K (2015) Efficient production of 2,5-diketo-D-gluconate *via* heterologous expression of 2-ketogluconate dehydrogenase in *Gluconobacter japonicus*. Appl Environ Microbiol 81(10):3552–3560. https://doi.org/10.1128/Aem.04176-14

Kawai S, Goda-Tsutsumi M, Yakushi T, Kano K, Matsushita K (2013) Heterologous overexpression and characterization of a flavoprotein-cytochrome c complex fructose dehydrogenase of *Gluconobacter japonicus* NBRC3260. Appl Environ Microbiol 79(5):1654–1660. https://doi.org/10.1128/Aem.03152-12

Ke X, Yu PH, Hu ZC, Chen L, Sun XQ, Zheng YG (2019) Synergistic improvement of PQQ-dependent D-sorbitol dehydrogenase activity from *Gluconobacter oxydans* for the biosynthesis of miglitol precursor 6-(N-hydroxyethyl)-amino-6-deoxy-alpha-L-sorbofuranose. J Biotechnol 300:55–62. https://doi.org/10.1016/j.jbiotec.2019.05.007

Kiefler I, Bringer S, Bott M (2015) SdhE-dependent formation of a functional *Acetobacter pasteurianus* succinate dehydrogenase in *Gluconobacter oxydans*-a first step toward a complete tricarboxylic acid cycle. Appl Microbiol Biotechnol 99(21):9147–9160. https://doi.org/10.1007/s00253-015-6972-8

Kiefler I, Bringer S, Bott M (2017) Metabolic engineering of *Gluconobacter oxydans* 621H for increased biomass yield. Appl Microbiol Biotechnol 101(13):5453–5467. https://doi.org/10.1007/s00253-017-8308-3

Kim TS, Hui G, Li JL, Kalia VC, Muthusamy K, Sohng JK, Kim IW, Lee JK (2019) Overcoming NADPH product inhibition improves D-sorbitol conversion to L-sorbose. Sci Rep 9. ARTN 815. https://doi.org/10.1038/s41598-018-37401-0

Kolesovs S, Semjonovs P (2020) Production of bacterial cellulose from whey-current state and prospects. Appl Microbiol Biotechnol. https://doi.org/10.1007/s00253-020-10803-9

Kondo K, Beppu T, Horinouchi S (1995) Cloning, sequencing, and characterization of the gene encoding the smallest subunit of the three-component membrane-bound alcohol dehydrogenase from *Acetobacter pasteurianus*. J Bacteriol 177(17):5048–5055. https://doi.org/10.1128/jb.177.17.5048-5055.1995

Kondo K, Horinouchi S (1997) Characterization of the genes encoding the three-component membrane-bound alcohol dehydrogenase from *Gluconobacter suboxydans* and their expression in *Acetobacter pasteurianus*. Appl Environ Microbiol 63(3):1131–1138. https://doi.org/10.1128/Aem.63.3.1131-1138.1997

Konjanda P, Yakushi T, Matsushita K, Theeragool G (2019) Enhanced growth and ethanol oxidation by overexpressed *caiA* gene encoding acyl-CoA dehydrogenase in *Komagataeibacter medellinensis* NBRC 3288. Chiang Mai J Sci 46(2):196–206

Kosciow K, Domin C, Schweiger P, Deppenmeier U (2016) Extracellular targeting of an active endoxylanase by a TolB negative mutant of *Gluconobacter oxydans*. J Ind Microbiol Biotechnol 43(7):989–999. https://doi.org/10.1007/s10295-016-1770-6

Kosciow K, Zahid N, Schweiger P, Deppenmeier U (2014) Production of a periplasmic trehalase in *Gluconobacter oxydans* and growth on trehalose. J Biotechnol 189:27–35. https://doi.org/10.1016/j.jbiotec.2014.08.029

Kostner D, Luchterhand B, Junker A, Volland S, Daniel R, Büchs J, Liebl W, Ehrenreich A (2015) The consequence of an additional NADH dehydrogenase paralog on the growth of *Gluconobacter oxydans* DSM3504. Appl Microbiol Biotechnol 99(1):375–386. https://doi.org/10.1007/s00253-014-6069-9

Kovach ME, Elzer PH, Hill DS, Robertson GT, Farris MA, Roop RM 2nd, Peterson KM (1995) Four new derivatives of the broad-host-

range cloning vector pBBR1MCS, carrying different antibiotic-resistance cassettes. Gene 166(1):175–176. https://doi.org/10.1016/0378-1119(95)00584-1

Kovach ME, Phillips RW, Elzer PH, Roop RM 2nd, Peterson KM (1994) pBBR1MCS: a broad-host-range cloning vector. Biotechniques 16(5):800–802

Kranz A, Busche T, Vogel A, Usadel B, Kalinowski J, Bott M, Polen T (2018) RNAseq analysis of α-proteobacterium *Gluconobacter oxydans* 621H. BMC Genomics 19. ARTN 24. https://doi.org/10.1186/s12864-017-4415-x

Kranz A, Vogel A, Degner U, Kiefler I, Bott M, Usadel B, Polen T (2017) High precision genome sequencing of engineered *Gluconobacter oxydans* 621H by combining long nanopore and short accurate Illumina reads. J Biotechnol 258:197–205. https://doi.org/10.1016/j.jbiotec.2017.04.016

Kretova M, Grones J (2006) Construction of shuttle vectors from pAP1 plasmid for cloning into *Escherichia coli* and *Acetobacter* strains. J Food Nutr Res 45(3):110–114

La China S, Zanichelli G, De Vero L, Gullo M (2018) Oxidative fermentations and exopolysaccharides production by acetic acid bacteria: a mini review. Biotechnol Lett 40(9-10):1289–1302. https://doi.org/10.1007/s10529-018-2591-7

Laureys D, Britton SJ, De Clippeleer J (2020) Kombucha tea fermentation: A review. J Am Soc Brew Chem 78(3):165–174. https://doi.org/10.1080/03610470.2020.1734150

Li KF, Mao XL, Liu L, Lin JP, Sun M, Wei DZ, Yang SL (2016a) Overexpression of membrane-bound gluconate-2-dehydrogenase to enhance the production of 2-keto-D-gluconic acid by *Gluconobacter oxydans*. Microbiol Cell Fact 15. ARTN 121. https://doi.org/10.1186/s12934-016-0521-8

Li MH, Wu JA, Lin JP, Wei DZ (2010a) Expression of *Vitreoscilla* hemoglobin enhances cell growth and dihydroxyacetone production in *Gluconobacter oxydans*. Curr Microbiol 61(5):370–375. https://doi.org/10.1007/s00284-010-9621-6

Li MH, Wu JA, Liu X, Lin JP, Wei DZ, Chen H (2010b) Enhanced production of dihydroxyacetone from glycerol by overexpression of glycerol dehydrogenase in an alcohol dehydrogenase-deficient mutant of *Gluconobacter oxydans*. Bioresource Technol 101(21):8294–8299. https://doi.org/10.1016/j.biortech.2010.05.065

Li S, Zhang JL, Xu H, Feng XH (2016b) Improved xylitol production from D-arabitol by enhancing the coenzyme regeneration efficiency of the pentose phosphate pathway in *Gluconobacter oxydans*. J Agr Food Chem 64(5):1144–1150. https://doi.org/10.1021/acs.jafc.5b05509

Liu D, Ke X, Hu ZC, Zheng YG (2020a) Combinational expression of D-sorbitol dehydrogenase and pyrroloquinoline quinone increases 6-(N-hydroxyethyl)-amino-6-deoxy-alpha-L-sorbofuranose production by *Gluconobacter oxydans* through cofactor manipulation. Enzyme Microbiol Tech 141. ARTN 109670. https://doi.org/10.1016/j.enzmictec.2020.109670

Liu LP, Yang X, Zhao XJ, Zhang KY, Li WC, Xie YY, Jia SR, Zhong C (2020b) A lambda Red and FLP/FRT-mediated site-specific recombination system in *Komagataeibacter xylinus* and its application to enhance the productivity of bacterial cellulose. ACS Synth Biol 9(11):3171–3180. https://doi.org/10.1021/acssynbio.0c00450

Liu M, Li SQ, Xie YZ, Jia SR, Hou Y, Zou Y, Zhong C (2018) Enhanced bacterial cellulose production by *Gluconacetobacter xylinus via* expression of *Vitreoscilla* hemoglobin and oxygen tension regulation. Appl Microbiol Biotechnol 102(3):1155–1165. https://doi.org/10.1007/s00253-017-8680-z

Lu LF, Wei LJ, Zhu K, Wei DZ, Hua Q (2012) Combining metabolic engineering and adaptive evolution to enhance the production of dihydroxyacetone from glycerol by *Gluconobacter oxydans* in a low-cost way. Bioresource Technol 117:317–324. https://doi.org/10.1016/j.biortech.2012.03.013

Lynch KM, Zannini E, Wilkinson S, Daenen L, Arendt EK (2019) Physiology of acetic acid bacteria and their role in vinegar and fermented beverages. Compr Rev Food Sci F 18(3):587–625. https://doi.org/10.1111/1541-4337.12440

Mamlouk D, Gullo M (2013) Acetic acid bacteria: Physiology and carbon sources oxidation. Indian J Microbiol 53(4):377–384. https://doi.org/10.1007/s12088-013-0414-z

Mangayil R, Rajala S, Pammo A, Sarlin E, Luo J, Santala V, Karp M, Tuukkanen S (2017) Engineering and characterization of bacterial nanocellulose films as low cost and flexible sensor material. ACS Appl Mater Inter 9(22):19048–19056. https://doi.org/10.1021/acsami.7b04927

Marx CJ, Lidstrom ME (2001) Development of improved versatile broad-host-range vectors for use in methylotrophs and other Gram-negative bacteria. Microbiol 147:2065–2075. https://doi.org/10.1099/00221287-147-8-2065

Masud U, Matsushita K, Theeragool G (2010) Cloning and functional analysis of *adhS* gene encoding quinoprotein alcohol dehydrogenase subunit III from *Acetobacter pasteurianus* SKU1108. Int J Food Microbiol 138(1-2):39–49. https://doi.org/10.1016/j.ijfoodmicro.2009.12.027

Matsumoto N, Hattori H, Matsutani M, Matayoshi C, Toyama H, Kataoka N, Yakushi T, Matsushita K (2018) A single-nucleotide insertion in a drug transporter gene induces a thermotolerance phenotype in *Gluconobacter frateurii* by increasing the NADPH/$NADP^+$ ratio *via* metabolic change. Appl Environ Microbiol 84(10) ARTN e00354-18. https://doi.org/10.1128/AEM.00354-18

Matsushita K, Yakushi T, Toyama H, Shinagawa E, Adachi O (1996) Function of multiple heme *c* moieties in intramolecular electron transport and ubiquinone reduction in the quinohemoprotein alcohol dehydrogenase cytochrome *c* complex of *Gluconobacter suboxydans*. J Biol Chem 271(9):4850–4857

Matsutani M, Yakushi T (2018) Pyrroloquinoline quinone-dependent dehydrogenases of acetic acid bacteria. Appl Microbiol Biotechnol 102(22):9531–9540. https://doi.org/10.1007/s00253-018-9360-3

Mehta K, Pfeffer S, Brown RM (2015) Characterization of an *acsD* disruption mutant provides additional evidence for the hierarchical cell-directed self-assembly of cellulose in *Gluconacetobacter xylinus*. Cellulose 22(1):119–137. https://doi.org/10.1007/s10570-014-0521-y

Merfort M, Herrmann U, Bringer-Meyer S, Sahm H (2006a) High-yield 5-keto-D-gluconic acid formation is mediated by soluble and membrane-bound gluconate-5-dehydrogenases of *Gluconobacter oxydans*. Appl Microbiol Biotechnol 73(2):443–451. https://doi.org/10.1007/s00253-006-0467-6

Merfort M, Herrmann U, Ha SW, Elfari M, Bringer-Meyer S, Gorisch H, Sahm H (2006b) Modification of the membrane-bound glucose oxidation system in *Gluconobacter oxydans* significantly increases gluconate and 5-keto-D-gluconic acid accumulation. Biotechnol J 1(5):556–563. https://doi.org/10.1002/biot.200600032

Meyer M, Schweiger P, Deppenmeier U (2013) Effects of membrane-bound glucose dehydrogenase overproduction on the respiratory chain of *Gluconobacter oxydans*. Appl Microbiol Biotechnol 97(8):3457–3466. https://doi.org/10.1007/s00253-012-4265-z

Meyer M, Schweiger P, Deppenmeier U (2015) Succinic semialdehyde reductase Gox1801 from *Gluconobacter oxydans* in comparison to other succinic semialdehyde-reducing enzymes. Appl Microbiol Biotechnol 99(9):3929–3939. https://doi.org/10.1007/s00253-014-6191-8

Mientus M, Kostner D, Peters B, Liebl W, Ehrenreich A (2017) Characterization of membrane-bound dehydrogenases of *Gluconobacter oxydans* 621H using a new system for their functional expression. Appl Microbiol Biotechnol 101(8):3189–3200. https://doi.org/10.1007/s00253-016-8069-4

Miksch G, Dobrowolski P (1995) Growth phase-dependent induction of stationary phase promoters of *Escherichia coli* in different Gram-

negative bacteria. J Bacteriol 177(18):5374–5378. https://doi.org/10.1128/jb.177.18.5374-5378.1995

Miksch G, Fiedler E, Dobrowolski P, Flaschel E (1997) Controlled secretion into the culture medium of a hybrid beta-glucanase by *Acetobacter methanolicus* mediated by the *kil* gene of *Escherichia coli* located on a Tn5-derived transposon. Appl Microbiol Biotechnol 47(5):530–536. https://doi.org/10.1007/s002530050968

Mogi T, Ano Y, Nakatsuka T, Toyama H, Muroi A, Miyoshi H, Migita CT, Ui H, Shiomi K, Omura S, Kita K, Matsushita K (2009) Biochemical and spectroscopic properties of cyanide-insensitive quinol oxidase from *Gluconobacter oxydans*. J Biochem 146(2): 263–271. https://doi.org/10.1093/jb/mvp067

Mostafa HE, Heller KJ, Geis A (2002) Cloning of *Escherichia coli lacZ* and *lacY* genes and their expression in *Gluconobacter oxydans* and *Acetobacter liquefaciens*. Appl Environ Microbiol 68(5):2619–2623. https://doi.org/10.1128/Aem.68.5.2619-2623.2002

Nakai T, Moriya A, Tonouchi N, Tsuchida T, Yoshinaga F, Horinouchi S, Sone Y, Mori H, Sakai F, Hayashi T (1998) Control of expression by the cellulose synthase (*bcsA*) promoter region from *Acetobacter xylinum* BPR 2001. Gene 213(1-2):93–100. https://doi.org/10.1016/S0378-1119(98)00191-7

Nakai T, Nishiyama Y, Kuga S, Sugano Y, Shoda M (2002) ORF2 gene involves in the construction of high-order structure of bacterial cellulose. Biochem Bioph Res Co 295(2):458–462. Pii S0006-291x(02)00696-4. https://doi.org/10.1016/S0006-291x(02)00696-4

Nakai T, Sugano Y, Shoda M, Sakakibara H, Oiwa K, Tuzi S, Imai T, Sugiyama J, Takeuchi M, Yamauchi D, Mineyuki Y (2013) Formation of highly twisted ribbons in a carboxymethylcellulase gene-disrupted strain of a cellulose-producing bacterium. J Bacteriol 195(5):958–964. https://doi.org/10.1128/Jb.01473-12

Nakai T, Tonouchi N, Konishi T, Kojima Y, Tsuchida T, Yoshinaga F, Sakai F, Hayashi T (1999) Enhancement of cellulose production by expression of sucrose synthase in *Acetobacter xylinum*. P Natl Acad Sci USA 96(1):14–18. https://doi.org/10.1073/pnas.96.1.14

Nakano S, Fukaya M, Horinouchi S (2004) Enhanced expression of aconitase raises acetic acid resistance in *Acetobacter aceti*. FEMS Microbiol Lett 235(2):315–322. https://doi.org/10.1016/j.femsle.2004.05.007

Nishikura-Imamura S, Matsutani M, Insomphun C, Vangnai AS, Toyama H, Yakushi T, Abe T, Adachi O, Matsushita K (2014) Overexpression of a type II 3-dehydroquinate dehydratase enhances the biotransformation of quinate to 3-dehydroshikimate in *Gluconobacter oxydans*. Appl Microbiol Biotechnol 98(7):2955–2963. https://doi.org/10.1007/s00253-013-5439-z

Okamoto-Kainuma A, Yan W, Fukaya M, Tukamoto Y, Ishikawa M, Koizumi Y (2004) Cloning and characterization of the *dnaKJ* operon in *Acetobacter aceti*. J Biosci Bioeng 97(5):339–342. https://doi.org/10.1016/S1389-1723(04)70216-9

Okamoto-Kainuma A, Yan W, Kadono S, Tayama K, Koizumi Y, Yanagida F (2002) Cloning and characterization of *groESL* operon in *Acetobacter aceti*. J Biosci Bioeng 94(2):140–147. https://doi.org/10.1263/jbb.94.140

Okumura H, Tagami H, Fukaya M, Masai H, Kawamura Y, Horinouchi S, Beppu T (1988) Cloning of the β-isopropylmalate dehydrogenase gene from *Acetobacter aceti* and its use for construction of a new host-vector system for *Acetobacter*. Agr Biol Chem 52(12):3125–3129. https://doi.org/10.1080/00021369.1988.10869191

Okumura H, Uozumi T, Beppu T (1985) Construction of plasmid vectors and a genetic transformation system for *Acetobacter aceti*. Agr Biol Chem 49(4):1011–1017. https://doi.org/10.1080/00021369.1985.10866859

Parachin NS, Mulder KC, Viana AAB, Dias SC, Franco OL (2012) Expression systems for heterologous production of antimicrobial peptides. Peptides 38(2):446–456. https://doi.org/10.1016/j.peptides.2012.09.020

Peters B, Mientus M, Kostner D, Daniel R, Liebl W, Ehrenreich A (2017) Expression of membrane-bound dehydrogenases from a mother of vinegar metagenome in *Gluconobacter oxydans*. Appl Microbiol Biotechnol 101(21):7901–7912. https://doi.org/10.1007/s00253-017-8479-y

Petroni EA, Bocca SN, Ielpi L (1996) Sequence-specific DNA modification in *Acetobacter xylinum*. Cell Mol Biol 42(5):759–767

Phathanathavorn T, Naloka K, Matsutani M, Yakushi T, Matsushita K, Theeragool G (2019) Mutated *fabG* gene encoding oxidoreductase enhances the cost-effective fermentation of jasmine rice vinegar in the adapted strain of *Acetobacter pasteurianus* SKU1108. J Biosci Bioeng 127(6):690–697. https://doi.org/10.1016/j.jbiosc.2018.12.006

Prust C, Hoffmeister M, Liesegang H, Wiezer A, Fricke WF, Ehrenreich A, Gottschalk G, Deppenmeier U (2005) Complete genome sequence of the acetic acid bacterium *Gluconobacter oxydans*. Nat Biotechnol 23(2):195–200. https://doi.org/10.1038/nbt1062

Quentmeier A, Friedrich CG (1994) Transfer and expression of degradative and antibiotic resistance plasmids in acidophilic bacteria. Appl Environ Microbiol 60(3):973–978. https://doi.org/10.1128/Aem.60.3.973-978.1994

Richhardt J, Bringer S, Bott M (2012) Mutational analysis of the pentose phosphate and Entner-Doudoroff pathways in *Gluconobacter oxydans* reveals improved growth of a Δ*edd* Δ*eda* mutant on mannitol. Appl Environ Microbiol 78(19):6975–6986. https://doi.org/10.1128/Aem.01166-12

Richhardt J, Luchterhand B, Bringer S, Büchs J, Bott M (2013) Evidence for a key role of cytochrome bo_3 oxidase in respiratory energy metabolism of *Gluconobacter oxydans*. J Bacteriol 195(18):4210–4220. https://doi.org/10.1128/Jb.00470-13

Roberto FF, Glenn AW, Bulmer D, Ward TE (1991) Genetic transfer in acidophilic bacteria which are potentially applicable in coal beneficiation. Fuel 70(5):595–598. https://doi.org/10.1016/0016-2361(91)90172-7

Rouws LFM, Meneses CHSG, Guedes HV, Vidal MS, Baldani JI, Schwab S (2010) Monitoring the colonization of sugarcane and rice plants by the endophytic diazotrophic bacterium *Gluconacetobacter diazotrophicus* marked with *gfp* and *gusA* reporter genes. Lett Appl Microbiol 51(3):325–330. https://doi.org/10.1111/j.1472-765X.2010.02899.x

Saito Y, Ishii Y, Hayashi H, Imao Y, Akashi T, Yoshikawa K, Noguchi Y, Soeda S, Yoshida M, Niwa M, Hosoda J, Shimomura K (1997) Cloning of genes coding for L-sorbose and L-sorbosone dehydrogenases from *Gluconobacter oxydans* and microbial production of 2-keto-L-gulonate, a precursor of L-ascorbic acid, in a recombinant *G. oxydans* strain. Appl Environ Microbiol 63(2):454–460. https://doi.org/10.1128/Aem.63.2.454-460.1997

Saito Y, Ishii Y, Hayashi H, Yoshikawa K, Noguchi Y, Yoshida S, Soeda S, Yoshida M (1998) Direct fermentation of 2-keto-L-gulonic acid in recombinant *Gluconobacter oxydans*. Biotechnol Bioeng 58(2-3):309–315. https://doi.org/10.1002/(Sici)1097-0290(19980420)58:2/3<309::Aid-Bit30>3.3.Co;2-Q

Salles JF, Gitahy PD, Skot L, Baldani JI (2000) Use of endophytic diazotrophic bacteria as a vector to express the *cry3A* gene from *Bacillus thuringiensis*. Braz J Microbiol 31(3):155–161

Saxena IM, Kudlicka K, Okuda K, Brown RM (1994) Characterization of genes in the cellulose-synthesizing operon (*acs* operon) of *Acetobacter xylinum* - Implications for cellulose crystallization. J Bacteriol 176(18):5735–5752. https://doi.org/10.1128/Jb.176.18.5735-5752.1994

Schleif R (2010) AraC protein, regulation of the L-arabinose operon in *Escherichia coli*, and the light switch mechanism of AraC action. FEMS Microbiol Rev 34(5):779–796. https://doi.org/10.1111/j.1574-6976.2010.00226.x

Schleyer U, Bringer-Meyer S, Sahm H (2008) An easy cloning and expression vector system for *Gluconobacter oxydans*. Int J Food

Microbiol 125(1):91–95. https://doi.org/10.1016/j.ijfoodmicro.2007.04.016

Schnappinger D, Ehrt S (2014) Regulated expression systems for mycobacteria and their applications. Microbiol Spectr 2(1). https://doi.org/10.1128/microbiolspec.MGM2-0018-2013

Schröder R, Engel J, Chistoserdov AY, Tsygankov YD (1989) Construction of a promoter-probe vector for the methanol-utilizing bacterium *Acetobacter methanolicus* MB 58. Acta Biotechnol 9(3):219–225. https://doi.org/10.1002/abio.370090306

Schröder R, Maassen A, Lippoldt A, Borner T, Vonbaehr R, Dobrowolski P (1991) Expression of the core antigen gene of hepatitis B virus (Hbv) in *Acetobacter methanolicus* using broad-host-range vectors. Appl Microbiol Biotechnol 35(5):631–637. https://doi.org/10.1007/Bf00169628

Schwab S, Pessoa CA, Bergami AAD, Figueiredo NLD, Teixeira KRD, Baldani JI (2016) Isolation and characterization of active promoters from *Gluconacetobacter diazotrophicus* strain PAL5 using a promoter-trapping plasmid. Arch Microbiol 198(5):445–458. https://doi.org/10.1007/s00203-016-1203-y

Setyawati MI, Chien LJ, Lee CK (2007) Expressing *Vitreoscilla* hemoglobin in statically cultured *Acetobacter xylinum* with reduced O-2 tension maximizes bacterial cellulose pellicle production. J Biotechnol 132(1):38–43. https://doi.org/10.1016/j.jbiotec.2007.08.012

Setyawati MI, Chien LJ, Lee CK (2009) Self-immobilized recombinant *Acetobacter xylinum* for biotransformation. Biochem Eng J 43(1):78–84. https://doi.org/10.1016/j.bej.2008.09.002

Shen Y, Zhou X, Xu Y (2020) Enhancement of *Gluconobacter oxydans* resistance to lignocellulosic-derived inhibitors in xylonic acid production by overexpressing thioredoxin. Appl Biochem Biotechnol 191(3):1072–1083. https://doi.org/10.1007/s12010-020-03253-6

Shi LL, Li KF, Zhang H, Liu X, Lin JP, Wei DZ (2014) Identification of a novel promoter gHp0169 for gene expression in *Gluconobacter oxydans*. J Biotechnol 175:69–74. https://doi.org/10.1016/j.jbiotec.2014.01.035

Shi YY, Li KF, Lin JP, Yang SL, Wei DZ (2015) Engineered expression vectors significantly enhanced the production of 2-keto-D-gluconic acid by *Gluconobacter oxidans*. J Agr Food Chem 63(22):5492–5498. https://doi.org/10.1021/acs.jafc.5b01652

Shinjoh M, Hoshino T (1995) Development of a stable shuttle vector and a conjugative transfer system for *Gluconobacter oxydans*. J Ferment Bioeng 79(2):95–99. https://doi.org/10.1016/0922-338x(95)94074-2

Shinjoh M, Tomiyama N, Asakura A, Hoshino T (1995) Cloning and nucleotide sequencing of the membrane-bound L-sorbosone dehydrogenase gene of *Acetobacter liquefaciens* IFO 12258 and its expression in *Gluconobacter oxydans*. Appl Environ Microbiol 61(2):413–420. https://doi.org/10.1128/Aem.61.2.413-420.1995

Shinjoh M, Tomiyama N, Miyazaki T, Hoshino T (2002) Main polyol dehydrogenase of *Gluconobacter suboxydans* IFO 3255, membrane-bound D-sorbitol dehydrogenase, that needs product of upstream gene, *sldB*, for activity. Biosci Biotechnol Biochem 66(11):2314–2322. https://doi.org/10.1271/bbb.66.2314

Siemen A, Kosciow K, Schweiger P, Deppenmeier U (2018) Production of 5-ketofructose from fructose or sucrose using genetically modified *Gluconobacter oxydans* strains. Appl Microbiol Biotechnol 102(4):1699–1710. https://doi.org/10.1007/s00253-017-8699-1

Singh SK, Banerjee PC (2007) Nucleotide sequence analysis of cryptic plasmid pAM5 from *Acidiphilium multivorum*. Plasmid 58(2):101–114. https://doi.org/10.1016/j.plasmid.2007.01.005

Soemphol W, Adachi O, Matsushita K, Toyama H (2008) Distinct physiological roles of two membrane-bound dehydrogenases responsible for D-sorbitol oxidation in *Gluconobacter frateurii*. Biosci Biotechnol Biochem 72(3):842–850. https://doi.org/10.1271/bbb.70720

Soemphol W, Deeraksa A, Matsutani M, Yakushi T, Toyama H, Adachi O, Yamada M, Matsushita K (2011) Global analysis of the genes involved in the thermotolerance mechanism of thermotolerant *Acetobacter tropicalis* SKU1100. Biosci Biotechnol Biochem 75(10):1921–1928. https://doi.org/10.1271/bbb.110310

Soemphol W, Toyama H, Moonmangmee D, Adachi O, Matsushita K (2007) L-sorbose reductase and its transcriptional regulator involved in L-sorbose utilization of *Gluconobacter frateurii*. J Bacteriol 189(13):4800–4808. https://doi.org/10.1128/Jb.01895-06

Soisson SM, MacDougall-Shackleton B, Schleif R, Wolberger C (1997) Structural basis for ligand-regulated oligomerization of AraC. Science 276(5311):421–425. https://doi.org/10.1126/science.276.5311.421

Subashini M, Priya AM, Sundarakrishnan B, Jayachandran S (2011) Recombinant *Gluconacetobacter diazotrophicus* containing *cry1Ac* gene codes for 130-kDa toxin protein. J Mol Microbiol Biotechnol 20(4):236–242. https://doi.org/10.1159/000331698

Sugiyama M, Suzuki S, Tonouchi N, Yokozeki K (2003) Cloning of the xylitol dehydrogenase gene from *Gluconobacter oxydans* and improved production of xylitol from D-arabitol. Biosci Biotechnol Biochem 67(3):584–591. https://doi.org/10.1271/bbb.67.584

Sunagawa N, Fujiwara T, Yoda T, Kawano S, Satoh Y, Yao M, Tajima K, Dairi T (2013) Cellulose complementing factor (Ccp) is a new member of the cellulose synthase complex (terminal complex) in *Acetobacter xylinum*. J Biosci Bioeng 115(6):607–612. https://doi.org/10.1016/j.jbiosc.2012.12.021

Tajima K, Nakajima K, Yamashita H, Shiba T, Munekata M, Takai M (2001) Cloning and sequencing of the beta-glucosidase gene from *Acetobacter xylinum* ATCC 23769. DNA Res 8(6):263–269. https://doi.org/10.1093/dnares/8.6.263

Takeda Y, Shimizu T (1992) Expression of cytochrome *c*-553(CO) gene that complements the second subunit deficiency of membrane-bound alcohol dehydrogenase in *Gluconobacter suboxydans* subsp. α. J Ferment Bioeng 73(2):89–93. https://doi.org/10.1016/0922-338x(92)90319-P

Takeda Y, Shimizu T, Matsushita K, Adachi O, Ameyama M (1992) Role of cytochrome *c*-553(CO), the second subunit of alcohol dehydrogenase, in the azide-insensitive respiratory chain and in oxidative fermentation of *Gluconobacter* species. J Ferment Bioeng 74(4):209–213. https://doi.org/10.1016/0922-338x(92)90111-7

Takemura H, Horinouchi S, Beppu T (1993a) Suppression of an ethanol-sensitive mutation of *Acetobacter pasteurianus* by overexpression of the *his1* gene encoding histidinol phosphate aminotransferase. J Ferment Bioeng 76(3):224–228. https://doi.org/10.1016/0922-338x(93)90013-X

Takemura H, Kondo K, Horinouchi S, Beppu T (1993b) Induction by ethanol of alcohol dehydrogenase activity in *Acetobacter pasteurianus*. J Bacteriol 175(21):6857–6866. https://doi.org/10.1128/jb.175.21.6857-6866.1993

Tang SY, Fazelinia H, Cirino PC (2008) AraC regulatory protein mutants with altered effector specificity. J Am Chem Soc 130(15):5267–5271. https://doi.org/10.1021/ja7109053

Teh MY, Ooi KH, Teo SXD, Bin Mansoor ME, Lim WZS, Tan MH (2019) An expanded synthetic biology toolkit for gene expression control in *Acetobacteraceae*. ACS Synth Biol 8(4):708–723. https://doi.org/10.1021/j.acssynbio.8b00168

Terpe K (2006) Overview of bacterial expression systems for heterologous protein production: from molecular and biochemical fundamentals to commercial systems. Appl Microbiol Biotechnol 72(2):211–222. https://doi.org/10.1007/s00253-006-0465-8

Theeragool G, Pitiwittayakul N, Matsutani M, Matsushita K (2018) Disruption of the groEL gene revealed a physiological role for chaperonin in the thermotolerant acetic acid bacterium, *Acetobacter pasteurianus* SKU1108. Chiang Mai J Sci 45(4):1623–1633

Tonouchi N, Horinouchi S, Tsuchida T, Yoshinaga F (1998a) Increased cellulose production from sucrose by *Acetobacter* after introducing the sucrose phosphorylase gene. Biosci Biotechnol Biochem 62(9): 1778–1780. https://doi.org/10.1271/bbb.62.1778

Tonouchi N, Sugiyama M, Yokozeki K (2003) Construction of a vector plasmid for use in *Gluconobacter oxydans*. Biosci Biotechnol Biochem 67(1):211–213. https://doi.org/10.1271/bbb.67.211

Tonouchi N, Thara N, Tsuchida T, Yoshinaga F, Beppu T, Horinouchi S (1995) Addition of a small amount of an endoglucanase enhances cellulose production by *Acetobacter xylinum*. Biosci Biotechnol Biochem 59(5):805–808. https://doi.org/10.1271/bbb.59.805

Tonouchi N, Tsuchida T, Yoshinaga F, Horinouchi S, Beppu T (1994) A host-vector system for a cellulose-producing *Acetobacter* strain. Biosci Biotechnol Biochem 58(10):1899–1901. https://doi.org/10.1271/bbb.58.1899

Tonouchi N, Yanase H, Kojima Y, Tsuchida T, Yoshinaga F, Horinouchi S (1998b) Increased cellulose production from sucrose with reduced levan accumulation by an *Acetobacter* strain harboring a recombinant plasmid. Biosci Biotechnol Biochem 62(5):833–836. https://doi.org/10.1271/bbb.62.833

Trcek J, Mira NP, Jarboe LR (2015) Adaptation and tolerance of bacteria against acetic acid. Appl Microbiol Biotechnol 99(15):6215–6229. https://doi.org/10.1007/s00253-015-6762-3

Urakami T, Tamaoka J, Suzuki K, Komagata K (1989) *Acidomonas* gen. nov., incorporating *Acetobacter methanolicus* as *Acidomonas methanolica* comb. nov. Int J Syst Bacteriol 39(1):50–55. https://doi.org/10.1099/00207713-39-1-50

Urzua LS, Vazquez-Candanedo AP, Sanchez-Espindola A, Ramirez CA, Baca BE (2013) Identification and characterization of an iron ABC transporter operon in *Gluconacetobacter diazotrophicus* PAL5. Arch Microbiol 195(6):431–438. https://doi.org/10.1007/s00203-013-0890-x

Valero F (2012) Heterologous expression systems for lipases: A review. Methods Mol Biol 861:161–178. https://doi.org/10.1007/978-1-61779-600-5_11

Valla S, Coucheron DH, Fjaervik E, Kjosbakken J, Weinhouse H, Ross P, Amikam D, Benziman M (1989) Cloning of a gene involved in cellulose biosynthesis in *Acetobacter xylinum* - Complementation of cellulose-negative mutants by the UDPG pyrophosphorylase structural gene. Mol Gen Genet 217(1):26–30. https://doi.org/10.1007/Bf00330938

Valla S, Coucheron DH, Kjosbakken J (1986) Conjugative transfer of the naturally-occurring plasmids of *Acetobacter xylinum* by IncP-plasmid-mediated mobilization. J Bacteriol 165(1):336–339. https://doi.org/10.1128/jb.165.1.336-339.1986

Valla S, Coucheron DH, Kjosbakken J (1987) The plasmids of *Acetobacter xylinum* and their interaction with the host chromosome. Mol Gen Genet 208(1-2):76–83. https://doi.org/10.1007/Bf00330425

Varotto-Boccazzi I, Epis S, Arnoldi I, Corbett Y, Gabrieli P, Paroni M, Nodari R, Basilico N, Sacchi L, Gramiccia M, Gradoni L, Tranquillo V, Bandi C (2020) Boosting immunity to treat parasitic infections: *Asaia* bacteria expressing a protein from *Wolbachia* determine M1 macrophage activation and killing of *Leishmania* protozoans. Pharmacol Res 105288. https://doi.org/10.1016/j.phrs.2020.105288

Velazquez-Hernandez ML, Baizabal-Aguirre VM, Cruz-Vazquez F, Trejo-Contreras MJ, Fuentes-Ramirez LE, Bravo-Patino A, Cajero-Juarez M, Chavez-Moctezuma MP, Valdez-Alarcon JJ (2011) *Gluconacetobacter diazotrophicus* levansucrase is involved in tolerance to NaCl, sucrose and desiccation, and in biofilm formation. Arch Microbiol 193(2):137–149. https://doi.org/10.1007/s00203-010-0651-z

Voss J, Ehrenreich A, Liebl W (2010) Characterization and inactivation of the membrane-bound polyol dehydrogenase in *Gluconobacter oxydans* DSM 7145 reveals a role in meso-erythritol oxidation. Microbiol 156:1890–1899. https://doi.org/10.1099/mic.0.037598-0

Walker KT, Goosens VJ, Das A, Graham AE, Ellis T (2019) Engineered cell-to-cell signalling within growing bacterial cellulose pellicles. Microbiol Biotechnol 12(4):611–619. https://doi.org/10.1111/1751-7915.13340

Wang B, Shao YC, Chen FS (2015) Overview on mechanisms of acetic acid resistance in acetic acid bacteria. World J Microb Biotechnol 31(2):255–263. https://doi.org/10.1007/s11274-015-1799-0

Wang PP, Xia Y, Li JH, Kang Z, Zhou JW, Chen J (2016) Overexpression of pyrroloquinoline quinone biosynthetic genes affects L-sorbose production in *Gluconobacter oxydans* WSH-003. Biochem Eng J 112:70–77. https://doi.org/10.1016/j.bej.2016.04.011

Wei LJ, Yang XP, Gao KL, Lin JP, Yang SL, Hua QA, Wei DZ (2010) Characterization of enzymes in the oxidation of 1,2-propanediol to D-(-)-lactic acid by *Gluconobacter oxydans* DSM 2003. Mol Biotechnol 46(1):26–33. https://doi.org/10.1007/s12033-010-9263-8

Wei LJ, Zhou JL, Zhu DN, Cai BY, Lin JP, Hua Q, Wei DZ (2012) Functions of membrane-bound alcohol dehydrogenase and aldehyde dehydrogenase in the bio-oxidation of alcohols in *Gluconobacter oxydans* DSM 2003. Biotechnol Bioproc Eng 17(6):1156–1164. https://doi.org/10.1007/s12257-012-0339-0

Wong HC, Fear AL, Calhoon RD, Eichinger GH, Mayer R, Amikam D, Benziman M, Gelfand DH, Meade JH, Emerick AW, Bruner R, Benbassat A, Tal R (1990) Genetic organization of the cellulose synthase operon in *Acetobacter xylinum*. P Natl Acad Sci USA 87(20):8130–8134. https://doi.org/10.1073/pnas.87.20.8130

Wu XF, Yao HL, Cao LL, Zheng Z, Chen XJ, Zhang M, Wei ZJ, Cheng JS, Jiang ST, Pan LJ, Li XJ (2017) Improving acetic acid production by over-expressing PQQ-ADH in *Acetobacter pasteurianus*. Front Microbiol 8. ARTN 1713. https://doi.org/10.3389/fmicb.2017.01713

Xu S, Wang XB, Du GC, Zhou JW, Chen J (2014) Enhanced production of L-sorbose from D-sorbitol by improving the mRNA abundance of sorbitol dehydrogenase in *Gluconobacter oxydans* WSH-003. Microbiol Cell Fact 13. ARTN 146. https://doi.org/10.1186/s12934-014-0146-8

Yadav V, Paniliatis BJ, Shi H, Lee K, Cebe P, Kaplan DL (2010) Novel *in vivo*-degradable cellulose-chitin copolymer from metabolically engineered *Gluconacetobacter xylinus*. Appl Environ Microbiol 76(18):6257–6265. https://doi.org/10.1128/Aem.00698-10

Yakushi T, Fukunari S, Kodama T, Matsutani M, Nina S, Kataoka N, Theeragool G, Matsushita K (2018a) Role of a membrane-bound aldehyde dehydrogenase complex AldFGH in acetic acid fermentation with *Acetobacter pasteurianus* SKU1108. Appl Microbiol Biotechnol 102(10):4549–4561. https://doi.org/10.1007/s00253-018-8940-6

Yakushi T, Komatsu K, Matsutani M, Kataoka N, Vangnai AS, Toyama H, Adachi O, Matsushita K (2018b) Improved heterologous expression of the membrane-bound quinoprotein quinate dehydrogenase from *Gluconobacter oxydans*. Protein Expres Purif 145:100–107. https://doi.org/10.1016/j.pep.2018.01.007

Yakushi T, Takahashi R, Matsutani M, Kataoka N, Hours RA, Ano Y, Adachi O, Matsushita K (2020) The membrane-bound sorbosone dehydrogenase of *Gluconacetobacter liquefaciens* is a pyrroloquinoline quinone-dependent enzyme. Enzyme Microbiol Tech 137. ARTN 109511. https://doi.org/10.1016/j.enzmictec.2020.109511

Yakushi T, Terada Y, Ozaki S, Kataoka N, Akakabe Y, Adachi O, Matsutani M, Matsushita K (2018c) Aldopentoses as new substrates for the membrane-bound, pyrroloquinoline quinone-dependent glycerol (polyol) dehydrogenase of *Gluconobacter* sp. Appl Microbiol Biotechnol 102(7):3159–3171. https://doi.org/10.1007/s00253-018-8848-1

Yamada Y (2014) Transfer of *Gluconacetobacter kakiaceti*, *Gluconacetobacter medellinensis* and *Gluconacetobacter maltaceti* to the genus *Komagataeibacter* as *Komagataeibacter kakiaceti* comb. nov., *Komagataeibacter medellinensis* comb. nov. and *Komagataeibacter maltaceti* comb. nov. Int J Syst Evol Microbiol 64(Pt 5):1670–1672. https://doi.org/10.1099/ijs.0.054494-0

Yamada Y, Hoshino K, Ishikawa T (1997) The phylogeny of acetic acid bacteria based on the partial sequences of 16S ribosomal RNA: the elevation of the subgenus *Gluconoacetobacter* to the generic level. Biosci Biotechnol Biochem 61(8):1244–1251. https://doi.org/10.1271/bbb.61.1244

Yamada Y, Yukphan P, Lan Vu HT, Muramatsu Y, Ochaikul D, Tanasupawat S, Nakagawa Y (2012) Description of *Komagataeibacter* gen. nov., with proposals of new combinations (*Acetobacteraceae*). J Gen Appl Microbiol 58(5):397–404. https://doi.org/10.2323/jgam.58.397

Yang XP, Wei LJ, Lin JP, Yin B, Wei DZ (2008) Membrane-bound pyrroloquinoline quinone-dependent dehydrogenase in *Gluconobacter oxydans* M5, responsible for production of 6-(2-hydroxyethyl) amino-6-deoxy-L-sorbose. Appl Environ Microbiol 74(16):5250–5253. https://doi.org/10.1128/Aem.00272-08

Yuan JF, Wu MB, Lin JP, Yang LR (2016a) Combinatorial metabolic engineering of industrial *Gluconobacter oxydans* DSM2343 for boosting 5-keto-D-gluconic acid accumulation. BMC Biotechnol 16. ARTN 42. https://doi.org/10.1186/s12896-016-0272-y

Yuan JF, Wu MB, Lin JP, Yang LR (2016b) Enhancement of 5-keto-D-gluconate production by a recombinant *Gluconobacter oxydans* using a dissolved oxygen control strategy. J Biosci Bioeng 122(1):10–16. https://doi.org/10.1016/j.jbiosc.2015.12.006

Zahid N, Deppenmeier U (2016) Role of mannitol dehydrogenases in osmoprotection of *Gluconobacter oxydans*. Appl Microbiol Biotechnol 100(23):9967–9978. https://doi.org/10.1007/s00253-016-7680-8

Zeng WZ, Cai W, Liu L, Du GC, Chen J, Zhou JW (2019) Efficient biosynthesis of 2-keto-D-gluconic acid by fed-batch culture of metabolically engineered *Gluconobacter japonicus*. Synth Syst Biotechnol 4(3):134–141. https://doi.org/10.1016/j.synbio.2019.07.001

Zhang H, Shi LL, Lin JP, Sun M, Wei DZ (2016) Effective improvement of the activity of membrane-bound alcohol dehydrogenase by overexpression of *adhS* in *Gluconobacter oxydans*. Biotechnol Lett 38(7):1131–1138. https://doi.org/10.1007/s10529-016-2084-5

Zhang JL, Li S, Xu H, Zhou P, Zhang LJ, Ouyang PK (2013) Purification of xylitol dehydrogenase and improved production of xylitol by increasing XDH activity and NADH supply in *Gluconobacter oxydans*. J Agr Food Chem 61(11):2861–2867. https://doi.org/10.1021/jf304983d

Zhang L, Lin JP, Ma YS, Wei DZ, Sun M (2010) Construction of a novel shuttle vector for use in *Gluconobacter oxydans*. Mol Biotechnol 46(3):227–233. https://doi.org/10.1007/s12033-010-9293-2

Zhang XL, Zheng Y, Xia ML, Wu YN, Liu XJ, Xie SK, Wu YF, Wang M (2020) Knowledge domain and emerging trends in vinegar research: A bibliometric review of the literature from WoSCC. Foods 9(2) ARTN 166. https://doi.org/10.3390/foods9020166

Zheng Y, Wang J, Bai XL, Chang YG, Mou J, Song J, Wang M (2018) Improving the acetic acid tolerance and fermentation of *Acetobacter pasteurianus* by nucleotide excision repair protein UvrA. Appl Microbiol Biotechnol 102(15):6493–6502. https://doi.org/10.1007/s00253-018-9066-6

Zhu HX, Jia SR, Yang HJ, Yan L, Li J (2012) The study of optimal conditions of electroporation in *Gluconacetobacter xylinum*. Adv Intel Soft Compu 115:17–24

Zhu JW, Xie JL, Wei LJ, Lin JP, Zhao L, Wei DZ (2018) Identification of the enzymes responsible for 3-hydroxypropionic acid formation and their use in improving 3-hydroxypropionic acid production in *Gluconobacter oxydans* DSM 2003. Bioresource Technol 265:328–333. https://doi.org/10.1016/j.biortech.2018.06.001

Zhu K, Lu LF, Wei LJ, Wei DZ, Imanaka T, Hua Q (2011) Modification and evolution of *Gluconobacter oxydans* for enhanced growth and biotransformation capabilities at low glucose concentration. Mol Biotechnol 49(1):56–64. https://doi.org/10.1007/s12033-011-9378-6

Zou XX, Lin JP, Mao XL, Zhao SY, Ren YH (2017) Biosynthesis of L-erythrose by assembly of two key enzymes in *Gluconobacter oxydans*. J Agr Food Chem 65(35):7721–7725. https://doi.org/10.1021/acs.jafc.7b02201

2.2 Highly tunable TetR-dependent target gene expression in the acetic acid bacterium *Gluconobacter oxydans*

Fricke, P. M., Lürkens, M., Hünnefeld, M., J., Sonntag, C., Bott, M., Davari, M. D. & Polen, T. (2021). Highly tunable TetR-dependent target gene expression in the acetic acid bacterium *Gluconobacter oxydans*. **Applied Microbiology and Biotechnology 105: 6835–6852**.

doi:10.1007/s00253-021-11473-x

Author's contributions:
PMF constructed the plasmids, carried out the growth experiments and analyzed the data. PMF and CS performed the FACS analysis and analyzed the data. PMF and MH obtained the microscopic images. ML and MDD conducted the computational simulations. TP designed and supervised the study. PMF, ML, MDD, MB and TP wrote and revised the manuscript. All authors read and approved the final version.

Overall contribution PF: 70%

Applied Microbiology and Biotechnology
https://doi.org/10.1007/s00253-021-11473-x

APPLIED GENETICS AND MOLECULAR BIOTECHNOLOGY

Highly tunable TetR-dependent target gene expression in the acetic acid bacterium *Gluconobacter oxydans*

Philipp Moritz Fricke[1] · Martha Lürkens[2] · Max Hünnefeld[1] · Christiane K. Sonntag[1] · Michael Bott[1] · Mehdi D. Davari[3] · Tino Polen[1]

Received: 18 June 2021 / Revised: 22 July 2021 / Accepted: 23 July 2021

Abstract

For the acetic acid bacterium (AAB) *Gluconobacter oxydans* only recently the first tight system for regulatable target gene expression became available based on the heterologous repressor-activator protein AraC from *Escherichia coli* and the target promoter P_{araBAD}. In this study, we tested pure repressor-based TetR- and LacI-dependent target gene expression in *G. oxydans* by applying the same plasmid backbone and construction principles that we have used successfully for the *araC*-P_{araBAD} system. When using a pBBR1MCS-5-based plasmid, the non-induced basal expression of the Tn*10*-based TetR-dependent expression system was extremely low. This allowed calculated induction ratios of up to more than 3500-fold with the fluorescence reporter protein mNeonGreen (mNG). The induction was highly homogeneous and tunable by varying the anhydrotetracycline concentration from 10 to 200 ng/mL. The already strong reporter gene expression could be doubled by inserting the ribosome binding site AGGAGA into the 3' region of the P_{tet} sequence upstream from *mNG*. Alternative plasmid constructs used as controls revealed a strong influence of transcription terminators and antibiotics resistance gene of the plasmid backbone on the resulting expression performance. In contrast to the TetR-P_{tet}-system, pBBR1MCS-5-based LacI-dependent expression from P_{lacUV5} always exhibited some non-induced basal reporter expression and was therefore tunable only up to 40-fold induction by IPTG. The leakiness of P_{lacUV5} when not induced was independent of potential read-through from the *lacI* promoter. Protein-DNA binding simulations for pH 7, 6, 5, and 4 by computational modeling of LacI, TetR, and AraC with DNA suggested a decreased DNA binding of LacI when pH is below 6, the latter possibly causing the leakiness of LacI-dependent systems hitherto tested in AAB. In summary, the expression performance of the pBBR1MCS-5-based TetR-P_{tet} system makes this system highly suitable for applications in *G. oxydans* and possibly in other AAB.

Key Points

- *A pBBR1MCS-5-based TetR-P_{tet} system was tunable up to more than 3500-fold induction.*
- *A pBBR1MCS-5-based LacI-P_{lacUV5} system was leaky and tunable only up to 40-fold.*
- *Modeling of protein-DNA binding suggested decreased DNA binding of LacI at pH < 6.*

Keywords Promoter · Induction · Expression · Plasmid · mNeonGreen · Membrane-bound dehydrogenase

✉ Tino Polen
t.polen@fz-juelich.de

Philipp Moritz Fricke
p.fricke@fz-juelich.de

Martha Lürkens
martha.luerkens@rwth-aachen.de

Max Hünnefeld
m.huennefeld@fz-juelich.de

Christiane K. Sonntag
c.sonntag@fz-juelich.de

Michael Bott
m.bott@fz-juelich.de

Mehdi D. Davari
mehdi.davari@ipb-halle.de

[1] Forschungszentrum Jülich GmbH, IBG-1: Biotechnology, Institute of Bio- and Geosciences, 52425 Jülich, Germany

[2] RWTH Aachen University, Institute of Biotechnology, Worringerweg 3, 52074 Aachen, Germany

[3] Department of Bioorganic Chemistry, Leibniz Institute of Plant Biochemistry, Weinberg 3, 06120 Halle, Germany

Published online: 27 August 2021

Introduction

The acetic acid bacterium (AAB) *Gluconobacter oxydans* harbors the beneficial ability of regio- and stereoselective incomplete oxidation of a variety of substrates (e.g., sugars and sugar alcohols) in the periplasm by membrane-bound dehydrogenases (mDHs) and release of resulting products into the cultivation medium (Mamlouk and Gullo 2013; Mientus et al. 2017; Pappenberger and Hohmann 2014). Because of this feature, *G. oxydans* is industrially used for oxidative biotransformations of carbohydrates to produce e.g. the vitamin C precursor L-sorbose, the tanning lotion additive dihydroxyacetone, and 6-amino-L-sorbose used for the production of the antidiabetic drug miglitol (Ameyama et al. 1981; Gupta et al. 2001; Hekmat et al. 2003; Saito et al. 1997; Tkac et al. 2001; Wang et al. 2016).

For the expression of target genes in *G. oxydans*, so far only constitutive promoters have been used due to the lack of a regulatable promoter demonstrated to be functional and tunable in *G. oxydans* (reviewed in Fricke et al. 2021). Only recently the first tight system became available for tunable induction of gene expression in *G. oxydans*. This system is based on AraC-P_{araBAD} and the induction by L-arabinose binding to the regulator protein AraC (Fricke et al. 2020). AraC typically represses the target promoter P_{araBAD} by DNA bending in the absence of the inducer L-arabinose and activates it in the presence of the inducer by a modified binding to the promoter DNA and thereby releasing the bending (Schleif 2010). However, in *G. oxydans*, P_{araBAD} is almost not active in the absence of *araC* and thus, repression by AraC is not required in *G. oxydans* for tightness of P_{araBAD} in the absence of the inducer (Fricke et al. 2020). In contrast, in *Gluconacetobacter* and *Komagataeibacter* plasmid-based AraC-P_{araBAD} was reported to be very leaky (Teh et al. 2019). While AraC typically is acting both as repressor and activator, the transcriptional regulators TetR and LacI only exert a repressor function and dissociate from their operator DNA when forming a complex with their respective inducer (Hillen et al. 1983; Khoury et al. 1991; Miller 1970; Sellitti et al. 1987; Wray and Reznikoff 1983). P_{tet} and P_{lac} then enable transcription of the downstream gene by RNA polymerase. In AAB both TetR- and LacI-dependent target gene expression have so far been reported to be very leaky or inhomogeneously induced. In *Komagataeibacter rhaeticus* iGEM, the TetR-P_{tet} system from transposon Tn*10* exhibited only approximately 1.5-fold induction due to high leakiness in the absence of the inducer anhydrotetracycline (Florea et al. 2016). With a LacI-based expression system in *K. xylinus*, the induction ratio also appeared to be low and only a fraction of cells showed some induction (Liu et al. 2020). For another LacI-based system, expression was also found to be very leaky in *G. oxydans* (Condon et al. 1991).

In this study, we aimed to test TetR- and LacI-dependent target gene expression in *G. oxydans* by applying the same plasmid backbone and construction principles that we have used recently for the construction of the *araC*-P_{araBAD} system (Fricke et al. 2020). With pBBR1MCS-5-based plasmid constructs, we found always some leakiness of the LacI-P_{lacuv5} system, yet extremely tight and optimally tunable target gene expression with TetR-P_{tet} making the latter system highly suitable for applications in *G. oxydans* and possibly in other AAB.

Materials and methods

Bacterial strains, plasmids, and culture conditions

All strains and plasmids created and used in this study are listed in Table 1. *G. oxydans* was routinely cultivated in D-mannitol medium (pH 6) containing 4% (w/v) D-mannitol, 5 g L^{-1} yeast extract, 2.5 g L^{-1} $MgSO_4 \times 7\ H_2O$, 1 g L^{-1} $(NH_4)_2SO_4$, 1 g L^{-1} KH_2PO_4 at 30 °C and 180 rpm, and supplemented with 50 µg mL^{-1} sodium cefoxitin. Besides D-mannitol and cefoxitin which were sterile filtered as stock solutions (20% (w/v) and 50 mg mL^{-1}), all components were autoclaved for sterilization (120 °C, 20 min). Unless stated otherwise, for shake flask cultivations 10 mL or 60 mL of D-mannitol medium was inoculated from overnight precultures to an initial optical density at 600 nm (OD_{600}) of 0.3 or 0.2 (UV-1800, Shimadzu) using 100 mL or 500 mL shaking flasks with three baffles. *G. oxydans* carrying pBBR1MCS-5- or pBBR1MCS-2-based plasmids were supplemented with 10 µg mL^{-1} gentamicin or 50 µg mL^{-1} kanamycin, respectively (Kovach et al. 1995). *Escherichia coli* strains were routinely grown at 37 °C and 160 rpm in lysogeny broth (LB) medium which was supplemented when appropriate with 10 µg mL^{-1} gentamicin or 50 µg mL^{-1} kanamycin. *G. oxydans* was transformed by conjugal transfer of plasmids from *E. coli* S17-1 (Kiefler et al. 2017). Competent *E. coli* cells were prepared by $CaCl_2$ procedure and transformed as described (Hanahan 1983).

Recombinant DNA work

All DNA oligonucleotides used for the construction of plasmids and sequencing are listed in Table S1 and were synthesized by Eurofins MWG. All restriction enzymes were purchased from Thermo Scientific. Polymerase chain reaction (PCR), restriction, and ligation reactions for DNA manipulations were conducted according to standard protocols (Sambrook et al. 1989). DNA fragments were amplified using Q5 polymerases according to

Table 1 Strains and plasmids used or constructed in this study

	Relevant characteristics	Reference / Source
Strain		
E. coli S17-1	Δ*recA*, *endA1*, *hsdR17*, *supE44*, *thi*-1, *tra*$^+$	Simon et al. 1983
G. oxydans 621H	DSM 2343	DSMZ
Plasmid		
pBBR1MCS-5	Derivative of pBBR1MCS; Gm^R	Kovach et al. 1995
pBBR1MCS-2	Derivative of pBBR1MCS; Km^R	Kovach et al. 1995
pBBR1-tetall-strep_long	Derivative of pBBR1MCS-2 with *tetR*-P_{tet} fragment from *E. coli* Tn*10*	Gift from Uwe Deppenmeier, University of Bonn
pBBR1MCS-5-T_{gdhM}-MCS-T_{0028}	Derivative of pBBR1MCS-5 with terminator sequences of GOX0265 (T_{gdhM}) and GOX0028 (T_{0028}) flanking the multiple cloning site	This work
pBBR1MCS-5-T_{gdhM}-*tetR*-P_{tet}-*mNG*-T_{BBa_B1002}-T_{0028}	Derivative of pBBR1MCS-5-T_{gdhM}-MCS-T_{0028} carrying fluorescent reporter gene *mNG* controlled by tetracycline-induced promoter P_{tet} and *tetR* encoding P_{tet} repressor TetR	This work
pBBR1MCS-5-*tetR*-P_{tet}-*mNG*-T_{BBa_B1002}-T_{0028}	Derivative of pBBR1MCS-5-T_{gdhM}-*tetR*-P_{tet}-*mNG*-T_{BBa_B1002}-T_{0028} lacking terminator T_{gdhM} downstream from *tetR*	This work
pBBR1MCS-5-T_{gdhM}-*tetR*-P_{tet}-*mNG*	Derivative of pBBR1MCS-5-T_{gdhM}-*tetR*-P_{tet}-*mNG*-T_{BBa_B1002}-T_{0028} lacking terminators T_{BBa_B1002} and T_{0028} downstream from *mNG*	This work
pBBR1MCS-5-*tetR*-P_{tet}-*mNG*	Derivative of pBBR1MCS-5-T_{gdhM}-*tetR*-P_{tet}-*mNG*-T_{BBa_B1002}-T_{0028} lacking the terminators downstream from *tetR* and *mNG*	This work
pBBR1MCS-5-T_{gdhM}-*tetR*-P_{tet}-RBS-*mNG*-T_{BBa_B1002}-T_{0028}	Derivative of pBBR1MCS-5-T_{gdhM}-*tetR*-P_{tet}-*mNG*-T_{BBa_B1002}-T_{0028} with ribosomal binding site AGGAGA (Hentschel et al. 2013) inserted upstream from *mNG*	This work
pBBR1MCS-5-T_{gdhM}-P_{tet}-*mNG*-T_{BBa_B1002}-T_{0028}	Derivative of pBBR1MCS-5-T_{gdhM}-*tetR*-P_{tet}-*mNG*-T_{BBa_B1002}-T_{0028} lacking *tetR*	This work
pBBR1MCS-2-T_{gdhM}-*tetR*-P_{tet}-*mNG*-T_{BBa_B1002}-T_{0028}	Derivative of pBBR1MCS-2 carrying *mNG* controlled by P_{tet} and *tetR*, with each gene flanked by terminators	This work
pBBR1MCS-5-P_{lacI}-*lacI*-P_{lacUV5}-RBS-*mNG*-T_{BBa_B1002}-T_{0028}	Derivative of pBBR1MCS-5 carrying *mNG* with RBS AGGAGA controlled by IPTG-induced promoter P_{lacUV5} and *lacI* encoding P_{lacUV5} repressor LacI	This work
pBBR1MCS-5-P_{lacUV5}-RBS-*mNG*-T_{BBa_B1002}-T_{0028}	Derivative of pBBR1MCS-5-P_{lacI}-*lacI*-P_{lacUV5}-RBS-*mNG*-tBBa-t28 lacking *lacI*	This work
pBBR1MCS-5-*lacI*-P_{lacI}-P_{lacUV5}-RBS-*mNG*-T_{BBa_B1002}-T_{0028}	Derivative of pBBR1MCS-5-P_{lacI}-*lacI*-P_{lacUV5}-RBS-*mNG*-T_{BBa_B1002}-T_{0028} with opposite orientation of P_{lacI}-*lacI* toward P_{lacUV5}	This work

the conditions recommended by the manufacturer (New England Biolabs). Unless stated otherwise for the construction of all reporter plasmids, amplified DNA fragments were integrated in the restricted broad-host vector pBBR1MCS-5 in a one-step isothermal Gibson assembly (50 °C, 1 h) (Gibson et al. 2009). All cloning steps to obtain desired plasmids were conducted in *E. coli* S17-1 and plasmids were isolated using a QIAprep spin miniprep kit (Qiagen). Inserts of all constructed plasmids were checked for correctness by DNA sequencing (Eurofins MWG).

Construction of plasmids

For the construction of plasmids, the empty vector pBBR1MCS-5-T_{gdhM}-MCS-T_{0028} was generated from pBBR1MCS-5. It carries the terminator sequences of GOX0265 (T_{gdhM}) and GOX0028 (T_{0028}) flanking the multiple cloning site (MCS) to minimize interfering effects between the plasmid backbone and expression of the inserted genes.

Plasmid pBBR1MCS-5-T_{gdhM}-*tetR*-P_{tet}-*mNG*-T_{BBa_B1002}-T_{0028} was constructed using the primer pair

PF1/PF2 to generate a 763 bp DNA fragment with *tetR*-P_{tet} from plasmid pBBR1-tetall-strep_long and primer pair PF3/PF4 to generate a 802 bp DNA fragment with *mNG* and the terminator BBa_B1002 from the iGEM parts library from pBBR1MCS-5-*araC*-P_{BAD}-*mNG* (Fricke et al. 2020). For insertion of the two DNA fragments in pBBR1MCS-5-T_{gdhM}-MCS-T_{0028}, the plasmid was restricted with *Xba*I and *Eco*RI.

Plasmid pBBR1MCS-5-*tetR*-P_{tet}-*mNG*-T_{BBa_B1002}-T_{0028} lacking terminator T_{gdhM} downstream from *tetR* was constructed by amplification of a 576 bp DNA fragment from pBBR1MCS-5-T_{gdhM}-*tetR*-P_{tet}-*mNG*-T_{BBa_B1002}-T_{0028} with primer pair PF5/PF6 and ligated with *Eco*81I/*Mun*I-digested pBBR1MCS-5-T_{gdhM}-*tetR*-P_{tet}-*mNG*-T_{BBa_B1002}-T_{0028} replacing T_{gdhM}-*tetR* by *tetR* only.

For the construction of pBBR1MCS-5-T_{gdhM}-*tetR*-P_{tet}-*mNG* lacking the terminators T_{BBa_1002} and T_{0028} downstream from *mNG*, the primer pairs PF7/PF8 and PF9/PF10 were used to amplify a 1,471 bp DNA fragment comprising *tetR*-P_{tet}-*mNG* and a 643 bp DNA fragment comprising a part of the pBBR1MCS-5 backbone using pBBR1MCS-5-T_{gdhM}-*tetR*-P_{tet}-*mNG*-T_{BBa_B1002}-T_{0028} as a template. Both DNA fragments were ligated with *Xba*I / *Bsp*1407I-digested pBBR1MCS-5-T_{gdhM}-MCS-T_{0028}.

The plasmid pBBR1MCS-5-*tetR*-P_{tet}-*mNG* lacking all terminators downstream from *tetR* and *mNG* was generated by removing T_{gdhM} from pBBR1MCS-5-T_{gdhM}-*tetR*-P_{tet}-*mNG* with primer pair PF5/PF6 as described above for the removal of T_{gdhM} from pBBR1MCS-5-T_{gdhM}-*tetR*-P_{tet}-*mNG*-T_{BBa_B1002}-T_{0028}.

In another construct, for comparing and enhancing resulting reporter protein level when using the P_{tet} region including its native ribosome binding site (RBS_{Ptet}) in *G. oxydans*, the RBS AGGAGA (RBS_{AGGAGA}), functional and strong in *G. oxydans*, was inserted upstream from *mNG* (Fricke et al. 2020; Hentschel et al. 2013). Therefore, the DNA fragments *tetR*-P_{tet}-RBS (761 bp) and RBS-*mNG* (811 bp) were amplified with the primer pairs PF1/PF12 and PF13/PF4, respectively, and ligated with *Xba*I/*Eco*RI-digested pBBR1MCS-5-T_{gdhM}-MCS-T_{0028} to obtain plasmid pBBR1MCS-5-T_{gdhM}-*tetR*-P_{tet}-RBS-*mNG*-T_{BBa_B1002}-T_{0028}.

For plasmid pBBR1MCS-5-T_{gdhM}-P_{tet}-*mNG*-T_{BBa_B1002}-T_{0028} lacking *tetR*, fragment P_{tet}-*mNG* (901 bp) was amplified from pBBR1MCS-5-T_{gdhM}-*tetR*-P_{tet}-*mNG*-T_{BBa_B1002}-T_{0028} with primer pair PF11/PF4 and ligated with *Xba*I / *Eco*RI-digested pBBR1MCS-5-T_{gdhM}-MCS-T_{0028}.

To change the plasmid backbone from pBBR1MCS-5 to pBBR1MCS-2 and create pBBR1MCS-2-T_{gdhM}-*tetR*-P_{tet}-*mNG*-T_{BBa_B1002}-T_{0028}, the DNA fragment with T_{gdhM}-*tetR*-P_{tet}-*mNG*-T_{BBa_B1002}-T_{0028} was excised from pBBR1MCS-5-T_{gdhM}-*tetR*-P_{tet}-*mNG*-T_{BBa_B1002}-T_{0028} and ligated with *Sac*I/*Xho*I-digested pBBR1MCS-2.

The plasmid pBBR1MCS-5-P_{lacI}-*lacI*-P_{lacUV5}-RBS-*mNG*-T_{BBa_B1002}-T_{0028} was constructed by ligating the DNA fragment P_{lacI}-*lacI*-P_{lacUV5}-*lacZα*-RBS (1855 bp) and *mNG*-T_{BBa_B1002}-T_{0028} (954 bp) with *Bsh*TI/*Sph*I-digested pBBR1MCS-5. Here, upstream from *mNG* the RBS AGGAGA known to be functional in *G. oxydans* was integrated into the construct (Hentschel et al. 2013). The DNA sequence of P_{lacI}-*lacI*-P_{lacUV5}-*lacZα* was derived from *E. coli* BL21 and obtained with primer pair PF14/PF15 and plasmid pK18*mobsacB*-DE3 (Kortmann et al. 2015). The DNA fragment *mNG*-T_{BBa_B1002}-T_{0028} was amplified with primer pair PF16/PF17 from plasmid pBBR1MCS-5-T_{gdhM}-*tetR*-P_{tet}-*mNG*-T_{BBa_B1002}-T_{0028}.

For the construction of plasmid pBBR1MCS-5-P_{lacUV5}-RBS-*mNG*-T_{BBa_B1002}-T_{0028} lacking the repressor gene *lacI*, the DNA fragment P_{lacUV5}-RBS-*mNG*-T_{BBa_B1002}-T_{0028} (1575 bp) was amplified with primer pair PF18/PF17 from pBBR1MCS-5-P_{lacI}-*lacI*-P_{lacUV5}-RBS-*mNG*-T_{BBa_B1002}-T_{0028} and ligated with *Bsh*TI/*Sph*I-digested pBBR1MCS-5.

The plasmid pBBR1MCS-5-*lacI*-P_{lacI}-P_{lacUV5}-RBS-*mNG*-T_{BBa_B1002}-T_{0028} with P_{lacI}-*lacI* in the opposite orientation to P_{lacUV5}-*mNG* was constructed by amplification of the DNA fragments P_{lacI}-*lacI* (1,261 bp) with the primer pair PF19/PF20 and P_{lacUV5}-*mNG*-T_{BBa_B1002}-T_{0028} (1556 bp) with the primer pair PF21/PF17. Both fragments were ligated into pBBR1MCS-5 digested with *Bsh*TI and *Sph*I.

Measurements of mNG fluorescence

Expression of promoter–reporter constructs in *G. oxydans* was monitored using the fluorescence protein mNeonGreen (mNG) as a reporter (Shaner et al. 2013). In shake flask experiments, the inducibility of P_{tet}-derived *mNG* expression in *G. oxydans* was tested by the addition of 200 ng mL^{-1} anhydrotetracycline (ATc) from a 0.2 mg mL^{-1} stock solution in 50% ethanol. Non-induced reference cultures were supplemented with an equal volume of 50% ethanol. For experiments with P_{lacUV5}-controlled *mNG* expression, 1 mM of isopropyl-β-D-1-thiogalactopyranoside (IPTG) was supplemented from a 100 mM stock solution in water. An equal volume of water was added to non-induced reference cultures. Throughout the cultivation samples were taken to monitor growth (OD_{600}) by a spectrophotometer (UV-1800, Shimadzu) and fluorescence emission using an Infinite M1000 PRO Tecan reader (λ_{ex} 504 nm / λ_{em} 517 nm, gain 60, ex/em bandwidth 5 nm, infinite M1000 PRO Tecan). Using a BioLector system, 800 µL batches of D-mannitol medium were inoculated from overnight starter cultures to an initial OD_{600} of 0.3 and incubated at 30 °C (1,200 rpm; 85% humidity) using 48-well Flowerplates® (m2p-labs). Backscattering light intensity ($A_{620\ nm}$) for growth and fluorescence emission (λ_{ex} 510 nm / λ_{em} 532 nm) were monitored online during the cultivation. Backscatter and fluorescence

signals were measured using gain 15 or 20 and 50 or 60, respectively, as indicated in the figure legends. Fluorescence values that did not exceed the emission signals from cell-free control samples were set to 1. Specific fluorescence was calculated by taking the quotient of the fluorescence signal per biomass value at a given time point. Specific fluorescence values lower than in the cell-free control samples were set to 0.01. All data presented in the same graphs were obtained in the same BioLector growth experiment using identical gains.

Cell flow cytometer analysis

Reporter gene expression was analyzed by measuring mNG fluorescence on the single cell level with *G. oxydans* 621H either carrying the plasmid pBBR1MCS-5-T_{gdhM}-*tetR*-P_{tet}-*mNG*-T_{BBa_B1002}-T_{0028}, pBBR1MCS-2-T_{gdhM}-*tetR*-P_{tet}-*mNG*-T_{BBa_B1002}-T_{0028}, or pBBR1MCS-5-P_{lacI}-*lacI*-P_{lacUV5}-RBS-*mNG*-T_{BBa_B1002}-T_{0028} using a FACSAria™ Fusion cell sorter (BD Biosciences) run with 70 psi sheath pressure and equipped with a 70 µm nozzle. Data acquisition and analysis of the flow cytometer was controlled by the FACSDiva 8.0.3 software (BD Biosciences). Using a 488-nm solid blue laser beam, the forward scatter (FSC) and side scatter (SSC) were employed for cell analysis. Particles/events with FSC-H and SSC-H signals below a threshold of 200 a.u. and 300 a.u. were excluded from the analysis. Detection of emitted mNG fluorescence from the SSC signal was performed by combining a 502-nm long-pass and 530/30-nm band-pass filter. The entire cell population was analyzed in a three-step gating strategy. Initially, the assessed cell population was gated in a FSC-H *vs*. SSC-H plot, to exclude signals originating from electronic noise and cell debris. From the resulting population, the FSC-H signal was plotted against the FSC-W signal. Subsequently, the obtained population was gated in a SSC-H *vs*. SSC-W plot, to ensure singlet discrimination. The gated singlet population was used for fluorescence acquisition in all experiments (fluorescence intensity *vs*. cell count). For all samples, 100,000 events were recorded with an event rate below 10,000 events/s. FlowJo 10.7.2 for Windows (FlowJo, LLC) was used for data analysis and visualization of all gated events ($n = 100{,}000$).

Fluorescence microscopy

For fluorescence microscopy, cells were placed on agarose-coated microscope slides and covered by a coverslip. Images were taken on a Zeiss AxioImager M2 imaging microscope that was equipped with a Plan-Apochromat 100×/1.40-numerical aperture phase-contrast oil-immersion objective and an AxioCam MRm camera. Fluorescence was measured using the 46 HE filter set (λ_{ex} 500/20 nm / λ_{em} 535/30 nm). For all images, identical exposure times were applied. Digital images were acquired and analyzed with AxioVision Rel. 4.8 software (Zeiss).

Total DNA extraction, library preparation, Illumina sequencing, and data analysis

Total DNA was purified from a culture aliquot using a NucleoSpin Microbial DNA Mini kit (MACHEREY–NAGEL). DNA concentrations were measured using a Qubit 2.0 fluorometer (Thermo Fisher Scientific). Illumina sequencing libraries of *tetR*-P_{tet} and *lacI*-P_{lacUV5} samples were prepared from 1 µg of isolated DNA using the NEBNext Ultra™ II DNA Library Prep Kit for Illumina according to the manufacturers' instructions (NEB). The libraries were evaluated by qPCR using the KAPA library quantification kit (Peqlab) and then normalized for sample pooling. Paired-end sequencing with a read length of 2 × 150 bases was performed in-house on an Illumina MiSeq system. The demultiplexed sequencing output (base calls) was obtained as fastq files and used for trimming and quality filtering, mapping, and coverage calculation using the CLC Genomics Workbench software (Qiagen). For the mappings, the improved genome sequence from *G. oxydans* 621H and the *tetR*-P_{tet} or *lacI*-P_{lacUV5} plasmid sequence was used (Kranz et al. 2017).

Computational methods

Homology modeling of TetR, LacI, and AraC structures was performed by YASARA Structure version 19.12.14 (Krieger et al. 2002) using the default settings (PSI-BLAST iterations: 6, E value cutoff: 0.5, templates: 5), and with oligomerization state adjusted to 2 for TetR and AraC, and to 4 for LacI (Altschul et al. 1997). A position-specific scoring matrix (PSSM) was used to score the obtained template structures (Jones 1999; Qiu and Elber 2006). The obtained hybrid models were further evaluated for protein geometry by VERIFY3D and ProSA (Eisenberg et al. 1997; Sippl 1993). Operator models of *tetO* and $araI_1$ were generated with Avogadro as B-shaped DNA (Hanwell et al. 2012). The initial coordinates for *lacO* were taken from the X-ray structure (PDB ID 1EFA, resolution 2.6 Å) (Bell and Lewis 2000).

Surface residues were determined with PyMol script (default cutoff of 2.5 $Å^2$). The protonation states of titratable residues were assigned on the basis of pK_a values obtained from the PROPKA 3.1 program for the pH values 7, 6, 5, and 4 (Olsson et al. 2011).

Modeling protein–protein and protein-DNA complexes was performed by using the HADDOCK Webserver (van Zundert et al. 2016). To understand the DNA binding behavior, protein-DNA docking simulations of the transcription factors and their respective operator sequence were done. In docking simulations, a dimeric model for TetR and LacI

and a monomeric model for AraC were used. The charge states of proteins were adjusted to the respective pH based on the previous pK_a calculations and were adjusted to the respective pH either directly within the PDB file according to the HADDOCK specifications (Asp, Glu), or within the HADDOCK interface (His). Oligomerization of proteins was computed by performing protein–protein docking with the transcription factor subunits, i.e., monomer–monomer docking for TetR and AraC, and dimer-dimer docking for LacI. Due to the fact that the LacI homology model was missing the second tetramerization helix, the dimer structure taken from the crystal structure (PDB ID 3EDC, resolution 2.10 Å) was used for the LacI tetramerization modeling (Stenberg and Vihinen 2009).

Results

A pBBR1MCS-5-based TetR-P_{tet} system was very tight and highly inducible and tunable

The *tetR*-P_{tet} region including its native RBS from transposon Tn*10* was used to construct a pBBR1MCS-5-based reporter plasmid using the reporter gene *mNeonGreen* (*mNG*). The *tetR* gene under the control of its native promoter P_{tetR} overlapping with the divergently oriented TetR-dependent promoter P_{tet} followed by *mNG* were integrated into the MCS of pBBR1MCS-5-T_{gdhM}-MCS-T_{0028} as described in Material and Methods. DNA sequences for transcription terminators were placed adjacent to the *tetR*-P_{tet}-*mNG* insert to create transcriptional barriers between the genetic elements on the insert and on the plasmid backbone.

The leakiness and inducibility of P_{tet} were tested in *G. oxydans* 621H harboring the plasmid pBBR1MCS-5-T_{gdhM}-*tetR*-P_{tet}-*mNG*-T_{BBa_B1002}-T_{0028} by omitting and adding anhydrotetracycline (ATc). A pre-culture was split and used to inoculate shake flasks for growth in D-mannitol medium without and with 200 ng mL^{-1} ATc. The highest mNG fluorescence signals were measured in induced cultures after 10 h of growth at the end of the exponential growth phase, followed by a slight decrease in the stationary phase (Fig. 1a). In the non-induced cultures, the mNG signals barely surpassed background signals of cell-free control samples, suggesting very tight repression of P_{tet} in the absence of inducer. Based on the absolute and the specific mNG fluorescence, the maximal induction ratios were calculated to be 2284 ± 263-fold and 2661 ± 180-fold, respectively. At the end of the cultivation (24 h), cells of an induced culture were harvested and total DNA was purified for Illumina sequencing. In the read data analysis, 99.5% of the reads mapped to the updated reference sequences of the *G. oxydans* 621H genome, the 5 endogenous plasmids, and the mNG expression plasmid with *tetR*-P_{tet} (Kranz et al. 2017). Thus, the sequencing results excluded undesired contaminations and verified that the P_{tet}-derived *mNG* expression was highly induced in *G. oxydans* 621H carrying the plasmid pBBR1MCS-5-T_{gdhM}-*tetR*-P_{tet}-*mNG*-T_{BBa_B1002}-T_{0028}. In microscale BioLector cultivations a similar induction profile of P_{tet} was observed as in shake flasks. The fluorescence in ATc-supplemented cultures peaked approximately after 8 h also followed by a decreased fluorescence level in the stationary phase (Fig. 1b). Again, the basal expression under non-induced conditions was barely detectable and the maximal induction ratio based on the specific fluorescence was calculated to be 3674 ± 193-fold. The drop in mNG fluorescence signals observed in shake flasks and in BioLector cultivations in the stationary phase was caused by the decreased pH of the medium (pH 4.6) and could be largely recovered at pH 6 as outlined below and described previously (Fricke et al. 2020).

To verify that TetR is responsible for the repression of P_{tet} also in *G. oxydans*, we constructed the plasmid pBBR1MCS-5-T_{gdhM}-P_{tet}-*mNG*-T_{BBa_B1002}-T_{0028} lacking the *tetR* gene. In the absence of the plasmid-encoded regulator TetR, in both conditions with ATc supplement and without, the *mNG* expression from P_{tet} was even higher than in the induced control cultures containing the *tetR* gene on the plasmid (Fig. S1). This indicated that in *G. oxydans* P_{tet} is also fully repressed by TetR like in *E. coli* and that non-blocked P_{tet} is highly active in *G. oxydans*. Interestingly, even without the *tetR* gene the addition of ATc resulted in a higher maximal specific fluorescence (28.8 ± 1.3 a.u.) than without ATc (23.5 ± 1.9 a.u). This suggested that in *G. oxydans* the P_{tet} activity could additionally be affected by an endogenous factor.

We then tested the tunability of the TetR-P_{tet} system in *G. oxydans* by varying the ATc concentration from 10 to 400 ng mL^{-1}. Gradual increase of the inducer concentration led to a gradual increase in mNG fluorescence illustrating the high dynamic range of P_{tet}-derived gene expression in *G. oxydans* with the pBBR1MCS-5 backbone (Fig. 1c). Comparing the peaking fluorescence signals, the system appeared to be almost fully induced with 150 to 200 ng mL^{-1} ATc. According to flow cytometry analysis (FACS) of samples taken 7 h after induction (Fig. 1a), in both ATc-induced and non-supplemented cultures high population homogeneity was observed (Fig. 1d). Ninety-five percent and 94% of the cells of a sample were found to exhibit either very low (~ 400 a.u., non-induced) or very high (~ 80,000 a.u., ATc-induced) mNG fluorescence signals. To visualize this high homogeneity by microscopy, images of induced and non-induced *G. oxydans* cells harboring the plasmid pBBR1MCS-5-T_{gdhM}-*tetR*-P_{tet}-*mNG*-T_{BBa_B1002}-T_{0028} were taken (Fig. S2). In accordance with the data obtained by flow cytometry, the microscopic images confirmed the

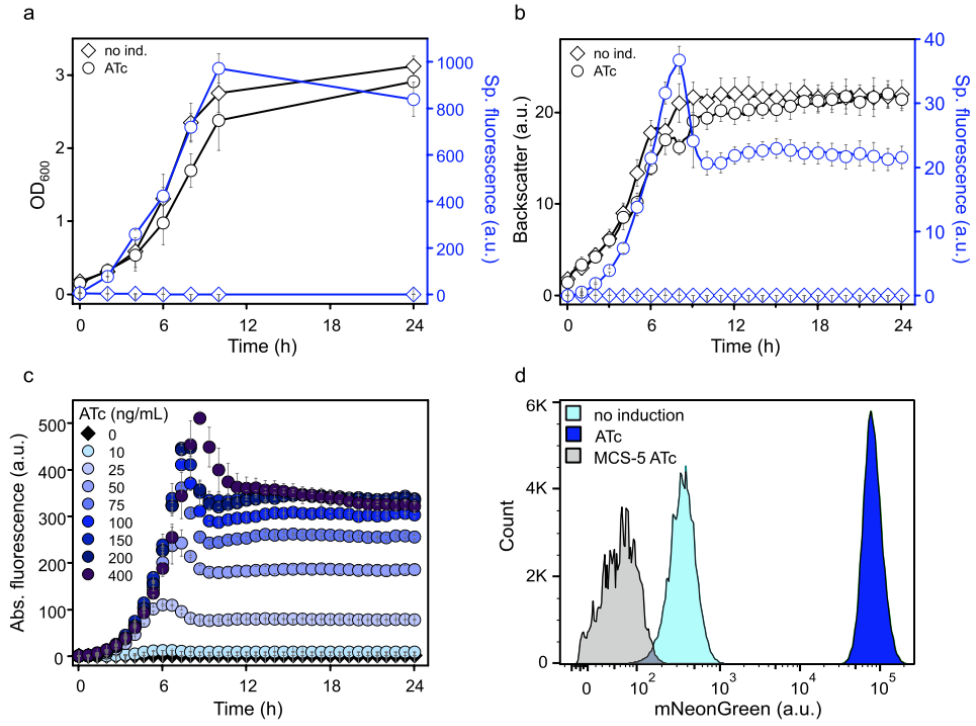

Fig. 1 Performance of the TetR-P_{tet} system in *G. oxydans* 621H. **a** Growth (OD_{600}) and specific mNG fluorescence in *G. oxydans* 621H carrying plasmid pBBR1MCS-5-T_{gdhM}-*tetR*-P_{tet}-*mNG*-T_{BBa_B1002}-T_{0028} in ATc-induced (200 ng mL^{-1}) and non-induced condition in shake flasks. The mNG fluorescence was measured in a Tecan reader (gain 60). The specific fluorescence was calculated from absolute fluorescence per OD_{600}. Data represent mean values and standard deviation from three biological replicates with three technical replicates each. **b** Growth according to backscatter (gain 15) and specific mNG fluorescence (with gain 50) of *G. oxydans* 621H carrying plasmid pBBR1MCS-5-T_{gdhM}-*tetR*-P_{tet}-*mNG*-T_{BBa_B1002}-T_{0028} in ATc-induced (200 ng mL^{-1}) and non-induced condition in microscale BioLector cultivations. Data represent mean values and standard deviation from four biological replicates with three technical replicates each. **c** Graded ATc-dependent *mNG* expression in *G. oxydans* 621H carrying plasmid pBBR1MCS-5-T_{gdhM}-*tetR*-P_{tet}-*mNG*-T_{BBa_B1002}-T_{0028} in microscale BioLector cultivations. Reporter gene expression measured as fluorescence (gain 50) was induced with increasing concentrations of ATc from 10 to 400 ng mL^{-1} as indicated. **d** FACS analysis of *G. oxydans* 621H carrying plasmid pBBR1MCS-5-T_{gdhM}-*tetR*-P_{tet}-*mNG*-T_{BBa_B1002}-T_{0028} or empty vector pBBR1MCS-5 (MCS-5) as a control. Cells were grown in shake flasks with D-mannitol medium without and with 200 ng mL^{-1} ATc. FACS analysis was performed 7 h after inoculation/induction. Total counts per sample represent 100.000 events

strong inducibility of pBBR1MCS-5-based TetR-P_{tet} and the highly homogenous induction response in *G. oxydans*.

During growth, the *G. oxydans* D-mannitol medium initially set to pH 6 is acidified to pH 4.7 which causes a loss of intracellular mNG fluorescence suggesting a decreased cytoplasmic pH, at least in the stationary phase (Fricke et al. 2020). We wanted to test experimentally whether an already initially lower medium pH could result in leakiness of P_{tet} in *G. oxydans* already during growth as observed in *Komagataeibacter* (Florea et al. 2016). Therefore, *G. oxydans* carrying the plasmid pBBR1MCS-5-T_{gdhM}-*tetR*-P_{tet}-*mNG*-T_{BBa_B1002}-T_{0028} was grown in D-mannitol medium initially adjusted to pH 6, 5, 4 and 3 both in the absence and presence of ATc. After 23 h cells were centrifuged and resuspended in fresh D-mannitol-free medium set to pH 6 to check for potential pH-dependent recovery of

mNG fluorescence above the respective levels monitored before that would indicate a leakiness of P_{tet} together with a loss of mNG fluorescence during growth. In all non-induced cultures, very low maximal fluorescence signals (0.6 ± 0.1 to 1.3 ± 0.2 a.u.) were measured independent of the initial medium pH (Fig. S3a-b). Cells grown in pH 3 exhibited the lowest signals and a different growth according to backscatter compared to all other cultures. No sufficient increase of mNG fluorescence was observed in any non-induced condition in the exponential growth phase to suggest a leakiness of P_{tet} in *G. oxydans*. Moreover, after transfer (23 h) of the cells into fresh D-mannitol-free medium adjusted to pH 6 no recovery of mNG fluorescence above the levels before could be observed. Thus, since the strong induction of P_{tet} by ATc in the cells grown in each medium of this pH series indicated that the mNG protein could always be produced during the exponential phase of growth and exhibited strong fluorescence property (Fig. S3c-d), the results together indicated that expression from P_{tet} was really tightly repressed in *G. oxydans* in all pH conditions, even in medium initially set to pH 3.

Terminators strongly affected mNG expression strength but not repression of P_{tet}

Since we did not observe and could not show leakiness of the TetR-P_{tet} system in growing *G. oxydans* cells *per se* or in dependence of the medium pH, we wanted to analyze the influence of terminator sequences on the functionality and leakiness of the TetR-P_{tet} system. Therefore, we constructed plasmids lacking terminators downstream from *tetR* or *mNG* and both and compared these constructs in regard to P_{tet}-derived *mNG* expression in *G. oxydans* (Fig. 2). The terminators downstream from *mNG* had a major influence on the resulting mNG fluorescence level. With plasmid pBBR1MCS-5-T_{gdhM}-*tetR*-P_{tet}-*mNG* not having T_{BBa_B1002} and T_{0028} downstream from *mNG*, the mNG fluorescence signals were reduced by half in ATc-induced *G. oxydans* cells. Compared to the reference plasmid including all terminators, the maximum in specific fluorescence dropped from 19.4 ± 2.9 a.u. to 10.5 ± 0.2 a.u. (Fig. 2e). The specific fluorescence signals of *G. oxydans* harboring the plasmid pBBR1MCS-5-*tetR*-P_{tet}-*mNG*-T_{BBa_B1002}-T_{0028} lacking T_{gdhM} downstream from *tetR* were significantly ($p = 0.0383$) higher (22.3 ± 1.1 a.u.) compared to the reference (19.4 ± 2.9 a.u.) suggesting a little positive effect on P_{tet}-derived induction and expression strength when T_{gdhM} downstream from *tetR* was absent. The construct pBBR1MCS-5-*tetR*-P_{tet}-*mNG* lacking all terminators performed similar (9.5 ± 0.7 a.u.) as pBBR1MCS-5-T_{gdhM}-*tetR*-P_{tet}-*mNG* lacking only the terminators downstream from *mNG* (10.5 ± 0.2 a.u.). Hence, in *G. oxydans* and in case of *mNG,* termination of the target gene transcription close to the 3' end might be important to achieve higher expression levels in *G. oxydans.* None of the terminators appeared to affect the repression of P_{tet} in the absence of ATc and a P_{tet} leakiness was not observed.

Comparison of the pBBR1MCS-2 / -5 backbones and insertion of AGGAGA as RBS

The broad-host-range vectors pBBR1MCS-5 and pBBR1MCS-2 differ in the antibiotics resistance they convey for clone selection. pBBR1MCS-5 *gmR* encodes for a gentamicin-3-acetyltransferase enabling growth on gentamicin and pBBR1MCS-2 *neoR/kanR* encodes for a neomycin/kanamycin phosphotransferase enabling growth on kanamycin (Kovach et al. 1995). Furthermore, *gmR* and *neoR/kanR* are located on different DNA strands which in the case of *neoR/kanR* could result in transcripts partially overlapping with and antisense to the mRNA of the target gene present in the cloned insert. To check whether the plasmid backbone and antibiotics resistance affect the inducibility of P_{tet} in *G. oxydans* we compared the performance of the TetR-P_{tet} system with pBBR1MCS-5 and pBBR1MCS-2.

In *G. oxydans* the pBBR1MCS-2-based TetR-P_{tet} system performed much worse compared to the pBBR1MCS-5-based system despite the similarities of the two plasmids. With pBBR1MCS-2, the specific mNG fluorescence with induced P_{tet} was almost halved and reached 19.2 ± 9.7 a.u. ~ 10 h after induction at the end of the exponential phase of growth, while with pBBR1MCS-5 the maximal fluorescence peaked at 36.7 ± 2.2 a.u. after 8 h (Fig. 3a). Nevertheless, the maximal induction ratios were high with both pBBR1MCS-2 and pBBR1MCS-5 and were calculated to be 1915 ± 757 and 3674 ± 193, respectively. The basal expression under non-induced conditions was not affected by the plasmid backbone. Notably, a much higher standard deviation was obtained with pBBR1MCS-2. FACS analysis with gating of cells in regard to their volume and complexity by forward and side scattering (FSC and SSC) of light revealed that a major part of the *G. oxydans* cells with the pBBR1MCS-2 derivative and kanamycin exhibited a very different non-typical elongated cell morphology that was not observed with the pBBR1MCS-5 derivative and gentamicin (Fig. 3b). Approximately only 42% of the population with the pBBR1MCS-2 derivative passed the FACS gate where almost 100% of *G. oxydans* cells without plasmid or with the pBBR1MCS-5 derivative passed. This high heterogeneity of *G. oxydans* carrying the pBBR1MCS-2 derivative was not affected by the inducer ATc. The occurrence of a portion of elongated cells with pBBR1MCS-2 backbone and kanamycin was also demonstrated by fluorescence microscopy (Fig. S4). Several *G. oxydans* cells carrying pBBR1MCS-2 or pBBR1MCS-2-*tetR*-P_{tet}-*mNG*-T_{BBa_B1002}-T_{0028} appeared to be 10–15 µm and > 40 µm long, while the 621H reference cells typically were 2–3 µm. Apparently, the altered

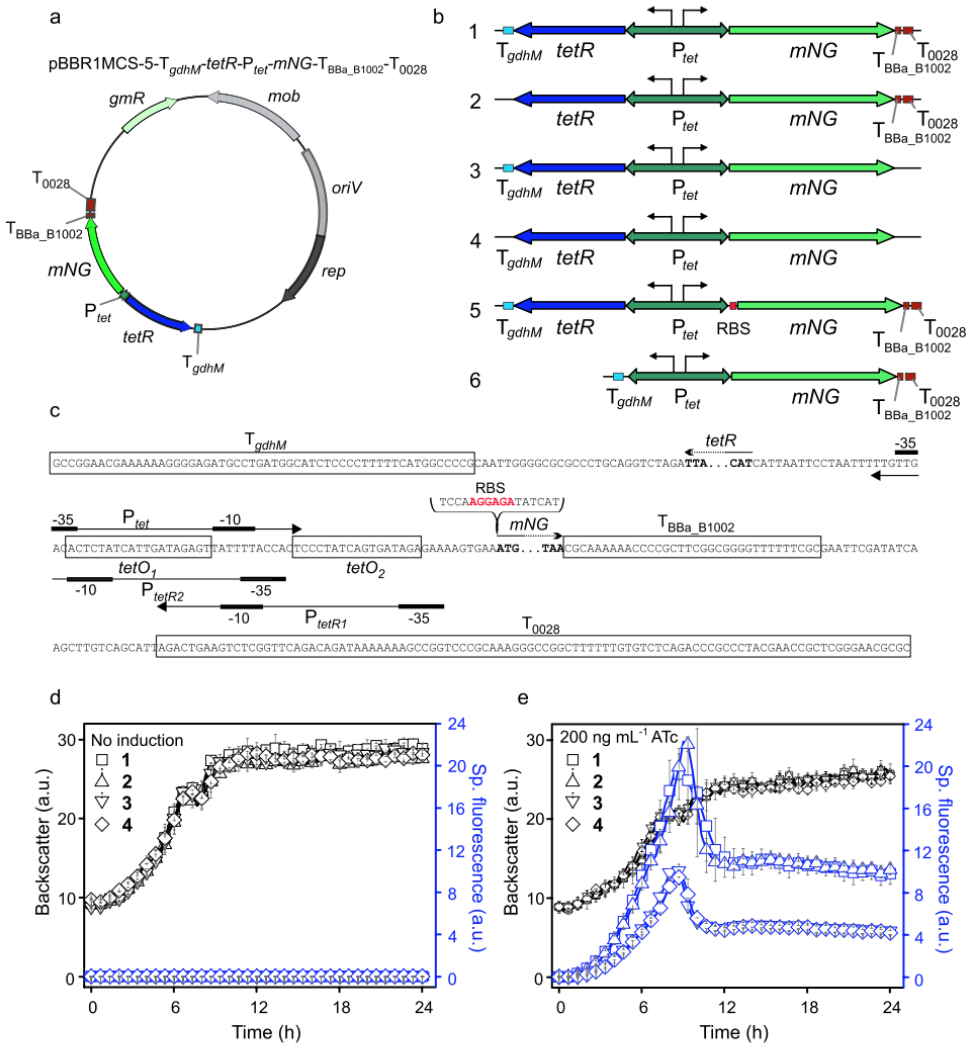

Fig. 2 Variants of pBBR1MCS-5-based expression plasmids with *tetR*-P_{tet} and reporter gene expression in *G. oxydans* 621H. **a** Map of plasmid pBBR1MCS-5-T_{gdhM}-*tetR*-P_{tet}-*mNG*-T_{BBa_B1002}-T_{0028} carrying the fluorescence reporter gene *mNeonGreen* (*mNG*) expressed from P_{tet} with the adjacent *tetR* gene and terminators T_{gdhM}, T_{BBa_B1002} and T_{0028}. **b** Variants of the plasmid insert with reporter gene *mNG* to test TetR-P_{tet}-dependent expression in the presence and absence of terminators downstream from *tetR* and *mNG*, with RBS AGGAGA (Hentschel et al. 2013) inserted in the 3' region of P_{tet} upstream from *mNG*, and without *tetR*. **c** DNA sequence details with P_{tet} region and TetR binding sites (*tetO1* and *tetO2*) and terminator sequences adjacent to *tetR* and *mNG*. **d** + **e**) Growth according to backscatter and specific mNG fluorescence in *G. oxydans* carrying either plasmid pBBR1MCS-5-T_{gdhM}-*tetR*-P_{tet}-*mNG*-T_{BBa_B1002}-T_{0028} (1), or the plasmid lacking T_{gdhM} (2) or T_{BBa_B1002}-T_{0028} (3) or all terminators (4) under non-induced (d) and ATc-induced (**e**) condition in microscale BioLector cultivations. For induction 200 ng mL^{-1} ATc was present in the D-mannitol medium. Data represent mean values and standard deviation from two biological replicates with three technical replicates each. T_{gdhM}: terminator sequence of *gdhM* (GOX0265); T_{0028}: terminator sequence of GOX0028. BioLector settings: backscatter gain 20, fluorescence gain 50

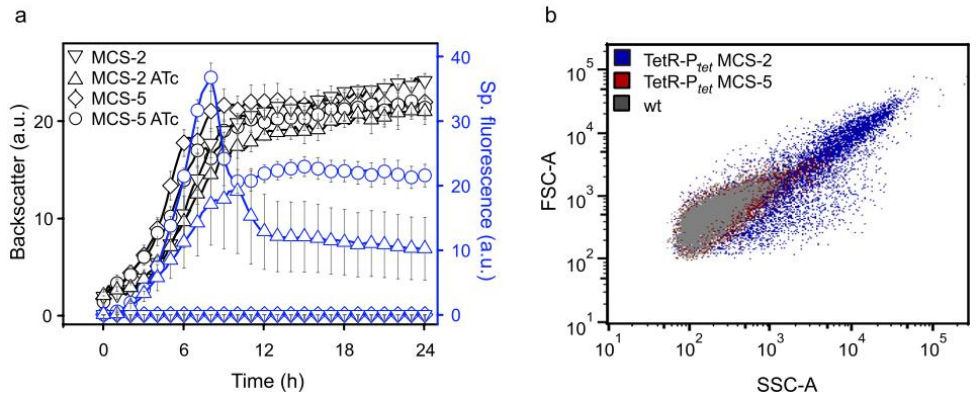

Fig. 3 Comparison of pBBR1MCS-5 and pBBR1MCS-2 with *tetR*-P_{tet}. **a** Growth according to backscatter (gain 15) and specific mNeonGreen (mNG) fluorescence (gain 50) in *G. oxydans* 621H carrying either plasmid pBBR1MCS-5-T_{gdhM}-*tetR*-P_{tet}-*mNG*-T_{BBa_B1002}-T_{0028} or pBBR1MCS-2-T_{gdhM}-*tetR*-P_{tet}-*mNG*-T_{BBa_B1002}-T_{0028} in microscale BioLector cultivations. For induction, always 200 ng mL^{-1} ATc was present in the D-mannitol medium. Data represent mean values and standard deviation from at least three biological replicates with three technical replicates each. **b** Cell morphology according to FACS analysis of *G. oxydans* 621H type strain (wt) without plasmid and with either the pBBR1MCS-5- or pBBR1MCS-2-based *tetR*-P_{tet} system, all without the inducer ATc

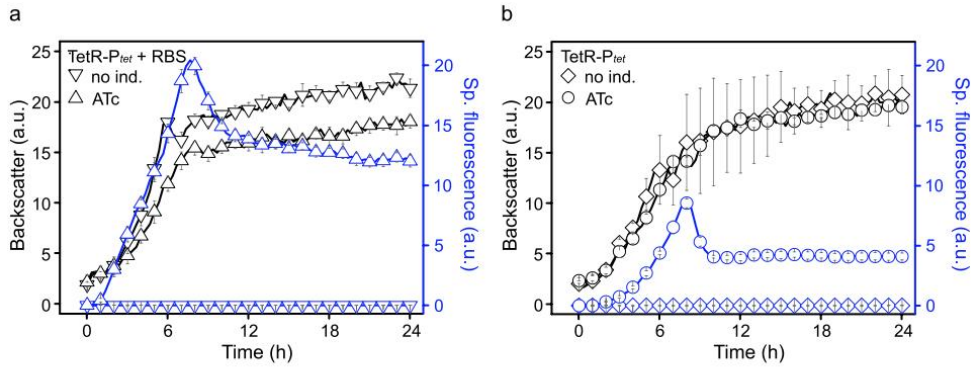

Fig. 4 Influence of the ribosome binding site AGGAGA on mNG reporter expression with the TetR-P_{tet} system. Growth according to backscatter and specific mNeonGreen (mNG) fluorescence in *G. oxydans* 621H carrying plasmid pBBR1MCS-5-T_{gdhM}-*tetR*-P_{tet}-RBS-*mNG*-T_{BBa_B1002}-T_{0028} with the RBS change (**a**) and with plasmid pBBR1MCS-5-T_{gdhM}-*tetR*-P_{tet}-*mNG*-T_{BBa_B1002}-T_{0028} as the control (**b**) in microscale BioLector cultivations. Cells were grown in D-mannitol medium without or with 200 ng mL^{-1} ATc for induction. Data represent mean values and standard deviation from two biological replicates with three technical replicates each. BioLector settings: backscatter gain 20, fluorescence gain 40

cell morphology had no direct effect on the inducibility of the TetR-P_{tet} system in *G. oxydans* as elongated cells also exhibited strong mNG fluorescence.

To test improved translation and thus resulting reporter protein levels in *G. oxydans*, we also constructed a plasmid with the RBS AGGAGA that we had also used in the *araC*-P_{araBAD} system and inserted it upstream from *mNG* and downstream from $tetO_2$ overlapping with the native RBS of the P_{tet} region (Fig. 2c). Thus, in this construct, RBS_{Ptet} and RBS_{AGGAGA} were consecutively upstream from *mNG*. The

impact on reporter expression and inducibility was measured in BioLector cultivations. Grown in D-mannitol medium and induced with 200 ng mL^{-1} ATc, the fluorescence signals of induced cells were further increased and reached > 4000-fold induction, yet at such a high level that the detector gain in the BioLector had to be set from 50 down to 40 to avoid signal saturation. For both constructs with gain 40 setting, the insertion of RBS_{AGGAGA} doubled up the specific fluorescence in induced cells from 8.6 ± 0.4 a.u. for the reference to 20.4 ± 0.5 a.u. (Fig. 4). The basal expression in the absence of ATc was again extremely low, and the calculated maximal induction ratio based on the specific fluorescence with gain 40 was increased from 855 ± 7 for the reference to 2042 ± 1 for the plasmid with RBS_{AGGAGA}.

pBBR1MCS-5-based LacI-P_{lacUV5} was leaking and therefore tunable only up to 40-fold

For the *lacI*-P_{lac} system, the insert containing *lacI* under control of its native promoter P_{lacI}, promoter P_{lacUV5} and *lacZα* was derived from *E. coli* BL21(DE3). The promotor P_{lacUV5} differs from the native *E. coli* P_{lac} promoter by three point mutations leading to enhanced activity and reduced cyclic adenosine monophosphate (cAMP)-dependency for induction in *E. coli* (Hirschel et al. 1980). Downstream from the P_{lacUV5}-controlled reporter gene *mNG*, the terminator T_{BBa_B1002} was placed and RBS_{AGGAGA} upstream from *mNG* (Fig. 5a, b). The *lacI*-P_{lac} system includes three different operator sites which typically are bound by LacI in the absence of an inducer molecule to repress P_{lac}-derived expression. Of these operator sites, O_1 is located in close proximity to the -10 region of P_{lac}, while O_3 and O_2 overlap with *lacI* and *lacZα*, respectively. In *E. coli* all three operator sites are bound by tetrameric LacI and are required for maximal repression (Oehler et al. 1990). Therefore, in order to enable full repression by LacI, the α-unit region of *lacZ* with O_2 was included in the insert.

We examined the inducibility of P_{lacUV5} by IPTG in *G. oxydans* 621H harboring the plasmid pBBR1MCS-5-P_{lacI}-*lacI*-P_{lacUV5}-RBS-*mNG*-T_{BBa_B1002}-T_{0028}. Cells were grown in shake flasks using D-mannitol medium supplemented with and without 1 mM IPTG. After 10 h at the end of the exponential growth phase, the highest fluorescence signal was measured. Due to the basal expression in the absence of IPTG, the maximal induction ratios by the absolute and by the specific fluorescence were calculated to be 18 ± 4 and 18 ± 5, respectively (Fig. 5c). When testing the inducibility of P_{lacUV5} in microscale BioLector cultivations, a similar trend was observed. Under induced conditions, the fluorescence peaked approximately 6 h after induction and subsequently slightly decreased in the stationary phase while in non-induced cultures a basal fluorescence was measured (Fig. 5d). Here, with 1 mM IPTG an average induction ratio of 41 ± 16 was calculated based on the specific fluorescence of the replicates in the BioLector. The P_{lacUV5}-derived mNG expression exhibited a tunability by IPTG concentrations ranging from 0.1 to 10 mM in *G. oxydans* (Fig. 5e). The *mNG* expression from P_{lacUV5} was gradually increased up to 3 mM IPTG. Above 3 mM IPTG, the *mNG* expression hardly increased further and thus appeared to be saturated and best-calculated induction ratios were again in the range of 40-fold. Illumina sequencing data obtained with total DNA purified from induced cells showed that 99.5% of the reads mapped to the updated reference sequences of the *G. oxydans* 621H genome, the 5 endogenous plasmids, and the mNG expression plasmid with *lacI* (Kranz et al. 2017). Thus, the sequencing results verified that the P_{lacUV5}-derived *mNG* expression was induced in *G. oxydans* carrying the intended plasmid pBBR1MCS-5-P_{lacI}-*lacI*-P_{lacUV5}-RBS-*mNG*-T_{BBa_B1002}-T_{0028}.

To analyze the induction of P_{lacUV5} in *G. oxydans* on the single cell level with regard to the homogeneity of *mNG* expression, flow cytometer analysis was applied (Fig. 5f). Within the chosen gate, 7 h after induction 95% of all induced cells exhibited high fluorescence (~ 11,000 a.u.) while under non-induced conditions in 96% of all cells, the fluorescence was at the somewhat leaky basal level (~ 1500 a.u.). This indicated that in the exponential growth phase, expression from induced P_{lacUV5} was very homogenous in *G. oxydans*. This was also supported by fluorescence microscopy (Fig. S5).

Similarly, as for TetR and P_{tet}, we tested experimentally if initially lower medium pH values could affect the leakiness of P_{lacUV5}. Therefore, *G. oxydans* carrying the plasmid pBBR1MCS-5-P_{lacI}-*lacI*-P_{lacUV5}-RBS-*mNG*-T_{BBa_B1002}-T_{0028} was grown in D-mannitol medium initially adjusted to pH 6, 5, 4, and 3 in the absence and presence of IPTG. After 23 h, cells were centrifuged and resuspended in fresh D-mannitol-free medium of pH 6 to check for potential pH-dependent recovery of mNG fluorescence above the respective levels monitored before that would indicate a higher leakiness of P_{lacUV5} together with a previous loss of mNG fluorescence already during growth (Fig. S3e-h). In all non-induced cultures, overall basal fluorescence signals up to 10 a.u. were measured with decreasing maxima in the exponential phase when the initial medium pH decreased. Again, cells grown in pH 3 exhibited the lowest signals and a different growth according to backscatter compared to all other cultures. Compared to the pH 6 condition, no sufficient increase of mNG fluorescence was observed in any non-induced pH condition (6 h) in the exponential growth phase to suggest a higher leakiness of P_{lacUV5}. Additionally, after the transfer (23 h) of the non-induced cells into fresh D-mannitol-free medium adjusted to pH 6 no recovery of mNG fluorescence above the levels with pH 6 could be observed in any condition. Interestingly, only for the non-induced pH 4 and pH 5

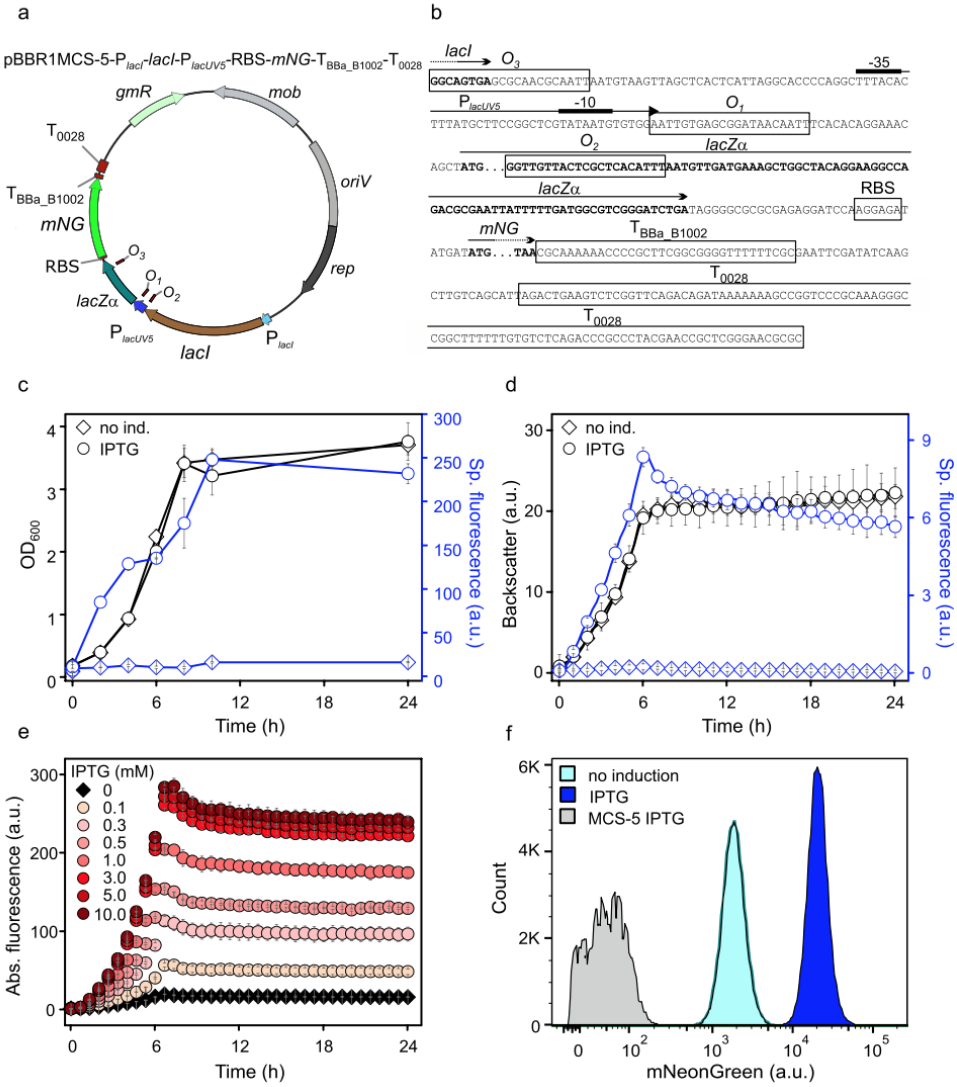

conditions, recovery of mNG fluorescence in pH 6 (24 h) above the respective maximal levels observed before in the exponential phase (6 h) were observed. This suggested that in the pH 4 and pH 5 conditions *G. oxydans* was not able to maintain its typical intracellular pH during growth and mNG fluorescence partially became inactive already in an early phase of growth (6 h).

◂**Fig. 5** pBBR1MCS-5-based expression plasmid with *lacI*-P_{lacUV5} and reporter gene expression in *G. oxydans* 621H. **a** Map of the pBBR1MCS-5-based *lacI*-P_{lacUV5} plasmid. **b** Sequence information details of the *lacI*-P_{lacUV5} plasmid. The promoter P_{lacUV5} comprises the LacI operator sites O_3, O_1, and O_2. The O_3 sites overlaps with the 3' end of *lacI*. The RBS AGGAGA was inserted upstream from *mNG*. The iGEM terminator sequence of BBa_B1002 was located downstream from *mNG* followed by terminator T_{0028} from GOX0028. **c** Shake flasks cultivations of *G. oxydans* 621H carrying plasmid pBBR1MCS-5-P_{lacI}-*lacI*-P_{lacUV5}-RBS-*mNG*-T_{BBa_B1002}-T_{0028} in IPTG-induced (1 mM) and non-induced condition. The mNG fluorescence was measured in a Tecan reader (gain 60. The specific fluorescence was calculated from absolute fluorescence per OD_{600}. **d** Microscale BioLector cultivations of *G. oxydans* 621H carrying plasmid pBBR1MCS-5-P_{lacI}-*lacI*-P_{lacUV5}-RBS-*mNG*-T_{BBa_B1002}-T_{0028} in IPTG-induced (1 mM) and non-induced condition. All data represent mean values and standard deviation from three biological replicates with three technical replicates each. Backscatter gain 15, fluorescence gain 60. **e** Microscale BioLector cultivations of *G. oxydans* 621H carrying plasmid pBBR1MCS-5-P_{lacI}-*lacI*-P_{lacUV5}-RBS-*mNG*-T_{BBa_B1002}-T_{0028} with increasing concentrations of IPTG as indicated. Fluorescence gain 60. **f** FACS analysis of *G. oxydans* 621H carrying plasmid pBBR1MCS-5-P_{lacI}-*lacI*-P_{lacUV5}-RBS-*mNG*-T_{BBa_B1002}-T_{0028}. Cells were grown in shake flasks with D-mannitol medium and 1 mM IPTG. FACS analysis was performed 7 h after inoculation and induction. Total counts per sample represent 100.000 events. As a control *G. oxydans* 621H carrying the empty vector pBBR1MCS-5 was used (MCS-5)

Strength of P_{lacUV5} was P_{lacI}-lacI-dependent and leaking was independent of read-through

Unlike most operons, in the *E. coli lac* operon, the regulatory gene *lacI* is located immediately upstream from the target operon and is transcribed in the same direction. The repressor LacI forms tetramers binding in the absence of an inducer to up to three operator sites, thereby preventing transcription from the *lac* promoter directly downstream from *lacI*. Nevertheless, despite LacI binding and the presence of a *lacI* terminator region coinciding with the LacI operator site O_1 directly downstream from the − 10 region, read-through is possible varying from 10 up to 80% (Horowitz and Platt 1982; Oehler et al. 1990). To check the possibility of read-through from P_{lacI} causing the leakiness observed in *G. oxydans* and interference by endogenous proteins on the P_{lacUV5} inducibility, we wanted to check and compare the pBBR1MCS-5-based reporter expression in the absence of P_{lacI}-*lacI*, as well as with P_{lacI}-*lacI* in opposite orientation toward P_{lacUV5}.

Firstly, we constructed the plasmid pBBR1MCS-5-P_{lacUV5}-RBS-*mNG*-T_{BBa_B1002}-T_{0028} lacking P_{lacI} and most of the *lacI* gene, while keeping a short 3' region of *lacI* to maintain all three operator sites of P_{lacUV5} including O_3 partly overlapping with the end of the *lacI* gene. The analysis of the IPTG-dependent inducibility of P_{lacUV5} in *G. oxydans* in the absence of P_{lacI}-*lacI* revealed no difference in fluorescence signals supplemented with IPTG or not (Fig. S6). This indicated that the inducibility observed in *G. oxydans* solely depended on derepression by LacI. Interestingly, compared to the original system with P_{lacI}-*lacI*, the maximal reporter expression from P_{lacUV5} was strongly reduced from 8.4 ± 0.4 to 2.3 ± 0.2 according to the specific fluorescence (6–7 h) when P_{lacI}-*lacI* was lacking. This suggested that a significant read-through from P_{lacI} appeared to contribute to the expression of the gene downstream from P_{lacUV5}, thus increasing the apparent P_{lacUV5} strength in *G. oxydans* almost fourfold when induced.

Secondly, we constructed plasmid pBBR1MCS-5-*lacI*-P_{lacI}-P_{lacUV5}-RBS-*mNG*-T_{BBa_B1002}-T_{0028} with P_{lacI}-*lacI* in opposite direction to exclude potential read-through toward P_{lacUV5}-mNG. Despite the opposite directions of P_{lacI} and P_{lacUV5}, an even somewhat higher leakiness of P_{lacUV5} was observed when not induced (Fig. S7). Therefore, with 1 mM IPTG the maximal induction fold-change (6.4 h) calculated was only 15.4 ± 0.9 based on the specific fluorescence, while the original P_{lacI}-*lacI*-P_{lacUV5} construct reached a maximal induction fold-change (6.7 h) of 39.7 ± 13.9. Surprisingly, the apparent induced P_{lacUV5} strength was restored according to the reporter fluorescence and reached the same levels as when P_{lacI}-*lacI* were in the same direction as P_{lacUV5}. Together, the results indicated that in *G. oxydans* the promoter strength of plasmid-based P_{lacUV5} appeared to depend on sequences further upstream and that the P_{lacUV5} leakiness was independent of potential read-through from P_{lacI}.

Modeling LacI and TetR binding to DNA at acidic pH values

Our results suggested that the leakiness of P_{lacUV5} in *G. oxydans* was independent of potential read-through from P_{lacI} and thus should result from transcription initiation from P_{lacUV5} and insufficient repression by LacI. Since the cytoplasmic pH of *G. oxydans* may readily be acidified to some extent already during growth when medium pH decreases, we modeled LacI- and TetR-DNA structures at different pH values using YASARA to predict if and how a potentially lower cytoplasmic hydrogen ion activity might affect the binding of LacI and TetR to DNA (Krieger et al. 2002). As a control, the AraC structure was also modeled since an L-arabinose-inducible AraC-P_{araBAD} system was shown to be fully functional in *G. oxydans* with plasmid pBBR1MSC-5, yet was very leaky in *Gluconacetobacter* and *Komagataeibacter* using another expression plasmid (Fricke et al. 2020; Teh et al. 2019). Protein-DNA bindings were simulated in two different steps for pH 7, 6, 5, and 4 (see supplementary Text S1 and S2).

Analysis of the HADDOCK simulations in different pH conditions showed that the HADDOCK scores of all five best-scoring clusters obtained in the TetR-DNA docking simulation for pH 7, 6, 5, and 4 lie within the standard

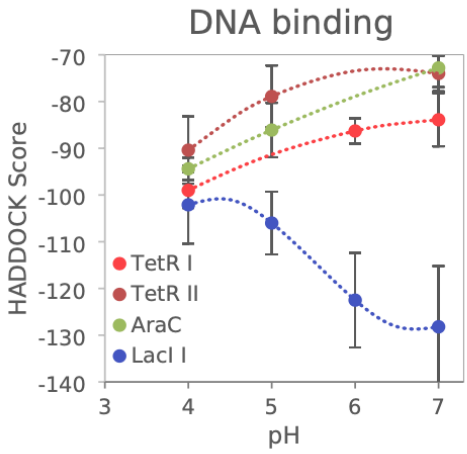

Fig. 6 Prediction of DNA-binding behavior of LacI, TetR, and AraC at different pH values computed by the HADDOCK web server. Each data point corresponds to a cluster of docking poses. The lower (more negative) the HADDOCK score the energetically more favorable the docking pose. Trend lines plotted are based on clusters containing similar docking poses. For details see supplementary Text S1 and Text S2

deviation of each other. To make a prediction of the DNA binding behavior in dependence of the pH value, similar docking positions were identified for each pH value and the cluster scores were compared. It can be observed that with decreasing pH values the scores decrease. The smaller the score, i.e., the more negative, the better is the predicted binding to DNA, suggesting an increased binding of TetR to DNA (Fig. 6). Similar results were obtained for AraC. Thus, when comparing the scores of clusters with corresponding docking positions, the values generally decreased with decreasing pH values, suggesting a generally increased binding to DNA for both TetR and AraC (Fig. 6). On the contrary, for LacI unique clusters with correlating docking poses identified for pH 7, 6, 5, and 4 exhibited increasing HADDOCK scores for decreasing pH values, suggesting a decreased DNA binding of LacI when pH decreases (Fig. 6 and Supplementary Text S1 and S2).

Discussion

In this study, we found with a pBBR1MCS-5-based TetR-P_{tet} system that inducible target gene expression based solely on de-repression of the heterologous target promoter can also perform extremely well in *G. oxydans*. With the pBBR1MCS-5-based plasmid constructed here, the anhydrotetracycline (ATc)-inducible promoter P_{tet} derived from the *E. coli* transposon Tn*10* exhibited excellently tunable expression performance in an inducer concentration-dependent manner with maximal induction ratios up to more than 3500-fold. This was due to extremely low basal reporter expression in the absence of an inducer, thus well repressed P_{tet}, and P_{tet} being very strong in *G. oxydans*.

In contrast, expression from P_{lacUV5} was always leaky when not induced and this appeared to be independent of potential read-through from P_{lacI} which was located with *lacI* immediately upstream from P_{lacUV5} and, unlike most regulator genes and target operons, coupled very close and transcribed in the same direction. Therefore, the transcription termination by the native *lacI* terminator is expected to be very effective in *G. oxydans* and the P_{lacUV5} leakiness is rather related to the early events after transcription initiation from P_{lacUV5}. In *E. coli*, the LacI repressor is not preventing *per se* the binding of RNA polymerase (RNAP), but is blocking the progress of RNAP which has bound to the DNA and has begun transcribing (Reznikoff et al. 1969). Transcription through roadblocks has been shown to depend on the cooperation of the leading and trailing RNAP molecules and thus depends on how many RNAP molecules are allowed to initiate from the same promoter upstream from the roadblock (Epshtein et al. 2003; Hao et al. 2014). In the case of P_{lac} or P_{lacUV5}, the distance from the transcriptional start (TSS) to the LacI binding site O_2 is rather short and site O_1 is even overlapping with the TSS; thus, only one RNAP molecule is expected to initiate upstream from the roadblock. Additionally, the *E. coli* σ^{70} subunit of RNAP mediates a pause at the *lac* promoter closely downstream from the transcriptional start which is proposed to function in limiting the downstream gene expression (Nickels et al. 2004). If the *G. oxydans* σ^{70} subunit of RNAP also mediates this pause at the *lac* promoter is unknown. Nevertheless, RNAP cooperation should not be possible and thus not contribute to the leakiness of P_{lacUV5} in *G. oxydans*, yet the extent of read-through can also be affected by accessory factors. For example, in *E. coli* GreA and GreB rescue backtracked (roadblocked) RNAP by cleavage of the RNA, regenerating a new 3' end at the catalytic site, and can aid passage of RNAP through a LacI roadblock in cells (Toulme et al. 2000). Furthermore, in *E. coli* the transcription-coupled repair protein Mfd binds to the DNA behind RNAP and uses ATP to push backtracked RNAP forward until the 3' end of RNA is back at the catalytic center, yet the forces generated by Mfd may also result in RNAP termination (Park et al. 2002). *E. coli* GreA (158 aa, b3181) and *G. oxydans* GreA (157 aa, GOX0324) share 54% sequence identity, *E. coli* GreB (158 aa, b3406) and *G. oxydans* GreB (168 aa, GOX1860) share 47%, and *E. coli* Mfd (1148 aa, b1114) and *G. oxydans* Mfd (1173 aa, GOX0055) share 39%. It is unknown how these factors support roadblocked RNAP and

read-through behind roadblocks in *G. oxydans* and AAB in general, yet the leakiness of P_{lac} or P_{lacUV5} is likely rather related to weaker binding of LacI to operator DNA and thus weaker promoter repression in *G. oxydans*.

Our docking simulations predicted that below pH 6 the binding of LacI to DNA is decreased which could cause or contribute to promoter leakiness. Neutralophilic bacteria maintain an intracellular pH between 7 and 8, while in acidophilic bacteria intracellular pH is considered to be maintained between 6 and 7 (Baker-Austin and Dopson 2007; Krulwich et al. 2011). The mannitol LB medium typically used for *G. oxydans* is initially set to pH 6 and can be acidified during growth in dependence of the carbon and energy sources, for example, to approximately pH 4.5 or 3.3 as well (Fricke et al. 2020). In such acidic pH conditions of the growth medium strongly decreased, intracellular fluorescence reporter activities of mNeonGreen (mNG) were observed in *G. oxydans* in the stationary phase (Fricke et al. 2020). Studies with isolated mNG revealed a strong decrease in fluorescence at pH 4.4 and below (Steiert et al. 2018). Therefore, the decrease in mNG fluorescence in *G. oxydans* cells was attributed to an acidified intracellular pH, at least in the stationary phase. The loss in mNG fluorescence in stationary *G. oxydans* cells can quickly be restored without protein synthesis just by short incubation in pH 6 condition as shown in this study and before (Fricke et al. 2020). Moreover, for the AAB *Acetobacter aceti*, the intracellular pH was reported to change from 5.8 to 3.9 already during growth when the medium pH acidified from 6.2 to 3.5 (Menzel and Gottschalk 1985). Despite intracellular pH maintenance mechanisms, it is conceivable that depending on the growth conditions in some or many AAB the cytoplasmic pH can decrease already during growth below the range of pH 6 to 7 considered to be typically maintained in acidophilic bacteria. According to our data, the mNG reporter fluorescence in *G. oxydans* cells with LacI-P_{lacUV5} grown in non-induced pH 4 and pH 5 conditions suggested that *G. oxydans* was not able to maintain its typical intracellular pH during growth and the mNG fluorescence became partially inactive already in the middle phase of growth (6 h). To get LacI-dependent systems tight and suitable for use in *G. oxydans* or AAB in general, the LacI protein may require engineering for increased binding to DNA in acidic pH condition. However, more intracellular pH data of AAB strains in various growth conditions are required. Besides leakiness, in *G. oxydans*, the strength of fully induced P_{lacUV5} was much lower compared to that of the fully induced P_{tet} (compare absolute fluorescence Fig. S3d and S3h). It was already reported before that P_{lac} is rather weak in *G. oxydans* 621H and the P_{lacUV5} mutant promoter exhibiting three base pair changes including two changes at positions − 9 and − 8 apparently also exhibits a similar low expression strength in *G. oxydans* (Hirschel et al. 1980; Kallnik et al. 2010). Thus, in *G. oxydans* the TetR-P_{tet} system will probably always be the choice for applications because of its extremely low basal expression and very high dynamic range of the tunable expression strength from P_{tet}.

Interestingly, in *K. rhaeticus* iGEM, the TetR-P_{tet} system tested exhibited high leakiness in the absence of the inducer (Florea et al. 2016). In *G. oxydans*, we could neither observe nor demonstrate relevant leakiness of TetR-P_{tet}, not with the pBBR1MCS-5-based construct variants (± terminators), not with the pBBR1MCS-2 backbone and kanamycin causing abnormal cell morphology, and not in the media of the pH series. Without terminators downstream from *mNG*, the length of the *mNG* transcript is assumed to exhibit an extended 3' UTR. This appeared to only decrease transcript stability or translation, since the mNG signals were reduced to half, yet repression of P_{tet} was not affected. For the *tetR* transcript, it is unknown how stability and translation are affected in *G. oxydans* when the 3' UTR is longer or shorter, yet altered repression of P_{tet} was also not observed with either of the constructs. A major difference of the two *tetR*-P_{tet} constructs tested in *K. rhaeticus* iGEM and in *G. oxydans* is that we maintained the opposite orientation of *tetR*-P_{tetR} and P_{tet} as originally present on Tn*10*, while in *K. rhaeticus* iGEM the construct tested contained the promoter J23118 or P_{lacI} for expression of *tetR* followed by a terminator sequence and all directly upstream from the target promoter P_{tet} and in the same direction as P_{tet} (Florea et al. 2016). It was assumed that the terminator is effective, yet it seemed to be unknown to what extend the terminator allowed potential read-through in these constructs. This could possibly cause the high leakiness of P_{tet} in *K. rhaeticus* iGEM, especially when cooperative RNAP molecules read through the TetR roadblock. On the other hand, our computational simulation also predicted that with decreasing pH value TetR dimerization decreases (Text S1 and Text S2). That could finally affect binding to DNA and thus promoter repression since TetR binds as a dimer (Hillen and Berens 1994). Thus, if the prediction holds true, in *G. oxydans* TetR dimerization is not sufficiently negatively affected by mild acidic intracellular pH. *Komagataeibacter* is typically grown in Hestrin – Schramm (HS) medium with glucose or in LGI medium with sucrose, both initially set to pH 6 or pH 4.5 and acidified further during growth (Florea et al. 2016; Hestrin and Schramm 1954). The intracellular pH of *A. aceti* was reported to change from 5.8 to 3.9 already during growth when the medium pH acidified from 6.2 to 3.5 (Menzel and Gottschalk 1985). The extent of being able to maintain the intracellular pH not only in the stationary phase but also during exponential growth could differ between AAB species. This could possibly be seen in the results with the LuxR-P_{lux} system in *Komagataeibacter* (Florea et al. 2016). The system exhibited condition-dependent induction only up to fivefold due to high leakiness, yet it also exhibited extremely low

leakiness and much better induction performance according to fluorescence microscopic analysis in cells inside cellulose pellicles. Cellulose pellicles generate a micro-environment with the advantage of potentially protecting the cells from harsh conditions which could also include protection from acidic environmental pH. Again, to better understand the pH-dependent binding of regulators to DNA and to improve the expression performance of heterologous regulatable expressions systems so far leaky in AAB and their growth conditions, more intracellular pH data of AAB strains are required for various growth conditions. Additionally, experimental pH-dependent protein–protein and protein-DNA interaction data are needed.

In summary, we could show that in *G. oxydans* the TetR-P_{tet} system tested was extremely well performing with the pBBR1MCS-5 backbone and exhibited very strong reporter expression when induced, while the LacI-P_{lacUV5} system was always leaking and thus resulting in much lower induction ratios. Therefore, the pBBR1MCS-5-based TetR-P_{tet} system with the low inducer concentrations required for gradually tuning target gene expression appeared to be highly suitable for applications in *G. oxydans* and possibly in other AAB.

Supplementary Information The online version contains supplementary material available at https://doi.org/10.1007/s00253-021-11473-x.

Acknowledgements The authors are grateful to Uwe Deppenmeier for the kind gift of plasmid pBBR1-tetall-strep_long. The authors also thank Astrid Bida and Ulrike Viets for the technical assistance with the Illumina sequencing.

Author contribution PMF constructed the plasmids, carried out the growth experiments, and analyzed the data. PMF and CS performed the FACS analysis and analyzed the data. PMF and MH obtained the microscopic images. ML and MDD conducted the computational simulations. TP designed and supervised the study. PMF, ML, MDD, MB, and TP wrote and revised the manuscript. All authors read and approved the final version.

Funding Open Access funding enabled and organized by Projekt DEAL. We are grateful to the Federal Ministry of Education and Research (BMBF) for the generous financial support of the project IMPRES (031B0370B). The funding organization did not influence the design of the study or collection, analysis, and interpretation of data, or writing the manuscript.

Data availability Data and material are available upon request.

Declarations

Ethical statement This article does not contain any studies with human participants or animals performed by any of the authors.

Conflict of interest The authors declare no competing interests.

References

Altschul SF, Madden TL, Schaffer AA, Zhang JH, Zhang Z, Miller W, Lipman DJ (1997) Gapped BLAST and PSI-BLAST: a new generation of protein database search programs. Nucleic Acids Res 25(17):3389–3402. https://doi.org/10.1093/nar/25.17.3389

Ameyama M, Shinagawa E, Matsushita K, Adachi O (1981) D-fructose dehydrogenase of *Gluconobacter industrius*: purification, characterization, and application to enzymatic microdetermination of D-fructose. J Bacteriol 145(2):814–823

Baker-Austin C, Dopson M (2007) Life in acid: pH homeostasis in acidophiles. Trends Microbiol 15(4):165–171. https://doi.org/10.1016/j.tim.2007.02.005

Bell CE, Lewis M (2000) A closer view of the conformation of the Lac repressor bound to operator. Nat Struct Biol 7(3):209–214

Condon C, Fitzgerald RJ, Ogara F (1991) Conjugation and heterologous gene expression in *Gluconobacter oxydans* ssp *suboxydans*. FEMS Microbiol Lett 80(2–3):173–178. https://doi.org/10.1016/0378-1097(91)90590-7

Eisenberg D, Luthy R, Bowie JU (1997) VERIFY3D: Assessment of protein models with three-dimensional profiles. Method Enzymol 277:396–404. https://doi.org/10.1016/S0076-6879(97)77022-8

Epshtein V, Toulme F, Rahmouni AR, Borukhov S, Nudler E (2003) Transcription through the roadblocks: the role of RNA polymerase cooperation. EMBO J 22(18):4719–4727. https://doi.org/10.1093/emboj/cdg452

Florea M, Hagemann H, Santosa G, Abbott J, Micklem CN, Spencer-Milnes X, Garcia LD, Paschou D, Lazenbatt C, Kong DZ, Chughtai H, Jensen K, Freemont PS, Kitney R, Reeve B, Ellis T (2016) Engineering control of bacterial cellulose production using a genetic toolkit and a new cellulose-producing strain. P Natl Acad Sci USA 113(24):E3431–E3440. https://doi.org/10.1073/pnas.1522985113

Fricke PM, Link T, Gätgens J, Sonntag C, Otto M, Bott M, Polen T (2020) A tunable L-arabinose-inducible expression plasmid for the acetic acid bacterium *Gluconobacter oxydans*. Appl Microbiol Biotechnol 104(21):9267–9282. https://doi.org/10.1007/s00253-020-10905-4

Fricke PM, Klemm A, Bott M, Polen T (2021) On the way toward regulatable expression systems in acetic acid bacteria: target gene expression and use cases. Appl Microbiol Biotechnol 105(9):3423–3456. https://doi.org/10.1007/s00253-021-11269-z

Gibson DG, Young L, Chuang RY, Venter JC, Hutchison CA, Smith HO (2009) Enzymatic assembly of DNA molecules up to several hundred kilobases. Nat Methods 6(5):343-U41. https://doi.org/10.1038/Nmeth.1318

Gupta A, Singh VK, Qazi GN, Kumar A (2001) *Gluconobacter oxydans*: its biotechnological applications. J Mol Microb Biotech 3(3):445–56

Hanahan D (1983) Studies on transformation of *Escherichia coli* with plasmids. J Mol Biol 166(4):557–80

Hanwell MD, Curtis DE, Lonie DC, Vandermeersch T, Zurek E, Hutchison GR (2012) Avogadro: an advanced semantic chemical

editor, visualization, and analysis platform. J Cheminformatics 4.https://doi.org/10.1186/1758-2946-4-17

Hao N, Krishna S, Ahlgren-Berg A, Cutts EE, Shearwin KE, Dodd IB (2014) Road rules for traffic on DNA - systematic analysis of transcriptional roadblocking in vivo. Nucleic Acids Res 42(14):8861–8872. https://doi.org/10.1093/nar/gku627

Hekmat D, Bauer R, Fricke J (2003) Optimization of the microbial synthesis of dihydroxyacetone from glycerol with *Gluconobacter oxydans*. Bioproc Biosyst Eng 26(2):109–16. https://doi.org/10.1007/s00449-003-0338-9

Hentschel E, Will C, Mustafi N, Burkovski A, Rehm N, Frunzke J (2013) Destabilized eYFP variants for dynamic gene expression studies in *Corynebacterium glutamicum*. Microb Biotechnol 6(2):196–201. https://doi.org/10.1111/j.1751-7915.2012.00360.x

Hestrin S, Schramm M (1954) Synthesis of cellulose by *Acetobacter xylinum*. II. Preparation of freeze-dried cells capable of polymerizing glucose to cellulose. Biochem J 58(2):345–52. https://doi.org/10.1042/bj0580345

Hillen W, Berens C (1994) Mechanisms underlying expression of Tn*10*-encoded tetracycline resistance. Annu Rev Microbiol 48:345–369. https://doi.org/10.1146/annurev.mi.48.100194.002021

Hillen W, Gatz C, Altschmied L, Schollmeier K, Meier I (1983) Control of expression of the Tn*10*-encoded tetracycline resistance genes - equilibrium and kinetic investigation of the regulatory reactions. J Mol Biol 169(3):707–721. https://doi.org/10.1016/S0022-2836(83)80166-1

Hirschel BJ, Shen V, Schlessinger D (1980) Lactose operon transcription from wild-type and L8-Uv5 *lac* promoters in *Escherichia coli* treated with chloramphenicol. J Bacteriol 143(3):1534–1537. https://doi.org/10.1128/Jb.143.3.1534-1537.1980

Horowitz H, Platt T (1982) A termination site for *lacI* transcription is between the CAP site and the *lac* promoter. J Biol Chem 257(19):11740–6

Jones DT (1999) Protein secondary structure prediction based on position-specific scoring matrices. J Mol Biol 292(2):195–202. https://doi.org/10.1006/jmbi.1999.3091

Kallnik V, Meyer M, Deppenmeier U, Schweiger P (2010) Construction of expression vectors for protein production in *Gluconobacter oxydans*. J Biotechnol 150(4):460–465. https://doi.org/10.1016/j.jbiotec.2010.10.069

Khoury AM, Nick HS, Lu P (1991) *In vivo* interaction of *Escherichia coli lac* repressor N-terminal fragments with the *lac* operator. J Mol Biol 219(4):623–34. https://doi.org/10.1016/0022-2836(91)90659-t

Kiefler I, Bringer S, Bott M (2017) Metabolic engineering of *Gluconobacter oxydans* 621H for increased biomass yield. Appl Microbiol Biotechnol 101(13):5453–5467. https://doi.org/10.1007/s00253-017-8308-3

Kortmann M, Kuhl V, Klaffl S, Bott M (2015) A chromosomally encoded T7 RNA polymerase-dependent gene expression system for *Corynebacterium glutamicum*: construction and comparative evaluation at the single-cell level. Microb Biotechnol 8(2):253–65. https://doi.org/10.1111/1751-7915.12236

Kovach ME, Elzer PH, Hill DS, Robertson GT, Farris MA, Roop RM 2nd, Peterson KM (1995) Four new derivatives of the broad-host-range cloning vector pBBR1MCS, carrying different antibiotic-resistance cassettes. Gene 166(1):175–6. https://doi.org/10.1016/0378-1119(95)00584-1

Kranz A, Vogel A, Degner U, Kiefler I, Bott M, Usadel B, Polen T (2017) High precision genome sequencing of engineered *Gluconobacter oxydans* 621H by combining long nanopore and short accurate Illumina reads. J Biotechnol 258:197–205. https://doi.org/10.1016/j.jbiotec.2017.04.016

Krieger E, Koraimann G, Vriend G (2002) Increasing the precision of comparative models with YASARA NOVA - a self-parameterizing force field. Proteins 47(3):393–402. https://doi.org/10.1002/prot.10104

Krulwich TA, Sachs G, Padan E (2011) Molecular aspects of bacterial pH sensing and homeostasis. Nat Rev Microbiol 9(5):330–43. https://doi.org/10.1038/nrmicro2549

Liu LP, Yang X, Zhao XJ, Zhang KY, Li WC, Xie YY, Jia SR, Zhong C (2020) A lambda Red and FLP/FRT-mediated site-specific recombination system in *Komagataeibacter xylinus* and its application to enhance the productivity of bacterial cellulose. ACS Synth Biol 9(11):3171–3180. https://doi.org/10.1021/acssynbio.0c00450

Mamlouk D, Gullo M (2013) Acetic Acid bacteria: physiology and carbon sources oxidation. Indian J Microbiol 53(4):377–84. https://doi.org/10.1007/s12088-013-0414-z

Menzel U, Gottschalk G (1985) The internal pH of *Acetobacterium wieringae* and *Acetobacter aceti* during growth and production of acetic acid. Arch Microbiol 143(1):47–51. https://doi.org/10.1007/Bf00414767

Mientus M, Kostner D, Peters B, Liebl W, Ehrenreich A (2017) Characterization of membrane-bound dehydrogenases of *Gluconobacter oxydans* 621H using a new system for their functional expression. Appl Microbiol Biotechnol 101(8):3189–3200. https://doi.org/10.1007/s00253-016-8069-4

Miller JH (1970). In: Beckwith JR, Zipser D (eds) The Lactose Operon. Cold Spring Harbor Laboratory Press, Cold Spring Harbor, pp 173–188

Nickels BE, Mukhopadhyay J, Garrity SJ, Ebright RH, Hochschild A (2004) The s^{70} subunit of RNA polymerase mediates a promoter-proximal pause at the *lac* promoter. Nat Struct Mol Biol 11(6):544–550. https://doi.org/10.1038/nsmb757

Oehler S, Eismann ER, Kramer H, Muller-Hill B (1990) The three operators of the *lac* operon cooperate in repression. EMBO J 9(4):973–9

Olsson MHM, Sondergaard CR, Rostkowski M, Jensen JH (2011) PROPKA3: consistent treatment of internal and surface residues in empirical pK(a) predictions. J Chem Theory Comput 7(2):525–537. https://doi.org/10.1021/ct100578z

Pappenberger G, Hohmann HP (2014) Industrial production of L-ascorbic Acid (vitamin C) and D-isoascorbic acid. Adv Biochem Eng Biotechnol 143:143–88. https://doi.org/10.1007/10_2013_243

Park JS, Marr MT, Roberts JW (2002) *E. coli* transcription repair coupling factor (Mfd protein) rescues arrested complexes by promoting forward translocation. Cell 109(6):757–767. https://doi.org/10.1016/S0092-8674(02)00769-9

Qiu J, Elber R (2006) SSALN: an alignment algorithm using structure-dependent substitution matrices and gap penalties learned from structurally aligned protein pairs. Proteins 62(4):881–891. https://doi.org/10.1002/prot.20854

Reznikoff WS, Miller JH, Scaife JG, Beckwith JR (1969) A mechanism for repressor action. J Mol Biol 43(1):201. https://doi.org/10.1016/0022-2836(69)90089-8

Saito Y, Ishii Y, Hayashi H, Imao Y, Akashi T, Yoshikawa K, Noguchi Y, Soeda S, Yoshida M, Niwa M, Hosoda J, Shimomura K (1997) Cloning of genes coding for L-sorbose and L-sorbosone dehydrogenases from Gluconobacter oxydans and microbial production of 2-keto-L-gulonate, a precursor of L-ascorbic acid, in a recombinant G oxydans strain. Appl Environ Microb 63(2):454–60

Sambrook J, Fritsch EF, Maniatis T (1989) Molecular cloning: a laboratory manual. Cold Spring Harbor Laboratory Press, Cold Spring Harbor

Schleif R (2010) AraC protein, regulation of the L-arabinose operon in *Escherichia coli*, and the light switch mechanism of AraC action. FEMS Microbiol Rev 34(5):779–96. https://doi.org/10.1111/j.1574-6976.2010.00226.x

Sellitti MA, Pavco PA, Steege DA (1987) *lac* repressor blocks in vivo transcription of *lac* control region DNA. P Natl Acad Sci USA 84(10):3199–203. https://doi.org/10.1073/pnas.84.10.3199

Shaner NC, Lambert GG, Chammas A, Ni Y, Cranfill PJ, Baird MA, Sell BR, Allen JR, Day RN, Israelsson M, Davidson MW, Wang J (2013) A bright monomeric green fluorescent protein derived from

Branchiostoma lanceolatum. Nat Methods 10(5):407–9. https://doi.org/10.1038/nmeth.2413

Simon R, Priefer U, Pühler A (1983) A broad host range mobilization system for in vivo genetic-engineering - transposon mutagenesis in Gram-negative bacteria. Bio-Technol 1(9):784–791. https://doi.org/10.1038/nbt1183-784

Sippl MJ (1993) Recognition of errors in 3-dimensional structures of proteins. Proteins 17(4):355–362. https://doi.org/10.1002/prot.340170404

Steiert F, Petrov EP, Schultz P, Schwille P, Weidemann T (2018) Photophysical behavior of mNeonGreen, an evolutionarily distant green fluorescent protein. Biophys J 114(10):2419–2431. https://doi.org/10.1016/j.bpj.2018.04.013

Stenberg KAE, Vihinen M (2009) Crystal structure of a 1,6-hexanediol bound tetrameric form of Escherichia coli lac-repressor refined to 2.1 Å resolution. Proteins 75(3):748–759. https://doi.org/10.1002/prot.22284

Teh MY, Ooi KH, Teo SXD, Bin Mansoor ME, Lim WZS, Tan MH (2019) An expanded synthetic biology toolkit for gene expression control in *Acetobacteraceae*. ACS Synth Biol 8(4):708–723. https://doi.org/10.1021/j.acssynbio.8b00168

Tkac J, Navratil M, Sturdik E, Gemeiner P (2001) Monitoring of dihydroxyacetone production during oxidation of glycerol by immobilized *Gluconobacter oxydans* cells with an enzyme biosensor. Enzyme Microb Tech 28(4–5):383–388

Toulme F, Mosrin-Hauman C, Sparkowski J, Das A, Leng M, Rahmouni AR (2000) GreA and GreB proteins revive backtracked RNA polymerase in vivo by promoting transcript trimming. EMBO J 19(24):6853–6859. https://doi.org/10.1093/emboj/19.24.6853

van Zundert GCP, Rodrigues J, Trellet M, Schmitz C, Kastritis PL, Karaca E, Melquiond ASJ, van Dijk M, de Vries SJ, Bonvin A (2016) The HADDOCK2.2 web server: User-friendly integrative modeling of biomolecular complexes. J Mol Biol 428(4):720–725. https://doi.org/10.1016/j.jmb.2015.09.014

Wang EX, Ding MZ, Ma Q, Dong XT, Yuan YJ (2016) Reorganization of a synthetic microbial consortium for one-step vitamin C fermentation. Microb Cell Fact 15:21. https://doi.org/10.1186/s12934-016-0418-6

Wray LV Jr, Reznikoff WS (1983) Identification of repressor binding sites controlling expression of tetracycline resistance encoded by Tn*10*. J Bacteriol 156(3):1188–91. https://doi.org/10.1128/JB.156.3.1188-1191.1983

2.3 The L-rhamnose-dependent regulator RhaS and its target promoters expand the toolkit for regulatable gene expression in the acetic acid bacterium *Gluconobacter oxydans*

Fricke P.M., Gries M., Mürköster M., Sonntag C., Gätgens J., Bott M., Polen T. The L-rhamnose-dependent regulator RhaS and its target promoters expand the toolkit for regulatable gene expression in the acetic acid bacterium *Gluconobacter oxydans*. Manuscript in preparation.

Author's contributions:
PMF, MG, and MM constructed the plasmids, carried out the growth experiments and analyzed the data. PMF and CS performed the FACS analysis and analyzed the data. JG performed the GC-TOF-MS experiments and analyzed the data. TP designed and supervised the study. PMF and TP wrote the manuscript.

Own contribution to this publication: about 50%.

The L-rhamnose-dependent regulator RhaS and its target promoters expand the toolkit for regulatable gene expression in the acetic acid bacterium *Gluconobacter oxydans*

Philipp Moritz Fricke, Mandy Gries, Maurice Mürköster, Christiane Sonntag, Jochem Gätgens, Michael Bott, and Tino Polen*

Forschungszentrum Jülich GmbH, IBG-1: Biotechnology, Institute of Bio- and Geosciences
52425 Jülich, Germany

Running title: RhaS-dependent gene expression in *Gluconobacter oxydans*

ORCID:	Philipp Moritz Fricke	orcid.org/0000-0002-3507-4881
ORCID:	Mandy Lynn Gries	orcid.org/0000-0002-9345-5463
ORCID:	Maurice Mürköster	orcid.org/0000-0002-3589-5065
ORCID:	Christiane Sonntag	orcid.org/0000-0003-3764-227X
ORCID	Jochem Gätgens	orcid.org/0000-0002-9232-180X
ORCID:	Michael Bott	orcid.org/0000-0002-4701-8254
ORCID:	Tino Polen	orcid.org/0000-0002-0065-3007

*** for correspondence:** Dr. Tino Polen
e-mail: t.polen@fz-juelich.de
phone: +49 2461 61 6205
fax: +49 2461 61 2710

Co-authors email address

Philipp Fricke	p.fricke@fz-juelich.de
Mandy Gries	m.gries@fz-juelich.de
Maurice Mürköster	m.muerkoester@fz-juelich.de
Christiane Sonntag	c.sonntag@fz-juelich.de
Jochem Gätgens	j.gaetgens@fz-juelich.de
Michael Bott	m.bott@fz-juelich.de

Keywords: promoter
regulation
plasmid
mNeonGreen
acetic acid bacteria
membrane-bound dehydrogenase

Abstract

For inducible target gene expression in the acetic acid bacterium (AAB) *Gluconobacter oxydans* only recently the first plasmids became available that enable AraC- and TetR-dependent induction. In this study we showed that the L-rhamnose-dependent RhaS regulator from *Escherichia coli* and its target promoters could also be used in *G. oxydans* as an alternative for regulatable target gene expression. Interestingly, in contrast to the responsiveness in *E. coli*, the apparent strong activity of the RhaS-regulated promoter P_{rhaBAD} was surprisingly gradually decreased in *G. oxydans* with increasing L-rhamnose concentrations down to only 10% residual reporter expression, while in the absence of L-rhamnose RhaS increased the apparent P_{rhaBAD} activity. The RhaS-dependent repression of P_{rhaBAD} and of a two-fold stronger synthetic promoter variant thereof containing another RhaS binding site ($P_{rhaBAD(+RhaS\text{-}BS)}$) was largely tunable between only 0.3% and 0% (w/v) L-rhamnose. Therefore, the RhaS-P_{rhaBAD} and the RhaS-$P_{rhaBAD(+RhaS\text{-}BS)}$ system derived from *E. coli* represent sensitive and, for the first time, effector-dependent down-regulatable expression systems in *G. oxydans*. In contrast to P_{rhaBAD}, the *E. coli* promoter P_{rhaT} was almost inactive in the absence of *rhaS*. In the presence of *rhaS*, the non-induced P_{rhaT} activity was very weak and the induced P_{rhaT} activity was weak to moderate and inducible up to a 10-fold induction. Therefore, the RhaS-P_{rhaT} system from *E. coli* could be a suitable alternative for expression of difficult enzymes and membrane proteins at lower levels. Like P_{rhaT}, P_{rhaSR} appeared positively auto-regulated by RhaS which was increased with L-rhamnose. In summary, the interplay of the L-rhamnose-dependent RhaS protein from *E. coli* and its target promoters P_{rhaBAD}, P_{rhaT}, and P_{rhaSR} offer very interesting characteristics potentially usable for repressible and inducible gene expression in basic and applied research including combinatorial metabolic engineering approaches in *G. oxydans* and possibly in other AAB.

Key Points

- *E. coli* P_{rhaBAD} was strong with a reversed RhaS-dependent responsiveness in *G. oxydans*.
- *E. coli* P_{rhaT} was very weak in *G. oxydans* and gradually inducible up to 10-fold induction.
- RhaS-P_{rha} systems open up new opportunities for dynamic gene expression regulation.

Introduction

In biotechnological applications and basic research, timed production of proteins in bacterial cell culture for various purposes by inducible or regulatable expression of target genes is a standard method well established in many bacteria except in acetic acid bacteria (see, for example, {Chen, 2012 #1}{Connell, 2001 #2}{Dilworth, 2018 #3}{Evans, 2015 #4}{Forstner, 2007 #5}{Gruber, 2015 #6}{Parachin, 2012 #7}{Schnappinger, 2014 #8}{Terpe, 2006 #9}{Valero, 2012 #10}. Members of the acetic acid bacteria (AAB) family (*Acetobacteraceae*) are interesting Gram-negative microorganisms that can be exploited to produce food and beverage, industrial chemicals, and biomaterials. For a long time, in AAB only constitutive target gene expression was applied and in a very few studies only weakly regulatable target gene expression were achieved (reviewed in {Fricke, 2021 #11}. The transfer and full functionality as well as tunability of well-known heterologous regulatable expression systems was demonstrated in AAB only recently for the AraC and TetR systems from *Escherichia coli* and hitherto only for the AAB *Gluconobacter oxydans* {Fricke, 2020 #12}{Fricke, 2021 #13}, while in the AAB *Komagataeibacter* and *Gluconacetobacter* both systems turned out to be very leaky on alternative plasmid constructs in the absence of inducer {Florea, 2016 #14}{Teh, 2019 #15}. Besides, in *K. rhaeticus*, *Ga. xylinus* and *Ga. hansenii*, an *N*-acyl homoserine lactone-inducible LuxR-P_{lux} system exhibited condition-dependent induction only up to 36-fold, yet an apparent more robust tightness and induction of fluorescence reporter expression when cells were encased in pellicles {Florea, 2016 #14}{Teh, 2019 #15}. LacI-dependent systems from *Escherichia coli* have also been found to always exhibit some non-induced basal reporter expression in AAB and thus low induction fold-changes only up to 40-fold, or inhomogeneous induction {Condon, 1991 #17}{Fricke, 2021 #13}{Liu, 2020 #16}. Protein-DNA binding simulations by computational modeling of LacI, TetR, and AraC with DNA predicted a decreased DNA binding of LacI when pH is below 6 while DNA binding of TetR and AraC was predicted to be increased {Fricke, 2021 #13}. Although it has not yet been shown experimentally, pH-dependent decreased DNA binding could cause the leakiness of the LacI-dependent systems hitherto tested in AAB. Therefore, the leakiness of LacI from neutralophilic *E. coli* was also discussed to be related to the internal pH in AAB species, which appears to be maintained to different extents during growth and depending on the acidic growth conditions. Besides LacI, the leakiness of other heterologous repressor-based systems tested and still leaky in AAB may also be related to the internal pH. For acidophilic bacteria such as AAB, the intracellular pH is considered to be maintained between 6 and 7, while neutralophilic bacteria such as *E. coli* are considered to maintain pH 7 to 8 {Baker-Austin, 2007 #19}{Krulwich, 1998 #20}. Despite pH maintenance mechanisms, the intracellular pH of the AAB *Acetobacter aceti* was reported to change from 5.8 to 3.9 already during growth when the medium pH acidified from 6.2 to 3.5 {Menzel, 1985 #18}. Furthermore,

expression data obtained with the pH-sensitive fluorescence reporter protein mNeonGreen suggested that also in *G. oxydans* the typical intracellular pH is not maintained during exponential growth in conditions initially set to pH 5 or pH 4, while this was not observed when grown in the standard condition initially set to pH 6 {Fricke, 2021 #13}. Recently, the pH-sensitive green fluorescent protein pHluorin2' was introduced to monitor and estimate the intracellular pH of *K. europaeus* and revealed a decrease from 6.3 to 4.7 already during cell growth {Ishii, 2021 #40}. The study also showed that the DNA-binding leucine-responsive regulatory protein Lrp from acetic acid bacteria is stable and functions at a wide range of intracellular pH levels. However, to better understand the pH-dependent binding of regulators to DNA and to possibly improve the expression performance of heterologous regulatable expression systems so far leaky in AAB species and their growth conditions, more protein-DNA interaction data and intracellular pH data of AAB strains in various growth conditions are required.

The AAB *G. oxydans* harbors the beneficial ability of regio- and stereoselective incomplete oxidation of a variety of sugars, sugar alcohols and other substrates in the periplasm by membrane-bound dehydrogenases (mDHs) and release of resulting products into the cultivation medium {Mamlouk, 2013 #21}{Mientus, 2017 #22}{Pappenberger, 2014 #23}. Therefore, *G. oxydans* is industrially used for oxidative biotransformations of carbohydrates to produce *e. g*. the tanning lotion additive dihydroxyacetone, the vitamin C precursor L-sorbose, and 6-amino-L-sorbose used for production of the antidiabetic drug miglitol {Ameyama, 1981 #24}{Gupta, 2001 #25}{Hekmat, 2003 #26}{Saito, 1997 #27}{Tkac, 2001 #28}{Wang, 2016 #29}. In *G. oxydans*, the derivatives of the pBBR1MCS plasmid family obtained from the endogenous plasmid pBBR1 isolated from *Bordetella bronchiseptica* are the most successful shuttle vectors for recombinant target gene expression {Antoine, 1992 #30}{Kovach, 1994 #32}{Kovach, 1995 #31}. Among the pBBR1MCS derivatives, pBBR1MCS-2 conferring kanamycin resistance and pBBR1MCS-5 conferring gentamicin resistance are by far the most used in *G. oxydans* (reviewed in {Fricke, 2021 #11}. Both plasmid backbones recently enabled full functionality and thus transfer of the AraC- and TetR-dependent systems from *E. coli* to *G. oxydans* 621H, yet the use of pBBR1MCS-2 resulted in abnormal cell morphology due to kanamycin and in reduced expression performance of the TetR-P_{tet} system {Fricke, 2020 #12}{Fricke, 2021 #13}. Therefore, in *G. oxydans* plasmid backbone pBBR1MCS-5 with gentamicin is likely to be the choice over pBBR1MCS-2.

Due to our recent success in demonstrating for the first time fully functional regulatable expressions systems in *G. oxydans* (AraC-P_{araBAD} and TetR-P_{tet}) by using the plasmid pBBR1MCS-5, we wanted to test another heterologous system with pBBR1MCS-5 to provide and establish a further alternative for regulatable target gene expression in *G. oxydans*. To this end, we chose the L-rhamnose-dependent RhaSR system from *E. coli* {Baldoma, 1990

#33}{Egan, 1993 #34}{Egan, 1994 #35}{Via, 1996 #36}{Bhende, 1999 #37}{Wickstrum, 2010 #38}. Compared to the AraC, TetR, and LacI systems from *E. coli*, the RhaRS system offers special features that could be particularly interesting and useful for applications in *G. oxydans* or AAB in general (Fig. S1).

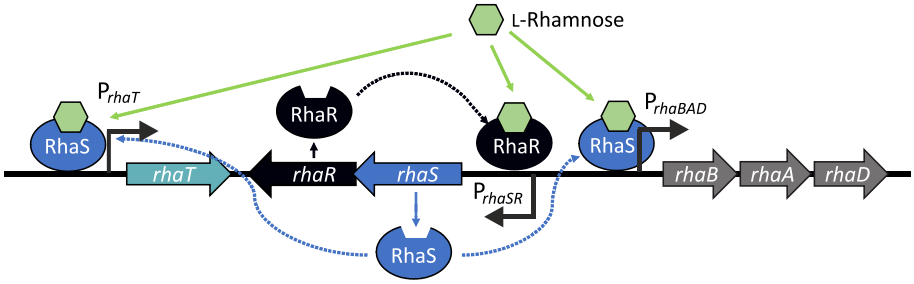

Fig. S1 The region of the P_{rhaBAD} promoter between the P_{rhaT} and *rhaBAD* genes illustrating the regulatory mode of action by the RhaR and RhaS regulator proteins in *E. coli* according to Egan & Schleif (1993) and VÍa et al. (1996).

Firstly, the system comprises not only one, but two transcriptional regulators both responding to L-rhamnose. Namely, the RhaR and RhaS protein encoded in the *rhaSR* operon expressed from the promoter P_{rhaSR}. In *E. coli*, basal expression from P_{rhaSR} is positively auto-regulated in the presence of L-rhamnose by RhaR resulting in increased expression of the *rhaSR* operon and in turn P_{rhaSR} is negatively auto-regulated by RhaS since RhaS is able to bind to the RhaR binding site at P_{rhaSR}. Secondly, the regulator RhaS furthermore targets two different promoters, namely P_{rhaBAD} and P_{rhaT}. P_{rhaBAD} drives transcription of the structural *rhaBAD* genes encoding the L-rhamnose catabolic enzymes rhamnulose kinase, L-rhamnose isomerase and rhamnulose-1-phosphate aldolase. P_{rhaT} drives transcription of *rhaT* encoding the L-rhamnose transport system. RhaS activates transcription from P_{rhaBAD} and P_{rhaT} in the presence of L-rhamnose. Furthermore, in *E. coli* the L-rhamnose metabolism is under catabolite repression by glucose, which is overcome by the binding of the cAMP receptor protein (CRP) to consensus recognition sequences found in all three P_{rha} promoters and interaction of CRP with RhaS and RhaR. In *G. oxydans* CRP is absent since the predicted CRP gene (GOX0974 / GOX_RS06010) turned out to encode an iron-sulfur cluster protein termed GoxR, an FNR-type transcriptional regulator of genes involved in respiration and redox metabolism {Schweikert, 2021 #39}. Overall, it seemed very interesting to analyze if and how RhaS, RhaR, and the promoters P_{rhaBAD}, P_{rhaT}, and P_{rhaSR} perform and could be useful for regulatable recombinant gene expression in *G. oxydans*.

We found with pBBR1MCS-5-based mNeonGreen (mNG) reporter plasmids that in *G. oxydans* the promoter P_{rhaBAD} surprisingly was regulated differently compared to *E. coli*. In

the absence of L-rhamnose, RhaS increased the expression from P_{rhaBAD}. Additionally, increased *rhaS* expression using different promoters increased *mNG* expression from P_{rhaBAD}, thus the apparent strength of P_{rhaBAD} was dependent from the RhaS level. In the presence of L-rhamnose, RhaS repressed the expression from P_{rhaBAD} down to only 7% to 10% residual plasmid-based mNG reporter activity. The RhaS-dependent repression of P_{rhaBAD} was largely tunable by L-rhamnose between 0% and only 0.3% (w/v). In contrast to P_{rhaBAD}, the very similar promoter P_{rhaT} was activated by RhaS, tunable, and rather weak in *G. oxydans*. The promoter P_{rhaSR} alone appeared also rather weak in *G. oxydans*, yet in the presence of the *rhaS* gene P_{rhaSR} appeared to be very strong indicating a positive auto-regulation of P_{rhaSR} by RhaS in the absence of RhaR. Together, the effects and properties of the L-rhamnose-dependent RhaS protein from *E. coli* and the promoters P_{rhaBAD}, P_{rhaT}, and P_{rhaSR} in *G. oxydans* offer very interesting characteristics usable for regulated gene expression in basic and applied research including combinatorial metabolic engineering approaches.

Materials and Methods

Bacterial strains, plasmids, media and growth conditions

Bacterial strains and plasmids used in this study and their relevant characteristics are listed in Table 1. *G. oxydans* cells were routinely cultivated in D-mannitol complex medium containing 40 g L^{-1} D-mannitol, 5 g L^{-1} yeast extract, 1 g L^{-1} KH_2PO_4, 1 g L^{-1} $(NH_4)_2SO_4$, and 2.5 g L^{-1} $MgSO_4$ x 7 H_2O at 30°C. The initial pH of the medium was set to 6 by the addition of KOH (5 M stock). Because *G. oxydans* possesses a natural resistance toward cefoxitin, 50 µg mL^{-1} of the antibiotic was routinely added to the medium as a precaution to prevent bacterial contaminations. Stock solution of cefoxitin (50 mg mL^{-1}) and D-mannitol (200 g L^{-1}) were sterile-filtered and added to autoclaved medium. Unless stated otherwise, for shake flask cultivations cells from 10 mL overnight pre-cultures were used to inoculate 50 mL D-mannitol medium in 500 mL shaking flasks with three baffles to an initial optical density at 600 nm (OD_{600}) of 0.3 (UV-1800, Shimadzu). All shake flasks cultures were grown on a rotary shaker at an agitation speed of 180 rpm. *G. oxydans* cells harboring pBBR1MCS-5-based plasmids were supplemented with 10 µg mL^{-1} gentamicin {Kovach, 1994 #32}. *Escherichia coli* strains were cultivated at 37 °C and 160 rpm in lysogeny broth (LB) medium. Medium of *E. coli* carrying pBBR1MCS-5-based plasmids was supplemented with 10 µg mL^{-1} gentamicin. *E. coli* S17-1 was used as donor strain to transform *G. oxydans* by conjugation {Kiefler, 2017 #41}. Competent *E. coli* S17-1 were made and transformed by $CaCl_2$ procedure as described {Hanahan, 1983 #42}.

Recombinant DNA work

All DNA oligonucleotides used in this study were obtained from Eurofins Genomics and are listed in Table S1. All enzymes required for recombinant DNA work were purchased

from Thermo Scientific. Polymerase chain reaction (PCR) used for DNA manipulation and plasmid verification followed standard protocols as described {Sambrook, 1989 #43}. For amplification of DNA fragments Q5 DNA polymerases were utilized as recommended by the manufacturer (New England Biolabs). All reporter plasmids were constructed in a one-step isothermal Gibson assembly (50°C, 1 h) by integrating amplified DNA fragments in the restricted broad-host vector pBBR1MCS-5 {Gibson, 2009 #44}. All DNA modifications to create desired plasmids were conducted in *E. coli* S17-1. For plasmid isolation a QIAprep spin miniprep kit (Qiagen) was used according to the manufacturer's protocol. Correctness of plasmid inserts were checked by DNA sequencing (Eurofins MWG).

Construction of plasmids

In this study, all plasmids were constructed using the empty vector pBBR1MCS-5-T_{gdhM}-MCS-T_{0028} that we created previously for the TetR-P_{tet} system as described {Fricke, 2021 #13}. The terminator sequences of GOX0265 (T_{gdhM}) and GOX0028 (T_{0028}) flank the multiple cloning site (MCS) to reduce potential interferences caused by genetic elements on the plasmid backbone. Unless stated otherwise, pBBR1MCS-5-T_{gdhM}-MCS-T_{0028} was restricted for insert integration with the restriction endonucleases *Xba*I and *Eco*RI. Furthermore, in all constructs using the promoter P_{rhaBAD}, P_{rhaSR}, P_{rhaT}, $P_{GOX0264}$ or $P_{GOX0452}$ to express the reporter gene *mNeonGreen* (*mNG*), upstream from *mNG* the ribosome binding site (RBS) AGGAGA was placed downstream from the naturally occurring RBS of the respective promoter region. This RBS was already shown to be functional and strong in *G. oxydans* {Fricke, 2020 #12}{Fricke, 2021 #13}.

For construction of plasmid pBBR1MCS-5-*rhaSR*-P_{rhaSR}-P_{rhaBAD}-*mNG*, two DNA fragments were inserted in pBBR1MCS-5-T_{gdhM}-MCS-T_{0028}: a 2112 bp DNA fragment with *rhaSR*-P_{rhaSR}-P_{rhaBAD}-RBS amplified with primer pair PF1/PF2 from the genome of *E. coli* LJ110 and a 806 bp DNA fragment with *mNG*-T_{BBa_B1002} amplified with the primer pair PF3/PF4 from pBBR1MCS-5-*araC*-P_{BAD}-*mNG* {Fricke, 2020 #12}. The second DNA fragment inserted the terminator BBa_B1002 from the iGEM parts library directly downstream from the reporter gene *mNG*.

The plasmid pBBR1MCS-5-*rhaS*-P_{rhaSR}-P_{rhaBAD}-*mNG* lacking *rhaR* was constructed by amplification of a 2021 bp DNA fragment from pBBR1MCS-5-*rhaSR*-P_{rhaSR}-P_{rhaBAD}-*mNG* with primer pair PF5/PF4 obtaining fragment *rhaS*-P_{rhaSR}-P_{rhaBAD}-RBS-*mNG*-T_{BBa_B1002} and subsequent integration of this fragment into pBBR1MCS-5-T_{gdhM}-MCS-T_{0028}.

To construct the plasmid pBBR1MCS-5-*rhaR*-P_{rhaSR}-P_{rhaBAD}-*mNG* lacking *rhaS*, the primer pairs PF1/PF6 and PF7/PF4 were used to amplify a 969 bp DNA fragment containing *rhaR* and a 1128 bp DNA fragment containing P_{rhaSR}-P_{rhaBAD}-RBS-*mNG*-T_{BBa_B1002}. Again, plasmid pBBR1MCS-5-*rhaSR*-P_{rhaSR}-P_{rhaBAD}-*mNG* was used as a PCR template. Due to the design of the primers, *rhaS*, being the first gene of the *rhaSR* operon, was deleted in such a

way that the first and last three codons of *rhaS* remained in frame in the plasmid, thereby in principle maintaining the original operon structure.

To construct the plasmid pBBR1MCS-5-P_{rhaSR}-P_{rhaBAD}-*mNG* lacking the whole *rhaSR* operon, a 1121 bp DNA fragment comprising of P_{rhaSR}-P_{rhaBAD}-RBS-*mNG*-T_{BBa_B1002} was generated with primer pair PF8/PF4 from pBBR1MCS-5-*rhaSR*-P_{rhaSR}-P_{rhaBAD}-*mNG* and integrated in pBBR1MCS-5-T_{gdhM}-MCS-T_{0028}.

The plasmid pBBR1MCS-5-*rhaS*-$P_{GOX0264}$-P_{rhaBAD}-*mNG* was assembled from three DNA fragments: The first fragment (943 bp) contained *rhaS* and was amplified with primer pair PF5/PF9 from pBBR1MCS-5-*rhaS*-P_{rhaSR}-P_{rhaBAD}-*mNG*. The second fragment (537 bp) contained RBS-$P_{GOX0264}$ and was amplified with primer pair PF10/PF11 from the genome of *G. oxydans* 621H. The third fragment (998 bp) contained P_{rhaBAD}-RBS-*mNG*-T_{BBa_B1002} and was amplified with primer pair PF12/PF4 from pBBR1MCS-5-*rhaS*-P_{rhaSR}-P_{rhaBAD}-*mNG*.

Similarly, plasmid pBBR1MCS-5-*rhaS*-$P_{GOX0452}$-P_{rhaBAD}-*mNG* was constructed from three DNA fragments: Again, the first fragment (943 bp) contained *rhaS* and was amplified with primer pair PF5/PF9 from pBBR1MCS-5-*rhaS*-P_{rhaSR}-P_{rhaBAD}-*mNG*. The second fragment (450 bp) contained RBS-$P_{GOX0452}$ and was amplified with primer pair PF13/PF14 from the genome of *G. oxydans* 621H. The third fragment (999 bp) contained P_{rhaBAD}-RBS-*mNG*-T_{BBa_B1002} and was amplified with primer pair PF15/PF4 from pBBR1MCS-5-*rhaS*-P_{rhaSR}-P_{rhaBAD}-*mNG*.

The plasmid pBBR1MCS-5-*mNG*-P_{rhaSR}-$P_{GOX0264}$-*rhaS* was created from the DNA fragment T_{BBa_B1002}-*mNG*-RBS-P_{rhaBAD} (993 bp) amplified with primer pair PF16/PF17 from pBBR1MCS-5-*rhaS*-P_{rhaSR}-P_{rhaBAD}-*mNG* and fragment $P_{GOX0264}$-RBS-*rhaS* (1338 bp) amplified with primer pair PF18/PF19 from pBBR1MCS-5-*rhaS*-$P_{GOX0264}$-P_{rhaBAD}-*mNG.*

Similarly, plasmid pBBR1MCS-5-*mNG*-P_{rhaSR}-$P_{GOX0452}$-*rhaS* was generated from DNA fragment T_{BBa_B1002}-*mNG*-RBS-P_{rhaBAD} (997 bp) amplified with primer pair PF16/PF20 from template pBBR1MCS-5-*rhaS*-P_{rhaSR}-P_{rhaBAD}-*mNG* and from DNA fragment $P_{GOX0452}$-RBS-*rhaS* (1305 bp) amplified with primer pair PF21/PF19 from template pBBR1MCS-5-*rhaS*-$P_{GOX0452}$-P_{rhaBAD}-*mNG*.

Plasmid pBBR1MCS-5-*mNG*-P_{rhaSR} was constructed with DNA fragment T_{BBa_B1002}-*mNG* (815 bp) amplified with primer pair PF16/PF22 and DNA fragment RBS-P_{rhaSR}-P_{rhaBAD} amplified with primer pair PF23/PF24, both fragments generated from plasmid pBBR1MCS-5-*rhaS*-P_{rhaSR}-P_{rhaBAD}-*mNG* as PCR template. In the resulting construct pBBR1MCS-5-*mNG*-P_{rhaSR}, the P_{rhaBAD} region directly neighborly located to P_{rhaSR} was included to keep the native DNA region upstream from P_{rhaSR}.

For construction of plasmid pBBR1MCS-5-*rhaS*-P_{rhaSR}-$P_{rhaBAD(+RhaS\text{-}BS)}$-*mNG* containing an additional RhaS-binding site (RhaS-BS) directly downstream from the -10 region of P_{rhaBAD}, a DNA fragment (933 bp) consisting of $_{(RhaS\text{-}BS)}$-RBS-*mNG*-T_{BBa_B1002} was amplified

with primer pair PF25/PF4 from pBBR1MCS-5-*rhaS*-P_{rhaSR}-P_{rhaBAD}-*mNG* and integrated into the *Eco*RI-restricted plasmid pBBR1MCS-5-*rhaS*-P_{rhaSR}-P_{rhaBAD}-*mNG*.

Plasmid pBBR1MCS-5-P_{rhaT}-*mNG* was constructed with the DNA fragments P_{rhaT}-RBS (334 bp) generated with primer pair PF26/PF27 from the genome of *E. coli* LJ110 and fragment *mNG*-T_{BBa_B1002} (806 bp) generated with primer pair PF28/PF4 from plasmid pBBR1MCS-5-*rhaS*-P_{rhaSR}-P_{rhaBAD}-*mNG*.

To construct plasmid pBBR1MCS-5-*rhaS*-P_{rhaSR}-P_{rhaT}-*mNG*, two DNA fragments were used. The first DNA fragment contained *rhaS*-P_{rhaSR} (1124 bp) amplified with primer pair PF5/PF29 from pBBR1MCS-5-*rhaS*-P_{rhaSR}-P_{rhaBAD}-*mNG*. The second DNA fragment contained P_{rhaT}-RBS-*mNG*-T_{BBa_B1002} (1085 bp) amplified with primer pair PF30/PF4 from pBBR1MCS-5-P_{rhaT}-*mNG*.

Measurements of fluorescence protein

The regulation and relative strength of the promoters on constructed plasmids was monitored in *G. oxydans* by means of expressing *mNeonGreen* (*mNG*) encoding the fluorescent reporter protein mNG {Shaner, 2013 #45}. For analysis of *mNG* expression with various promoters, *G. oxydans* test cultures were supplemented with L-rhamnose (w/v) at indicated concentrations using a 40% (w/v) stock solution. Equal volumes of medium were added to non-supplemented reference cultures. Throughout the cultivation, growth (OD_{600}) and fluorescence emission were monitored in intervals using a spectrophotometer (UV-1800, Shimadzu) and an Infinite M1000 PRO Tecan reader (λ_{ex} 504 nm / λ_{em} 517 nm, ex/em bandwidth 5 nm, infinite M1000 PRO Tecan). For microscale BioLector cultivations, overnight starter cultures were used to inoculate 800 µL batches of D-mannitol medium in 48-well Flowerplates® (m2p-labs) to an initial OD_{600} of 0.3. Sealed with disposable foil (m2p-labs), plates were cultivated for 24 h at 1200 rpm, 85% humidity and 30 °C while growth was monitored in each well according to backscatter light intensities ($A_{620\ nm}$) and fluorescence emission (λ_{ex} 510 nm / λ_{em} 532 nm). For backscatter signal amplification gain 20 was applied. Signal amplification of fluorescence emission varied (gain 40 - 70) and is indicated in the figure legends. All BioLector data shown in a diagram were measured in the same run of a growth experiment.

Cell flow cytometer analysis

For single cell analysis, a FACSAria™ cell sorter controlled by FACSDiva 8.0.3 software (BD Biosciences) was used to analyze the mNG reporter protein signals in *G. oxydans* 621H harboring either plasmid pBBR1MCS-5-*rhaS*-P_{rhaSR}-P_{rhaBAD}-*mNG* or pBBR1MCS-5-*rhaS*-P_{rhaSR}-P_{rhaT}-*mNG*. The FACS was operated with a 70 µm nozzle and run with a sheath pressure of 70 psi. The forward scatter (FSC) and side scatter (SSC) were recorded as small-angle scatter and orthogonal scatter, respectively, by means of a 488 nm solid blue laser beam. For analysis, only particles/events above a 200 a.u. for FSC-H and

300 a.u. for SSC-H as the thresholds were considered. mNG fluorescence emission was detected from the SSC through the combination of a 502 nm long-pass and 530/30 nm band-pass filter. Prior to data acquisition, the FSC-H *vs*. SSC-H plot was employed to gate the population and to exclude signals originating from cell debris or electronic noise. In a second and third gating step, from the resulting population, the SSC-H signal was plotted against the SSC-W signal and this population was subsequently gated in a FSC-H *vs*. FSC-W plot to exclude doublets. From this resulting singlet population, 100,000 events were recorded at a rate of <10,000 events/s for fluorescence data acquisition. For data analysis and visualization of all gated events (n=100,000) FlowJo 10.7.2 for Windows (FlowJo, LLC) was applied.

L-Rhamnose biotransformation test assay and GC-TOF-MS analysis

G. oxydans cells were grown to an OD_{600} of 1.3, centrifuged (4000 x *g*, 5 min) and washed twice with 50 mM phosphate buffer (pH 6). After the second washing step, cells were resuspended in biotransformation buffer (6.6 g L^{-1} Na_2HPO_4, 3 g L^{-1} KH_2PO_4, 1 g L^{-1} NH_4Cl, 0.5 g L^{-1} NaCl, 0.49 g L^{-1} $MgSO_4$, 0.02 g L^{-1} $CaCl_2$) supplemented with 2% (w/v) L-rhamnose and incubated for 24 h at 30 °C and 200 rpm. Then, the cells were removed from the buffer (4000 x *g*, 5 min) and the supernatant was used for analysis by gas chromatography (Agilent 6890N, Agilent Technologies) coupled to a Waters Micromass GCT Premier high-resolution time-of-flight mass spectrometer (Waters). Sample handling for derivatization, GC-TOF-MS operation, and peak identification were carried out as described {Paczia, 2012 #46}. As a control, samples from biotransformation buffer with L-rhamnose and without cells as well as biotransformation buffer without L-rhamnose yet with cells were prepared.

Total DNA extraction, library preparation, Illumina sequencing, and data analysis

Total DNA was purified from a culture aliquot using a NucleoSpin Microbial DNA Mini kit (MACHEREY–NAGEL). DNA concentrations were measured using a Qubit 2.0 fluorometer (Thermo Fisher Scientific). Illumina sequencing and data analysis of the indicated P_{rhaBAD} DNA sample was carried out as described {Fricke, 2021 #13}. For the read mapping, the improved genome sequence from *G. oxydans* 621H and the indicated P_{rhaBAD} plasmid sequence were used {Kranz, 2017 #47}.

Results

L-Rhamnose does not affect growth and is barely oxidized by *G. oxydans*

In the present study, we tested L-rhamnose-inducible *E. coli* promoters in *G. oxydans* 621H using the plasmid backbone pBBR1MCS-5 to expand the growing genetic toolbox for gene expression in AAB by another regulatory system as an alternative to AraC-P_{araBAD} and TetR-P_{tet} in *G. oxydans*. Similarly to AraC-P_{araBAD} and its effector L-arabinose, the RhaSR-P_{rhaBAD} system from *E. coli* responds to the abundant monosaccharide rhamnose in the uncommon L conformation. In *E. coli*, L-rhamnose needs to enter the cell to interact with the

regulators RhaR and RhaS {Tobin, 1987 #48}. In contrast to L-arabinose, for more than 90% of the strains in the genus *Gluconobacter* no acid formation from L-rhamnose has been reported {Kersters, 1990 #51}. *G. oxydans* 621H whole-cell enzyme activity assays using the artificial electron acceptor DCPIP also revealed no detectable mDH activity with L-rhamnose as substrate {Peters, 2013 #49}. To further check if *G. oxydans* 621H could possibly consume or convert L-rhamnose to a product, we carried out biotransformation assays and GC-TOF-MS analysis. According to the results, no substantial conversion or consumption of L-rhamnose was observed since no new peaks other than the L-rhamnose peaks were detected in 24 h samples, and the areas of GC peaks assigned to L-rhamnose were very similar for both after 24 h and 0 h samples (Fig. S2). Hence, if at all, L-rhamnose is degraded or converted by strain 621H so slowly that the effector is hardly diminished during potential applications.

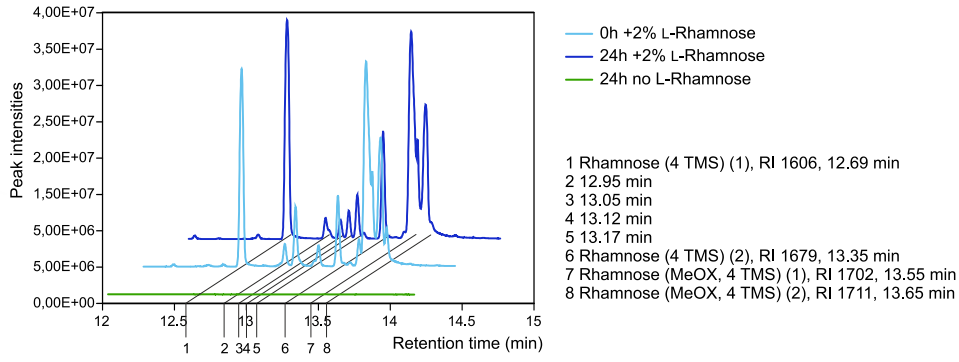

Fig. S2 Chromatograms of GC-TOF-MS analysis of L-rhamnose oxidation by *G. oxydans* 621H. Cell suspensions with an OD_{600} of 1.3 were incubated for 24 h at 30°C and 200 rpm in biotransformation buffer supplemented with 2% (w/v) L-rhamnose. Then cell-free culture supernatant was prepared for GC-TOF-MS analysis.

To check if L-rhamnose as the effector of the RhaSR-system somehow affects the growth of *G. oxydans* 621H, we added L-rhamnose to the medium. With 1% (w/v) L-rhamnose instead of D-mannitol, there was no growth of *G. oxydans* 621H and the initial start OD_{600} of 0.04 did not change within 24 h (Fig. 1). In 4% (w/v) D-mannitol medium supplemented with 1% (w/v) L-rhamnose, the strain 621H grew very similar compared to the D-mannitol reference medium and reached a similar final OD_{600}. Therefore, up to 1% (w/v) there was no negative effect of L-rhamnose on the growth of *G. oxydans* 621H.

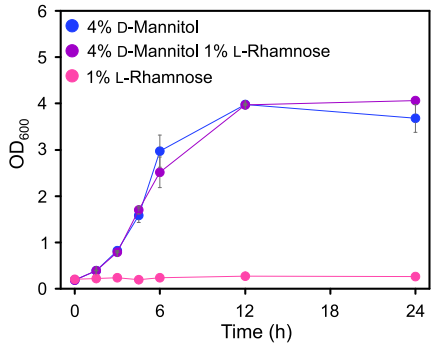

Fig. 1 Growth of *G. oxydans* 621H with L-rhamnose

Growth of *G. oxydans* 621H in shake flask with 4% (w/v) D-mannitol reference medium, reference medium supplemented with 1% (w/v) L-rhamnose, and medium containing 1% (w/v) L-rhamnose instead of 4% (w/v) D-mannitol. The data represent mean values of two biological replicates.

In *G. oxydans* P_{rhaBAD} from *E. coli* is repressed in the presence of L-rhamnose

A special feature of the L-rhamnose-inducible P_{rhaBAD} system from *E. coli* is the involvement of two transcriptional regulators. In *E. coli*, RhaS activates transcription from P_{rhaBAD} in the presence of a suitable inducer while RhaR auto-regulates the P_{rhaSR} promoter for transcription of the *rhaSR* operon itself, which affects the resulting RhaS level making P_{rhaBAD} highly inducible {Egan, 1993 #34}{Egan, 1994 #35}{Kelly, 2016 #50}. First, we tested the inducibility of P_{rhaBAD} in *G. oxydans* by constructing a pBBR1MCS-5-based plasmid placing the required elements in the same order as present in *E. coli*, thus the *rhaSR* operon under control of its native promoter P_{rhaSR} in divergent orientation to P_{rhaBAD}. The fluorescent reporter mNeonGreen (mNG) was used to measure P_{rhaBAD}-derived expression. On the plasmid, the elements *rhaSR*-P_{rhaSR}-P_{rhaBAD}-*mNG* were flanked by three terminators, T_{gdhM} downstream from *rhaR* and T_{BBa_B1002} and $T_{GOX0028}$ downstream from *mNG*. Furthermore, downstream from the native ribosome binding site (RBS) present within P_{rhaBAD} the RBS 5'-AGGAGA was inserted upstream from *mNG*. This RBS upstream from *mNG* is strong in *G. oxydans* and was also used in the regulatable AraC-P_{araBAD} and TetR-P_{tet} expression systems {Fricke, 2020 #12}{Fricke, 2021 #13}. The inducibility of the resulting plasmid pBBR1MCS-5-*rhaSR*-P_{rhaSR}-P_{rhaBAD}-*mNG* was tested in *G. oxydans* 621H with 1% L-rhamnose. Overnight pre-cultures were split to inoculate main cultures with D-mannitol medium either without or supplemented with 1% L-rhamnose. Growth and mNG fluorescence was monitored in a BioLector. As expected from the previous growth test in shake flasks, also all microscale cultures exhibited similar growth regardless of L-rhamnose supplementation (Fig. 2a). With and without L-rhamnose, in both conditions the growth medium was acidified to pH 4.3 (24 h) also suggesting no relevant

oxidation of L-rhamnose to a corresponding acid. However, surprisingly and contrary to our expectation, the mNG fluorescence of the cultures without L-rhamnose strongly increased during growth and peaked approximately 6 h after inoculation when cells entered the stationary phase (Fig. 2b). Contrary, in cultures with L-rhamnose only a slight increase of mNG fluorescence was observed corresponding to approximately 28% of the mNG signals of the non-supplemented cultures. Thus, in *G. oxydans mNG* expression from P_{rhaBAD} appeared to be repressed in the presence of L-rhamnose suggesting that the responsiveness of the RhaSR-P_{rhaBAD} system is *vice versa* compared to *E. coli*. According to the mNG fluorescence in the absence of L-rhamnose, P_{rhaBAD} appeared to be very strong in *G. oxydans*.

To verify the expected and regular responsiveness of the plasmid-based RhaSR-P_{rhaBAD} system, it was tested in *E. coli* S17-1. As expected, in LB medium supplemented with 1% (w/v) L-rhamnose, the mNG fluorescence of induced *E. coli* cultures was approximately 2200-fold higher compared to the mNG signals in the non-induced reference cultures (data not shown). This clearly demonstrated that all the required elements of the RhaSR-P_{rhaBAD} system on the plasmid were fully functional and that the system showed the regular responsiveness in *E. coli*. To further verify that the reversed responsiveness of RhaSR-P_{rhaBAD} was observed in *G. oxydans* 621H carrying the intended plasmid without mutations possibly acquired during growth, cells of an induced culture were harvested at the end of the cultivation (24 h) for isolation of total DNA and Illumina sequencing. In the read data analysis 99.48% of the reads mapped to the mNG expression plasmid with *rhaSR*-P_{rhaSR}-P_{rhaBAD}-*mNG* (1011-fold coverage), the updated reference sequences of the *G. oxydans* 621H genome (88-fold coverage), and the 5 endogenous plasmids {Kranz, 2017 #47}. Thus, the sequencing results excluded undesired contaminations in the culture and mutations on the plasmid, thereby verified that the P_{rhaBAD}-derived mNG expression was indeed expressed and repressed in *G. oxydans* 621H carrying the plasmid pBBR1MCS-5-*rhaSR*-P_{rhaSR}-P_{rhaBAD}-*mNG*.

RhaS is responsible for the regulation of P_{rhaBAD}

To analyze whether RhaS and/or RhaR, or an endogenous *G. oxydans* protein is responsible for the reversed responsiveness of the RhaSR-P_{rhaBAD} system, we constructed derivatives of the expression plasmid lacking in-frame a substantial part of either *rhaS*, *rhaR* or both, yet keeping all the elements upstream and downstream from *rhaS* and *rhaR* (Fig. 2c). *G. oxydans* clones carrying one of the three described plasmid derivatives of pBBR1MCS-5-*rhaSR*-P_{rhaSR}-P_{rhaBAD}-*mNG* were grown in D-mannitol medium without and with 1% (w/v) L-rhamnose and cultivated in a BioLector to monitor growth and mNG fluorescence. Regardless of the plasmid derivative, all *G. oxydans* cultures exhibited similar growth with and without L-rhamnose (Fig. 2d). The differences in mNG signals without and with L-rhamnose clearly indicated that RhaS alone is either directly or indirectly responsible for the regulation of

P_{rhaBAD}. All cultured clones with the plasmid lacking *rhaS* exhibited a moderate maximal mNG fluorescence after ~6 h (220-228 a.u.) regardless of L-rhamnose supplementation (Fig. 2e). Similarly unchanged, yet almost 50% higher was the mNG fluorescence with the plasmid lacking both *rhaSR*, suggesting a little negative effect of RhaR on P_{rhaBAD} activity regardless of L-rhamnose. Here, the mNG signals of all cultured clones also peaked at 6 h (314-338 a.u.). With the plasmid lacking only *rhaR*, expression from P_{rhaBAD} was strongly reduced in the presence of L-rhamnose suggesting that RhaS repressed P_{rhaBAD}-derived *mNG* expression. Interestingly, compared to the plasmid pBBR1MCS-5-*rhaSR*-P_{rhaSR}-P_{rhaBAD}-*mNG* with both regulator genes, the lack of *rhaR* increased expression from P_{rhaBAD} in the absence of L-rhamnose by ~20% from 431 a.u. to 513 a.u. and reduced expression from P_{rhaBAD} with 1% (w/v) L-rhamnose by ~23% from 122 a.u. to 94 a.u.. Furthermore, when compared to cells with plasmid pBBR1MCS-5-P_{rhaSR}-P_{rhaBAD}-*mNG* lacking both regulators, it appeared that the presence of *rhaS* increased P_{rhaBAD}-derived *mNG* expression also in the absence of L-rhamnose. This suggested that in *G. oxydans* the regulator RhaS is not only involved in repression of P_{rhaBAD} when L-rhamnose is present, but is also involved in transcriptional activation of P_{rhaBAD} in the absence of L-rhamnose (Fig. 2e).

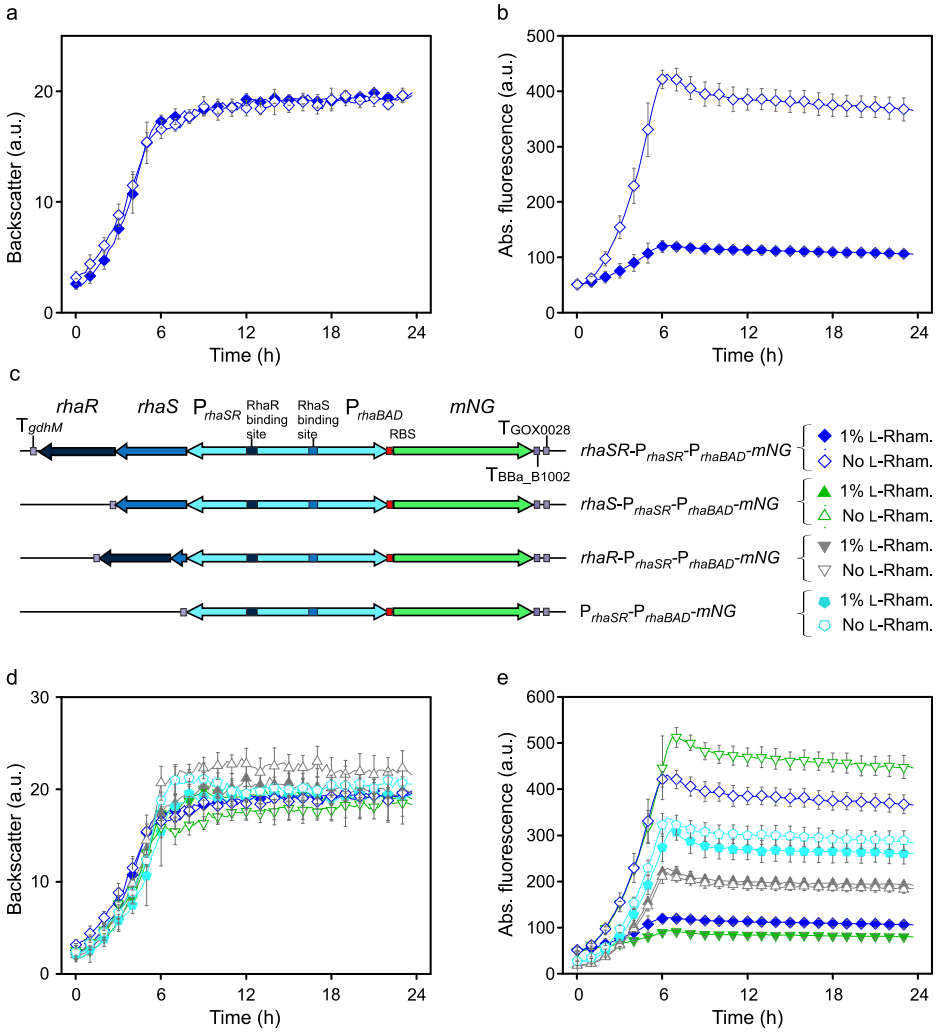

Fig. 2 pBBR1MCS-5-based expression plasmids and analysis of the regulation of the RhaSR-P_{rhaBAD} system from *E. coli* in *G. oxydans* 621H.

(**a**) Growth according to backscatter and (**b**) absolute mNG fluorescence of *G. oxydans* carrying plasmid pBBR1MCS-5-*rhaSR*-P_{rhaSR}-P_{rhaBAD}-*mNG* grown in D-mannitol medium without and with 1% (w/v) L-rhamnose in microscale (BioLector). (**c**) Schematic illustration of the plasmid variants with reporter gene *mNG* to test L-rhamnose-dependent regulation of P_{rhaBAD} expression in the presence and absence of RhaS and RhaR. T_{gdhM}: terminator sequence of *gdhM* (GOX0265); T_{0028}: terminator sequence of GOX0028. The RBS 5'-AGGAGA was inserted in the 3' region of P_{rhaBAD} upstream from *mNG*. (**d**) Growth according to backscatter and (**e**) absolute mNG fluorescence of *G. oxydans* carrying either plasmid pBBR1MCS-5-*rhaSR*-P_{rhaSR}-P_{rhaBAD}-*mNG*, or a plasmid lacking either *rhaR*, or *rhaS*, or both *rhaSR*. Cells were grown in microscale (BioLector) in D-mannitol medium without and with 1% (w/v) L-rhamnose. All data represent mean values and standard deviation from two biological replicates (clones) with three technical replicates each. BioLector settings: backscatter gain 20, fluorescence gain 50.

Without L-rhamnose, strength of *rhaS* expression affected the activated apparent strength of P_{rhaBAD}

The *mNG* expression obtained from P_{rhaBAD} with the previous plasmid derivatives either lacking *rhaS* or not suggested that in *G. oxydans* RhaS activates P_{rhaBAD} in the absence of L-rhamnose. If so, the apparent strength of P_{rhaBAD} could partially be tuned by the *rhaS* expression strength. To test this and the resulting down-regulation of P_{rhaBAD}-derived *mNG* expression from the different resulting levels in the presence of L-rhamnose, we constructed derivatives of pBBR1MCS-5-*rhaS*-P_{rhaSR}-P_{rhaBAD}-*mNG* expressing *rhaS* constitutively either from the *G. oxydans* promoter $P_{GOX0264}$ or $P_{GOX0452}$ (Fig. 3a). $P_{GOX0264}$ and $P_{GOX0452}$ have been shown previously to be a strong and a moderate promoter in *G. oxydans* {Kallnik, 2010 #52}. With the resulting plasmids pBBR1MCS-5-*rhaS*-$P_{GOX0264}$-P_{rhaBAD}-*mNG* and pBBR1MCS-5-*rhaS*-$P_{GOX0452}$-P_{rhaBAD}-*mNG*, the *mNG* expression were compared to that with pBBR1MCS-5-*rhaS*-P_{rhaSR}-P_{rhaBAD}-*mNG* in microscale BioLector cultivations (Fig. 3b). Without L-rhamnose, constitutive expression of *rhaS* from strong $P_{GOX0264}$ reduced P_{rhaBAD}-derived *mNG* expression by more than half and from this level *mNG* expression was further reduced by half when expressing *rhaS* from the moderate $P_{GOX0452}$ (Fig. 3c). Thus, expression of *rhaS* from its native promoter P_{rhaSR} led to the highest mNG signals (514 a.u. after ~7 h) in the absence of L-rhamnose, suggesting either P_{rhaSR} is extremely strong in *G. oxydans* or is positively auto-regulated by RhaS. In the presence of 1% (w/v) L-rhamnose, the strong *mNG* expression obtained with *rhaS*-P_{rhaSR}-P_{rhaBAD}-*mNG* in the absence of L-rhamnose was reduced to approximately 18% (from 514 a.u. to 90 a.u.). The *mNG* expression obtained with *rhaS*-$P_{GOX0264}$-P_{rhaBAD}-*mNG* and with *rhaS*-$P_{GOX0452}$-P_{rhaBAD}-*mNG* were reduced to 23% (from 212 a.u. to 48 a.u.) and 32% (from 95 a.u. to 30 a.u.), respectively, by 1% (w/v) L-rhamnose. Despite the absence of L-rhamnose, the mNG fluorescence obtained with pBBR1MCS-5-*rhaS*-$P_{GOX0452}$-P_{rhaBAD}-*mNG* (95 a.u.) only reached approximately the same level as the mNG fluorescence obtained with pBBR1MCS-5-*rhaS*-P_{rhaSR}-P_{rhaBAD}-*mNG* in the presence of L-rhamnose (90 a.u.). This also indicated that the apparent strength of P_{rhaSR} is very high compared to $P_{GOX0452}$ and $P_{GOX0264}$.

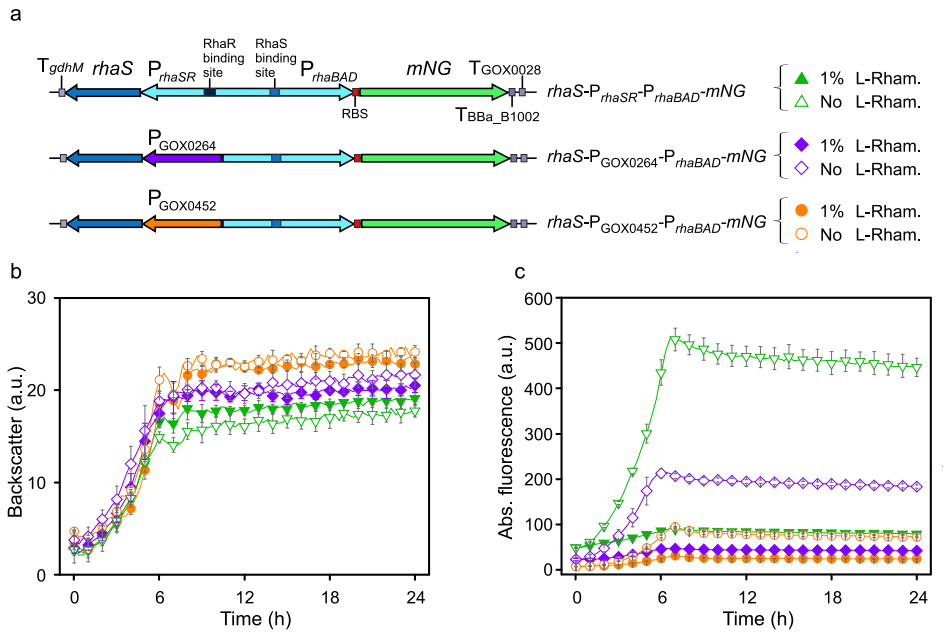

Fig. 3 P_{rhaBAD}-derived *mNG* expression in dependence of *rhaS* expression strength and presence of L-rhamnose.

(**a**) Schematic illustration of the plasmid variants for constitutive expression of *rhaS* from the strong and moderate *G. oxydans* promoter $P_{GOX0264}$ and $P_{GOX0452}$. T_{gdhM}: terminator sequence of *gdhM* (GOX0265); $T_{GOX0028}$: terminator sequence of GOX0028. RBS: 5'-AGGAGA inserted in the 3' region of P_{rhaBAD} upstream from *mNG*. (**b**) Growth according to backscatter and absolute mNG fluorescence (**c**) of *G. oxydans* 621H carrying either plasmid pBBR1MCS-5-*rhaS*-P_{rhaSR}-P_{rhaBAD}-*mNG*, or pBBR1MCS-5-*rhaS*-$P_{GOX0264}$-P_{rhaBAD}-*mNG*, or pBBR1MCS-5-*rhaS*-$P_{GOX0452}$-P_{rhaBAD}-*mNG*. Repression of *mNG* expression from P_{rhaBAD} was tested with 1% (w/v) L-rhamnose. Data represent mean values and standard deviation from two biological replicates (clones) with three technical replicates each. BioLector settings: backscatter gain 20, fluorescence gain 50.

P_{rhaSR} is rather weak in *G. oxydans* yet activated in the presence of *rhaS* and further with L-rhamnose

In *E. coli*, RhaS negatively auto-regulates expression of the *rhaSR* operon by competing with RhaR for the same binding site in the P_{rhaSR} region. While RhaR bound to the promoter increases CRP-dependent transcription activation from P_{rhaSR}, RhaS inhibits CRP-promoter interaction and thereby reduces transcription from P_{rhaSR} {Wickstrum, 2010 #38}. Since in *G. oxydans* CRP is absent and the apparent strength of P_{rhaSR} appeared to be high in the presence of *rhaS* as concluded from RhaS-dependent P_{rhaBAD}-derived mNG fluorescence (Fig. 2), we also wanted to analyze the influence of the *rhaS* expression strength on P_{rhaSR} activity by P_{rhaSR}-derived *mNG* expression. Therefore, we created plasmids with *mNG* under control of P_{rhaSR} and either lacking *rhaS* or with *rhaS* under the control of $P_{GOX0452}$ or $P_{GOX0264}$, and cultivated the respective *G. oxydans* strains in a BioLector (Fig. 4a, b). In the absence of

L-rhamnose, moderate $P_{GOX0452}$-derived *rhaS* expression resulted in a similar *mNG* expression from P_{rhaSR} as without *rhaS*, while the stronger $P_{GOX0264}$-derived *rhaS* expression resulted in a higher *mNG* expression from P_{rhaSR} and thus suggesting a positive effect of RhaS on P_{rhaSR} activity (Fig. 4c, d). In the presence of L-rhamnose, *mNG* expression from P_{rhaSR} was always increased with *rhaS* while there was no effect by L-rhamnose when *rhaS* was absent. With moderate *rhaS* expression in *G. oxydans* harboring pBBR1MCS-5-*mNG*-P_{rhaSR}-$P_{GOX0452}$-*rhaS*, the mNG fluorescence increased ~2.5-fold from 74 a.u. to 189 a.u. with 1% (w/v) L-rhamnose. This L-rhamnose-dependent increase was less pronounced with *rhaS* under control of the stronger $P_{GOX0264}$ where RhaS levels are expected to be higher. Here, the mNG fluorescence increased only 1.3-fold from 144 a.u. to 187 a.u. (Fig. 4d). Together, in contrast to P_{rhaBAD} which is repressed in *G. oxydans* by RhaS and L-rhamnose, P_{rhaSR} is activated in *G. oxydans* by RhaS and is further activated by RhaS in the presence of L-rhamnose.

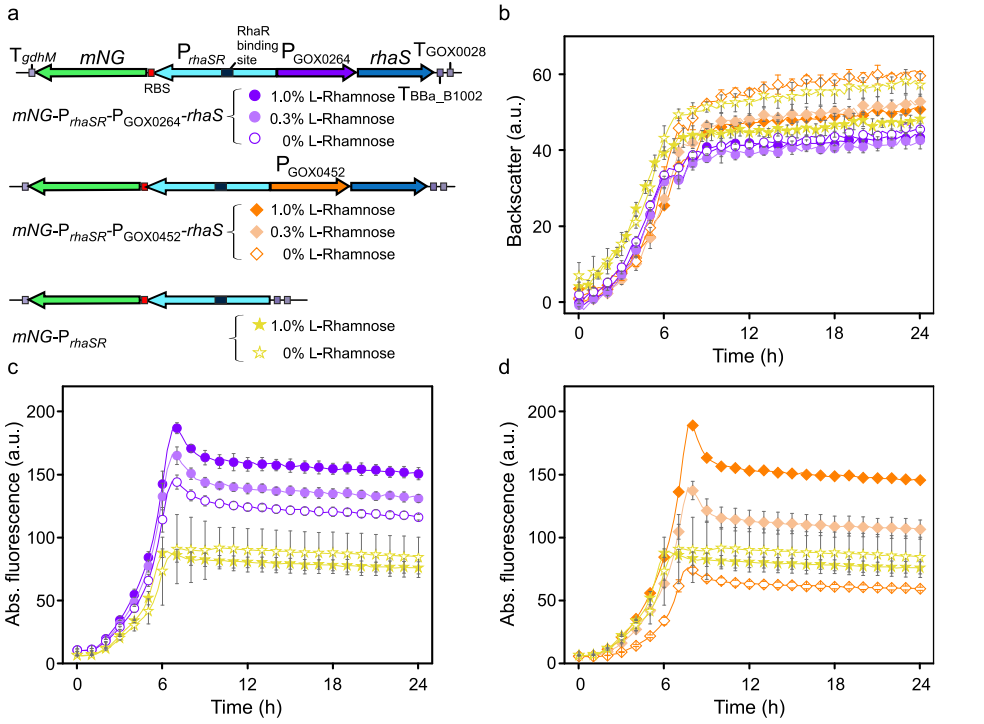

Fig. 4 P_{rhaSR}-derived *mNG* expression in dependence of *rhaS* expression strength and presence of L-rhamnose.

(**a**) Schematic illustration of pBBR1MCS-5-derived plasmid variants with insert *mNG*-P_{rhaSR}-$P_{GOX0264}$-*rhaS*, *mNG*-P_{rhaSR}-$P_{GOX0452}$-*rhaS* or *mNG*-P_{rhaSR}. (**b**) Growth according to backscatter of *G. oxydans* 621H carrying plasmid pBBR1MCS-5-*mNG*-P_{rhaSR}-$P_{GOX0264}$-*rhaS*, pBBR1MCS-5-*mNG*-P_{rhaSR}-$P_{GOX0452}$-*rhaS*, or pBBR1MCS-5-*mNG*-P_{rhaSR} in microscale BioLector cultivations. Absolute fluorescence of *G. oxydans* 621H with (**c**) plasmid pBBR1MCS-5-*mNG*-

P_{rhaSR}-$P_{GOX0264}$-*rhaS* and with (**d**) pBBR1MCS-5-*mNG*-P_{rhaSR}-$P_{GOX0452}$-*rhaS*, both graphs with *G. oxydans* 621H carrying pBBR1MCS-5-*mNG*-P_{rhaSR} lacking *rhaS*. L-Rhamnose was supplemented with 0.3% or 1% (w/v). Data represent mean values and standard deviation from two biological replicates with two and three technical replicates each. BioLector settings: backscatter gain 20, fluorescence gain 70.

Repression of P_{rhaBAD} was tunable by low L-rhamnose concentrations and homogeneous

Since from all tested variants the plasmid lacking *rhaR* and with *rhaS* under control of the auto-regulated P_{rhaSR} exhibited the highest P_{rhaBAD} activity in the absence of L-rhamnose, the construct pBBR1MCS-5-*rhaS*-P_{rhaSR}-P_{rhaBAD}-*mNG* was analyzed further in regard to repression of the *mNG* expression. The tunability of repression and residual *mNG* expression was tested in D-mannitol medium with 0.3%, 1% and 3% (w/v) L-rhamnose in a BioLector (Fig. 5a, b). Compared to non-supplemented cultures, the mNG fluorescence of cells grown with 0.3% (w/v) L-rhamnose was strongly reduced after ~7 h to 25% residual *mNG* expression (225 a.u. *vs*. 55 a.u.). This indicated that the RhaS-P_{rhaBAD} system is very sensitive and already low L-rhamnose concentrations should enable a tuning of reduced target gene expression. Supplementation with 1% and 3% (w/v) L-rhamnose reduced mNG fluorescence further representing 17% (38 a.u.) and 15% (34 a.u.) residual *mNG* expression, respectively. This suggested that already 1% (w/v) L-rhamnose is sufficient to reach almost maximal possible repression of P_{rhaBAD} when using the plasmid pBBR1MCS-5-*rhaS*-P_{rhaSR}-P_{rhaBAD}-*mNG*.

The sensitivity of P_{rhaBAD}-derived expression toward relatively low L-rhamnose concentration was also observed in scale-up cultivations in shake flask. When grown in 50 mL D-mannitol medium supplemented with 0.25% or 1% (w/v) L-rhamnose, the mNG fluorescence was already highly reduced in the presence of 0.25% (w/v) L-rhamnose (from 3,267 a.u. to 783 a.u. after 9 h) representing 24% residual *mNG* expression (Fig. 5c, d). In shake flask cultures with 1% (w/v) L-rhamnose, the mNG fluorescence was reduced to 553 a.u., again representing 17% residual *mNG* expression.

Flow cytometer analysis (FACS) was used to analyze the repression of P_{rhaBAD}-derived *mNG* expression on the single cell level. In the absence of L-rhamnose, 7 h after inoculation 95.5% of all measured cells showed strong mNG fluorescence (~100,000 a.u.) representing a very high population homogeneity. With 1% (w/v) L-rhamnose, 96.4% of all measured cells showed a strongly reduced fluorescence (~11,000 a.u.) also representing a very high population homogeneity (Fig. 5e). Thus, the results of the FACS analysis suggested approximately 11% residual *mNG* expression in the presence of 1% (w/v) L-rhamnose.

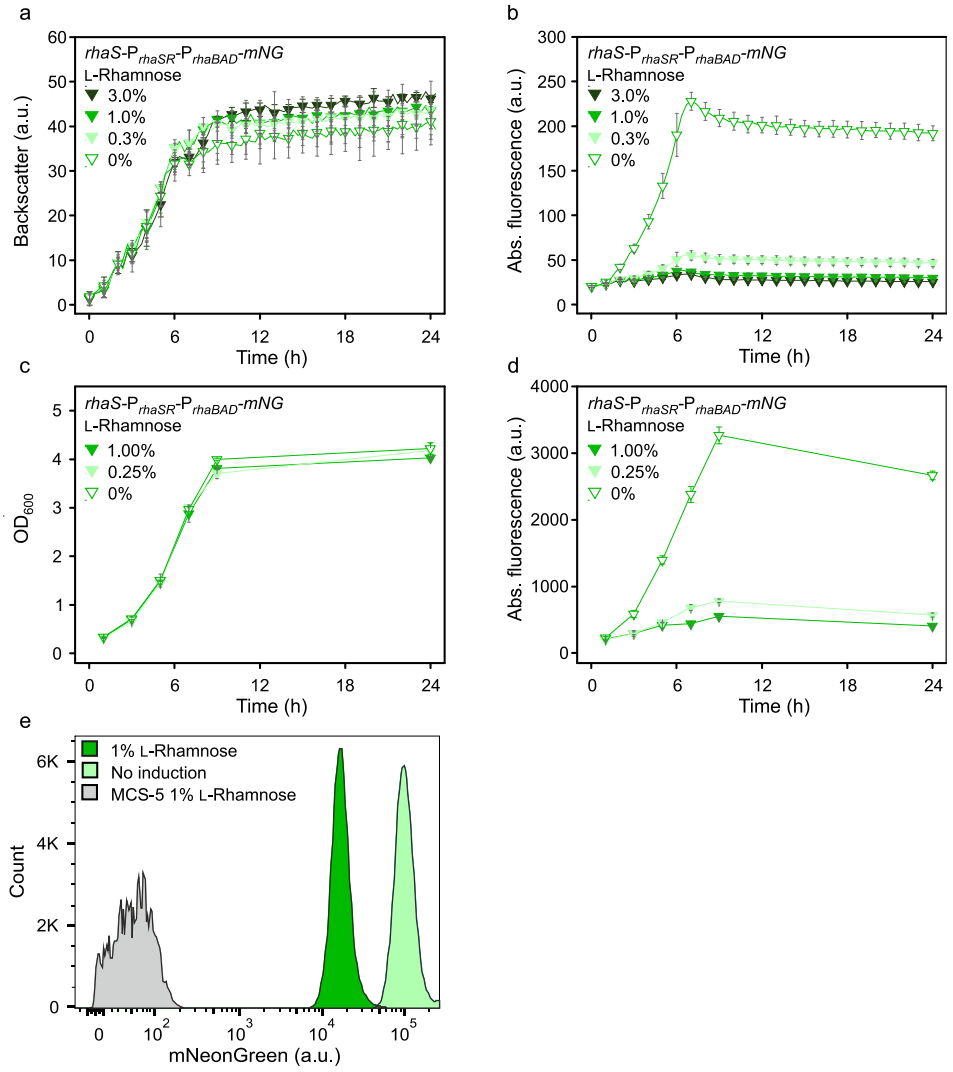

Fig. 5 RhaS-dependent repression of P_{rhaBAD} in *G. oxydans* in the presence of L-rhamnose.

(**a**) Growth according to backscatter and (**b**) absolute mNG fluorescence in *G. oxydans* 621H with plasmid pBBR1MCS-5-*rhaS*-P_{rhaSR}-P_{rhaBAD}-*mNG* in microscale BioLector cultivations without or with L-rhamnose (w/v) as indicated. BioLector settings: backscatter gain 20, fluorescence gain 40. (**c**) Growth (OD_{600}) and (**d**) absolute mNG fluorescence in *G. oxydans* 621H with plasmid pBBR1MCS-5-*rhaS*-P_{rhaSR}-P_{rhaBAD}-*mNG* in shake flask cultivations without and with L-rhamnose (w/v) as indicated. mNG fluorescence was measured in a Tecan reader (gain 60). Data represent mean values and standard deviation from two biological replicates with three technical replicates each. (**e**) FACS analysis of *G. oxydans* 621H with plasmid pBBR1MCS-5-*rhaS*-P_{rhaSR}-P_{rhaBAD}-*mNG* or empty vector pBBR1MCS-5 as a control (MCS-5). Cells were grown in shake flasks with D-mannitol medium without and with 1% (w/v) L-rhamnose. FACS analysis was performed 7 h after inoculation/induction. Total counts per sample represent 100,000 events.

Additional RhaS binding site downstream from the -10 region increased P_{rhaBAD}-derived expression almost two-fold and expanded the dynamic range of repression

The results described above demonstrated that with plasmid pBBR1MCS-5-*rhaS*-P_{rhaSR}-P_{rhaBAD}-*mNG* a strong P_{rhaBAD}-derived target gene expression could be achieved. This strong expression was repressible by only 1% (w/v) L-rhamnose down to approximately 11% (FACS measurements) or 17% (BioLector and Tecan reader measurements) residual *mNG* expression which could be reduced a little more by higher L-rhamnose concentrations. However, to possibly increase repression of P_{rhaBAD} and thereby further reduce residual P_{rhaBAD}-derived expression by RhaS already with lower L-rhamnose concentrations, we constructed and tested a plasmid with an additional RhaS binding site (+RhaS-BS) directly downstream from the -10 region of P_{rhaBAD}. Additional binding of the RhaS-L-rhamnose complex should contribute to repression of P_{rhaBAD}. It was also interesting to know the effect this RhaS-BS on the P_{rhaBAD} activity in the absence of L-rhamnose.

We used pBBR1MCS-5-*rhaS*-P_{rhaSR}-P_{rhaBAD}-*mNG* as the parental plasmid and created a copy of the 50 bp region comprising the native RhaS-BS present within P_{rhaBAD}. This copy was inserted between the -10 region and the annotated *E. coli* transcription start site of P_{rhaBAD}. The resulting plasmid was termed pBBR1MCS-5-*rhaS*-P_{rhaSR}-$P_{rhaBAD(+RhaS\text{-}BS)}$-*mNG* (Fig. 6a-c). The *mNG* expression in *G. oxydans* with plasmid pBBR1MCS-5-*rhaS*-P_{rhaSR}-$P_{rhaBAD(+RhaS\text{-}BS)}$-*mNG* containing +RhaS-BS was compared to *G. oxydans* with pBBR1MCS-5-*rhaS*-P_{rhaSR}-P_{rhaBAD}-*mNG* containing the parental P_{rhaBAD}. Grown in D-mannitol medium without and with 1% (w/v) L-rhamnose, both strains showed comparable growth independent of the plasmids or L-rhamnose supplementation (Fig. 6d). Interestingly, in the absence of L-rhamnose, the maximal mNG fluorescence with the plasmid carrying +RhaS-BS almost doubled (405 a.u.) compared to the parental plasmid (225 a.u.). This indicated additional activation of P_{rhaBAD} by RhaS in the absence of L-rhamnose (Fig. 6e). However, the levels of the absolute *mNG* expression in the presence of 1% (w/v) L-rhamnose were very similar for both constructs. Thus, +RhaS-BS did not decrease the absolute level of residual target gene expression in the presence of L-rhamnose, yet the relative residual expression level was decreased to 11% by +RhaS-BS due to the higher expression strength in the absence of L-rhamnose (parental: 225 a.u. *vs.* 38 a.u. representing 17%; +RhaS-BS: 405 a.u. *vs*. 45 a.u. representing 11%).

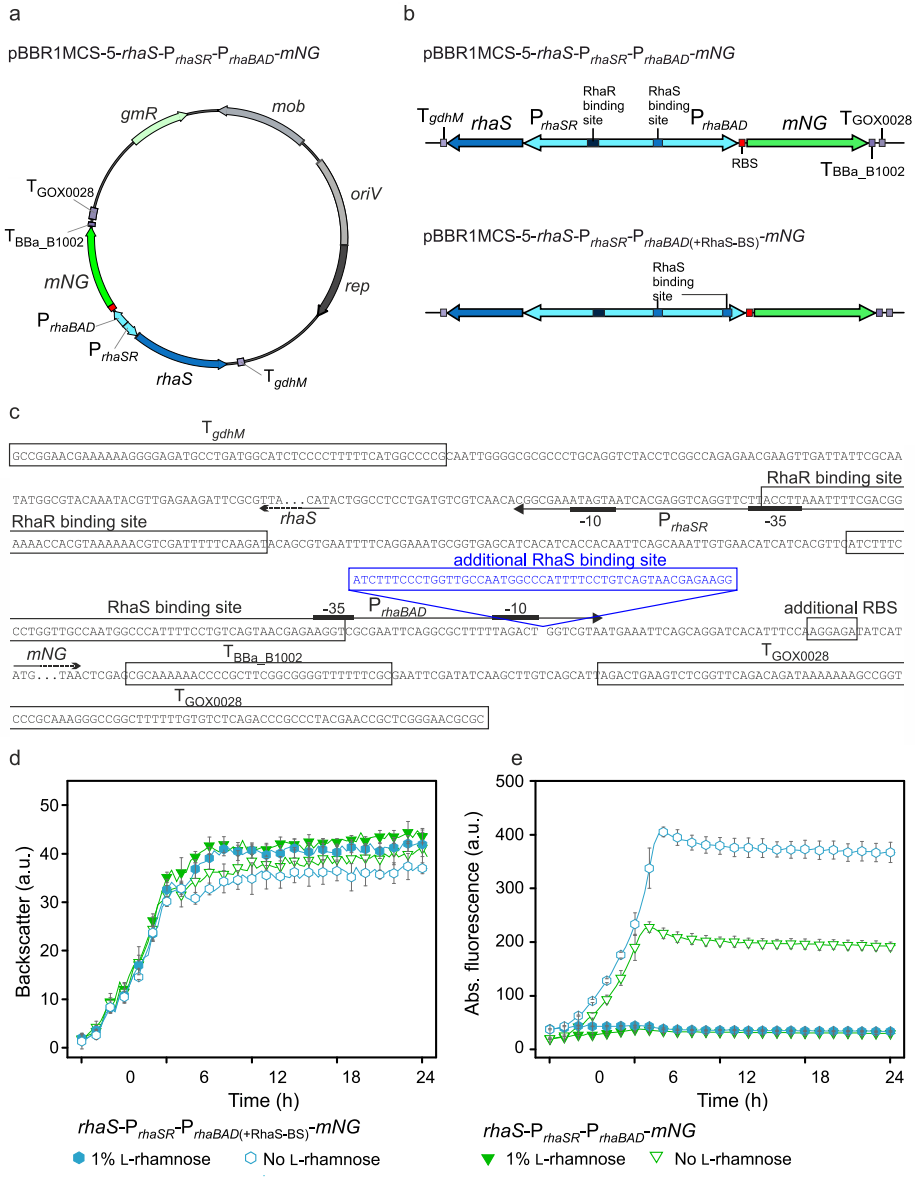

Fig. 6 Insertion of additional RhaS binding site downstream from -10 region increases apparent P_{rhaBAD} promoter strength.

(**a**) Map of plasmid pBBR1MCS-5-*rhaS*-P_{rhaSR}-P_{rhaBAD}-*mNG*. (**b**) Schematic illustration of the pBBR1MCS-5 inserts *rhaS*-P_{rhaSR}-P_{rhaBAD}-*mNG* and its variant *rhaS*-P_{rhaSR}-$P_{rhaBAD(+RhaS-BS)}$-*mNG* harboring an additional RhaS binding site directly downstream from the -10 region, all flanked by terminators. (**c**) DNA sequence details of fragment *rhaS*-P_{rhaSR}-$P_{rhaBAD(+RhaS-BS)}$-*mNG* with RhaS and RhaR binding sites as well as terminator sequences adjacent to *rhaS* and *mNG*. The promoter elements are given according to the literature {Egan, 1993 #34}. (**d**) Growth according to backscatter and (**e**) absolute mNG fluorescence of *G. oxydans* 621H carrying either plasmid pBBR1MCS-5-*rhaS*-P_{rhaSR}-P_{rhaBAD}-*mNG* (P_{rhaBAD}) or pBBR1MCS-5-*rhaS*-P_{rhaSR}-$P_{rhaBAD(+RhaS-BS)}$-*mNG* ($P_{rhaBAD(+RhaS-BS)}$) in the absence and in the presence of 1% (w/v)

L-rhamnose in microscale BioLector cultivations. Data represent mean values and standard deviation from two biological replicates with three technical replicates each. BioLector settings: backscatter gain 20, fluorescence gain 40.

For $P_{rhaBAD(+RhaS\text{-}BS)}$, the tunability of repression was tested with 0.05%, 0.1%, 0.2%, 0.3%, 1%, and 3% (w/v) L-rhamnose (Fig. 7a-d). With 1% and 3% (w/v), the reduction of the mNG fluorescence was very similar from 405 a.u. to 43 a.u. and 41 a.u., respectively, indicating that $P_{rhaBAD(+RhaS\text{-}BS)}$ like P_{rhaBAD} is almost maximally repressed by 1% (w/v) L-rhamnose. For both concentrations, the calculated residual *mNG* expression from $P_{rhaBAD(+RhaS\text{-}BS)}$ was 11% and 10%, respectively. With 0.3% (w/v) L-rhamnose, the residual mNG fluorescence was 17% (405 a.u. *vs*. 69 a.u.). With 0.05% (w/v) L-rhamnose, the mNG fluorescence was reduced approximately by half (from 406 a.u. to 197 a.u.) underlining the high sensitivity and tunability of the two P_{rhaBAD} promoters. Plotting the relative P_{rhaBAD}- and $P_{rhaBAD(+RhaS\text{-}BS)}$-derived *mNG* expression against the L-rhamnose concentrations illustrates the sensitive responsiveness of both promoters toward already low L-rhamnose concentrations (Fig. 8). While repression of both promoters exhibited similar sensitivity, non-repressed $P_{rhaBAD(+RhaS\text{-}BS)}$ was two-fold stronger than P_{rhaBAD}. In scaled-up shake flask cultivations with 0.25% and 1% (w/v) L-rhamnose, $P_{rhaBAD(+RhaS\text{-}BS)}$ showed a similar repression performance as in microscale BioLector conditions. After 9 h of growth, the maximal mNG fluorescence of the non-supplemented condition (5,833 a.u.) was reduced to 1,060 a.u. and 600 a.u. by 0.25% and 1% (w/v) L-rhamnose (Fig. 7e, f). This reduction represented 18% and 10% residual *mNG* expression.

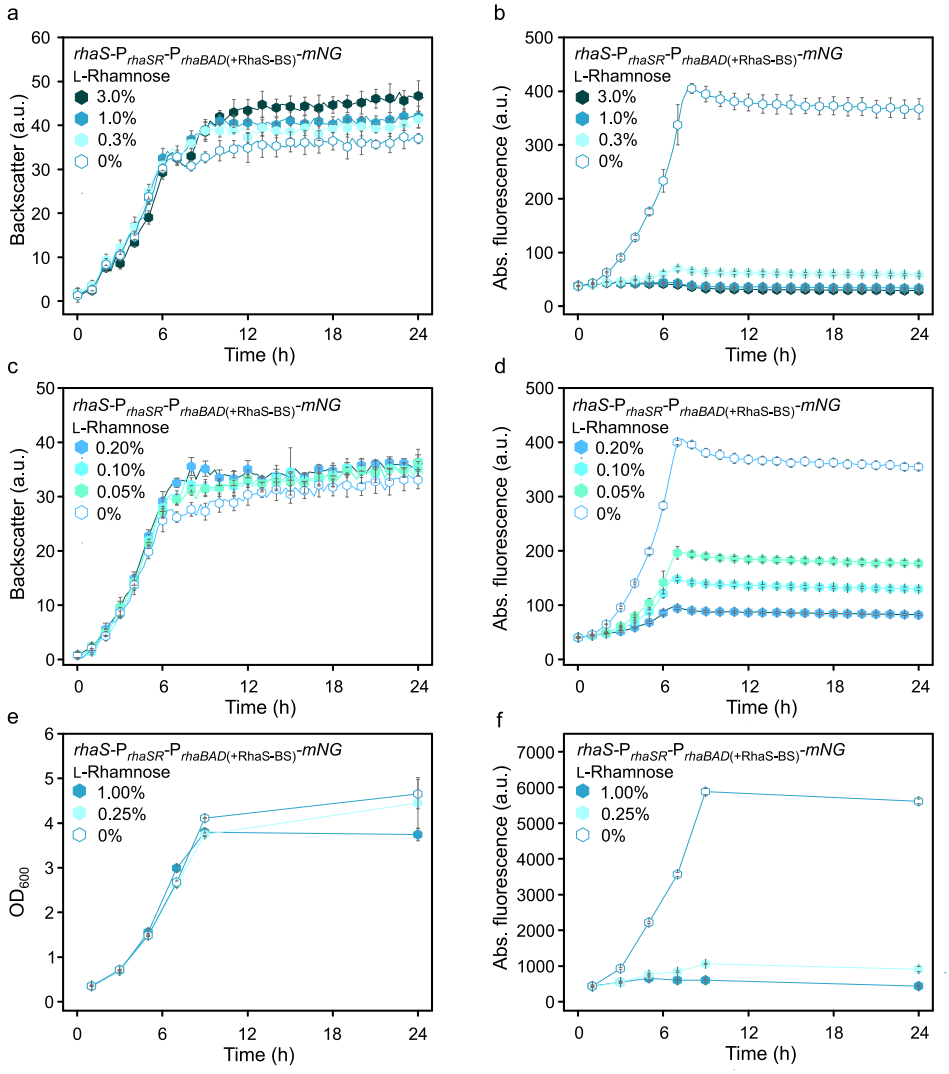

Fig. 7 Tunability of the RhaS-P$_{rhaBAD(+RhaS-BS)}$ system in *G. oxydans* 621H.

(**a, c**) Growth according to backscatter and (**b, d**) absolute mNG fluorescence of *G. oxydans* carrying plasmid pBBR1MCS-5-*rhaS*-P$_{rhaSR}$-P$_{rhaBAD(+RhaS-BS)}$-*mNG* in BioLector cultivations. L-rhamnose was supplemented in concentrations ranging from 0.05% to 3% (w/v). All data represent mean values and standard deviation from two biological replicates with three technical replicates each. BioLector settings: backscatter gain 20, fluorescence gain 40. (**e**) Growth and (**f**) absolute mNG fluorescence in shake flasks. The mNG fluorescence was measured in a Tecan reader (gain 60).

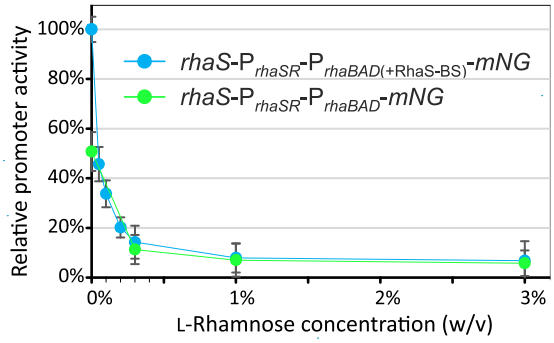

Fig. 8 Comparison of the relative P_{rhaBAD} and $P_{rhaBAD(+RhaS\text{-}BS)}$ promoter activity.

The maximal mNG fluorescence of *G. oxydans* 621H carrying either plasmid pBBR1MCS-5-*rhaS*-P_{rhaSR}-P_{rhaBAD}-*mNG* or pBBR1MCS-5-*rhaS*-P_{rhaSR}-$P_{rhaBAD(+RhaS\text{-}BS)}$-*mNG* in response to different L-rhamnose concentrations was used to calculate the relative promoter activities. The maximal $P_{rhaBAD(+RhaS\text{-}BS)}$ activity in the absence of L-rhamnose was set to 100%.

Promoter P_{rhaT} is weak and inducible in *G. oxydans*

As mentioned above, in *E. coli* RhaS also targets the promoter P_{rhaT} of the L-rhamnose permease gene. Similar to P_{rhaBAD}, P_{rhaT} contains two regulatory elements, one for RhaS and one for CRP binding and activation. Contrary to P_{rhaBAD}, the RhaS-BS on P_{rhaT} is differently composed and slightly shifted so that the binding site does not overlap with the -35 element of P_{rhaT} {Via, 1996 #36}{Wickstrum, 2010 #38}. To test whether these differences affect the regulation of P_{rhaT} by RhaS in *G. oxydans*, we constructed reporter plasmid pBBR1MCS-5-*rhaS*-P_{rhaSR}-P_{rhaT}-*mNG*. As a control, plasmid pBBR1MCS-5-P_{rhaSR}-P_{rhaT}-*mNG* lacking *rhaS* was also constructed (Fig. 9).

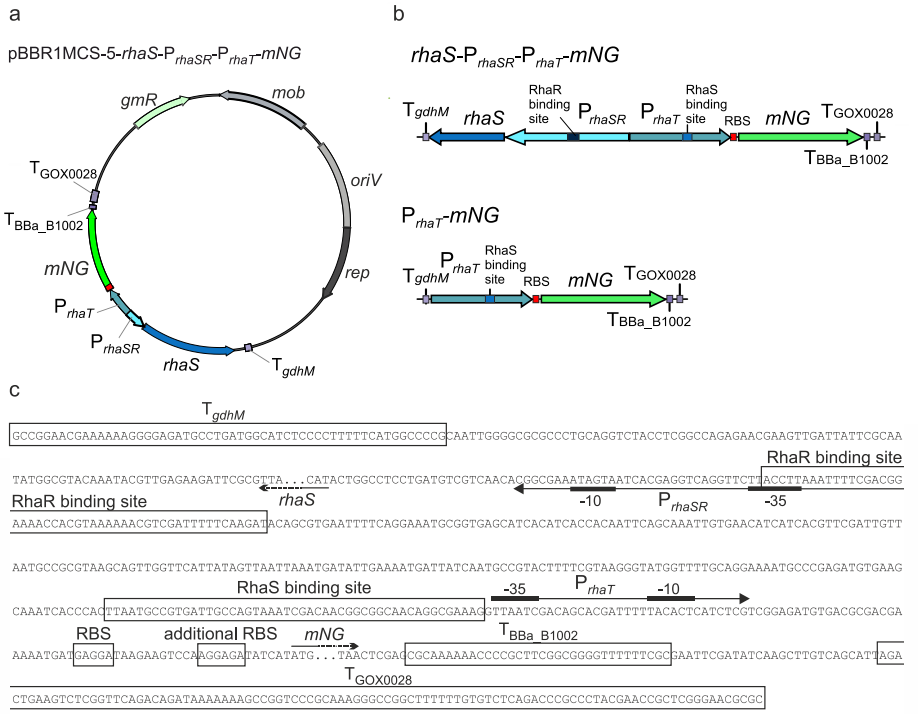

Fig. 9 Reporter plasmids with P_{rhaT} and sequence details.

(**a**) Map of plasmid pBBR1MCS-5-*rhaS*-P_{rhaSR}-P_{rhaT}-*mNG* with the fluorescence reporter gene *mNeonGreen* (*mNG*) under control of the L-rhamnose permease promoter P_{rhaT} with the adjacent *rhaS* gene, all flanked by the terminators T_{gdhM}, T_{BBa_B1002} and $T_{GOX0028}$. (**b**) Schematic illustration of the pBBR1MCS-5 inserts *rhaS*-P_{rhaSR}-P_{rhaT}-*mNG* and its variant P_{rhaT}-*mNG* lacking *rhaS*-P_{rhaSR}. (**c**) DNA sequence details with RhaS and RhaR binding sites and terminator sequences downstream from *rhaS* and *mNG*. P_{rhaT} promoter elements are given according to {Via, 1996 #36}.

In microscale BioLector cultivations, *G. oxydans* cells with pBBR1MCS-5-*rhaS*-P_{rhaSR}-P_{rhaT}-*mNG* or pBBR1MCS-5-P_{rhaT}-*mNG* also showed very similar growth independent of the plasmid or L-rhamnose (Fig. 10a). Interestingly and different to P_{rhaBAD} in *G. oxydans*, with P_{rhaT} the *mNG* expression was induced by L-rhamnose. The supplementation of 1% (w/v) L-rhamnose increased P_{rhaT}-derived mNG fluorescence ~7.5-fold (from 36 a.u. to 266 a.u.) after ~8 h of growth/induction. Together with the absolute mNG fluorescence values, this indicates a weak or moderate strength of P_{rhaT} in *G. oxydans* (Fig. 10b). Almost no mNG fluorescence was observed with plasmid pBBR1MCS-5-P_{rhaT}-*mNG* lacking *rhaS*. Thus, on the one hand P_{rhaT} was apparently not active in *G. oxydans* without RhaS and an endogenous *G. oxydans* protein did not interfere. On the other hand, RhaS activated P_{rhaT} already in the absence of L-rhamnose since with plasmid pBBR1MCS-5-*rhaS*-P_{rhaSR}-P_{rhaT}-*mNG* a low basal mNG fluorescence was observed in the absence of L-rhamnose exceeding the extremely low

mNG signals when *rhaS* was absent (Fig. 10b). It should be noted that due to the relatively weak expression from P_{rhaT} compared to P_{rhaBAD} in these BioLector cultivations the fluorescence signals were monitored with gain 70 instead of 40.

The tunability of P_{rhaT} induction was tested with L-rhamnose concentrations ranging from 0.25% to 4% (w/v). Again, growth of *G. oxydans* cells with pBBR1MCS-5-*rhaS*-P_{rhaSR}-P_{rhaT}-*mNG* was not affected differently (Fig. 10c). The P_{rhaT}-derived *mNG* expression increased gradually in an inducer-dependent manner (Fig. 10d). With 4% (w/v) L-rhamnose the induction was 9.2-fold (36 a.u. *vs*. 330 a.u.). With 0.25% (w/v) already half of the induction compared to 4% (w/v) was reached showing that the weak to moderate P_{rhaT}-derived *mNG* expression could be nicely tuned by low L-rhamnose concentrations (Fig. 10e). The low expression strength from P_{rhaT} and its tunability could be of particular interest for (membrane) proteins difficult to express.

The homogeneity of P_{rhaT} induction was analyzed by FACS using cells harvested after 7 h of growth in D-mannitol medium without or with 1% (w/v) L-rhamnose (Fig. 10f). In the absence of L-rhamnose, 97.4% of all measured cells with pBBR1MCS-5-*rhaS*-P_{rhaSR}-P_{rhaT}-*mNG* showed relatively low fluorescence signals (~1,000 a.u.). In the presence of 1% (w/v) L-rhamnose, 96.9% of the population showed about 10-fold higher mNG fluorescence signals (~10,000 a.u.). We also tested the inducible P_{rhaT}-derived *mNG* expression in scaled-up shake flask conditions with 0.3% and 1% (w/v) L-rhamnose. In all conditions, the *G. oxydans* cells with pBBR1MCS-5-*rhaS*-P_{rhaSR}-P_{rhaT}-*mNG* exhibited very similar growth (Fig. 10g). The *mNG* expression was similarly induced as in the microscale BioLector cultivations (Fig. 10h). The maximal mNG fluorescence was reached after 9 h of growth and represented 4-fold and 6-fold induction with 0.3% (50 a.u. *vs*. 210 a.u.) and 1% (w/v) L-rhamnose (50 a.u. *vs*. 297 a.u.), respectively.

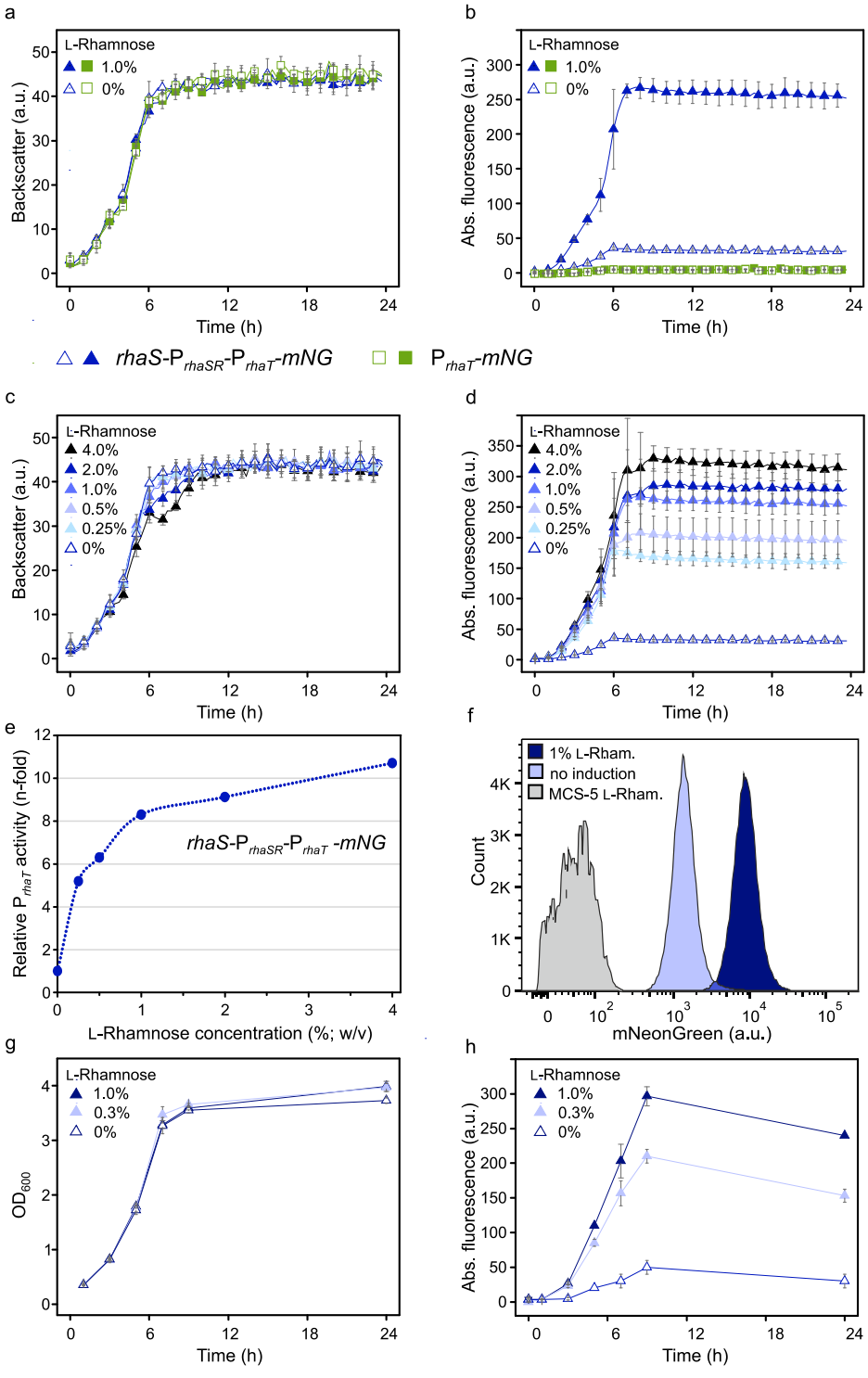
a
L-Rhamnose
1.0%
0%
Backscatter (a.u.)
Time (h)
b
L-Rhamnose
1.0%
0%
Abs. fluorescence (a.u.)
Time (h)
rhaS-P rhaSR -P rhaT -mNG
P rhaT -mNG
c
L-Rhamnose
4.0%
2.0%
1.0%
0.5%
0.25%
0%
Backscatter (a.u.)
Time (h)
d
L-Rhamnose
4.0%
2.0%
1.0%
0.5%
0.25%
0%
Abs. fluorescence (a.u.)
Time (h)
e
Relative P rhaT activity (n-fold)
rhaS-P rhaSR -P rhaT -mNG
L-Rhamnose concentration (%; w/v)
f
1% L-Rham.
no induction
MCS-5 L-Rham.
Count
mNeonGreen (a.u.)
g
L-Rhamnose
1.0%
0.3%
0%
OD600
Time (h)
h
L-Rhamnose
1.0%
0.3%
0%
Abs. fluorescence (a.u.)
Time (h)

Fig. 10 Performance of the RhaS-P_{rhaT} system in *G. oxydans* 621H.

(**a**) Growth according to backscatter and (**b**) absolute mNG fluorescence of *G. oxydans* 621H carrying plasmid pBBR1MCS-5-*rhaS*-P_{rhaSR}-P_{rhaT}-*mNG* or pBBR1MCS-5-P_{rhaT}-*mNG* lacking *rhaS*-P_{rhaSR} in microscale BioLector cultivations without and with 1% (w/v) L-rhamnose. (**c**) Growth (backscatter) and (**d**) absolute mNG fluorescence of *G. oxydans* 621H carrying plasmid pBBR1MCS-5-*rhaS*-P_{rhaSR}-P_{rhaT}-*mNG* in microscale BioLector cultivations with L-rhamnose concentrations from 0.25% to 4% (w/v) as indicated. BioLector settings: backscatter gain 20, fluorescence gain 70. (**e**) Correlation between the relative n-fold P_{rhaT} activity in *G. oxydans* 621H carrying plasmid pBBR1MCS-5-*rhaS*-P_{rhaSR}-P_{rhaT}-*mNG* and the L-rhamnose concentrations. The maximal mNG fluorescence in the absence of L-rhamnose was set to 1. (**f**) FACS analysis of *G. oxydans* 621H carrying plasmid pBBR1MCS-5-*rhaS*-P_{rhaSR}-P_{rhaT}-*mNG* or empty vector pBBR1MCS-5 (MCS-5) as a control. Cells were grown in shake flasks with D-mannitol medium without and with 1% (w/v) L-rhamnose. FACS analysis was performed 7 h after inoculation/induction. Total counts per sample represent 100,000 events. (**g**) Growth (OD_{600}) and (**h**) L-rhamnose-induced mNG fluorescence of *G. oxydans* 621H carrying plasmid pBBR1MCS-5-*rhaS*-P_{rhaSR}-P_{rhaT}-*mNG* in shake flask cultivations. The mNG fluorescence was measured in a Tecan reader (gain 60). All data represent mean values and standard deviation from two biological replicates with three technical replicates each.

Declarations

Authors' contributions
PMF and MG constructed the plasmids, carried out the growth experiments and analyzed the data. PMF and CS performed the FACS analysis and analyzed the data. JG performed the GC-TOF-MS experiments and analyzed the data. TP designed and supervised the study. PMF and TP wrote the manuscript.

Funding
We are grateful to the Federal Ministry of Education and Research (BMBF) for financial support of the project IMPRES (031B0370B). The funding organization did not influence the design of the study or collection, analysis, and interpretation of data, or writing the manuscript.

Conflicts of interest/Competing interests
The authors declare that they have no conflict of interest.

Ethical statement
This article does not contain any studies with human participants or animals performed by any of the authors.

TABLES

Table 1 Strains and plasmids used or constructed in this study.

Strain	Relevant characteristics	Reference / Source
E. coli S17-1	Δ*recA*, *endA1*, *hsdR17*, *supE44*, *thi*-1, *tra*$^+$	{Simon, 1983 #}
G. oxydans 621H	DSM 2343	DSMZ
Plasmid		
pBBR1MCS-5	Derivative of pBBR1MCS; Gm^R	{Kovach, 1995 #31}
pBBR1MCS-5-T_{gdhM}-MCS-T_{0028}	Derivative of pBBR1MCS-5 with terminator sequences of GOX0265 (T_{gdhM}) and GOX0028 ($T_{GOX0028}$) flanking the multiple cloning site	{Fricke, 2021 #13}
pBBR1MCS-5-*rhaSR*-P_{rhaSR}-P_{rhaBAD}-*mNG*	Derivative of pBBR1MCS-5-T_{gdhM}-MCS-T_{0028} with DNA fragment *rhaSR*-P_{rhaSR}-P_{rhaBAD} from *E. coli* with L-rhamnose-regulated promoter P_{rhaBAD} controlling fluorescent reporter gene *mNG* expression	This work
pBBR1MCS-5-*rhaS*-P_{rhaSR}-P_{rhaBAD}-*mNG*	Derivative of pBBR1MCS-5-*rhaSR*-P_{rhaSR}-P_{rhaBAD}-*mNG* lacking regulator gene *rhaR*	This work
pBBR1MCS-5-*rhaR*-P_{rhaSR}-P_{rhaBAD}-*mNG*	Derivative of pBBR1MCS-5-*rhaSR*-P_{rhaSR}-P_{rhaBAD}-*mNG* lacking regulator gene *rhaS*	This work
pBBR1MCS-5-P_{rhaSR}-P_{rhaBAD}-*mNG*	Derivative of pBBR1MCS-5-*rhaSR*-P_{rhaSR}-P_{rhaBAD}-*mNG* lacking operon *rhaSR*	This work
pBBR1MCS-5-*rhaS*-$P_{GOX0264}$-P_{rhaBAD}-*mNG*	Derivative of pBBR1MCS-5-*rhaS*-P_{rhaSR}-P_{rhaBAD}-*mNG* with *rhaS* constitutively expressed from strong promoter $P_{GOX0264}$	This work
pBBR1MCS-5-*rhaS*-$P_{GOX0452}$-P_{rhaBAD}-*mNG*	Derivative of pBBR1MCS-5-*rhaS*-P_{rhaSR}-P_{rhaBAD}-*mNG* with *rhaS* constitutively expressed from moderate promoter $P_{GOX0452}$	This work
pBBR1MCS-5-*mNG*-P_{rhaSR}-$P_{GOX0264}$-*rhaS*	Derivative of pBBR1MCS-5-*rhaS*-P_{rhaSR}-P_{rhaBAD}-*mNG* with *mNG* expressed from P_{rhaSR} and, in opposite direction, *rhaS* constitutively expressed from strong promoter $P_{GOX0264}$	This work
pBBR1MCS-5-*mNG*-P_{rhaSR}-$P_{GOX0452}$-*rhaS*	Derivative of pBBR1MCS-5-*rhaS*-P_{rhaSR}-P_{rhaBAD}-*mNG* with *mNG* expressed from P_{rhaSR} and, in opposite direction, *rhaS* constitutively expressed from moderate promoter $P_{GOX0452}$	This work
pBBR1MCS-5-*mNG*-P_{rhaSR}	Derivative of pBBR1MCS-5-*mNG*-P_{rhaSR}-$P_{GOX0264}$-*rhaS* lacking $P_{GOX0264}$-*rhaS*	This work
pBBR1MCS-5-*rhaS*-P_{rhaSR}-$P_{rhaBAD(+RhaS\text{-}BS)}$-*mNG*	Derivative of pBBR1MCS-5-*rhaS*-P_{rhaSR}-P_{rhaBAD}-*mNG* with an additional copy of the RhaS-binding site (RhaS-BS) in P_{rhaBAD}	This work
pBBR1MCS-5-*rhaS*-P_{rhaSR}-P_{rhaT}-*mNG*	Derivative of pBBR1MCS-5-*rhaS*-P_{rhaSR}-P_{rhaBAD}-*mNG* with P_{rhaT} controlling *mNG* expression	This work
pBBR1MCS-5-P_{rhaT}-*mNG*	Derivative of pBBR1MCS-5-*rhaS*-P_{rhaSR}-P_{rhaT}-*mNG* lacking regulator gene *rhaS*	This work

References

Ameyama M, Shinagawa E, Matsushita K, Adachi O (1981) D-fructose dehydrogenase of *Gluconobacter industrius*: purification, characterization, and application to enzymatic microdetermination of D-fructose. J Bacteriol 145(2):814-23

Antoine R, Locht C (1992) Isolation and molecular characterization of a novel broad-host-range plasmid from *Bordetella bronchiseptica* with sequence similarities to plasmids from Gram-positive organisms. Mol Microbiol 6(13):1785-99 doi:10.1111/j.1365-2958.1992.tb01351.x

Baker-Austin C, Dopson M (2007) Life in acid: pH homeostasis in acidophiles. Trends Microbiol 15(4):165-71 doi:10.1016/j.tim.2007.02.005

Baldoma L, Badia J, Sweet G, Aguilar J (1990) Cloning, mapping and gene product identification of *rhaT* from *Escherichia coli* K12. FEMS Microbiol Lett 60(1-2):103-7 doi:10.1016/0378-1097(90)90353-r

Bhende PM, Egan SM (1999) Amino acid-DNA contacts by RhaS: an AraC family transcription activator. J Bacteriol 181(17):5185-92 doi:10.1128/JB.181.17.5185-5192.1999

Chen R (2012) Bacterial expression systems for recombinant protein production: *E. coli* and beyond. Biotechnol Adv 30(5):1102-7 doi:10.1016/j.biotechadv.2011.09.013

Condon C, Fitzgerald RJ, Ogara F (1991) Conjugation and heterologous gene expression in *Gluconobacter oxydans* ssp. *suboxydans*. FEMS Microbiol Lett 80(2-3):173-178 doi:10.1016/0378-1097(91)90590-7

Connell ND (2001) Expression systems for use in actinomycetes and related organisms. Curr Opin Biotechnol 12(5):446-449 doi:10.1016/S0958-1669(00)00243-3

Dilworth MV, Piel MS, Bettaney KE, Ma P, Luo J, Sharples D, Poyner DR, Gross SR, Moncoq K, Henderson PJF, Miroux B, Bill RM (2018) Microbial expression systems for membrane proteins. Methods 147:3-39 doi:10.1016/j.ymeth.2018.04.009

Egan SM, Schleif RF (1993) A regulatory cascade in the induction of *rhaBAD*. J Mol Biol 234(1):87-98 doi:10.1006/jmbi.1993.1565

Egan SM, Schleif RF (1994) DNA-dependent renaturation of an insoluble DNA binding protein. Identification of the RhaS binding site at *rhaBAD*. J Mol Biol 243(5):821-9 doi:10.1006/jmbi.1994.1684

Evans JC, Mizrahi V (2015) The application of tetracyclineregulated gene expression systems in the validation of novel drug targets in *Mycobacterium tuberculosis*. Front Microbiol 6:812 doi:10.3389/fmicb.2015.00812

Florea M, Hagemann H, Santosa G, Abbott J, Micklem CN, Spencer-Milnes X, Garcia LD, Paschou D, Lazenbatt C, Kong DZ, Chughtai H, Jensen K, Freemont PS, Kitney R, Reeve B, Ellis T (2016) Engineering control of bacterial cellulose production using a genetic toolkit and a new cellulose-producing strain. P Natl Acad Sci USA 113(24):E3431-E3440 doi:10.1073/pnas.1522985113

Forstner M, Leder L, Mayr LM (2007) Optimization of protein expression systems for modern drug discovery. Expert Rev Prot 4(1):67-78 doi:10.1586/14789450.4.1.67

Fricke PM, Klemm A, Bott M, Polen T (2021a) On the way toward regulatable expression systems in acetic acid bacteria: target gene expression and use cases. Appl Microbiol Biotechnol 105(9):3423-3456 doi:10.1007/s00253-021-11269-z

Fricke PM, Link T, Gätgens J, Sonntag C, Otto M, Bott M, Polen T (2020) A tunable L-arabinose-inducible expression plasmid for the acetic acid bacterium *Gluconobacter oxydans*. Appl Microbiol Biotechnol 104(21):9267-9282 doi:10.1007/s00253-020-10905-4

Fricke PM, Lürkens M, Hunnefeld M, Sonntag CK, Bott M, Davari MD, Polen T (2021b) Highly tunable TetR-dependent target gene expression in the acetic acid bacterium *Gluconobacter oxydans*. Appl Microbiol Biotechnol 105(18):6835-6852 doi:10.1007/s00253-021-11473-x

Gibson DG, Young L, Chuang RY, Venter JC, Hutchison CA, Smith HO (2009) Enzymatic assembly of DNA molecules up to several hundred kilobases. Nat Methods 6(5):343-U41 doi:10.1038/Nmeth.1318

Gruber S, Schwab H, Koefinger P (2015) Versatile plasmid-based expression systems for Gram-negative bacteria - General essentials exemplified with the bacterium *Ralstonia eutropha* H16. New Biotechnol 32(6):552-558 doi:10.1016/j.nbt.2015.03.015

Gupta A, Singh VK, Qazi GN, Kumar A (2001) *Gluconobacter oxydans*: its biotechnological applications. J Mol Microb Biotech 3(3):445-56

Hanahan D (1983) Studies on transformation of *Escherichia coli* with plasmids. J Mol Biol 166(4):557-80

Hekmat D, Bauer R, Fricke J (2003) Optimization of the microbial synthesis of dihydroxyacetone from glycerol with *Gluconobacter oxydans*. Bioproc Biosyst Eng 26(2):109-16 doi:10.1007/s00449-003-0338-9

Ishii Y, Shige Y, Akasaka N, Trinugraha AC, Higashikubo H, Fukuda W, Fujiwara S (2021) Leucine-responsive regulatory protein in acetic acid bacteria is stable and functions at a wide range of intracellular pH levels. J Bacteriol 203(18):e0016221 doi:10.1128/JB.00162-21

Kallnik V, Meyer M, Deppenmeier U, Schweiger P (2010) Construction of expression vectors for protein production in *Gluconobacter oxydans*. J Biotechnol 150(4):460-465 doi:10.1016/j.jbiotec.2010.10.069

Kelly CL, Liu Z, Yoshihara A, Jenkinson SF, Wormald MR, Otero J, Estevez A, Kato A, Marqvorsen MH, Fleet GW, Estevez RJ, Izumori K, Heap JT (2016) Synthetic chemical inducers and genetic decoupling enable orthogonal control of the *rhaBAD* promoter. ACS Synth Biol 5(10):1136-1145 doi:10.1021/acssynbio.6b00030

Kersters K, Lisdiyanti P, Komagata K, Swings J (1990) The family *Acetobacteraceae*: The genera *Acetobacter*, *Acidomonas*, *Asaia*, *Gluconacetobacter*, *Gluconobacter*, and *Kozakia*. In: Dworkin M., Falkow S., Rosenberg E., Schleifer KH., Stackebrandt E. (eds) The Prokaryotes. Springer, New York, NY

Kiefler I, Bringer S, Bott M (2017) Metabolic engineering of *Gluconobacter oxydans* 621H for increased biomass yield. Appl Microbiol Biotechnol 101(13):5453-5467 doi:10.1007/s00253-017-8308-3

Kovach ME, Elzer PH, Hill DS, Robertson GT, Farris MA, Roop RM, 2nd, Peterson KM (1995) Four new derivatives of the broad-host-range cloning vector pBBR1MCS, carrying different antibiotic-resistance cassettes. Gene 166(1):175-6 doi:10.1016/0378-1119(95)00584-1

Kovach ME, Phillips RW, Elzer PH, Roop RM, 2nd, Peterson KM (1994) pBBR1MCS: a broad-host-range cloning vector. Biotechniques 16(5):800-2

Kranz A, Vogel A, Degner U, Kiefler I, Bott M, Usadel B, Polen T (2017) High precision genome sequencing of engineered *Gluconobacter oxydans* 621H by combining long nanopore and short accurate Illumina reads. J Biotechnol 258:197-205 doi:10.1016/j.jbiotec.2017.04.016

Krulwich TA, Ito M, Hicks DB, Gilmour R, Guffanti AA (1998) pH homeostasis and ATP synthesis: studies of two processes that necessitate inward proton translocation in extremely alkaliphilic *Bacillus* species. Extremophiles 2(3):217-22 doi:10.1007/s007920050063

Liu LP, Yang X, Zhao XJ, Zhang KY, Li WC, Xie YY, Jia SR, Zhong C (2020) A lambda Red and FLP/FRT-mediated site-specific recombination system in *Komagataeibacter xylinus* and its application to enhance the productivity of bacterial cellulose. ACS Synth Biol 9(11):3171-3180 doi:10.1021/acssynbio.0c00450

Mamlouk D, Gullo M (2013) Acetic Acid bacteria: physiology and carbon sources oxidation. Indian J Microbiol 53(4):377-84 doi:10.1007/s12088-013-0414-z

Menzel U, Gottschalk G (1985) The internal pH of *Acetobacterium wieringae* and *Acetobacter aceti* during growth and production of acetic acid. Arch Microbiol 143(1):47-51 doi:10.1007/Bf00414767

Mientus M, Kostner D, Peters B, Liebl W, Ehrenreich A (2017) Characterization of membrane-bound dehydrogenases of *Gluconobacter oxydans* 621H using a new system for their functional expression. Appl Microbiol Biotechnol 101(8):3189-3200 doi:10.1007/s00253-016-8069-4

Paczia N, Nilgen A, Lehmann T, Gatgens J, Wiechert W, Noack S (2012) Extensive exometabolome analysis reveals extended overflow metabolism in various microorganisms. Microb Cell Fact 11:122 doi:10.1186/1475-2859-11-122

Pappenberger G, Hohmann HP (2014) Industrial production of L-ascorbic acid (vitamin C) and D-isoascorbic acid. Adv Biochem Eng Biotechnol 143:143-88 doi:10.1007/10_2013_243

Parachin NS, Mulder KC, Viana AAB, Dias SC, Franco OL (2012) Expression systems for heterologous production of antimicrobial peptides. Peptides 38(2):446-456 doi:10.1016/j.peptides.2012.09.020

Peters B, Mientus M, Kostner D, Junker A, Liebl W, Ehrenreich A (2013) Characterization of membrane-bound dehydrogenases from *Gluconobacter oxydans* 621H *via* whole-cell activity assays using multideletion strains. Appl Microbiol Biotechnol 97(14):6397-412 doi:10.1007/s00253-013-4824-y

Saito Y, Ishii Y, Hayashi H, Imao Y, Akashi T, Yoshida M, Niwa M, Hosoda J, Shimomura K (1997) Cloning of genes coding for L-sorbose and L-sorbosone dehydrogenases from *Gluconobacter oxydans* and microbial production of 2-keto-L-gulonate, a precursor of L-ascorbic acid, in a recombinant *G. oxydans* strain. Appl Environ Microb 63(2):454-60

Sambrook J, Fritsch EF, Maniatis T (1989) Molecular cloning: a laboratory manual. Cold Spring Harbor Laboratory Press, Cold Spring Harbor, NY

Schnappinger D, Ehrt S (2014) Regulated expression systems for mycobacteria and their applications. Microbiol Spectr 2(1) doi:10.1128/microbiolspec.MGM2-0018-2013

Schweikert S, Kranz A, Yakushi T, Filipchyk A, Polen T, Etterich H, Bringer S, Bott M (2021) FNR-type regulator GoxR of the obligatorily aerobic acetic acid bacterium *Gluconobacter oxydans* affects expression of genes involved in respiration and redox metabolism. Appl Environ Microbiol 87(11) doi:10.1128/AEM.00195-21

Shaner NC, Lambert GG, Chammas A, Ni Y, Cranfill PJ, Baird MA, Sell BR, Allen JR, Day RN, Israelsson M, Davidson MW, Wang J (2013) A bright monomeric green fluorescent protein derived from *Branchiostoma lanceolatum*. Nat Methods 10(5):407-9 doi:10.1038/nmeth.2413

Simon R, Priefer U, Pühler A (1983) A broad-host range mobilization system for *in vivo* genetic-engineering - transposon mutagenesis in Gram-negative bacteria. Bio-Technol 1(9):784-791 doi:DOI 10.1038/nbt1183-784

Teh MY, Ooi KH, Teo SXD, Bin Mansoor ME, Lim WZS, Tan MH (2019) An expanded synthetic biology toolkit for gene expression control in *Acetobacteraceae*. ACS Synth Biol 8(4):708-723 doi:10.1021/j.acssynbio.8b00168

Terpe K (2006) Overview of bacterial expression systems for heterologous protein production: from molecular and biochemical fundamentals to commercial systems. Appl Microbiol Biotechnol 72(2):211-22 doi:10.1007/s00253-006-0465-8

Tkac J, Navratil M, Sturdik E, Gemeiner P (2001) Monitoring of dihydroxyacetone production during oxidation of glycerol by immobilized *Gluconobacter oxydans* cells with an enzyme biosensor. Enzyme Microb Tech 28(4-5):383-388

Tobin JF, Schleif RF (1987) Positive regulation of the *Escherichia coli* L-rhamnose operon is mediated by the products of tandemly repeated regulatory genes. J Mol Biol 196(4):789-799 doi:10.1016/0022-2836(87)90405-0

Valero F (2012) Heterologous expression systems for lipases: A review. Methods Mol Biol 861:161-178 doi:10.1007/978-1-61779-600-5_11

Via P, Badia J, Baldoma L, Obradors N, Aguilar J (1996) Transcriptional regulation of the *Escherichia coli rhaT* gene. Microbiology 142 (Pt 7):1833-40 doi:10.1099/13500872-142-7-1833

Wang EX, Ding MZ, Ma Q, Dong XT, Yuan YJ (2016) Reorganization of a synthetic microbial consortium for one-step vitamin C fermentation. Microb Cell Fact 15:21 doi:10.1186/s12934-016-0418-6

Wickstrum JR, Skredenske JM, Balasubramaniam V, Jones K, Egan SM (2010) The AraC/XylS family activator RhaS negatively autoregulates *rhaSR* expression by preventing cyclic AMP receptor protein activation. J Bacteriol 192(1):225-32 doi:10.1128/JB.00829-08

3 Discussion

The AAB *G. oxydans* is well-known among industrially relevant microorganisms due to its ability to incompletely oxidize a wide range of carbohydrates stereo- and regioselectively. For this reason, *G. oxydans* has been used since the 1930s in various applications of which the synthesis of L-sorbose, a precursor for vitamin C production, is the most prominent one. Despite this long-time experience, hitherto no regulatable, low-cost, tight, and strongly inducible expression system has been reported in the literature for *G. oxydans*. Moreover, also in the other most frequently used and studied AAB genera *Komagataeibacter*, *Acetobacter*, *Gluconacetobacter*, and *Acidiphilium* only one inducible expression system with low to moderate induction ratios has been reported (Teh et al. 2019, reviewed in Fricke et al. 2021a). Therefore, in this work the regulator-promoter pairs AraC-P_{araBAD}, TetR-P_{tet}, LacI-P_{lacUV5}, as well as RhaSR-P_{rhaBAD} were tested and could successfully be used to establish pBBR1MCS-5-based plasmid expression systems in *G. oxydans* 621H, which form the basis of a well-characterized, comprehensive genetic toolkit that enables controlled target gene expression in *G. oxydans* and possibly other AAB. Furthermore, the genome of *G. oxydans* was screened for regulatable promoters by global transcriptome analyses in stimulon-response experiments and two promising candidates, $P_{GOX0536}$ and $P_{GOX0532}$, were found that might be usable for controlled target gene expression in *G. oxydans* strains classified as non-GMOs.

3.1 The AraC-P_{araBAD} system in *G. oxydans*

The regulator-promoter pair AraC-P_{araBAD} from *E. coli* K12 MC4100 performed very well in *G. oxydans* as it combined strong L-arabinose-inducible and tunable target gene expression with very low basal expression in the absence of L-arabinose, leading to up to 480-fold induction ratios. Many regulatable expression systems, such as the TetR-P_{tet} and LacI-P_{lac}, systems, are based on promoter repression and release of specific promoter target sequences depending on the presence of the effector molecule of corresponding transcriptional regulator. However, in the AraC-P_{araBAD} system, apo-AraC acts as a repressor of P_{araBAD} by binding operator sites in the absence of L-arabinose and looping the DNA, thereby preventing transcription. Being also involved in transcription activation, the AraC-L-arabinose complex unloops promoter DNA and stimulates P_{araBAD}-driven expression, thus sensing L-arabinose in the environment (Soisson et al. 1997, Schleif, 2010). Besides AraC-dependent regulation, transcription from the promoter P_{araBAD} in *E. coli* is also activated by the cAMP receptor protein (CRP) in the absence of a preferred carbon and energy source through opening of the DNA loop and enabling either RNA polymerase binding or the transition from the closed to the open complex (Lobell & Schleif, 1991, Schleif, 2010). There is only one

regulator termed GoxR (GOX0974) encoded in the genome of *G. oxydans* that belongs to the CRP/fumarate-nitrate reduction regulator (FNR) superfamily of proteins. GoxR is a member of the FNR subfamily and not a cAMP-binding protein, making the AraC-P_{araBAD} system independent of CRP-based catabolite repression in *G. oxydans* (Schweikert et al. 2021). Furthermore, the conducted experiments with the plasmid pBBR1MCS-5-P_{araBAD}-*mNG* lacking *araC* demonstrated that in *G. oxydans* transcription from P_{araBAD} without AraC does not take place and induction of P_{araBAD} by L-arabinose specifically requires AraC and no *G. oxydans* protein interferes. This indicated that *E. coli* AraC interacts with *G. oxydans* RNAP for transcription activation. Interestingly, since no expression of *mNG* with *G. oxydans* harboring pBBR1MCS-5-P_{araBAD}-*mNG* could be detected, AraC is not needed for repression of P_{araBAD} in *G. oxydans*. Nevertheless, it cannot be ruled out that endogenous *G. oxydans* proteins with a lower affinity for the P_{araBAD} promoter than AraC are involved in promoter repression when plasmids are used that are lacking *araC*.

Previous studies on the implementation of the *E. coli* AraC-P_{araBAD} system in the AAB *Gluconacetobacter xylinus* 700178, *Gluconacetobacter hansenii* 53582, and *Komagataeibacter rhaeticus* reported 5- to 12-fold induction upon the supplementation of 4% L-arabinose. In spite of strong reporter gene expression in induced cultures, only low induction ratios were achieved due to high basal expression in the absence of L-arabinose (Teh et al. 2019). The reasons for the leakiness of P_{araBAD}-controlled expression in these AAB are unknown. In contrast to *G. oxydans* where P_{araBAD} is inactive without AraC and thus does not require repression by AraC in the non-induced condition, P_{araBAD} could be active in *Komagataeibacter* and *Gluconacetobacter* without AraC and thus does require repression by AraC in the absence of the inducer. Possibly, the regulator AraC may not bind to the operator DNA as strongly in these AAB as required for full repression.

While in *E. coli* expression from P_{araBAD} is fully induced with 0.2% L-arabinose (Guzman et al. 1995), much higher L-arabinose concentrations of 1% were required for maximal target gene expression in *G. oxydans* carrying plasmid pBBR1MCS-5-*araC*-P_{araBAD}-*mNG*. The fact that effector concentrations up to 4% were also required for full induction in *K. xylinus*, *Ga. hansenii*, and *K. rhaeticus* reflects an altered inducer responsiveness of the AraC-P_{araBAD} system in *G. oxydans* and AAB in general. Possibly, like for *G. oxydans*, L-arabinose is metabolized by these AAB, thereby reducing the actual effector concentration in the cells. For *G. oxydans*, previous studies and GC-TOF-MS analysis conducted in this work showed that the membrane-bound glucose dehydrogenase (GdhM) oxidized L-arabinose to L-arabinonic acid (Mientus et al. 2017). Surprisingly, using the multi-deletion strain BP.6, which lacks GdhM and is therefore incapable of L-arabinose oxidation, did not alter the inducer responsiveness of the system when compared to strain 621H. Based on these results, it seems unlikely that effector degradation was responsible for the poor performance of the AraC-P_{araBAD}

system in other AAB than *G. oxydans*. Possibly the need for higher effector concentrations for fully induced P_{araBAD}-derived expression in *G. oxydans* and other AAB was rather caused by an inefficient uptake of L-arabinose into the cells. The fact that in the case of the aromatic inducer molecule anhydrotetracycline of the TetR-P_{tet} system, which passes membranes by diffusion, similar concentrations were required in *G. oxydans* and *E. coli* supports the assumption that the uptake of effectors that cannot cross the membrane by diffusion is responsible for different sensitivities. Little is known about sugar uptake in *G. oxydans* in general and no L-arabinose transporter has been described in literature or annotated in the genome (Prust et al. 2005). Searching for a potential L-arabinose transporter in *G. oxydans* with the amino acid sequence of the *E. coli* L-arabinose transporter AraE using BLASTP revealed three proteins of which two are annotated as galactose-proton symporters (GOX0808: 56% identity; GOX1971: 46% identity) and one as a sugar-proton symporter (GOX0649: 51% identity). No data on these transporters concerning substrate-specificity or physiological function are available. Hence, it can only be assumed that at least one of them is promiscuous and imports L-arabinose in small quantities as a side reaction. Trying to increase effector uptake in *G. oxydans* by co-expressing *E. coli araE* together with *araC* from the *araC* promoter P_C did not improve the responsiveness of the AraC-P_{araBAD} system towards lower effector concentrations. On the contrary, P_{araBAD}-derived *mNG* expression even decreased with this construct. While the reasons for this result remain unclear, it can be hypothesized that co-expression of *araC* and *araE* destabilized the mRNA due to the longer transcripts, thereby reducing AraC activator protein abundance with the consequence of less P_{araBAD}-derived *mNG* expression. Nevertheless, overall the obtained results proved the functionality and potential of the AraC-P_{araBAD} system in *G. oxydans* and possibly also other AAB.

3.2 L-Arabinonic acid production with *G. oxydans*

In this study, it was shown that *G. oxydans* bears the potential to be an excellent producer of the valuable compound L-arabinonic acid by oxidation of L-arabinose with the membrane-bound glucose DH GdhM. Already without strain and process optimization, *G. oxydans* 621H grown in pH-controlled fed-batch bioreactors with complex D-mannitol medium and repeated 8% (w/v) L-arabinose feeding produced 133 g/L (801 mM) L-arabinonic acid in 144 h. In previous studies, it was reported that expression of the L-arabinose/ D-galactose 1-dehydrogenase AraDH from *Rhizobium leguminosarum* in *Saccharomyces cerevisiae* resulted in 18 g/L L-arabinonic acid from L-arabinose within 118 h (Aro-Kärkkäinen et al. 2014). This product titer was increased with an engineered *E. coli* strain characterized by an inactivated L-arabinose metabolism. Here the expression of the L-arabinose dehydrogenase AraDH from *Azospirillum brasilense* led to an L-arabinonic acid titer of 43.9 g/L

in 36 h (Liu et al. 2014). While with *G. oxydans* 621H the previously reported product titers were tripled, productivity of *G. oxydans* overexpressing plasmid-borne *gdhM* did not meet the expectations. Constitutive *gdhM* expression from plasmid pMM4a resulted in reduced growth and presumably increased sensitivity towards stress. The plasmid pMM4a conveys resistance towards the antibiotic kanamycin for selection. Our previous study showed that the use of plasmid pBBR1MCS-2 also encoding kanamycin resistance correlated with abnormal cell morphology in *G. oxydans* (Fricke et al. 2021b). Therefore, it might be that selection for pMM4a maintenance with kanamycin in combination with the constitutive overexpression of *gdhM* was detrimental for cell membrane integrity under the osmotic stress conditions caused by the base titration for pH maintenance and the high L-arabinose and L-arabinonic acid concentrations. The plasmid pBBR1MCS-5 could be a valuable alternative for pMM4a as it uses gentamicin for selection and was shown not to effect cell morphology of plasmid-harboring strains. Moreover, it is very likely that in an optimized process, *e.g.* with adapted feeding strategies and timely regulated and tuned expression of *gdhM*, the L-arabinonic acid titer and productivity could be further increased.

3.3 The TetR-P_{tet} system in *G. oxydans*

With the pBBR1MCS-5-based regulator-promoter pair TetR-P_{tet}, an inducible expression system was found for *G. oxydans* that even outperformed the previously presented AraC-P_{araBAD} system. Based on the *E. coli* transposon Tn*10*, expression from the promoter P_{tet} was barely detectable in the absence of the effector anhydrotetracycline (ATc) and very strong when fully induced. The expression strength of target genes controlled by P_{tet} could be tuned over a wide range of induction ratios by adapting the ATc concentration. Due to the extremely low basal expression in the absence of ATc and P_{tet} being a very strong promoter in *G. oxydans*, induction ratios of more than 3,500-fold were obtained. These results demonstrate that regulatable expression systems that solely rely on heterologous repressor proteins that dissociate from the promoter after binding their respective effector can perform very well in *G. oxydans*.

In previous studies, the TetR-P_{tet} system was tested for controlled target gene expression in the AAB *K. rhaeticus* iGEM using the fluorescent protein mRFP1 as a reporter (Florea et al. 2016). Here the system was characterized by an overall moderate expression, a high basal expression in the absence of ATc, and induction ratios <2 when 1 µg mL^{-1} ATc was added to the cultures. The reasons for the high leakiness are unclear. In all tests conducted in our study with the TetR-P_{tet} system in *G. oxydans* under no circumstances strong basal expression was observed, independent of the plasmid backbone, the use of terminators, or the pH of the medium. When compared, a striking difference in the composition of the constructs used in *K. rhaeticus* iGEM and in *G. oxydans* was noticed. While in the *G. oxydans* plasmid

tetR and P_{tet} were organized as on transposon Tn*10* with *tetR* being controlled by P_{tetR} and divergently oriented toward P_{tet}, in the *K. rhaeticus* iGEM plasmid *tetR* was expressed from the promoter P_{J23118} or P_{lacI} upstream and in the same orientation as P_{tet} with two terminators between *tetR* and P_{tet}. Furthermore, the promoter P_{tet} in *K. rhaeticus* iGEM contained two copies of the operator sequence $tetO_2$ being 6 bp apart, whereas within P_{tet} of Tn*10* two slightly different operator sites ($tetO_1$ and $tetO_2$) are located 11 bp apart (Florea et al. 2016). For *G. oxydans*, it was shown that minor differences in DNA sequence, such as a single base pair exchange between the ribosome binding site and the start codon of P_{araBAD} or the insertion of a recognition site for a restriction endonuclease between the stop codon and the adjacent downstream terminator, or even both, affected the overall performance of the expression system (Fricke et al. 2020). Assuming that the terminators placed downstream from *tetR* were effective in preventing potential read-through in *K. rhaeticus* iGEM, a low expression of *tetR* and/or an inefficient binding of TetR to its operator sites might be responsible for the inability to repress P_{tet} in *K. rhaeticus* iGEM.

Since 2006, most publications on *Gluconobacter* reporting recombinant gene expression have used broad-host-range pBBR1MCS-based plasmids, making it the major expression plasmid lineage used in this genus. Plasmids pBBR1MCS-2 and pBBR1MCS-5 were the most popular representatives, being used in 25 and 27 studies, respectively (Fricke et al. 2021a). They harbor the genes *neoR*/*kanR* and *aacC1* that confer resistance against kanamycin and gentamicin, respectively. In case of *neoR*/*kanR,* transcription of this gene could lead to antisense transcripts to the mRNA of the target gene (here *mNeonGreen*) due to the orientation of the resistance cassette (Kovach et al. 1995). In our study we showed that the TetR-P_{tet} system performed much worse in pBBR1MCS-2- than in pBBR1MCS-5-based plasmids. While repression of P_{tet} was not affected by the plasmid backbone, reporter gene expression in induced cells was almost reduced by half in the pBBR1MCS-2-based plasmid. Furthermore, unlike with the pBBR1MCS-5 derivative, *G. oxydans* harboring pBBR1MCS-2-based plasmids exhibited an unusual elongated cell morphology. It is unclear whether the abnormal morphology was caused by the supplemented kanamycin or the neomycin/kanamycin 3'-phosphotransferase activity conveying the resistance. For *G. oxydans*, it was shown that osmotic stress, caused for example by high concentrations of sucrose or glycerol, may cause involution forms which are characterized by enlarged swollen cells, long filamentous cells, or other abnormal morphologies (Ohrem & Voß, 1996, De Muynck et al. 2007, Zahid et al. 2015). Furthermore, sublethal concentrations of the aminoglycoside amikacin led to cell elongations in *E. coli*, possibly due to the inability to properly assemble the Z ring (Possoz et al. 2007). Since the applied kanamycin concentrations certainly do not cause osmotic stress, the exact reasons for the anomalous cell morphology or the worse performance of expression plasmids with kanamycin resistance remain to be elucidated. Therefore, in *G.*

oxydans the pBBR1MCS-5 derivative with gentamicin resistance should always be the first choice for expression plasmids.

3.4 The LacI-P_{lacUV5} system in *G. oxydans*

Our studies showed that in *G. oxydans* 621H the LacI-P_{lacUV5} system from *E. coli* BL21 suffered from leaky expression in the absence of IPTG. Additionally, in comparison with the promoters P_{araBAD} or P_{tet}, P_{lacUV5} reached only moderate expression levels when fully induced, resulting in merely 40-fold maximal induction ratios. A previous study already reported that expression from *E. coli* P_{lac} was rather weak in *G. oxydans* 621H, probably due to inefficient recognition of the promoter by the *G. oxydans* RNAP (Kallnik et al. 2010). Our study showed that P_{lacUV5}, differing from P_{lac} by three base pair changes of which two are at positions −9 and −8, is equally weak in *G. oxydans* than the parental promoter P_{lac} (Hirschel et al. 1980).

Even though P_{lac} is the most used heterologous promoter in AAB, only three studies previously reported the use of IPTG-induced gene expression from P_{lac} or one of its derivatives in AAB (reviewed in Fricke et al. 2021a). The first study reported a 4-6-fold induction of *lacZ* expression in *G. oxydans*, pointing out that induced activity was less than 5% compared to fully induced levels in *E. coli* and that repression of P_{lac} was highly leaky in the absence of IPTG (Condon et al. 1991). The other two studies describing IPTG-induced expression from P_{lac} or one of its derivatives in *Komagataeibacter xylinus* and *Acetobacter orleanensis* did not present data on the basal expression in the absence of IPTG (Bugala et al. 2016, Liu et al. 2020). Therefore no general rule on leakiness of P_{lac} in AAB can be derived from these studies.

To exclude the possibility that endogenous proteins of *G. oxydans* interfered with P_{lacUV5}-derived expression, we constructed and tested a plasmid lacking P_{lacI}-*lacI*. The experiment showed that the inducibility of P_{lacUV5} solely depended on the derepression by LacI. Interestingly, the lack of P_{lacI}-*lacI* drastically reduced expression strength from P_{lacUV5}. Different from most regulator genes and their target promoters, *lacI* is located directly upstream of P_{lacUV5} and transcribed in the same direction as the *lac* operon. Thus, the obtained results suggested that read-through from P_{lacI}-*lacI* contributed to the expression of P_{lacUV5}-*mNG*. To circumvent potential read-through from P_{lacI}, a plasmid was constructed placing P_{lacI}-*lacI* in the opposite orientation toward P_{lacUV5}-*mNG*. Contrary to the expectation, this modification did not alter induced *mNG* expression and even increased leakiness of P_{lacUV5}, thereby reducing induction ratios by ~50%. Horowitz & Platt (1982) determined in *in vitro* transcription experiments mRNA species using a DNA construct as a template on which the *trp* promoter is placed upstream of *lacI*-P_{lac}-*lacZ*. Besides two mRNA species resulting from transcription initiated from the two promoters until the end of the template, a third mRNA was identified that was the product of P_{trp} promoted transcription and termination between the stop codon of *lacI* and P_{lac}. Despite little resemblance of the DNA sequence where the transcription was terminated to classic

terminator structures, this site was found to clearly function as a terminator preventing read-through from P_{lacI}-*lacI*. Furthermore, it was reported that the site exhibits homology to the atypical, factor-dependent termination sites *rrnB* t_L and *trp t'* that were shown to respond to the elongation factor NusA (Greenblatt et al. 1980, Kingston & Chamberlin, 1981, Platt, 1981, Horowitz & Platt, 1982). In the genome of *G. oxydans*, GOX1580 is annotated as *nusA* and the encoded protein shows 44% sequence identity to *E. coli* NusA (Prust et al. 2005). It is not clear whether the putative terminator site between *lacI* and P_{lacUV5} requires NusA for termination or whether *G. oxydans* NusA is capable to recognize the secondary mRNA termination structure described by Horowitz & Platt (1982). Since the tests with inverted P_{lacI}-*lacI* conducted in this work did not reduce basal expression from P_{lacUV5} in *G. oxydans*, it is unlikely that failed transcription termination between *lacI* and P_{lacUV5} caused the high leakiness. It appeared more probable that insufficient repression of P_{lacUV5} by LacI is responsible for the high basal expression from the promoter in the absence of IPTG. One possible reason might be a reduced ability of LacI to bind the operator sites at lower pH as suggested by computational protein-DNA binding simulations (Fricke et al. 2021b). When the AraC-P_{araBAD} system was tested, it was shown that the oxidation of the inducer L-arabinose to L-arabinonic acid strongly acidified the medium and resulted in drastically decreased intracellular reporter activity. This loss of activity could be regained when cells were transferred into fresh medium of pH 6, indicating that the intracellular pH was affected by the acidification of the medium (Fricke et al. 2020). During growth, the pH of the routinely used D-mannitol medium initially set to 6 drops to pH 4.6-4.7 independent of the supplementation of IPTG (Fricke et al. 2021b). Whether cytoplasmic pH and as a result LacI-dependent repression of P_{lacUV5} are affected by this acidification is not known.

For functionality of the *lac* operon in *E. coli*, some basal expression from P_{lac} is required as LacZ, encoded by the first gene of the operon, catalyzes the reaction that produces the inducer molecule allolactose from lactose. The second gene of the operon, *lacY*, codes for a lactose permease, which contributes to the dynamic process of P_{lac} induction. For *E. coli* it was shown that although the allolactose-analogon IPTG can pass the cell membrane independently of LacY at higher concentrations, at lower concentrations the lactose permease is the main route to enter the cell (Jensen et al. 1993, Marbach & Bettenbrock, 2012, Fernández-Castané et al. 2012). In *G. oxydans*, ~3 mM IPTG were required for full induction of P_{lacUV5}-derived expression. A protein BLAST search with LacY in the proteome of *G. oxydans* revealed a homologous protein with 33% identity annotated as DHA2 family efflux MFS transporter permease subunit. It is unknown whether this protein transports IPTG into the cell. Since it is annotated as an efflux pump, it seems not very likely that it is involved in the uptake of IPTG. Hence, the lack of a transporter that also imports IPTG is likely the reason for the high inducer concentrations required for full induction in *G. oxydans.* Alternatively, the possibility

cannot be excluded that in *G. oxydans* IPTG is altered by one or more enzymes. For example, it was shown that IPTG is acetylated by LacA, converting the effector to 6-O-acetyl-β-D-thiogalactopyranoside, which does not induce transcription from P_{lac} (Herzenberg, 1961). A biotransformation experiment with IPTG as previously performed with L-arabinose could help to determine if this molecule is metabolized by *G. oxydans* (Fricke et al. 2020).

3.5 The RhaS-P_{rhaBAD} system in *G. oxydans*

The regulatable promoters P_{rhaBAD} and P_{rhaT} from *E. coli* turned out to be suitable candidates to further expand the expression toolbox available for *G. oxydans* 621H and potentially other AAB. With P_{rhaBAD}, the first promoter for *G. oxydans* was found that allows the controlled down-regulation of target gene expression by gradually increasing the effector concentration. In plasmid-based assays with pBBR1MCS-5 derivatives, the otherwise very strong *mNG* expression from P_{rhaBAD} could be dimmed as desired to a minimum of approximately 8% residual expression by increasing the L-rhamnose concentration up to 3% (w/v) compared to the non-supplemented reference culture. In doing so, the RhaS-P_{rhaBAD} system exhibited a reverse responsiveness in *G. oxydans* compared to *E. coli* where P_{rhaBAD}-driven expression is induced by L-rhamnose. Interestingly, for the *E. coli* promoter P_{rhaT} no reverse responsiveness towards L-rhamnose was observed in *G. oxydans*. P_{rhaT}-driven expression was inducible reaching low expression levels with 4% L-rhamnose resulting in a maximal induction ratio of only 9.2-fold.

RhaR and RhaS both belong to the AraC/XylS family of transcriptional regulators (Tobin & Schleif, 1987). Within this protein family most regulators interact with the C-terminal domain (CTD) of the α-subunit of the RNAP to activate transcription (reviewed in Ebright & Busby, 1995). Also for RhaSR-P_{rhaBAD} it was shown that deletion of the α-CTD in combination with a truncated P_{rhaBAD} promoter that permitted only RhaS activation reduced expression 180-fold in *E. coli*, suggesting a direct interaction of RhaS and the α-subunit of the RNAP (Holcroft & Egan, 2000). Nevertheless, some members of the AraC/XylS family may also activate transcription through interaction of the regulators with the sigma 70 factor (σ^{70}) subunit RpoD of the RNAP. This mode of activation is often indicated by overlapping regulator binding sites and –35 elements (Lonetto et al. 1998, Bhende & Egan, 2000). Within P_{rhaBAD} 4 bp of the RhaS binding site overlap with the –35 hexamer of the promoter. Among the family of σ^{70} transcription factors, the C-terminus is highly conserved as it contains DNA-binding domains and well-defined functional regions (Hakimi et al. 2000, reviewed in Paget, 2015). In alanine substitution experiments, it was shown that D241 and D250 of RhaS and K593 and R599 of σ^{70} are likely interacting residues required for RhaS-dependent activation of P_{rhaBAD} (Bhende & Egan, 2000, Wickstrum & Egan, 2004). Since RhaS-P_{rhaBAD} showed a reverse responsiveness in

G. oxydans and *E. coli*, the C-terminal regions of the σ^{70} factors were compared in an amino acid sequence alignment (Fig. 1).

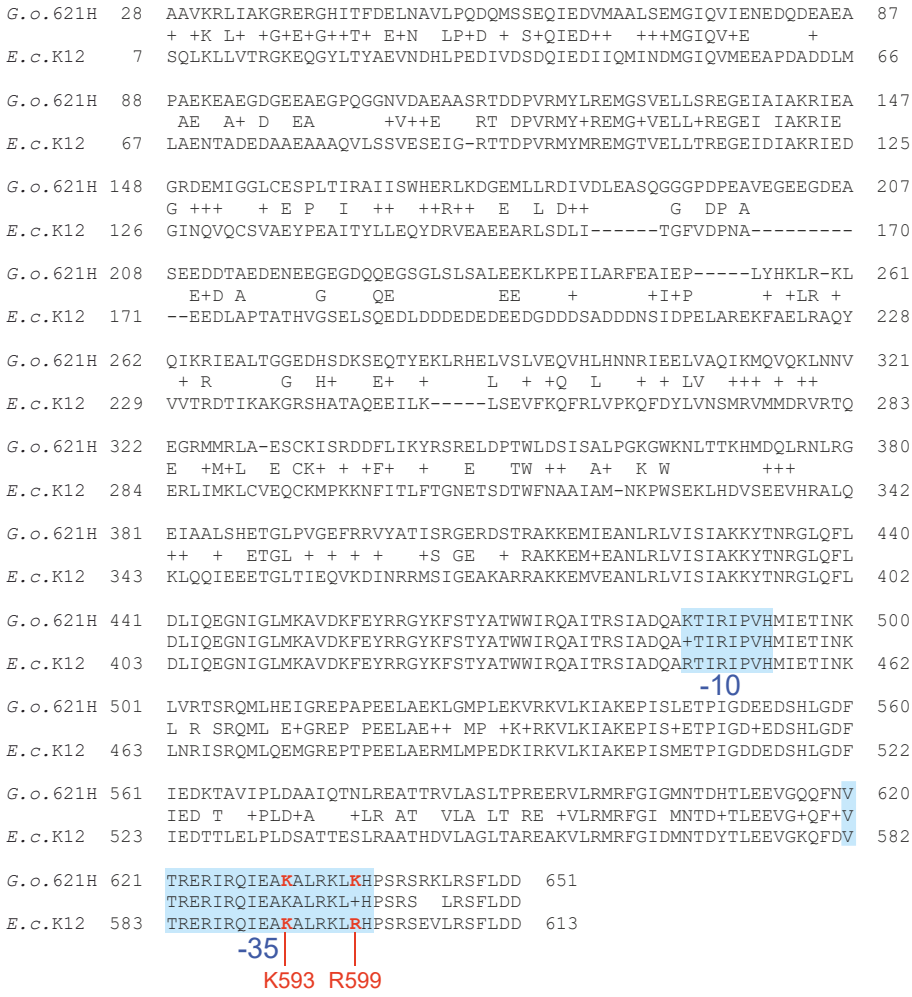

Fig. 1 Amino acid sequence alignment of the sigma factors σ^{70} from *G. oxydans* 621H and *E. coli* K12. Regions containing amino acid residues suggested to be involved in –10 and –35 promoter element recognition are marked in blue (Kelly et al. 2018). Amino acid residues K593 and R599 required for interaction with RhaS in *E. coli* are highlighted in red (Bhende & Egan, 2000, Wickstrum & Egan, 2004).

While the entire σ^{70} amino acid sequence of *G. oxydans* exhibited only 49% identity when compared to σ^{70} of *E. coli* K12, primarily due to little similarities at the N-terminus, the C-terminal region shared 84% identity with *E. coli* σ^{70}. Overall the C-terminal regions of the σ^{70} factors differed merely in few amino acids, of which only two were found in the regions likely involved in –10 and –35 recognition (Fig. 1). In both cases, an arginine in *E. coli* σ^{70} was replaced by a lysine in *G. oxydans* σ^{70}. Interestingly, the amino acids R599 involved in –35

recognition and also needed for RhaS interaction in *E. coli* was exchanged by K537 in *G. oxydans*. It is unclear whether this or other amino acid substitutions are responsible for the reversed responsiveness of RhaS in *G. oxydans*. In spite of their similarity as amino acids with cationic side chains, it cannot be excluded that the R599/K537 exchange caused the reverse effect on the protein interaction. Moreover, it should be noted that the –35 element within promoter P_{rhaT}, which is L-rhamnose-inducible in *G. oxydans* and *E. coli*, does not overlap with the RhaS binding site (Vía et al. 1996). Possibly the slightly different organization of these promoter elements is responsible for the inducibility of P_{rhaT} and repression of P_{rhaBAD} in *G. oxydans*.

GC-TOF-MS analysis performed in this study showed that no substantial metabolization of L-rhamnose occurs in *G. oxydans*. It is unknown how L-rhamnose enters the cell. A BLAST search with the amino acid sequence of RhaT in the proteome of *G. oxydans* did not reveal homologous transporters that may import the effector. The fact that even as low concentrations as 0.05% L-rhamnose reduced expression from P_{rhaBAD} by half, may be an indication that the effector uptake is not a bottle neck of this expression system.

In this study it was shown that in *G. oxydans* RhaS activated expression from P_{rhaBAD} in the absence of L-rhamnose and repressed expression when L-rhamnose was present. This indicated that in *G. oxydans*, RhaS supports transcription activation without L-rhamnose likely through DNA binding and interaction with RNAP but also decreases transcription by reducing RNAP binding, *e.g.* by altering the DNA structure once L-rhamnose is bound. Furthermore, L-rhamnose-bound RhaS stimulated its own expression from the P_{rhaSR} promoter. In *E. coli*, RhaR is required for strong expression of the *rhaSR* operon. It is known that in *E. coli* also RhaS binds the RhaR binding site within P_{rhaSR}, leading to lower transcription levels of the *rhaSR* operon than RhaR. This was explained by the fact that RhaR enables CRP to interact with RNAP whereas RhaS prevents CRP to efficiently coactivate RNAP for transcription. In the absence of CRP, which is given in *G. oxydans*, both regulators activate transcription of the *rhaSR* operon to the same level (Wickstrum et al. 2010). Kolin et al. (2008) observed that RhaS, different than RhaR, requires L-rhamnose to effectively bind operator sites within P_{rhaBAD} while RhaS interaction with RNAP is not affected by L-rhamnose binding. Perhaps in *G. oxydans*, RhaS exhibits some affinity for the RhaS binding site within P_{rhaBAD} also in the absence of L-rhamnose thereby lightly promoting expression from P_{rhaBAD}. Bound to L-rhamnose, the affinity of RhaS for the respective operator sites highly increases causing a RhaS dimer to simultaneously bind RhaR binding sites within P_{rhaSR} thereby looping the DNA in the P_{rhaSR}-P_{rhaBAD} region and making P_{rhaBAD} inaccessible for transcription.

No improved repression was observed when an additional RhaS binding site was inserted directly downstream from the –10 region and upstream from the transcription start of P_{rhaBAD}. It is unlcear and was not tested if RhaS binds to this additional binding site in

G. oxydans. Due to the promoter modification, expression from $P_{rhaBAD(+RhaS\text{-}BS)}$ almost doubled in the absence of L-rhamnose. Since the inserted second RhaS binding site contained promoter elements of P_{rhaBAD} (upstream element, 4 bp of –35 element), it may be that unintentionally a second promoter was created that contributed to transcription of *mNG*, thereby overall increasing reporter gene expression. Due to the fact that the degree of repression in the presence of L-rhamnose was maintained and non-repressed expression doubled, the range of P_{rhaBAD}-driven expression levels increased by the modification.

All in all, the exact mechanisms involved in the reversed regulation of P_{rhaBAD} by RhaS in *G. oxydans* remain unclear. Nevertheless, with the RhaS-P_{rhaBAD}/P_{rhaT} system, the repertoire of genetic tools available for *G. oxydans* was expanded by two regulatable promoters: Firstly, a promoter that allows the effector concentration-dependent knock-down of target genes. Secondly, a weak inducible promoter whose expression is controlled by the same effector molecule. These promoters, alone or in combination with others, could find use in industrial applications or basic research involving *G. oxydans* or other AAB.

3.6 Endogenous regulatable expression system

In this study, endogenous promoters from *G. oxydans* were identified that responded to the supplementation of a chemical substance by substantially increasing gene transcription. When tested on pBBR1MCS-5-based plasmids, expression from the promoters $P_{GOX0532}$ and $P_{GOX0536}$ induced by high concentrations of citrate (>50 mM) could be tuned by varying the effector concentration and reached induction ratios up to more than 430-fold. Also, genomically integrated copies of the promoters were citrate-inducible with up to 100-fold induction ratios. Therefore, the promoters $P_{GOX0532}$ and $P_{GOX0536}$ may form the basis of the first *G. oxydans* expression strain that enables controlled target gene expression but is not classified as a GMO. Based on the fact that the genes GOX0532 and GOX0536 encode proteins involved in the uptake of iron-loaded siderophores, it was assumed that both promoters were induced by iron limitation caused by the addition of the iron-chelating citrate. This hypothesis was supported by the observation that the supplementation of iron ions to the medium substantially reduced the otherwise relatively high basal expression from $P_{GOX0532}$ and $P_{GOX0536}$.

Citrate-chelated iron, also known as dinuclear ferric citrate, is taken up by *E. coli* through the ferric citrate uptake system, of which FecA is a TonB-dependent transporter in the outer membrane (reviewed by Braun, 2003). In *E. coli*, expression of *tonB* is activated upon iron-depletion (Hantke, 1981). Even though a homologue to the extracytoplasmic sigma factor (ECF) FecI responsible for regulation of genes encoding proteins of the ferric citrate uptake system could be identified when *G. oxydans* was sequenced, it is unlikely that the bacterium uses this system as not all required genes were found in the genome (Prust et al. 2005).

In most Gram-negative bacteria, the global regulator Fur (ferric uptake regulator) is responsible for iron homeostasis (reviewed in Fillat, 2014, Sarvan et al. 2018). Therefore, it was expected that the protein encoded by GOX0771, annotated as *fur*, which exhibits 37% sequence identity with *E. coli* Fur in a protein BLAST search, controls expression from $P_{GOX0532}$ and $P_{GOX0536}$ (Prust et al. 2005). In *E. coli*, Fur preferably binds promoter sites composed of 3-4 repeats of the motif GATAAT with 2 hexamers in the forward orientation separated by a single base pair from 1-2 hexamers in the reverse orientation (f-f-x-r or f-f-x-r-r) called Fur box (Escolar et al. 1998, Lavrrar & McIntosh, 2003). Also the putative promoters of the citrate-upregulated genes GOX0532 and GOX0536 contained potential Fur-binding sites in the f-f-x-r-r conformation. These consensus sequences within $P_{GOX0532}$ and $P_{GOX0536}$ were located 38 bp and 130 bp upstream from the start codon of GOX0532 and GOX0536, respectively. Nevertheless, a prediction about the mode of regulation is difficult as for both promoters the transcription start side and core elements, such as –10 or –35 sites, are unknown.

In spite of various attempts, deletion of GOX0771 did not succeed, suggesting that the gene could be essential for survival of *G. oxydans*. While for several bacterial species *fur* gene knockout mutants were obtained, in other species *fur* was described as an essential gene (Pasqua et al. 2017). Interestingly, due to the inability to create *fur* deletion mutants in *Pseudomonas putida* and *Pseudomonas aeruginosa*, the regulator was considered to be essential for many years (Venturi et al. 1995, Barton et al. 1996). This paradigm was changed when Pasqua et al. (2017) demonstrated that conditional *fur* knockout mutants of *P. aeruginosa* were unable to form colonies on solid media but that Fur was not essential for growth in liquid media. All attempts to delete *fur* in *G. oxydans* by homologous recombination using the plasmid pKOS6b-ΔGOX0771 conducted in this work used mannitol agar plates containing 5-fluorocytosine for selection. Possibly the inability of *G. oxydans* ΔGOX0771 mutants to grow on solid media could explain why no deletion mutants were obtained and selection in liquid media might allow deletion of *fur* also in *G. oxydans*.

To determine the role of GOX0771 for the regulation of $P_{GOX0532}$- and $P_{GOX0536}$-driven expression, *in vivo* Fur binding sites were searched in the genome of *G. oxydans* using ChAP-Seq. For that purpose, different plasmids were constructed with the aim to replace *fur* with a modified gene encoding a Fur variant with a Strep-tag in the genome of *G. oxydans*. Since no strain with tagged Fur encoded from its original locus could be obtained, ChAP-Seq analysis was performed with a C-terminally tagged Fur protein whose gene was integrated in intergenic region 3 (igr3) (Battling et al. 2020). Under the applied conditions, the promoter region of $P_{GOX0536}$ was enriched with Strep-tagged Fur and a Fur-binding motif resembling the Fur box described for *E. coli* was identified (Escolar et al. 1998). The promoter region of $P_{GOX0532}$ was not enriched by ChAP-Seq.

Sarvan et al. (2019) compared the ability of untagged and N-terminally tagged Fur to bind the metal ion required for regulation in *Campylobacter jejuni*. They found that untagged Fur incorporated metal ions with a higher efficiency. Moreover, *C. jejuni* Fur without a Strep-tag was able to bind DNA with higher affinity than tagged Fur, all in all indicating that an N-terminal tag is detrimental for the activity of the regulator in *C. jejuni* (Sarvan et al. 2019). Possibly a restricted functionality explains the inability to obtain a *G. oxydans* strain encoding an N-terminally tagged Fur protein. Therefore, in this study all ChAP-Seq experiments were conducted with a C-terminally tagged Fur variant encoded at a different locus in the genome than the native *fur* gene.

Overall, considerably less binding sites were found in the ChAP-Seq experiment than expected for a global transcription factor such as Fur. Since the native *fur* gene at its original locus remained together with modified *fur* gene inserted into the genome at the igr3 locus, tagged and untagged Fur proteins competed for the same DNA-binding sites. Furthermore, tagged and untagged Fur monomers may have formed heterodimers, which in case of an impaired tagged Fur variant might have weakened DNA-binding of the dimer thereby resulting in a reduced enrichment of Fur-regulated promoters. Trying to delete the *fur* in the *G. oxydans* strain containing the *fur* copy encoding the tagged Fur variant failed, suggesting that the tagged Fur protein could not compensate the native Fur. Further experiments are required to verify Fur-dependent regulation of $P_{GOX0532}$ through binding of the predicted Fur boxes within the promoter in the presence of iron ions.

3.7 Conclusions and outlook

In this study the collection of promoters available for target gene expression in the AAB *G. oxydans* 621H was expanded by the first regulatable promoters that allow dynamic external control of gene expression through the addition of specific effector molecules. Six tunable expression systems were established for *G. oxydans*, of which five systems enabled very strong (TetR-P_{tet}), strong (AraC-P_{araBAD}, Fur-$P_{GOX0532/6}$), moderate (LacI-P_{lacUV5}) and weak (RhaS-P_{rhaT}) induction of the target gene, whereas one system caused repression of the target gene in an effector-dependent manner (RhaS-P_{rhaBAD}). Four systems responded to low-cost effector molecules, such as sugars (L-arabinose, L-rhamnose) or a carboxylic acid (citrate), one to an antibiotic derivative (ATc), and one to a sugar derivative (IPTG). Five systems were based on well-characterized expression system from other bacteria (TetR-P_{tet}, AraC-P_{araBAD}, LacI-P_{lacUV5}, RhaS-P_{rhaBAD}, RhaS-P_{rhaT}), one system responding differently than in its native host (RhaS-P_{rhaBAD}), whereas one system exclusively required endogenous, so far not characterized regulatory elements from *G. oxydans* to be fully functional (Fur-$P_{GOX0532/6}$). Three of the established expression systems were successfully published (AraC-P_{araBAD}, TetR-P_{tet},

LacI-P_{lacUV5}), for two systems (RhaS-P_{rhaBAD}, RhaS-P_{rhaT}) a manuscript is in preparation, and one system (Fur-$P_{GOX0532/6}$) still requires experimental work for completion.

However, the established regulatable expression systems in *G. oxydans* bear the potential for improvements. For example, when compared to their use in *E. coli*, the AraC-P_{araBAD}- and LacI-P_{lacUV5}-systems require relative high effector concentrations to achieve maximal effects on target gene expression in *G. oxydans*. The TetR-P_{tet} system and its diffusible inducer anhydrotetracycline needed similar inducer concentrations for full induction in *E. coli* and *G. oxydans*. This indicated that an inefficient uptake of L-arabinose and IPTG might limit intracellular effector concentrations. Plasmid-encoded co-expression of *araE* and *araC*, with *araE* encoding an L-arabinose transporter, did not improve the sensitivity of the AraC-P_{araBAD} system in *G. oxydans* (Fricke et al. 2020). Trying to genomically express the genes *araE* and *lacY* encoding an L-arabinose and lactose permease, respectively, using promoters of different strength might help to create *G. oxydans* strains with an improved effector uptake and higher responsiveness towards low effector concentrations.

In case of the AraC-P_{araBAD} system, Tang et al. (2008) engineered the regulator AraC in such a way that it solely responded to D-arabinose instead of L-arabinose. Using *E. coli* as host, FACS-mediated screening was used to identify AraC mutants with randomized binding pocket residues that activated transcription only in response to D-arabinose (Tang et al. 2008). Using this modified AraC in *G. oxydans* would prevent the oxidation of L-arabinose and the corresponding acidification of the medium, thereby circumventing the need for a Δ*gdhM* strain or pH-controlled fermentations (Fricke et al. 2020).

A major drawback of the LacI-P_{lacUV5} system in *G. oxydans* is the relatively high basal expression in the absence of an inducer. The amino acid sequence of the regulator LacI contains 27 codons that exhibit a considerably lower frequency in *G. oxydans* than in *E. coli* including six codons with only 0.8% usage in *G. oxydans vs*. 15% usage frequency in *E. coli*. Therefore, a *lacI* gene codon-optimized for *G. oxydans* might increase abundance of functional LacI and thereby improve repression of P_{lacUV5} promoted transcription.

The inability to obtain *G. oxydans* strains lacking the gene GOX0771 encoding the regulator Fur suggested that the protein is essential for survival of the bacterium. However, it might be that the applied conditions prevented a successful deletion of GOX0771. Possibly, GOX0771 could be placed under the control of a regulatable promoter, such as P_{tet} or P_{rhaBAD}, at its original locus in the genome of *G. oxydans*. Different effector concentration could be tested with such a strain to determine how a conditional downregulation of *fur* expression would affect viability of *G. oxydans*. Furthermore, strong plasmid-based *mNG* expression from the promoters $P_{GOX0532}$ and $P_{GOX0536}$ in *G. oxydans* ΔGOX0771 in medium supplemented with iron would demonstrate the regulatory role of Fur for $P_{GOX0532/6}$ promoted expression. The predicted Fur binding sites within $P_{GOX0532}$ and $P_{GOX0536}$ strongly indicate that both promoters are

controlled by the regulator Fur. However, in ChAP-Seq experiments only the expected Fur box within $P_{GOX0536}$ could be enriched. Modifying the experimental set-up by applying different iron concentration that are maintained during the entire process might be needed to find optimal conditions to also enrich $P_{GOX0532}$.

Last but not least, the new established regulatable expression systems should be tested in basic research and for relevant applications involving *G. oxydans*. The above described conditional expression of genome-encoded GOX0771 might be suitable to investigate the Fur regulon in *G. oxydans*. Furthermore, plasmid-based regulatable overexpression of *gdhM* using P_{araBAD} or P_{tet} possibly allows to improve L-arabinonic acid production by *G. oxydans.*

4 References:

Ahmer, B. M. M., Thomas, M. G., Larsen, R. A., & Postle, K. (1995). Characterization of the *exbBD* operon of *Escherichia coli* and the role of ExbB and ExbD in TonB function and stability. *Journal of Bacteriology*, *177*(16), 4742–4747. doi:10.1128/jb.177.16.4742-4747.1995

Ameyama, M., Matsushita, K., Shinagawa, E., & Adachi, O. (1987). Sugar-oxidizing respiratory chain of *Gluconobacter suboxydans*. Evidence for a branched respiratory chain and characterization of respiratory chain-linked cytochromes. *Agricultural and Biological Chemistry*, *51*(11), 2943–2950. doi:10.1080/00021369.1987.10868527

Antoine, R., & Locht, C. (1992). Isolation and molecular characterization of a novel broad-host-range plasmid from *Bordetella bronchiseptica* with sequence similarities to plasmids from Gram-positive organisms. *Molecular Microbiology*, *6*(13), 1785–1799. doi:10.1111/j.1365-2958.1992.tb01351.x

Aro-Kärkkäinen, N., Toivari, M., Maaheimo, H., & Ylilauri, M. (2014). L-Arabinose/D-galactose 1-dehydrogenase of *Rhizobium leguminosarum* bv. *trifolii* characterised and applied for bioconversion of L-arabinose to L-arabonate with *Saccharomyces cerevisiae*. *Applied Micr*, 9653–9665. doi:10.1007/s00253-014-6039-2

Bagg, A., & Neilands, J. B. (1987). Ferric uptake regulation protein acts as a repressor, employing iron(II) as a cofactor to bind the operator of an iron transport operon in *Escherichia coli*, (1970), 5471–5477. doi:10.1021/bi00391a039

Bailey, T. L., & Gribskov, M. (1998). Combining evidence using p-values: Application to sequence homology searches. *Bioinformatics*, *14*(1), 48–54. doi:10.1093/bioinformatics/14.1.48

Barton, H. A., Johnson, Z., Cox, C. D., Vasil, A. I., & Vasil, M. L. (1996). Ferric uptake regulator mutants of *Pseudomonas aeruginosa* with distinct alterations in the iron-dependent repression of exotoxin A and siderophores in aerobic and microaerobic environments. *Molecular Microbiology*, *21*(5), 1001–1017. doi:10.1046/j.1365-2958.1996.381426.x

Battling, S., Wohlers, K., Igwe, C., Kranz, A., Pesch, M., Wirtz, A., … Bott, M. (2020). Novel plasmid-free *Gluconobacter oxydan*s strains for production of the natural sweetener 5-ketofructose. *Microbial Cell Factories*, *19*(1), 1–10. doi:10.1186/s12934-020-01310-7

Bertram, R., & Hillen, W. (2008). The application of Tet repressor in prokaryotic gene regulation and expression. *Microbial Biotechnology*, *1*, 2–16. doi:10.1111/j.1751-7915.2007.00001.x

Bhende, P. M., & Egan, S. M. (2000). Genetic evidence that transcription activation by RhaS involves specific amino acid contacts with sigma 70. *Journal of Bacteriology*, *182*(17), 4959–4969. doi:10.1128/JB.182.17.4959-4969.2000

Blank, M., & Schweiger, P. (2018). Surface display for metabolic engineering of industrially important acetic acid bacteria. *PeerJ*, *6*, 1–19. doi:10.7717/peerj.4626

Braun, V. (2003). Iron uptake by *Escherichia coli*. *Frontiers in Bioscience*, 1409–1421. doi:10.2741/1232

Brautaset, T., Lale, R., & Valla, S. (2009). Positively regulated bacterial expression systems. *Microbial Biotechnology*, *2*(1), 15–30. doi:10.1111/j.1751-7915.2008.00048.x

Bringer, S., & Bott, M. (2016). Central carbon Mmetabolism and respiration in *Gluconobacter oxydans*. In *Acetic Acid Bacteria* (pp. 235–253). doi:10.1007/978-4-431-55933-7_11

Brown, N. L., Stoyanov, J. V., Kidd, S. P., & Hobman, J. L. (2003). The MerR family of transcriptional regulators. *FEMS Microbiology Reviews*, *27*(2–3), 145–163. doi:10.1016/S0168-6445(03)00051-2

Browning, D. F., & Busby, S. J. W. (2004). The regulation of bacterial transcription initiation. *Nature Reviews Microbiology*, *2*(1), 57–65. doi:10.1038/nrmicro787

Browning, D. F., & Busby, S. J. W. (2016). Local and global regulation of transcription initiation in bacteria. *Nature Reviews Microbiology*, *14*(10), 638–650. doi:10.1038/nrmicro.2016.103

Bugala, J., Cimova, V., Grones, P., & Grones, J. (2016). Characterization of newly identified DnaA and DnaB proteins from *Acetobacter*. *Research in Microbiology*, *167*(8), 655–668. doi:10.1016/j.resmic.2016.06.010

Celia, H., Noinaj, N., & Buchanan, S. K. (2020). Structure and stoichiometry of the Ton molecular motor. *International Journal of Molecular Sciences*, *21*(2), 1–15. doi:10.3390/ijms21020375

Chen, R. R. (2007). Permeability issues in whole-cell bioprocesses and cellular membrane engineering. *Applied Microbiology and Biotechnology*, *74*(4), 730–738. doi:10.1007/s00253-006-0811-x

Condon, C., FitzGerald, R. J., & O'Gara, F. (1991). Conjugation and heterologous gene expression in *Gluconobacter oxydans* ssp. *suboxydans*. *FEMS Microbiology Letters*, *80*, 173–178. doi:10.1111/j.1574-6968.1991.tb04656.x

Dauner, M., Sonderegger, M., Hochuli, M., Szyperski, T., Wüthrich, K., Hohmann, H. P., … Bailey, J. E. (2002). Intracellular carbon fluxes in riboflavin-producing *Bacillus subtilis* during growth on two-carbon substrate mixtures. *Applied and Environmental Microbiology*, *68*(4), 1760–1771. doi:10.1128/AEM.68.4.1760-1771.2002

De Muynck, C., Pereira, C. S. S., Naessens, M., Parmentier, S., Soetaert, W., & Vandamme, E. J. (2007). The genus *Gluconobacter oxydans*: Comprehensive overview of biochemistry and biotechnological applications. *Critical Reviews in Biotechnology*, *27*(3), 147–171. doi:10.1080/07388550701503584

Degenkolb, J., Takahashi, M., Ellestad, G. a, & Hillen, W. (1991). Structural requirements of tetracycline-Tet repressor interaction: Determination of equilibrium binding constants for tetracycline analogs with the Tet repressor. *Antimicrobial Agents and Chemotherapy*, *35*(8), 1591. doi:10.1128/aac.35.8.1591

Deppenmeier, U., Hoffmeister, M., & Prust, C. (2002). Biochemistry and biotechnological applications of *Gluconobacter* strains. *Applied Microbiology and Biotechnology*, *60*(3), 233–242. doi:10.1007/s00253-002-1114-5.

Dunn, T. M., & Schleif, R. (1984). Deletion analysis of the *Escherichia coli ara* P_C and P_{BAD} promoters. *Journal of Molecular Biology*, *180*(1), 201–204. doi:10.1016/0022-2836(84)90437-6

Ebright, R. H., & Busby, S. (1995). The *Escherichia coli* RNA polymerase α-subunit: structure and function. *Current Opinion in Genetics and Development*, *5*(2), 197–203. doi:10.1016/0959-437X(95)80008-5

Egan, S. M., & Schleif, R. F. (1993). A regulatory cascade in the induction of *rhaBAD*. *Journal of Molecular Biology*. doi:10.1006/jmbi.1993.1565

Ernst, F. D., Bereswill, S., Waidner, B., Stoof, J., Mäder, U., Kusters, J. G., … Homuth, G. (2005). Transcriptional profiling of *Helicobacter pylori* Fur- and iron-regulated gene expression. *Microbiology*, *151*(2), 533–546. doi:10.1099/mic.0.27404-0

Escolar, L., Pérez-Martín, J., & De Lorenzo, V. (1998). Binding of the Fur (ferric uptake regulator) repressor of *Escherichia coli* to arrays of the GATAAT sequence. *Journal of Molecular Biology*, *283*(3), 537–547. doi:10.1006/jmbi.1998.2119

Fernández-Castané, A., Vine, C. E., Caminal, G., & López-Santín, J. (2012). Evidencing the role of lactose permease in IPTG uptake by *Escherichia coli* in fed-batch high cell density cultures. *Journal of Biotechnology*, *157*(3), 391–398. doi:10.1016/j.jbiotec.2011.12.007

Fillat, M. F. (2014). The FUR (ferric uptake regulator) superfamily: Diversity and versatility of key transcriptional regulators. *Archives of Biochemistry and Biophysics*, *546*, 41–52. doi:10.1016/j.abb.2014.01.029

Florea, M., Santosa, G., Hagemann, H., Reeve, B., Abbott, J., Freemont, P. S., … Spencer-Milnes, X. (2016). Engineering control of bacterial cellulose production using a genetic toolkit and a new cellulose-producing strain. *Proceedings of the National Academy of Sciences*, *113*(24), E3431–E3440. doi:10.1073/pnas.1522985113

Fricke, P. M., Klemm, A., Bott, M., & Polen, T. (2021a). On the way toward regulatable expression systems in acetic acid bacteria: Target gene expression and use cases. *Applied Microbiology and Biotechnology*. doi:10. 1007/ s00253- 021- 11269-z

Fricke, P. M., Link, T., Gätgens, J., Sonntag, C., Otto, M., Bott, M., & Polen, T. (2020). A tunable L-arabinose-inducible expression plasmid for the acetic acid bacterium *Gluconobacter oxydans*. *Applied Microbiology and Biotechnology*. doi:10.1007/s00253-020-10905-4

Fricke, P. M., Lürkens, M., Hünnefeld, M., Sonntag, C. K., Bott, M., Davari, M. D., & Polen, T. (2021b). Highly tunable TetR-dependent target gene expression in the acetic acid bacterium *Gluconobacter oxydans*. *Applied Microbiology and Biotechnology*. doi:10.1007/s00253-021-11473-x

Fukaya, M., Okumura, H., Masai, H., Uozumi, T., & Beppu, T. (1985). Development of a host-vector system for *Gluconobacter suboxydans*. *Agricultural and Biological Chemistry*, *49*(8), 2407–2411. doi:10.1080/00021369.1985.10867095

Gätgens, C., Degner, U., Bringer-Meyer, S., & Herrmann, U. (2007). Biotransformation of glycerol to dihydroxyacetone by recombinant *Gluconobacter oxydans* DSM 2343. *Applied Microbiology and Biotechnology*, *76*(3), 553–559. doi:10.1007/s00253-007-1003-z

Greenblatt, J., Li, J., Adhyat, S., Friedmanf, D. I., Baron, L. S., Redfieldt, B., … Weissbachi, H. (1980). L factor that is required for *β*-galactosidase synthesis is the *nusA* gene product involved in transcription termination. *Proc.Natl.Acad.Sci.U.S.A*, *77*(4), 1991–1994. doi:10.1073/pnas.77.4.1991

Grkovic, S., Brown, M. H., & Skurray, R. A. (2002). Regulation of bacterial drug export systems. *Microbiology and Molecular Biology Reviews*, *66*(4), 671–701. doi:10.1128/MMBR.66.4.671-701.2002

Gross, J., & Englesberg, E. (1959). Determination of the order of mutational sites governing L-arabinose utilization in *Escherichia coli* B/r by transduction with phage P1bt. *Virology*, *9*(3), 314–331. doi:10.1016/0042-6822(59)90125-4

Gupta, A., Singh, V. K., Qazi, G. N., & Kumar, A. (2001). *Gluconobacter oxydans*: Its biotechnological applications. *Journal of Molecular Microbiology and Biotechnology*, *3*(3), 445–456.

Guzman, L., Belin, D., Carson, M. J., & Beckwith, J. (1995). Tight regulation, modulation, and high-level expression by vectors containing the arabinose P_{BAD} promoter. *Journal of Applied Microbiology*, *177*(14), 4121–4130. doi:10.1128/jb.177.14.4121-4130.1995

Hansen, L. H., Knudsen, S., & Sørensen, S. J. (1998). The effect of the *lacY* gene on the induction of IPTG inducible promoters, studied in *Escherichia coli* and *Pseudomonas fluorescens*. *Current Microbiology*, *36*(6), 341–347. doi:10.1007/s002849900320

Hahn, S., & Schleif, R. (1983). *In vivo* regulation of the *Escherichia coli araC* promoter. *Journal of Bacteriology*, *155*(2), 593–600. doi:10.1128/jb.155.2.593-600.1983

Hahn, S., Dunn, T., & Schleif, R. (1984). Upstream repression and CRP stimulation of the *Escherichia coli* L-arabinose operon. *Journal of Molecular Biology*, *180*(1), 61–72. doi:10.1016/0022-2836(84)90430-3

Hakimi, M. A., Privat, I., Valay, J. G., & Lerbs-Mache, S. (2000). Evolutionary conservation of C-terminal domains of primary sigma^{70}-type transcription factors between plants and bacteria. *Journal of Biological Chemistry*, *275*(13), 9215–9221. doi:10.1074/jbc.275.13.9215

Hanke, T., Nöh, K., Noack, S., Polen, T., Bringer, S., Sahm, H., … Bott, M. (2013). Combined fluxomics and transcriptomics analysis of glucose catabolism via a partially cyclic pentose phosphate pathway in *Gluconobacter oxydans* 621H. *Applied and Environmental Microbiology*, *79*(7), 2336–2348. doi:10.1128/AEM.03414-12

Hanke, T., Richhardt, J., Polen, T., Sahm, H., Bringer, S., & Bott, M. (2012). Influence of oxygen limitation, absence of the cytochrome bc_1 complex and low pH on global gene expression in *Gluconobacter oxydans* 621H using DNA microarray technology. *Journal of Biotechnology*, *157*(3), 359–372. doi:10.1016/j.jbiotec.2011.12.020

Hantke, K. (1981). Regulation of ferric iron transport in *Escherichia coli* K12: Isolation of a constitutive mutant. *MGG Molecular & General Genetics*, *182*(2), 288–292. doi:10.1007/BF00269672

Harmer, T., Wu, M., & Schleif, R. (2001). The role of rigidity in DNA looping-unlooping by AraC. *Proceedings of the National Academy of Sciences of the United States of America*, *98*(2), 427–431. doi:10.1073/pnas.98.2.427

Haugen, S. P., Ross, W., & Gourse, R. L. (2008). Advances in bacterial promoter recognition and its control by factors that do not bind DNA. *Nature Reviews Microbiology*, *6*(7), 507–519. doi:10.1038/nrmicro1912

Herweg, E., Schöpping, M., Rohr, K., Siemen, A., Frank, O., Hofmann, T., … Büchs, J. (2018). Production of the potential sweetener 5-ketofructose from fructose in fed-batch cultivation with *Gluconobacter oxydans*. *Bioresource Technology*, *259*(March), 164–172. doi:10.1016/j.biortech.2018.03.038

Herzenberg, L. A. (1961). Isolotion and identification of derivatives formed in the course of intracellular accumulation of thiogalactosides by *Escherichia coli*. *Archives of Biochemistry and Biophysics*, *93*(2), 314–315. doi:10.1016/0003-9861(61)90270-3

Higgs, P. I., Larsen, R. A., & Postle, K. (2002). Quantification of known components of the *Escherichia coli* TonB energy transduction system: TonB, ExbB, ExbD and FepA. *Molecular Microbiology*, *44*(1), 271–281. doi:10.1046/j.1365-2958.2002.02880.x

Hirschel, B. J., Shen, V., & Schlessinger, D. (1980). Lactose operon transcription from wild-type and L8-UV5 *lac* promoters in *Escherichia coli* treated with chloramphenicol. *Journal of Bacteriology*, *143*(3), 1534–1537. doi:10.1128/jb.143.3.1534-1537.1980

Hoffmann, J. J., Hövels, M., Kosciow, K., & Deppenmeier, U. (2020). Synthesis of the alternative sweetener 5-ketofructose from sucrose by fructose dehydrogenase and invertase producing *Gluconobacte*r strains. *Journal of Biotechnology*, *307*(October 2019), 164–174. doi:10.1016/j.jbiotec.2019.11.001

Holcroft, C. C., & Egan, S. M. (2000). Interdependence of activation at *rhaSR* by cyclic AMP receptor protein, the RNA polymerase alpha subunit C-terminal domain, and RhaR. *Journal of Bacteriology*, *182*(23), 6774–6782. doi:10.1128/JB.182.23.6774-6782.2000

Horazdovsky, B. F., & Hogg, R. W. (1989). Genetic reconstitution of the high-affinity L-arabinose transport system. *Journal of Bacteriology*, *171*(6), 3053–3059. doi:10.1128/jb.171.6.3053-3059.1989

Horowitz, H., & Platt, T. (1982). A termination site for *lacI* transcription is between the CAP site and the *lac* promoter. *Journal of Biological Chemistry*, *257*(19), 11740–11746. doi:10.1016/s0021-9258(18)33825-0

Hu, Y., Wan, H., Li, J., & Zhou, J. (2015). Enhanced production of L-sorbose in an industrial *Gluconobacter oxydans* strain by identification of a strong promoter based on proteomics analysis. *Journal of Industrial Microbiology and Biotechnology*, *42*(7), 1039–1047. doi:10.1007/s10295-015-1624-7

Jacob, F., & Monod, J. (1961). Genetic regulatory mechanisms in the synthesis of proteins. *Journal of Molecular Biology*, *3*(3), 318–356. doi:10.1016/S0022-2836(61)80072-7

Jensen, P. R., Westerhoff, H. V., & Michelsen, O. (1993). The use of *lac*-type promoters in control analysis. *European Journal of Biochemistry*, *211*(1–2), 181–191. doi:10.1111/j.1432-1033.1993.tb19885.x

Kallnik, V. (2012). Untersuchungen zur Polyoloxidation in *Gluconobacter oxydans* und *Thermotoga maritima*.

Kallnik, V., Meyer, M., Deppenmeier, U., & Schweiger, P. (2010). Construction of expression vectors for protein production in *Gluconobacter oxydans*. *Journal of Biotechnology*, *150*(4), 460–465. doi:10.1016/j.jbiotec.2010.10.069

Kania, J., & Brown, D. T. (1976). The functional repressor parts of a tetrameric *lac* repressor-*β*-galactosidase chimaera are organized as dimers. *Proceedings of the National Academy of Sciences of the United States of America*, *73*(10), 3529–3533. doi:10.1073/pnas.73.10.3529

Kelly, C. L., Taylor, G. M., Hitchcock, A., Torres-Méndez, A., & Heap, J. T. (2018). A rhamnose-inducible system for precise and temporal control of gene expression in *Cyanobacteria*. *ACS Synthetic Biology*, *7*(4), 1056–1066. doi:10.1021/acssynbio.7b00435

Kersters, K., & De Ley, J. (1968). The occurrence of the Entner-Doudoroff pathway in bacteria. *Antonie van Leeuwenhoek*, *34*(1), 393–408. doi:10.1007/BF02046462

Kersters, K., Linsdiyanti, P., Komagata, K., & Swings, J. (2006). The family *Acetobacteraceae*: The genera *Acetobacter*, *Acidomonas*, *Asaia*, *Gluconacetobacter*, *Gluconobacter*, and *Kozakia*. *Prokaryotes*.

Kiefler, I. (2016). Strain development of *Gluconobacter oxydans*: Complementation of non-functional metabolic pathways and increase of carbon flux.

Kiefler, I., Bringer, S., & Bott, M. (2015). SdhE-dependent formation of a functional *Acetobacter pasteurianus* succinate dehydrogenase in *Gluconobacter oxydans* − a first step toward a complete tricarboxylic acid cycle. *Applied Microbiology and Biotechnology*, *99*(21), 9147–9160. doi:10.1007/s00253-015-6972-8

Kiefler, I., Bringer, S., & Bott, M. (2017). Metabolic engineering of *Gluconobacter oxydans* 621H for increased biomass yield. *Applied Microbiology and Biotechnology*, 5453–5467. doi:10.1007/s00253-017-8308-3

Kingston, R. E., & Chamberlin, M. J. (1981). Pausing and attenuation of *in vitro* transcription in the *rrnB* operon of *E. coli*. *Cell*, *27*(3 PART 2), 523–531. doi:10.1016/0092-8674(81)90394-9

Kitova, A., Tarasov, S., Plekhanova, Y., Bykov, A., & Reshetilov, A. (2021). Direct bioelectrocatalytic oxidation of glucose by *Gluconobacter oxydans* membrane fractions in PEDOT:PSS/TEG-modified biosensors. *Biosensors*, *11*(5), 144. doi:10.3390/bios11050144

Kleinschmidt, C., Tovar, K., & Hillen, W. (1991). Computer simulations and experimental studies of gel mobility patterns for weak and strong non-cooperative protein binding to two targets on the same DNA: Application to binding of Tet repressor variants to multiple and single *tet* operator sites. *Nucleic Acids Research*, *19*(5), 1021–1028. doi:10.1093/nar/19.5.1021

Kolin, A., Balasubramaniam, V., Skredenske, J. M., Wickstrum, J. R., & Egan, S. M. (2008). Differences in the mechanism of the allosteric L-rhamnose responses of the AraC/XylS family transcription activators RhaS and RhaR. *Molecular Microbiology*, *68*(2), 448–461. doi:10.1111/j.1365-2958.2008.06164.x

Kolodrubetz, D., & Schleif, R. (1981). Regulation of the L-arabinose transport operons in *Escherichia coli*. *Journal of Molecular Biology*, *151*(2), 215–227. doi:10.1016/0022-2836(81)90512-X

Kondo, K., & Horinouchi, S. (1997). Characterization of the genes encoding the three-component membrane-bound alcohol dehydrogenase from *Gluconobacter suboxydans* and their expression in *Acetobacter pasteurianus*. *Applied and Environmental Microbiology*, *63*(3), 1131–1138. doi:10.1128/aem.63.3.1131-1138.1997

Kosciow, K., Zahid, N., Schweiger, P., & Deppenmeier, U. (2014). Production of a periplasmic trehalase in *Gluconobacter oxydans* and growth on trehalose. *Journal of Biotechnology*, *189*, 27–35. doi:10.1016/j.jbiotec.2014.08.029

Kosciow, K., Domin, C., Schweiger, P., & Deppenmeier, U. (2016). Extracellular targeting of an active endoxylanase by a TolB negative mutant of *Gluconobacter oxydans*. *Journal of Industrial Microbiology & Biotechnology*, *43*(7), 989–999. doi:10.1007/s10295-016-1770-6

Kostner, D., Peters, B., Mientus, M., Liebl, W., & Ehrenreich, A. (2013). Importance of *codB* for new *codA*-based markerless gene deletion in *Gluconobacter strains*. *Applied Microbiology and Biotechnology*, *97*(18), 8341–8349. doi:10.1007/s00253-013-5164-7

Kovach, M. E., Elzer, P. H., Hill, D. S., Robertson, G. T., Farris, M. A., Roop, R. M., & Peterson, K. M. (1995). Four new derivatives of the broad-host-range cloning vector pBBR1MCS, carrying different antibiotic resistance cassettes. *Gene*, *166*(1), 175–176. doi:10.1089/152045500436104

Krajewski, V., Simic, P., Mouncey, N. J., Bringer, S., Sahm, H., & Bott, M. (2010). Metabolic engineering of *Gluconobacter oxydans* for improved growth rate and growth yield on glucose by elimination of gluconate formation, *76*(13), 4369–4376. doi:10.1128/AEM.03022-09

Kranz, A., Vogel, A., Degner, U., Kiefler, I., Bott, M., Usadel, B., & Polen, T. (2017). High precision genome sequencing of engineered *Gluconobacter oxydans* 621H by combining long nanopore and short accurate Illumina reads. *Journal of Biotechnology*, *258*(January), 197–205. doi:10.1016/j.jbiotec.2017.04.016

Kulhánek, M. (1989). Microbial dehydrogenations of monosaccharides. *Advances in Applied Microbiology*, *34*, 141–182. doi:10.1016/S0065-2164(08)70318-6

Lavrrar, J. L., & McIntosh, M. A. (2003). Architecture of a Fur binding site: A comparative analysis. *Journal of Bacteriology*, *185*(7), 2194–2202. doi:10.1128/JB.185.7.2194-2202.2003

Lee, D. J., Minchin, S. D., & Busby, S. J. W. (2012). Activating transcription in bacteria. *Annual Review of Microbiology*, *66*, 125–152. doi:10.1146/annurev-micro-092611-150012

Ley, J. De, Gillis, M., & Swings, J. (1984). The genus *Gluconobacter*. In N. R. Krieg & J. G. Holt (Eds.), *Bergey's Manual of Systematic Bacteriology* (pp. 267–278).

Liu, H., Valdehuesa, K. N. G., Ramos, K. R. M., Nisola, G. M., Lee, W.-K., & Chung, W.-J. (2014). L-arabinoate and D-galactonate production by expressing a versatile sugar dehydrogenase in metabolically engineered *Escherichia coli*. *Bioresource Technology*, *159*, 455–459. doi:10.1016/j.biortech.2014.03.056.

Liu, L. P., Yang, X., Zhao, X. J., Zhang, K. Y., Li, W. C., Xie, Y. Y., … Zhong, C. (2020). A lambda red and FLP/FRT-mediated site-specific recombination system in *Komagataeibacter xylinus* and its application to enhance the productivity of bacterial cellulose. *ACS Synthetic Biology*, *9*(11), 3171–3180. doi:10.1021/acssynbio.0c00450

Lobell, R. B., & Schleif, R. F. (1991). AraC-DNA looping: Orientation and distance-dependent loop breaking by the cyclic AMP receptor protein. *Journal of Molecular Biology*, *218*(1), 45–54. doi:10.1016/0022-2836(91)90872-4

Lonetto, M. A., Rhodius, V., Lamberg, K., Kiley, P., Busby, S., & Gross, C. (1998). Identification of a contact site for different transcription activators in region 4 of the *Escherichia coli* RNA polymerase σ^{70} subunit. *Journal of Molecular Biology*, *284*(5), 1353–1365. doi:10.1006/jmbi.1998.2268

Marbach, A., & Bettenbrock, K. (2012). *lac* operon induction in *Escherichia coli*: Systematic comparison of IPTG and TMG induction and influence of the transacetylase LacA. *Journal of Biotechnology*, *157*(1), 82–88. doi:10.1016/j.jbiotec.2011.10.009

Matsushita, K., Toyama, H., & Adachi, O. (1994). Respiratory chains and bioenergetics of acetic acid bacteria. *Advances in Microbial Physiology*, *36*, 247–301. doi:10.1016/s0065-2911(08)60181-2.

McMurry, L., Petrucci, R. E., & Levy, S. B. (1980). Active efflux of tetracycline encoded by four genetically different tetracyline resistance determinants in *Escherichia coli*. *Proceedings of the National Academy of Sciences of the United States of America*, *77*(7 II), 3974–3977. doi:10.1073/pnas.77.7.3974

Meier, I., Wray, L. V., & Hillen, W. (1988). Differential regulation of the Tn*10*-encoded tetracycline resistance genes *tetA* and *tetR* by the tandem *tet* operators *O1* and *O2*. *The EMBO Journal*, *7*(2), 567–572. doi:10.1002/j.1460-2075.1988.tb02846.x

Merfort, M., Herrmann, U., Bringer-Meyer, S., & Sahm, H. (2006). High-yield 5-keto-D-gluconic acid formation is mediated by soluble and membrane-bound gluconate-5-dehydrogenases of *Gluconobacter oxydans*. *Applied Microbiology and Biotechnology*, *73*, 443–451. doi:10.1007/s00253-006-0467-6

Merfort, Marcel, Herrmann, U., Ha, S. W., Elfari, M., Bringer-Meyer, S., Görisch, H., & Sahm, H. (2006). Modification of the membrane-bound glucose oxidation system in *Gluconobacter oxydans* significantly increases gluconate and 5-keto-D-gluconic acid accumulation. *Biotechnology Journal*, *1*(5), 556–563. doi:10.1002/biot.200600032

Mergulhão, F. J. M., & Monteiro, G. A. (2004). Secretion capacity limitations of the Sec pathway in *Escherichia coli*. *Journal of Microbiology and Biotechnology*, 128–133.

Meyer, M., Schweiger, P., & Deppenmeier, U. (2013). Effects of membrane-bound glucose dehydrogenase overproduction on the respiratory chain of *Gluconobacter oxydans*. *Applied Microbiology and Biotechnology*, *97*(8), 3457–3466. doi:10.1007/s00253-012-4265-z

Mientus, M., Kostner, D., Peters, B., Liebl, W., & Ehrenreich, A. (2017). Characterization of membrane-bound dehydrogenases of *Gluconobacter oxydans* 621H using a new system for their functional expression. *Applied Microbiology and Biotechnology*, 3189–3200. doi:10.1007/s00253-016-8069-4

Mill, J. H. (1992). *A short course in bacterial genetics*. Cold Spring Harbor: Cold Spring Harbor Laboratory Press.

Müller-Hill, B. (1998). The function of auxiliary operators. *Molecular Microbiology*, *29*(1), 13–18. doi:10.1046/j.1365-2958.1998.00870.x

Nguyen, T. N. M., Phan, Q. G., Duong, L. P., Bertrand, K. P., & Lenski, R. E. (1989). Effects of carriage and expression of the Tn*10* tetracycline-resistance operon on the fitness of *Escherichia coli* K12. *Molecular Biology and Evolution*, *6*(3), 213–225. doi:10.1093/oxfordjournals.molbev.a040545

Noel, R. J., & Reznikoff, W. S. (2000). Structural studies of *lac*UV5-RNA polymerase interactions *in vitro*. Ethylation interference and missing nucleoside analysis. *Journal of Biological Chemistry*, *275*(11), 7708–7712. doi:10.1074/jbc.275.11.7708

Oehler, S., Eismann, E. R., Kramer, H., & Muller-Hill, B. (1990). The three operators of the *lac* operon cooperate in repression. *EMBO Journal*, *9*(4), 973–979. doi:10.1002/j.1460-2075.1990.tb08199.x

Ohrem, H. L., & Voß, H. (1996). Inhibitory effects of glycerol on *Gluconobacter oxydans*. *Biotechnology Letters*, *18*(3), 245–250. doi:10.1007/bf00142939

Olijve, W., & Kok, J. J. (1979). An analysis of the growth of *Gluconobacter oxydans* in chemostat cultures. *Archives of Microbiology*, *121*(3), 291–297. doi:10.1007/BF00425070

Oliva, B., Gordon, G., Mcnicholas, P., Ellestad, G., & Choprat, I. a N. (1992). Evidence that tetracycline analogs whose primary target is not the bacterial ribosome cause lysis of *Escherichia coli*. *Antimicrobial Agents and Chemotherapy*, *36*(5), 913–919. doi:10.1128/AAC.36.5.913

Paget, M., & Helmann, J. (2003). The σ^{70} family of sigma factors. *Genome Biology*, *4*(1), 1–6. doi:10.1186/gb-2003-4-1-203.

Paget, M. S. (2015). Bacterial sigma factors and anti-sigma factors: Structure, function and distribution. *Biomolecules*, *5*(3), 1245–1265. doi:10.3390/biom5031245

Pappenberger, G., & Hohmann, H.-P. (2014). Industrial production of L-ascorbic acid (vitamin C) and D-isoascorbic acid. *Advances in Biochemical Engineering/Biotechnology*, *143*, 143–188. doi:10.1007/10_2013_243

Pasqua, M., Visaggio, D., Sciuto, A. Lo, Genah, S., Banin, E., Visca, P., & Imperi, F. (2017). Ferric uptake regulator Fur is conditionally essential in *Pseudomonas aeruginosa*. *Journal of Bacteriology*, *199*(22), 1–17. doi:10.1128/JB.00472-17

Peters, B., Mientus, M., Kostner, D., Junker, A., Liebl, W., Ehrenreich, A., & Received: (2013). Characterization of membrane-bound dehydrogenases from *Gluconobacter oxydans* 621H via whole-cell activity assays using multideletion strains. *Applied Microbiology and Biotechnology*, *97*, 6397–6412. doi:10.1007/s00253-013-4824-y

Philips, S. J., Canalizo-Hernandez, M., Yildirim, I., Schatz, G. C., Mondragón, A., & O'Halloran, T. V. (2015). Allosteric transcriptional regulation via changes in the overall topology of the core promoter. *Science*, *349*(6250), 877–881. doi:10.1126/science.aaa9809

Platt, T. (1981). Termination of transcription and its regulation in the tryptophan operon of *E. coli*. *Cell*, *24*(1), 10–23. doi:10.1016/0092-8674(81)90496-7

Possoz, C., Newmark, J., Sorto, N., Sherratt, D. J., & Tolmasky, M. E. (2007). Sublethal concentrations of the aminoglycoside amikacin interfere with cell division without affecting chromosome dynamics. *Antimicrobial Agents and Chemotherapy*, *51*(1), 252–256. doi:10.1128/AAC.00892-06

Power, J. (1967). The L-rhamnose genetic system in *Escherichia coli* K-12. *Genetics*, *55*(3), 557–568. doi:10.1093/genetics/55.3.557

Pramanik, A., Zhang, F., Schwarz, H., Schreiber, F., & Braun, V. (2010). ExbB protein in the cytoplasmic membrane of *Escherichia coli* forms a stable oligomer. *Biochemistry*, 8721–8728. doi:10.1021/bi101143y

Prust, C., Hoffmeister, M., Liesegang, H., Wiezer, A., Fricke, W. F., Ehrenreich, A., … Deppenmeier, U. (2005). Complete genome sequence of the acetic acid bacterium *Gluconobacter oxydans*. *Nature Biotechnology*, *23*(2), 195–200. doi:10.1038/nbt1062

Raspor, P., & Goranovič, D. (2008). Biotechnological applications of acetic acid bacteria. *Critical Reviews in Biotechnology*, *28*(2), 101–124. doi:10.1080/07388550802046749

Reznikoff, W. S. (1992). The lactose operon-controlling elements: A complex paradigm. *Molecular Microbiology*, *6*(17), 2419–2422. doi:10.1111/j.1365-2958.1992.tb01416.x

Richhardt, J., Bringer, S., & Bott, M. (2012). Mutational analysis of the pentose phosphate and Entner-Doudoroff pathways in *Gluconobacter oxydans* reveals improved growth of a Δ*edd* Δ*eda* mutant on mannitol. *Applied and Environmental Microbiology*, *78*(19), 6975–6986. doi:10.1128/AEM.01166-12

Richhardt, J., Bringer, S., & Bott, M. (2013). Role of the pentose phosphate pathway and the Entner-Doudoroff pathway in glucose metabolism of *Gluconobacter oxydans* 621H. *Applied Microbiology Biotechnology*, *97*(10), 4315–4323. doi:10.1007/s00253-013-4707-2

Richhardt, J., Luchterhand, B., Bringer, S., Büchs, J., & Bott, M. (2013). Evidence for a key role of cytochrome bo_3 oxidase in respiratory energy metabolism of *Gluconobacter oxydans*. *Journal of Bacteriology*, *195*(18), 4210–4220. doi:10.1128/JB.00470-13

Rosenberg, H. F. (1998). Isolation of recombinant secretory proteins by limited induction and quantitative harvest. *BioTechniques*, *24*(2), 188–192. doi:10.2144/98242bm03

Saïda, F., Uzan, M. ., Odaert, B., & Bontems, F. (2006). Expression of highly toxic genes in *E. coli*: Special strategies and genetic tools. *Current Protein and Peptide Science*, *7*, 47–56. doi:10.2174/138920306775474095

Saito, Y., Ishii, Y., Hayashi, H., Imao, Y., Akashi, T., Yoshikawa, K., … Shimomura, K. (1997). Cloning of genes coding for L-sorbose and L-sorbosone dehydrogenases from *Gluconobacter oxydans* and microbial production of 2-keto-L-gulonate, a precursor of L-ascorbic acid, in a recombinant *G. oxydans* strain. *Applied and Environmental Microbiology*, *63*(2), 454–460. doi:10.1128/aem.63.2.454-460.1997

Santillán, M., & Mackey, M. C. (2008). Quantitative approaches to the study of bistability in the *lac* operon of *Escherichia coli*. *Journal of the Royal Society Interface*, *5*, S29–S39. doi:10.1098/rsif.2008.0086.focus

Sarvan, S., Butcher, J., Stintzi, A., & Couture, J. F. (2018). Variation on a theme: Investigating the structural repertoires used by ferric uptake regulators to control gene expression. *BioMetals*, *31*(5), 681–704. doi:10.1007/s10534-018-0120-8

Sarvan, S., Yeung, A., Charih, F., Stintzi, A., & Couture, J. F. (2019). Purification and characterization of *Campylobacter jejuni* ferric uptake regulator. *BioMetals*, *32*(3), 491–500. doi:10.1007/s10534-019-00177-5

Schauer, K., Rodionov, D. A., & de Reuse, H. (2008). New substrates for TonB-dependent transport: Do we only see the "tip of the iceberg"? *Trends in Biochemical Sciences*, *33*(7), 330–338. doi:10.1016/j.tibs.2008.04.012

Schedel, M. (2001). Regioselective oxidation of aminosorbitol with *Gluconobacter oxydans,* key reaction in the industrial 1-deoxynojirimycin synthesis (Vol. 8), 295–311.

Schleif, R. (2010). AraC protein, regulation of the L-arabinose operon in *Escherichia coli*, and the light switch mechanism of AraC action. *FEMS Microbiology Reviews*, *34*(5), 779–796. doi:10.1111/j.1574-6976.2010.00226.x

Schweikert, S., Kranz, A., Yakushi, T., Filipchyk, A., Polen, T., Etterich, H., … Bott, M. (2021). The FNR-type regulator GoxR of the obligatory aerobic acetic acid bacterium *Gluconobacter oxydans* affects expression of genes involved in respiration and redox metabolism. *Applied and Environmental Microbiology*, (January), 1–9. doi:10.1128/aem.00195-21

Semsey, S., Tolstorukov, M. Y., Virnik, K., Zhurkin, V. B., & Adhya, S. (2004). DNA trajectory in the Gal repressosome. *Genes and Development*, *18*(15), 1898–1907. doi:10.1101/gad.1209404

Shi, L., Li, K., Zhang, H., Liu, X., Lin, J., & Wei, D. (2014). Identification of a novel promoter *gHp0169* for gene expression in *Gluconobacter oxydans*. *Journal of Biotechnology*, *175*, 69–74. doi:10.1016/j.jbiotec.2014.01.035

Siemen, A., Kosciow, K., Schweiger, P., & Deppenmeier, U. (2018). Production of 5-ketofructose from fructose or sucrose using genetically modified *Gluconobacter oxydans* strains. *Applied Microbiology and Biotechnology*, *102*(4), 1699–1710. doi:10.1007/s00253-017-8699-1

Silverstone, A. E., Arditti, R. R., & Magasanik, B. (1970). Catabolite-insensitive revertants of *lac* promoter mutants. *Proceedings of the National Academy of Sciences of the United States of America*, *66*(3), 773–779. doi:10.1073/pnas.66.3.773

Soini, J., Ukkonen, K., & Neubauer, P. (2008). High cell density media for *Escherichia coli* are generally designed for aerobic cultivations - consequences for large-scale bioprocesses and shake flask cultures. *Microbial Cell Factories*, *7*, 1–11. doi:10.1186/1475-2859-7-26

Soisson, S. M., MacDougall-Shackleton, B., Schleif, R., & Wolberger, C. (1997). Structural basis for ligand-regulated oligomerization of AraC. *Science*, *276*(5311), 421–425. doi:10.1126/science.276.5311.421

Studier, F. W., & Moffatt, B. A. (1986). Use of bacteriophage T7 RNA polymerase to direct selective high-level expression of cloned genes. *Journal of Molecular Biology*, *189*(1), 113–130. doi:10.1016/0022-2836(86)90385-2

Švitel, J., Tkáč, J., Voštiar, I., Navrátil, M., Štefuca, V., Bučko, M., & Gemeiner, P. (2006). *Gluconobacter* in biosensors: Applications of whole cells and enzymes isolated from *Gluconobacter* and *Acetobacter* to biosensor construction. *Biotechnology Letters*, *28*(24), 2003–2010. doi:10.1007/s10529-006-9195-3

Swint-Kruse, L. and Matthews, K. S. (2009). Allostery in the LacI/GalR family: Variations on a theme. *Current Opinion Microbiology*, *12*(2), 129–137. doi:10.1016/j.mib.2009.01.009

Tang, S. Y., Fazelinia, H., & Cirino, P. C. (2008). AraC regulatory protein mutants with altered effector specificity. *Journal of the American Chemical Society*, *130*(15), 5267–5271. doi:10.1021/ja7109053

Teh, M. Y., Ooi, K. H., Danny Teo, S. X., Bin Mansoor, M. E., Shaun Lim, W. Z., & Tan, M. H. (2019). An expanded synthetic biology toolkit for gene expression control in *Acetobacteraceae*. *ACS Synthetic Biology*, *8*(4), 708–723. doi:10.1021/acssynbio.8b00168

Teixidó, L., Carrasco, B., Alonso, J. C., Barbé, J., & Campoy, S. (2011). Fur activates the expression of *Salmonella enterica* pathogenicity island 1 by directly interacting with the *hilD* operator *in vivo* and *in vitro*. *PLoS ONE*, *6*(5). doi:10.1371/journal.pone.0019711

Terpe, K. (2006). Overview of bacterial expression systems for heterologous protein production: From molecular and biochemical fundamentals to commercial systems. *Applied Microbiology and Biotechnology*, *72*(2), 211–222. doi:10.1007/s00253-006-0465-8

Tobin, J. F., & Schleif, R. F. (1987). Positive regulation of the *Escherichia coli* L-rhamnose operon is mediated by the products of tandemly repeated regulatory genes. *Journal of Molecular Biology*, *196*(4), 789–799. doi:10.1016/0022-2836(87)90405-0

Tonouchi, N., Sgiyama, M., & Yokozeki, K. (2003). Construction of a vector plasmid for use in *Gluconobacter oxydans*. *Bioscience Biotechnology Biochemistry*, *67*(1), 211–213. doi:10.1271/bbb.67.211

Venturi, V., Ottevanger, C., Bracke, M., & Weisbeek, P. (1995). Iron regulation of siderophore biosynthesis and transport in *Pseudomonas putida* WCS358: Involvement of a transcriptional activator and of the Fur protein. *Molecular Microbiology*, *15*(6), 1081–1093. doi:10.1111/j.1365-2958.1995.tb02283.x

Vía, P., Badía, J., Baldomà, L., Obradors, N., & Aguilar, J. (1996). Transcriptional regulation of the *Escherichia coli rhaT* gene. *Microbiology*, *142*(7), 1833–1840. doi:10.1099/13500872-142-7-1833

Wickstrum, J. R., & Egan, S. M. (2004). Amino acid contacts between sigma 70 domain 4 and the transcription activators RhaS and RhaR. *Journal of Bacteriology*, *186*(18), 6277–6285. doi:10.1128/JB.186.18.6277-6285.2004

Wickstrum, J. R., Skredenske, J. M., Balasubramaniam, V., Jones, K., & Egan, S. M. (2010). The AraC/XylS family activator RhaS negatively autoregulates *rhaSR* expression by preventing cyclic AMP receptor protein activation. *Journal of Bacteriology*, *192*(1), 225–232. doi:10.1128/JB.00829-08

Wilderman, P. J., Sowa, N. A., FitzGerald, D. J., FitzGerald, P. C., Gottesman, S., Ochsner, U. A., & Vasil, M. L. (2004). Identification of tandem duplicate regulatory small RNAs in *Pseudomonas aeruginosa* involved in iron homeostasis. *Proceedings of the National Academy of Sciences of the United States of America*, *101*(26), 9792–9797. doi:10.1073/pnas.0403423101

Yamada, Y., & Yukphan, P. (2008). Genera and species in acetic acid bacteria. *International Journal of Food Microbiology*, *125*(1), 15–24. doi:10.1016/j.ijfoodmicro.2007.11.077

Yuan, J., Wu, M., Lin, J., & Yang, L. (2016). Combinatorial metabolic engineering of industrial *Gluconobacter oxydans* DSM2343 for boosting 5-keto-D-gluconic acid accumulation. *BMC Biotechnology*, *16*(1), 1–14. doi:10.1186/s12896-016-0272-y

Zahid, N., Schweiger, P., Galinski, E., & Deppenmeier, U. (2015). Identification of mannitol as compatible solute in *Gluconobacter oxydans*. *Applied Microbiology and Biotechnology*, 5511–5521. doi:10.1007/s00253-015-6626-x

Zhang, L., Lin, J., & Ma, Y. (2010). Construction of a novel shuttle vector for use in *Gluconobacter oxydans*. *Molecular Biotechnology*, *46*, 227–233. doi:10.1007/s12033-010-9293-2

5 Appendix

5.1 Endogenous promoters enabling tunable citrate-dependent target gene expression in the acetic acid bacterium *Gluconobacter oxydans*.

As a part of this thesis, endogenous *G. oxydans* regulator-promoter pairs were searched that permit controlled expression of target genes in an effector-dependent manner. Two inducible *G. oxydans* promoters as well as the corresponding regulator were identified and characterized experimentally. While the research on an endogenous regulatable expression system for *G. oxydans* is ongoing, the results presented here will form the core of a manuscript that is in preparation.

In their natural habitat bacteria are confronted with a fast-changing environment that often requires rapid phenotype adaptation to cope with fluctuations in nutrients, toxins, temperature or pH-level. This adaptation is usually driven by transcription factors (TF) that respond to particular changes by altering gene expression as required. In case of nutrients or toxins, a TF binds a specific effector molecule which triggers a conformational change that alters its affinity for particular promoter sites, thereby activating, deactivating, repressing or derepressing transcription of the corresponding gene or operon. To identify endogenous regulated promoters in *G. oxydans*, the mRNA level of 2,687 genes was analyzed in reaction to various substances supplemented to the medium using microarray technology. Giving a 1-2 h pulse of a potential effector in a 1 or 2% (w/v) concentration, the effect of L-arabinose, D-ribose, glycerol, cefoxitin (*G. oxydans* possesses a natural resistance towards the antibiotic), citrate, iso-citrate, α-ketoglutarate, and malate on the transcriptome of *G. oxydans* 621H was tested. Due to the fact that *G. oxydans* rapidly oxidizes many carbohydrates in the periplasm, which might alter a potential effector molecule before it enters the cytoplasm, not only *G. oxydans* 621H but also *G. oxydans* BP.9, lacking nine prominent dehydrogenases active in the periplasm, was used for these experiments (Peters et al. 2013). From all compounds tested, only high concentrations of citrate led to a strong change in mRNA level with a ratio of supplemented *vs.* non-supplemented >10.

Promoters $P_{GOX0532}$ and $P_{GOX0536}$ respond to high citrate concentrations

Transcription levels of the genes GOX0532 and GOX0536 were 46- and 45-fold elevated, when *G. oxydans* 621H was exposed to medium containing 1% (w/v) (~50 mM) citrate for 2 h. The gene GOX0532 clusters with GOX0531 and GOX0530 with GOX0532 being

the first gene of the operon and showing the strongest increase in transcription upon citrate supplementation (Fig. 1a, b). GOX0536 is located in close proximity of GOX0532 but transcribes as monocistronic mRNA. The GOX0532-0 operon encodes the proteins ExbB, ExbD and TonB and GOX0536 a hydroxamate-type ferrisiderophore receptor (Prust et al. 2005). In Gram-negative bacteria, ExbB, ExbD and TonB form a complex that transfers energy derived from the proton motive force at the cytoplasmic membrane to outer membrane transporter proteins of scarce nutrients. The ExbD-ExbB-TonB transfer system is illustrated in Figure 1c. Synthesized in a ratio of 7:2:1 for ExbB:ExbD:TonB and anchored in the cytoplasmic membrane, the complex enables TonB-dependent transporters the energy-dependent uptake of substrates that are either too large to pass non-specific porin channels in the outer membrane or require a high-affinity transport system (Ahmer et al. 1995, Higgs et al. 2002, Pramanik et al. 2010). Such substrates may be iron-loaded siderophores, vitamin B12, or different carbohydrates (reviewed by Schauer et al. 2008). The ferrisiderophore receptor encoded by GOX0536 is likely a TonB-dependent transporter of iron-loaded siderophores.

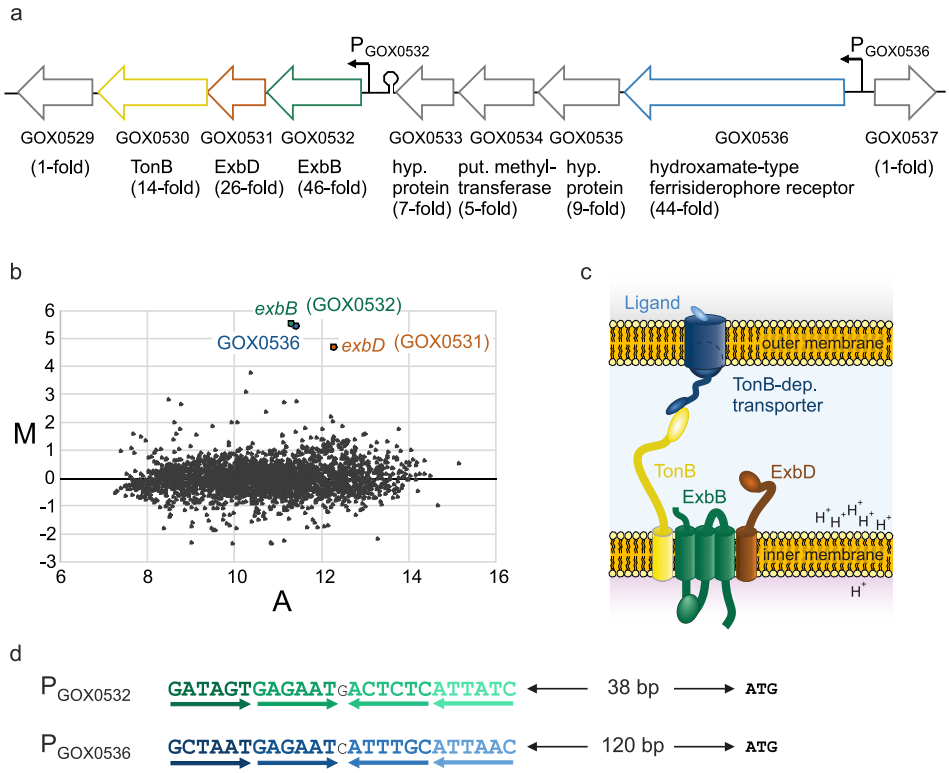

Fig. 1 Elevated expression of the genes GOX0532 and GOX0536 in *G. oxydans* 621H incubated in medium supplemented with citrate and putative binding sites of the ferric uptake regulator.

(**a**) Organization of the operon GOX0532-0 and monocistronic GOX0536 with adjacent genes in the genome of *G. oxydans*. Underneath encoded proteins according to annotation and ratio of mRNA levels (in brackets) when exposed to a 2 h pulse of 50 mM citrate (pH 6 by KOH) determined by microarray analysis. (**b**) Microarray analysis of *G. oxydans* exposed to 50 mM citrate in a MA plot showing $\log_2$ of the red/green fluorescence intensity ratios (M) *vs.* the average $\log_2$ intensity of both channels. Signals of genes GOX0531, GOX0532 and GOX0536 are highlighted and labeled. (**c**) ExbD-ExbB-TonB energy transfer system (adapted from Celia et al. 2020). Energy derived from the proton gradient at the cytoplasmic membrane is transferred via ExbD-ExbB-TonB to TonB-dependent receptors at the outer membrane for the uptake of scarce compounds such as iron siderophores. (**d**) Predicted Fur binding sites in the putative promoter regions of the genes GOX0532 and GOX0536 resembling Fur binding sites in *E. coli*.

Citrate is a known chelator of Fe^{3+}. During the incubation of *G. oxydans* with 50 mM citrate, probably the iron accessibility was reduced which in turn induced adaptational processes in genome. Iron homeostasis in most Gram-negative bacteria is regulated by the TF Fur (ferric uptake regulator) that acts primarily as a repressor upon binding of iron (reviewed by Fillat, 2014). However, it has been shown that dimeric Fur-Fe^{2+} may also activate gene expression or apo-Fur may repress transcription (Bagg & Neilands, 1987, Ernst et al. 2005, Teixidó et al. 2011, Fillat, 2014). Genome sequencing of *G. oxydans* confirmed the presence of a *E. coli* Fur homolog encoded by GOX0771 exhibiting in a protein BLAST search 38% sequence identity with Fur from *E. coli* K12 (Prust et al. 2005).

Fur likely transcription factor for $P_{GOX0532}$ and $P_{GOX0536}$

Multiple attempts conducted during this work trying to delete GOX0771 in order to investigate the role of Fur in *G. oxydans* failed, suggesting that the regulator is essential for survival of the bacterium. Promoters regulated by Fur often contain a ~19 bp palindromic consensus sequence also known as a FUR-box that is bound by iron-loaded FUR for the repression of gene transcription in the presence of iron. The FUR-box is characterized by a minimum of three repeats of the hexameric motif 5'-GATAAT-3'. These can be slightly imperfect and the third motif has often a reverse orientation and is separated by a single base pair from the first two hexamers (Escolar *et al* 1998, Fillat 2014, Seo *et al* 2014). Scanning the putative promoter regions for potential Fur binding sites using 300 bp upstream of the respective start codons of GOX0532 and GOX0536, so called Fur-boxes were identified that resemble Fur-boxes of other bacteria (Fig. 1d) (reviewed by Filat, 2014). These potential Fur-boxes within $P_{GOX0532}$ and $P_{GOX0536}$ are located 38 bp and 120 bp upstream from the start codons of GOX0532 and GOX0536, respectively. Since for both genes the transcription start sites are unknown, no prediction on the mode of regulation could be made. To verify these Fur-binding motives on $P_{GOX0532}$ and $P_{GOX0536}$ by chromatin affinity purification DNA sequencing (ChAP-Seq), attempts were made to genomically modify GOX0771 to obtain N- or C-terminally Strep-tagged Fur as a gene product. Similar to the deletion of GOX0771, no *G. oxydans* strain with a modified GOX0771 gene and tagged Fur could be generated. As an alternative, a copy

of modified GOX0771 encoding C-terminally tagged Fur and expressed from its native promoter was genomically integrated in the known and previously used intergenic region 3 (igr3) between GOX0038 and GOX0039 (Battling et al. 2020). A *G. oxydans* strain with modified GOX0771 encoding N-terminally tagged Fur in igr3 could until now not be obtained.

Maintaining high iron concentrations (>300 µM) during cultivation and protein purification, ChAP-Seq analysis with C-terminally tagged Fur encoded from modified GOX0771 integrated in igr3 confirmed the putative Fur-binding site within $P_{GOX0536}$. Next to $P_{GOX0536}$, binding sites within the promoters of the genes GOX1246 and GOX0641 were enriched (Tab. 1). GOX1246 and GOX0641 encode TonB-dependent and ferrisiderophore receptors, respectively. Within $P_{GOX0532}$ no Fur box was enriched by ChAP-Seq. Surprisingly, among others within the putative promoter of GOX1191, encoding bacterioferritin, no potential Fur box was identified. Bacterioferritin is involved in iron storage and positively activated by iron-loaded Fur *e.g.* in *Pseudomonas aeruginosa* (Wilderman et al. 2004).

Table 1 ChAP-Seq analysis with C-terminally tagged Fur integrated in intergenic region 3

Genes and annotated proteins with potential Fur-DNA binding sites obtained by ChAP-Seq with *G. oxydans* 621H containing a copy of modified GOX0771 encoding C-terminally tagged Fur integrated in intergenic region 3 (Battling et al. 2020). Genes were ranked according to the peak coverage. Binding sequences were identified using *E. coli* Fur box 5'-GATAATGATAATCATTATC-3' for comparison and the MASTMEME motif search tool (Bailey & Gribskov, 1998) (Fillat, 2014).

Rank	Gene	Annotation	Fur-binding motif sequence (5'→3')
1	GOX0536	ferrisiderophore receptor (hydroxamate-type)	**G**C**TAATGA**G**AAT**C**ATT**TG**CATTA**A**C**
2	GOX1191	bacterioferritin	
3	GOX2731	pGOX4, transposase	
4	GOX1246	TonB-dependent receptor	**GAGAATGA**G**AAT**CT**TT**CG**CA**A**T**G**T**T
5	GOX2588	pGOX1	
6	GOX2584	pGOX1, hypothetical protein	
7	GOX2714	pGOX4, transposase	
8	GOX0641	ferrisiderophore receptor (hydroxamate-type)	**GA**G**AAT**A**ATTATCATT**CG**C**
9	GOX2718	pGOX4, transposase	
10	GOX2097	sorbitol-dehydrogenase (small subunit)	
11	GOX2699	pGOX3, hypothetical protein	
12	GOX0442	hypothetical protein	

Performance of $P_{GOX0532/6}$ with enzyme reporter UidA

In preliminary experiments, the plasmids pBBR1MCS-2-$P_{GOX0532}$-*uidA* and pBBR1MCS-2-$P_{GOX0536}$-*uidA* were constructed by fusing 300 bp upstream from GOX0532 and GOX0536 to the gene *uidA*, which encodes the reporter enzyme β-D-glucuronidase, and integrated into the multiple cloning site of pBBRMCS-2. The transcription terminator sequence T_{gdhM} taken from the gene GOX0265 and proven to be effective in *G. oxydans* was placed downstream of *uidA*. Grown in shake flasks with D-mannitol complex medium and induced by 50 mM citrate upon inoculation, *uidA* expression from both promoter was determined by Miller assay (Miller, 1992). Measuring enzyme activity after 3 and 4 h showed that *uidA* expression from $P_{GOX0536}$ was considerably higher than from $P_{GOX0532}$ (Fig. 2b). For $P_{GOX0532}$ and $P_{GOX0536}$, UidA activity in induced cultures was with 17,800 Miller units (MU) and 2268,900 MU approximately 9- and 4-fold higher than in non-induced cultures ($P_{GOX0532}$: 2,000 MU, $P_{GOX0536}$: 550,300 MU). Overall, induction fold-ratios were significantly reduced due to the strong basal expression of both promoters in the absence of citrate.

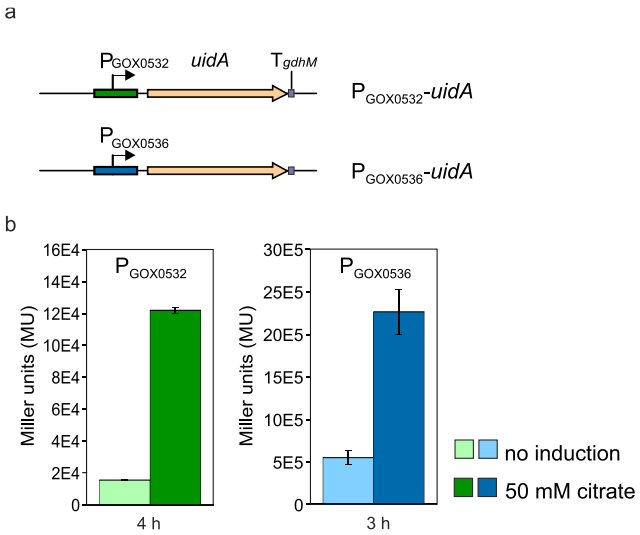

Fig. 2 pBBR1MCS-5-based expression plasmids and analysis of the inducibility of $P_{GOX0532/6}$ by citrate using *uidA* as reporter.

(**a**) Schematic illustration of the plasmid inserts $P_{GOX0532}$-*uidA* and $P_{GOX0536}$-*uidA* with terminator sequence T_{gdhM} derived from *gdhM* (GOX0265) (**b**) Inducibility of $P_{GOX0532}$ and $P_{GOX0536}$ in *G. oxydans* 621H carrying plasmid pBBR1MCS-2-$P_{GOX0536}$-*uidA* or pBBR1MCS-2-$P_{GOX0536}$-*uidA*. Grown in shake flasks with 4% D-mannitol medium, *uidA* expression was induced upon inoculation with 50 mM citrate and determined 4 and 3 h after induction as β-D-glucuronidase activity shown in Miller units (MU).

Performance of $P_{GOX0532/6}$ with fluorescent reporter mNeonGreen

For continuous determination of reporter gene expression in microscale BioLector cultivations, plasmids encoding the fluorescence reporter protein mNeonGreen (mNG) were

constructed. Additionally, to avoid undesired side-effects such as an abnormal cell morphology resulting from the pBBR1MCS-2 plasmid backbone, $P_{GOX0532}$ and $P_{GOX0536}$ were integrated into the pBBR1MCS-5 plasmid, which was shown to not have these effects on the morphology (Fricke et al. 2021b). Furthermore, on the pBBR1MCS-5-based plasmids $P_{GOX0532}$-*mNG* and $P_{GOX0536}$-*mNG* were flanked on both sides by terminator sequences to create transcriptional barriers between the genetic elements within the inserts and the plasmid backbone. A schematic illustration of the pBBR1MCS-5 inserts is given in Figure 3a. The terminators T_{gdhM} and $T_{GOX0028}$ are DNA sequences derived from the genes GOX0265 and GOX0028, respectively, while terminator T_{BBa_B1002} was taken from the iGEM parts library.

Since both promoters exhibited high basal expression in the absence of citrate, it was tested whether the supplementation of the medium with iron ions would reduce leakiness. Basal expression significantly decreased when the medium was supplemented with iron sulfate ($Fe(II)SO_4$), supporting the hypothesis that citrate did induce expression from $P_{GOX0532}$ and $P_{GOX0536}$ through iron limitation (data not shown). Furthermore, different induction strategies were tested. Grown in D-mannitol medium, the effect of 50-250 mM citrate supplemented in intervals of 1.5 h up to 5 times on $P_{GOX0532/6}$ promoted expression in *G. oxydans* was tested by means of *mNG* expression. Now routinely cultivated in medium supplemented with 4-8 µM $Fe(II)SO_4$ for reduced basal expression, best induction ratios were obtained when 5 x 50 mM citrate was added in intervals (Fig. 3b, c).

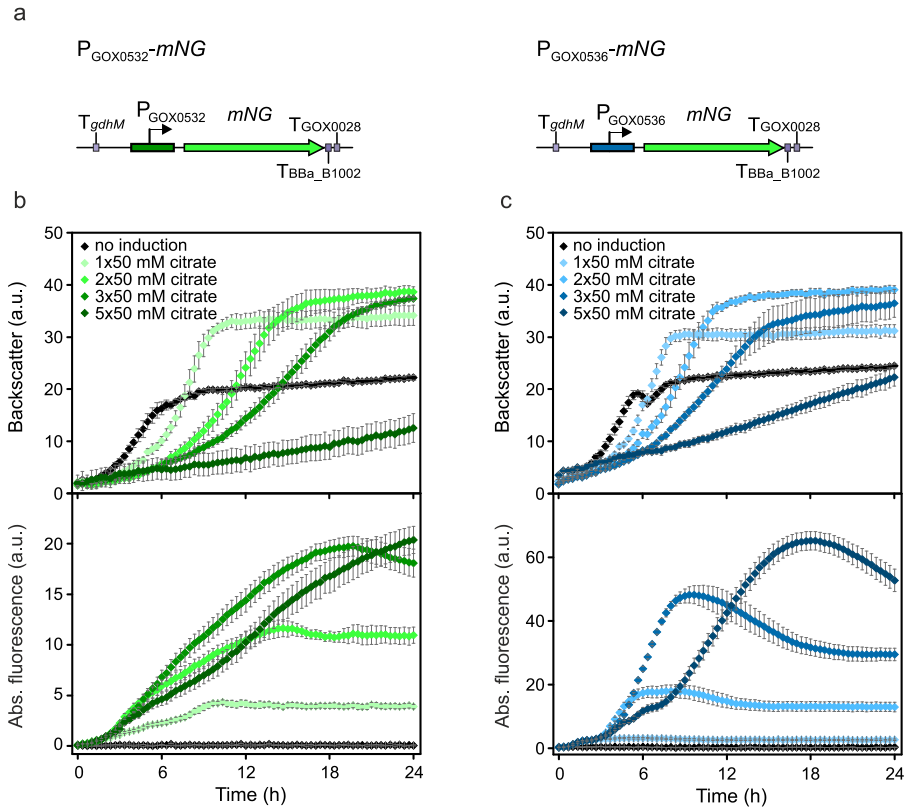

Fig. 3 pBBR1MCS-5-based expression plasmids and analysis of the inducibility of $P_{GOX0532/6}$ by citrate using *mNG* as reporter.

Performance of citrate-inducible promoters $P_{GOX0532}$ and $P_{GOX0536}$ in *G. oxydans* 621H. Growth according to backscatter and absolute mNG fluorescence of *G. oxydans* carrying plasmid pBBR1MCS-5-$P_{GOX0532}$-*mNG* (**b**) or pBBR1MCS-5-$P_{GOX0536}$-*mNG* (**c**) in citrate-induced and non-induced condition in microscale BioLector cultivations. Grown in D-mannitol medium supplemented with 8 µM Fe(II)SO_4, reporter gene expression was induced by adding 1 x, 2 x, 3 x or 5 x 50 mM citrate in 1.5 h intervals from pH-neutral 2 M stock solution. BioLector settings: backscatter gain 4, fluorescence gain 8. Data represent mean values and standard deviation from two biological replicates with three technical replicates each.

Overall, increasing citrate concentrations in the medium of *G. oxydans* harboring pBBR1MCS-5-$P_{GOX0532/6}$-*mNG* led to stronger *mNG* expression and high induction ratios when compared to non-supplemented cultures. Additionally, the lag growth phase of cultures prolonged with higher citrate concentrations (Fig. 3b, c). Moreover, backscatter signals indicated considerably higher final cell densities of citrate supplemented cultures compared to non-supplemented reference cultures. For example, the addition of 3 x 50 mM citrate increased backscatter values from ~24 to ~37 a.u. after 24 h. Trying to verify the final backscatter values by photometer, only a slightly higher optical density of maximal 10% of induced *vs.* non-

induced cultures was observed. Hence, it can be assumed that the backscatter values higher than those of the reference without citrate posed an artifact. Therefore, in this work only absolute but no biomass-specific fluorescence is presented.

For both promoters, basal expression in the absence of supplemented citrate was barely detectable. The strongest fluorescence values with 21 a.u. after 24 h for *G. oxydans* carrying pBBR1MCS-5-P_{GOX053}-*mNG* and 65 a.u. after 18 h for *G. oxydans* carrying pBBR1MCS-5-$P_{GOX0536}$-*mNG* were obtained when culture were supplemented with 5 x 50 mM citrate (Fig. 3b, c). At this time point, highest induction ratios for *G. oxydans* with the $P_{GOX0532}$-(433-fold) and $P_{GOX0536}$-plasmid (291-fold) were obtained. However, due to the severely retarded growth, the induction strategy using 5 x 50 mM citrate seemed not expedient. Since growth of *G. oxydans* in medium supplemented with 3 x 50 mM citrate was less impaired but cultures still exhibited strong *mNG* expression ($P_{GOX0532}$: 20 a.u. after 20 h; $P_{GOX0536}$: 48 a.u. after 9 h) and high induction ratios ($P_{GOX0532}$: 378-fold; $P_{GOX0536}$: 264-fold), the addition of 3 x 50 mM citrate seemed the preferable induction strategy. All induction ratios obtained with *G. oxydans* carrying pBBR1MCS-5-$P_{GOX0532}$-*mNG* or pBBR1MCS-5-$P_{GOX0536}$-*mNG* are summarized in table 2.

Table 2 Citrate-dependent induction fold changes of $P_{GOX0532/6}$ in pBBR1MCS-5-based expression plasmids.

Citrate-dependent induction fold changes calculated from mNG fluorescence signals in *G. oxydans* 621H carrying plasmid pBBR1MCS-5-$P_{GOX0532}$-*mNG* or pBBR1MCS-5-$P_{GOX0536}$-*mNG.* Citrate was added to BioLector cultivations in intervals of 1.5 h. In brackets the time after inoculation is given when maximal induction fold changes were measured.

Citrate (1.5 h intervals)	$P_{GOX0532}$-*mNG*	$P_{GOX0536}$-*mNG*
1 x 50 mM	72 (10 h)	10 (6 h)
2 x 50 mM	258 (15 h)	71 (8 h)
3 x 50 mM	378 (20 h)	101 (9 h)
5 x 50 mM	433 (24 h)	274 (18 h)

Using a flow cytometer, the citrate inducibility of $P_{GOX0536}$ in *G. oxydans* harboring pBBR1MCS-5-$P_{GOX0536}$-*mNG* was tested on single cell level. Grown in shake flask, induced and uninduced cells exhibited a high population homogeneity 7 h after inoculation (Fig. 4). Approximately 97% of all cells in non-induced and citrate-supplemented cultures showed low fluorescence (~1,000 a.u.) and high fluorescence (10,000 a.u.), respectively.

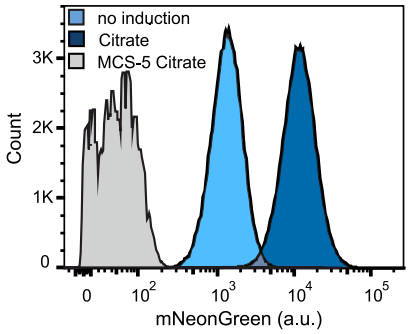

Fig. 4 Citrate-dependent induction of $P_{GOX0536}$ in *G. oxydans* on single cell level.

FACS analysis of *G. oxydans* 621H carrying plasmid pBBR1MCS-5-$P_{GOX0536}$-*mNG* or for reference empty vector pBBR1MCS-5 (MCS-5). Grown in shake flasks with D-mannitol medium supplemented with 4 µM Fe(II)SO_4 *mNG* expression was induced by the addition of 5 x 50 mM citrate in intervals of 1.5 h. Empty vector control cultures were also supplemented with 5 x 50 mM citrate. FACS analysis was performed 7 h after inoculation. Total counts per sample represent 100.000 events.

Regulation of genomically integrated $P_{GOX0532}$ and $P_{GOX0536}$

To create a non-GMO (genetically modified organism) *G. oxydans* strain that enables induced target gene expression from the promoters $P_{GOX0532}$ and $P_{GOX0536}$ and grows independent of antibiotics for plasmid selection, $P_{GOX0532}$ and $P_{GOX0536}$ were integrated into the genome of *G. oxydans* 621H in the same intergenic region igr3 described above (Battling et al. 2020). For markerless genome integration, the plasmid pKOS6b with *E. coli codA* was used as described by Kostner et al. (2013). To avoid interference with adjacent genes or genetic elements of igr3, the DNA sequences inserted contained the same three terminator sequences flanking the inserts as on the plasmids pBBR1MCS-5-$P_{GOX0532}$-*mNG* and pBBR1MCS-5-$P_{GOX0536}$-*mNG*. For proof of principle, induced *mNG* expression from both genomically integrated promoters was tested by supplementing the modified *G. oxydans* strains with up to 3 x 50 mM citrate. Due to the reduced copy number per cell of genomically expressed *mNG* in comparison to plasmid-based constructs, detection of fluorescence signals required stronger amplification than with plasmid encoded promoter-reporter pairs. Furthermore, a BioLector of a different generation was used, making a direct comparison with the previously shown plasmid-based system difficult.

Expressing genome encoded *mNG* from $P_{GOX0532}$ and $P_{GOX0536}$ in the created *G. oxydans* strains, a fairly similar growth profile was observed than in the above presented tests with expression plasmids. According to backscatter values, increased citrate

concentrations prolonged the lag growth phase of the cells with in case of 3 x 50 mM citrate resulting in the strongest effect (Fig. 5a, b).

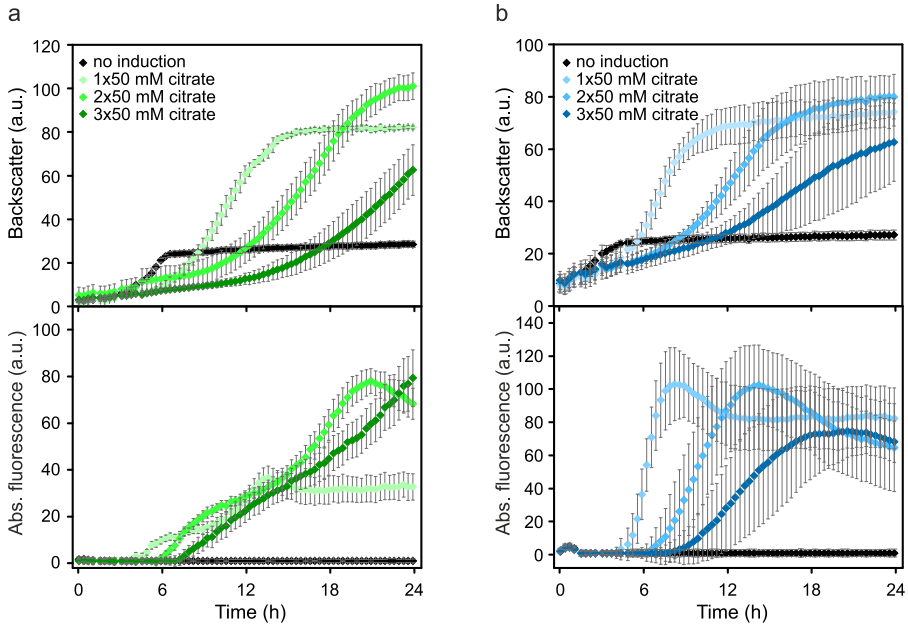

Fig. 5 Inducibility of genomically integrated $P_{GOX0532/6}$ by citrate using *mNG* as reporter.

Citrate-inducible *mNG* expression in the *G. oxydans* strains igr3::$P_{GOX0532}$-*mNG* and igr3::$P_{GOX0536}$-*mNG.* Growth according to backscatter and absolute mNG fluorescence of *G. oxydans* 621H with $P_{GOX0532}$-*mNG* (**a**) or $P_{GOX0536}$-*mNG* (**b**) genomically integrated in intergenic region igr3 (Battling et al. 2020). Using microscale BioLector cultivations, cells were grown in D-mannitol medium supplemented with 8 µM $Fe(II)SO_4$. Upon inoculation reporter gene expression was induced by adding 1 x, 2 x or 3 x 50 mM citrate in 1.5 h intervals from pH-neutral 2 M stock solution. BioLector settings: backscatter gain 20, fluorescence gain 100. Data represent mean values and standard deviation from three biological replicates with three technical replicates each.

First supplemented with 50 mM citrate 1.5 h after inoculation, fluorescence signals in *G. oxydans* igr3::$P_{GOX0532}$-*mNG* and *G. oxydans* igr3::$P_{GOX0536}$-*mNG* were only detectable approximately 4-5 h after induction (Fig. 5a, b). For *G. oxydans* igr3::$P_{GOX0532}$-*mNG* the highest induction fold-changes of 81±3 were obtained with 3 x 50 mM citrate at the end of the experiment after 24 h. While in uninduced cultures fluorescence was barely detectable, in induced cultures values of ~82 a.u. were measured. The data indicate that the maximum had not been reached at that point. Supplementing with 1 x 50 and 2 x 50 mM citrate led to maximal fluorescence of ~37 a.u. and ~78 a.u. with calculated induction fold-change of 37±4 after 14 h and 78±2 after 21 h, respectively (Fig. 5a, b).

In the case of *G. oxydans* igr3::$P_{GOX0536}$-*mNG*, basal expression in uninduced cultures was too low to detect of mNG fluorescence (Fig. 5a, b). Therefore, for calculation of induction fold-changes values were set to 1. In cultures with *G. oxydans* igr3::$P_{GOX0536}$-*mNG*, multiple additions of 50 mM citrate did not result in an increased *mNG* expression. Inducing with 1 x 50 and 2 x 50 mM citrate both led to 103 a.u. and a 103-fold increase in fluorescence, with the difference that with a single supplementation, fluorescence signals peaked after 8 h while with two supplementations similar intensities were reached only after 14 h. Adding 3 x 50 mM citrate reduced induction fold-changes in cultures with *G. oxydans* igr3::$P_{GOX0536}$-*mNG* again. Hence, after 21 h maximal fold-changes of 75±12 were calculated. All induction ratios of genome encoded and citrate-induced *mNG* expression in the *G. oxydans* strains igr3::$P_{GOX0532}$-*mNG* and igr3::$P_{GOX0536}$-*mNG* are summarized in table 3.

Table 3 Citrate-dependent induction fold changes of genomically integrated $P_{GOX0532/6}$

Citrate-dependent induction fold changes calculated from mNG fluorescence signals in the *G. oxydans* strains igr3::$P_{GOX0532}$-*mNG* and igr3::$P_{GOX0536}$-*mNG*. Both strain were created by genomically integrating T_{gdhM}-$P_{GOX0532}$-*mNG*-$T_{BBa\text{-}B1002}$-$T_{GOX0028}$ or T_{gdhM}-$P_{GOX0536}$-*mNG*-$T_{BBa\text{-}B1002}$-$T_{GOX0028}$ in intergenic region igr3 (Battling et al. 2020). Citrate was added to BioLector cultivations in intervals of 1.5 h. In brackets the time after inoculation is given when maximal induction fold changes were measured.

Citrate (1.5 h intervals)	$P_{GOX0532}$-*mNG* (igr3)	$P_{GOX0536}$-*mNG* (igr3)
1 x 50 mM	37±4 (14 h)	103±22 (8 h)
2 x 50 mM	78±2 (21 h)	103±23 (14 h)
3 x 50 mM	81±3 (24 h)	75±12 (21 h)

The regulatable endogenous promoters $P_{GOX0532}$ and $P_{GOX0536}$ may form the basis of an industrial *G. oxydans* strain that combines inducible gene expression with a non-GMO classification. The experiments conducted in this work showed that both promoters combine low basal expression in iron supplemented medium with strong controlled target gene expression and high induction fold changes when fully induced with citrate. Since the high citrate concentrations required for strong target gene expression impaired growth, it needs to be evaluated whether increased expression can compensate for the strong retardation of growth in citrate-supplemented cultures. Furthermore, it is very likely that both promoters are induced due to an iron limitation in the medium caused by the high citrate concentrations and therefore regulated by the global TF Fur encoded by GOX0771. Using a regulatable expression system that depends on a global TF poses the risk of interfering with other fundamental regulatory networks of the cell. The inability to delete *fur* in *G. oxydans* might indicate that the TF plays a key role in very basic mechanisms needed for survival of the bacterium.

Nonetheless, in spite of the questionable feasibility of this endogenous expression system, this research shed some light on an essential regulon of *G. oxydans* that so far has not been investigated.

Danksagung

Ich möchte mich bei Prof. Dr. Michael Bott für die Überlassung des spannenden Themas bedanken, dass trotz eines einfach anmutenden Titels viele interessante Facetten beinhaltete. Ich habe unsere Diskussionen immer als engagiert und hilfreich empfunden. Außerdem danke ich für zügige Durchsicht der Manuskripte und der Doktorarbeit.

Bei Prof. Dr. Vlada Urlacher bedanke ich mich dafür, dass sie das Zweitgutachten angenommen hat.

Mein besonderer Dank gilt meinem engagierten Gruppenleiter Dr. Tino Polen. Ich danke ihm für die vielen konstruktiven Diskussionen und Anregungen, die mich immer sehr motiviert haben. Auch habe ich unseren regen wissenschaftlichen und freundschaftlichen Austausch bei unseren laufenden Gruppentreffen im Jülicher Wald sehr geschätzt. Außerdem danke ich ihm für die Korrektur der Manuskripte und der Doktorarbeit.

Bei den Mitarbeitern der AG Polen, mit Namen Astrid Wirtz und Ursula Degner, möchte ich mich für die angenehme Arbeitsatmosphäre und gute Zusammenarbeit bedanken. Bei Fragen zu Laborarbeiten konnte ich immer mit einem offenen Ohr rechnen. Auch unsere Prä-Corona Freizeitaktivitäten haben mir immer Spaß gemacht.

Dem gesamten IMPRES Team möchte für die gute Kooperation danken. Die konstruktiven Diskussionen mit den Gruppenleitern und Doktoranden der AG Deppenmeier der Universität Bonn, der AG Büchs der RWTH Aachen, der AG Baumgart/Bott des Forschungszentrums Jülich sowie den Mitarbeitern von Pfeifer & Langen waren immer informativ und unterstützend.

Mein großer Dank gilt auch den Bachelor- und Masterstudenten Tobias Link, Sabrina Derksen, Angelika Klemm, Mandy Gries, Claudia Tahiraj und Maurice Mürköster, die ich während meiner Doktorarbeit bei ihren Abschlussarbeiten betreuen durfte. Mir hat die Arbeit mit ihnen sehr viel Freude bereitet und sie haben alle durch ihre Laborarbeit zum Gelingen meiner Dissertation beigetragen.

Erklärung

Ich versichere an Eides Statt, dass die Dissertation von mir selbständig und ohne unzulässige fremde Hilfe unter Beachtung der „Grundsätze zur Sicherung guter wissenschaftlicher Praxis an der Heinrich-Heine-Universität Düsseldorf“ erstellt worden ist. Ich habe bisher keine erfolglosen Promotionsversuche unternommen. Diese Dissertation wurde bisher an keiner anderen Fakultät vorgelegt.

Jülich,

Philipp Moritz Fricke

Band / Volume 246
Tailoring neuroelectronic interfaces via combinations of oxides and molecular layers
X. Yuan (2021), 113 pp
ISBN: 978-3-95806-572-7

Band / Volume 247
Stoichiometric control and magnetoelectric coupling in artificial multiferroic heterostructures
P. Schöffmann (2021), vii, 176 pp
ISBN: 978-3-95806-575-8

Band / Volume 248
A Unified Framework for Functional Renormalisation Group Calculations and its Application to Three Dimensional Hubbard Models
J. Ehrlich (2021), xvi, 213 pp
ISBN: 978-3-95806-582-6

Band / Volume 249
Photoemission electron microscopy of magneto-ionic effects in $La_{0.7}Sr_{0.3}MnO_3$
M. Wilhelm (2021), 134 pp
ISBN: 978-3-95806-592-5

Band / Volume 250
Development of a Multiplexer System and Measurement of the Neutron Yield for a Low-Energy Accelerator-Driven Neutron Source
M. Rimmler (2021), v, 200 pp
ISBN: 978-3-95806-600-7

Band / Volume 251
Resolving interface effects in voltage controlled magnetic heterostructures using advanced neutron scattering and electron microscopy methods
T. Bhatnagar-Schöffmann (2021), ix, 171 pp
ISBN: 978-3-95806-604-5

Band / Volume 252
Strain development of *Gluconobacter oxydans* and *Pseudomonas putida* for production of the sweetener 5-ketofructose
K. Wohlers (2022), VI, 118 pp
ISBN: 978-3-95806-612-0

Band / Volume 253
Topological magnonic properties of two-dimensional magnetic materials
L. Zhang (2022), xx, 154 pp
ISBN: 978-3-95806-621-2

Band / Volume 254
Role of secondary metabolites in antiphage defense in *Streptomyces*
Aël Hardy (2022), IV, 193 pp
ISBN: 978-3-95806-633-5

Band / Volume 255
Neutron Scattering
Lectures of the JCNS Laboratory Course held at Forschungszentrum Jülich and at the Heinz-Maier-Leibnitz Zentrum Garching
edited by T. Brückel, S. Förster, M. Kruteva**,** M. Zobel, and R. Zorn (2022), ca. 300 pp
ISBN: 978-3-95806-634-2

Band / Volume 256
Magnetoelectric Interactions in Multiferroic Thin-film Heterosystems and Nanostructures
H. Gökdemir (2022), x, 140 pp
ISBN: 978-3-95806-635-9

Band / Volume 257
High-Performance Computing Approach to Hybrid Functionals in the All-Electron DFT Code FLEUR
M. Redies (2022), xi, 109 pp
ISBN: 978-3-95806-639-7

Band / Volume 258
Establishing regulatable expression systems in the acetic acid bacterium *Gluconobacter oxydans* 621H
P. M. Fricke (2022), VIII, 187 pp
ISBN: 978-3-95806-642-7

Schlüsseltechnologien / Key Technologies
Band / Volume 258
ISBN 978-3-978-3-95806-642-7

Mitglied der Helmholtz-Gemeinschaft

JÜLICH
Forschungszentrum